

# **Genetic diversity and reproductive systems of myxomycetes**

I n a u g u r a l d i s s e r t a t i o n

zur

Erlangung des akademischen Grades eines

Doktors der Naturwissenschaften (Dr. rer. nat.)

der

Mathematisch-Naturwissenschaftlichen Fakultät

der

Ernst-Moritz-Arndt-Universität Greifswald

vorgelegt von

Yun Feng

geboren am 11.06.1970

in Beijing

Greifswald, im November 2015

Dekan: Prof. Dr. Werner Weitschies

1. Gutachter: Prof. Dr. Martin Schnittler

2. Gutachter: Prof. Dr. Steven L. Stephenson

Tag der Promotion: 16.12.2015

# Contents

1. Summary	5
1.1 English	7
1.2 German	9
2. Introduction	11
3. Publications	27
3.1 Sex or no sex? Group I introns and independent marker genes reveal the existence of three sexual but reproductively isolated biospecies in <i>Trichia varia</i> (Myxomycetes)	29
3.2 What an intron may tell: several sexual biospecies coexist in <i>Meriderma</i> spp. (Myxomycetes)	49
3.3 Morphological or biological species? A revision of <i>Meriderma</i> spp. (Myxomycetes)	69
3.4 Molecular or morphological species? Myxomycete diversity in a deciduous forest in northeastern Germany	93
4. Declaration	115
5. Curriculum Vitae	121
6. Acknowledgements	125



## 1. Summary



Myxomycetes (Amoebozoa, plasmodial slime molds) are one of the last larger groups of organisms where the biodiversity is not yet investigated by molecular methods, except for a very few cultivable model species. Based on the first phylogenies for the group produced in 2012 and 2013, this thesis work explores the genetic diversity of wild populations of myxomycetes, addressing two questions: 1. *Does diversity and phylogenetic trees found with barcode markers fit the current morphological species concept, and do barcode markers reveal a lower or higher diversity than found by morphological characters?* In the first case, morphological characters seen as decisive for species differentiation would be plastic (shaped by the environment), in the second case we must assume the existence of cryptic species. 2. *Can genetic markers be used to see if natural populations of myxomycetes reproduce mainly sexual or asexual?* Sexuality is proven to occur in the Amoebozoa, but asexual reproduction should be advantageous for habitat colonization. Experiments with cultivable species have shown that both reproductive modes occur in the myxomycetes.

Two species complexes were chosen for an in-depth investigation. The first species is the common wood-inhabiting myxomycete *Trichia varia* (Pers. ex J.F. Gmel.) Pers., one of the first myxomycetes to be described and always seen as a variable, yet single, species. The second example involves a snowbank species so far known as *Lamproderma atrosporium* Meyl., which was recently transferred to a genus on its own, *Meriderma* Mar. Mey. & Poulain, and a morphological species concept, including several taxa, was proposed.

*Trichia varia* belongs to the bright-spored myxomycetes. Partial sequences of three independent markers (nuclear small-subunit ribosomal RNA gene, SSU, extrachromosomal; protein elongation factor 1 alpha gene, EF1A, chromosomal; cytochrome oxidase subunit 1 gene, COI, mitochondrial) from 198 specimens resulted in a three-gene phylogeny containing three groups, within each group combinations of the single-marker genotypes occurred exclusively. Complete SSU sequences were generated for 66 specimens, which revealed six positions that can carry group I introns and putatively functional or degenerated homing endonuclease genes in two groups. All observations (genotypic combinations of the three markers, signs of recombination, intron patterns) fit well into a pattern of three cryptic biological species that reproduce predominantly sexual but are reproductively isolated. The pattern of group I introns and inserted homing endonuclease genes mounts evidence that the Goddard-Burt intron life cycle model applies to naturally occurring myxomycete populations.

A total of 89 specimens of the dark-spored myxomycete genus *Meriderma* from five European mountain ranges were sequenced for partial genes of SSU and EF1A. The latter gene includes an extremely variable spliceosomal intron. Three clades, the two morphologically recognizable taxa *M. fuscatum*, *M. aggregatum*, and the morphologically complicated complex species *M. atrosporium* agg., were recovered. The EF1A-based phylogeny of the 81 specimens of *M. atrosporium* agg. resulted in seven subclades, with the two EF1A-haplotypes of a sequence sharing always one subclade for each of the 50 heterozygous specimens, a pattern consistent with the existence of several independent but sexually reproducing biospecies. Identical EF1A genotypes occurred more often within a regional population than in between. A simulation assuming panmixis within a biospecies but not in between, and isolation between mountain ranges suggested that similar numbers of shared genotypes can be created by chance through sexual reproduction alone. Numbers of haplotypes shared between mountain ranges correlate with geographical distance, suggesting occasional long-distance dispersal by spores.

An enlarged data set containing 227 partial SSU sequences of *Meriderma* spp. identified 53 ribotypes, with a ribotype accumulation curve indicating  $68.4 \pm 14.5$  ribotypes to expect according to the Chao2 estimator. The topology of the SSU phylogeny generally confirms results from the partial SSU and EF1A data set of 89 specimens, where several putative biospecies could be recognized. A novel method for automated analyses of SEM images allows to derive quantitative descriptors for spore ornamentation, which were subjected to multivariate analyses. Spore ornamentation provided traits with the highest explanatory power in a multivariate statistics, whereas spore size and stalk length were much less significant. For some but not all putative biospecies a unique combination of morphological characters was found, which is in accordance with the hypothesis of instant sympatric

speciation via mutations creating incompatible strains splitting from existing biospecies. The morphologically recognizable taxa of the genus are described and a key for the genus *Meriderma* is given.

To compare morphological and molecular diversity in lignicolous myxomycetes, all specimens found in a study covering the late-autumn aspect were sequenced, using partial SSU gene as a barcode marker. A total of 161 logs in the old-growth forest Eldena, northeastern Germany, was surveyed, resulting in 530 collections representing 27 taxa from 14 genera. Bright-spores species were far more abundant than dark-spored taxa. A phylogeny based on partial SSU sequences for bright-spored myxomycetes revealed morphospecies to be largely consistent with phylogenetic groups. Most but not all morphospecies may contain multiple ribotypes that cannot be differentiated by light microscopy. This first study backing up a traditional morphology-based survey by a full molecular component demonstrates that partial SSU sequences can function as reliable barcode markers for myxomycetes, but reveals as well a significant, yet not infinite, amount of hidden diversity.

The main conclusions of this work, set up in the frame of a project funded by the German Research Council (DFG), are the following:

1. Sexual reproduction seems to be an important, if not the dominating mode (apart from clonal myxamoebal populations built up by binary fission) of reproduction in naturally occurring populations of myxomycetes.
2. From the two investigated species complexes we can expect many, if not most, morphospecies to be composed of reproductively isolated, sexually reproducing, biospecies.
3. Partial SSU sequences, as most widely used in this study, seem to represent suitable barcode markers for the group and can be used to distinguish the (usually cryptic) biospecies, although they alone do not allow any conclusions about reproductive isolation and speciation processes.
4. We have to expect a significant amount of hidden diversity in myxomycetes, which will increase the number of taxa from ca. 1000 recognized morphologically by a factor between two and ten.



Myxomyceten (Amoebozoa, plasmodiale Schleimpilze) sind eine der letzten größeren Organismengruppen, deren Diversität noch nicht mit molekularen Methoden untersucht wurde; lediglich einige kultivierbare Modellarten bilden eine Ausnahme. Basierend auf den Ergebnissen erster molekularer Phylogenien der Gruppe, die 2012 und 2013 publiziert wurden, steht die genetische Diversität wildlebender Populationen im Fokus dieser Arbeit, die vorrangig zwei Fragen bearbeitet: 1. *Korrelieren die mit barcoding-Markern gefundene Diversität und deren Phylogenien mit dem gegenwärtig verwendeten morphologischen Artkonzept, und zeigen diese Marker eine geringere oder höhere Diversität als die mit morphologischen Merkmalen ermittelte?* Im ersten Fall ist anzunehmen, dass sich für die Art differenzierung verwendete morphologische Merkmale als plastisch erweisen (also durch die Umweltbedingungen während der Bildung der Fruktifikationen beeinflusst werden); im zweiten Fall ist die Existenz kryptischer Arten anzunehmen. 2. *Können genetische Marker Aufschluss über die Vermehrungssysteme bei wildlebenden Myxomyceten geben, insbesondere ob sexuelle oder asexuelle Vermehrung vorherrscht?* Sexuelle Vermehrung wurde vielfach bei Vertretern der Amoebozoa nachgewiesen, aber asexuelle Vermehrung sollte Vorteile bei der Kolonisierung neuer Habitate bringen. Experimente mit kultivierbaren Arten zeigten, dass beide Reproduktionssysteme bei Myxomyceten vorkommen können.

Zwei Arten wurden für eine tiefergehende Analyse ausgewählt. Die erste ist die häufige, Totholz bewohnende *Trichia varia* (Pers. ex J.F. Gmel.) Pers., einer der ersten beschriebenen Myxomyceten. Dieses Taxon wurde bisher stets als eine, jedoch variable, Art angesehen. Das zweite Beispiel bildet eine nivicole Art, die bisher als *Lamproderma atrosporum* Meyl. bekannt ist, aber unter dem Namen *Meriderma* Mar. Mey. & Poulain als eigene Gattung aufgefasst wird. Für diese Gattung wurde ein morphologisches Konzept mit mehreren Taxa vorgeschlagen.

*Trichia varia* gehört zu den hellsporigen Myxomyceten. Partialsequenzen dreier, voneinander unabhängig vererbter Marker (kleine Untereinheit der nuklearen ribosomalen DNA, SSU, Vererbung extrachromosomal; Protein-Elongationsfaktor 1 alpha, EF1A, chromosomal; Cytochrom-Oxydase Untereinheit 1, COI; mitochondrial) wurden für 198 Aufsammlungen erstellt. Eine aus diesen drei Genen erstellte Phylogenie zeigte drei Gruppen, die jeweils durch mehrere, nur in der entsprechenden Gruppe vorkommende Kombinationen dieser Marker charakterisiert sind. Komplette SSU Sequenzen wurden für 66 Aufsammlungen generiert; dabei wurden sechs Positionen gefunden, in denen group I introns und vermutlich funktionale bzw. degenerierte Gene von Homing-Endonukleasen vorkommen können. Alle Befunde (Kombinationen der drei Markergene, Rekombinationssignale, Vorkommen der Introns) passen gut zur Annahme dreier kryptischer Arten, die sich vorwiegend sexuell vermehren, aber voneinander reproduktiv isoliert sind. Die gefundenen Muster der group I introns und der in ihnen inserierten Gene von Homing-Endonukleasen lassen vermuten, dass das von Goddard & Burt postulierte Modell evolutionärer Lebenszyklen bei Introns auf natürlich vorkommende Populationen von Myxomyceten zutrifft.

Für 89 Aufsammlungen aus fünf europäischen Gebirgen der Gattung *Meriderma* (dunkelsporige Myxomyceten) wurden partielle Sequenzen zweier Marker, SSU und EF1A, generiert. Das letztere Gen enthält ein extrem variables spliceosomales Intron. Die damit erstellten Phylogenien zeigten übereinstimmend drei Hauptgruppen, die den morphologisch erkennbaren Taxa *M. fuscatum*, *M. aggregatum*, und einem Artkomplex, hier *M. atrosporum* agg. genannt, entsprechen. Eine EF1A-basierte Phylogenie für 81 Aufsammlungen von *M. atrosporum* agg. ergab sieben Untergruppen, und die beiden EF1A-Hyplotypen einer Sequenz wurden stets in der gleichen Untergruppe für jede der 50 heterozygoten Sequenzen positioniert. Diese Muster ist konsistent mit der Annahme von sieben, voneinander reproduktiv isolierten Biospecies. Identische EF1A-Genotypen sind häufiger innerhalb einer Regionalpopulation als verteilt über mehrere zu finden. Eine Simulationsrechnung, die ausschliesslich sexuelle Vermehrung (Panmixis) innerhalb, aber nicht zwischen, den hypothetischen Biospecies annimmt, und die Gebirgszüge als voneinander isoliert betrachtet, ergab, dass ein ähnliches Muster von Genotypen unter diesen Annahmen rein zufällig entstehen kann. Die Zahl der EF1A-Haplotypen, die mehreren Gebirgszügen gemeinsam ist, korreliert mit deren geographischer Entfernung, welches auf gelegentliche Fernverbreitung von Sporen hinweist.

Ein erweiterter Datensatz mit 227 SSU-Partialsequenzen von *Meriderma* spp. ergab 53 Ribotypen. Eine Akkumulationskurve dieser Ribotypen zeigte, dass  $68.4 \pm 14.5$  Ribotypen bei unbegrenzter Zahl untersuchter Aufsammlungen nach dem Chao2 Estimator zu erwarten wären. Die mit diesem Datensatz erstellte SSU-Phylogenie stimmt in ihrer Topologie mit der aus kombinierten SSU- und EF1A-Sequenzen für 89 Aufsammlungen erstellten Phylogenie überein und zeigt ebenfalls eine Aufspaltung in mehrere hypothetische Biospecies. Eine neu entwickelte Methode für die automatisierte Auswertung von rasterelektronenmikroskopischen Aufnahmen der Sporen ermöglichte es, quantitative Deskriptoren für deren Ornamente abzuleiten. Diese Merkmale erklärten am besten die in multivariaten statistischen Analysen gefundene Varianz, während Sporengröße und Länge des Stieles der Sporokarprien weniger beitrugen. Für einige, aber nicht alle der hypothetischen Biospecies wurde eine einzigartige Kombination morphologischer Merkmale gefunden; dies passt zu der Annahme einer plötzlichen Artbildung durch Mutationen, die inkompatible Linien aus existierenden Biospecies abspaltet. Die morphologisch erkennbaren Taxa innerhalb der Gattung werden beschrieben und ein Schlüssel zur Identifikation vorgestellt.

Um morphologische und molekulare Diversität in totholzbewohnenden Myxomyceten zu vergleichen, wurden für alle Aufsammlungen aus Untersuchung des Spätherbstaspektes partielle SSU-Sequenzen erstellt. Dazu wurden 161 tote Stämme aus dem Waldgebiet Eldena (Nordostdeutschland) systematisch abgesucht, welches 530 Aufsammlungen ergab, die zu 27 Arten aus 14 Gattungen gehörten. Hellsporige Myxomyceten waren in dieser Untersuchung wesentlich häufiger als dunkelsporige Arten. Eine Phylogenie der SSU-Sequenzen zeigte, dass die morphologisch bestimmten Arten weitgehend mit phylogenetischen Gruppen übereinstimmten. Viele, jedoch nicht alle morphologischen Arten enthalten mehrere Ribotypen, welche durch traditionelle Artbestimmung (Lichtmikroskopie) nicht zu unterscheiden sind. Diese Untersuchung, die erstmals eine traditionell morphologiebasierte Erhebung durch eine durchgängige molekulare Komponente ergänzt, zeigt, dass partielle SSU-Sequenzen als verlässliche barcodes für Myxomyceten dienen können und einen beachtlichen, aber begrenzten Anteil kryptischer Diversität offenbaren.

Die wichtigsten Schlussfolgerungen dieser Arbeit, die im Zuge eines DFG-geförderten Projektes entstand, sind die folgenden:

1. Sexuelle Vermehrung scheint eine wichtige, vielleicht sogar die dominierende Vermehrungsart bei natürlich vorkommenden Myxomyceten zu sein (neben durch Zellteilung entstehenden klonalen Populationen von Myxamöben).
2. Die zwei untersuchten Artenkomplexe lassen erwarten, dass viele, eventuell die Mehrzahl der morphologisch erkennbaren Arten aus mehreren reproduktiv isolierten, sexuellen Biospecies besteht.
3. Partielle SSU-Sequenzen, die in dieser Arbeit am meisten verwendet wurden, scheinen verlässliche Barcodes für Myxomyceten darzustellen und können auch die (gewöhnlich kryptischen) Biospecies unterscheiden. Sie allein erlauben aber nicht, reproduktive Isolation festzustellen oder Artbildungsprozesse zu verfolgen.
4. Bei Myxomyceten ist ein beträchtlicher Anteil kryptischer Diversität zu erwarten, dies sollte die Zahl der bisher ca. 1000 morphologisch unterscheidbarer Arten um einen Faktor zwischen 2 und 10 erhöhen.

## 2. Introduction



## Species diversity in different forms of life

Macroscopically visible forms of life, as we know them, belong mostly to three major taxonomic groups (Adl et al. 2012): Metazoa (animals), Chloroplastida (vascular plants and mosses), and Dikarya (higher fungi). In addition, a part of green, red, and brown algae displays a macroscopic appearance. However, deep phylogenies of Eukaryotes (Baldauf et al. 2000, 2003) brought the insight that only a minor fraction of the genetic diversity of Eukaryotes is included in the three abovementioned groups, even if they account for about three quarters of all hitherto described species. This contradiction between taxonomic and genetic diversity is caused mainly by the various groups of unicellular eukaryotic life summarized as Protista (Adl et al. 2012). Most of these groups are poor in species, which is in part due to the paucity of morphological characters (Fig. 1).

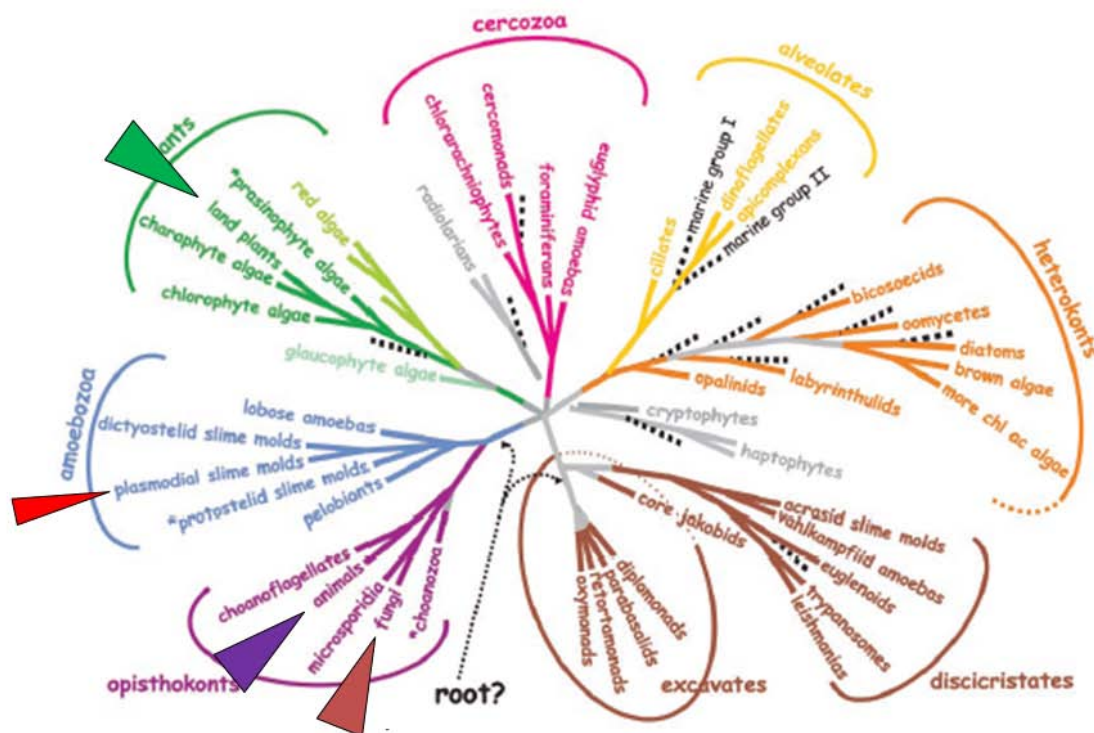


Fig. 1. A simplified phylogeny of Eukaryotes constructed from sequences of four major genes ( $\alpha$ -tubulin,  $\beta$ -tubulin, actin, and protein elongation factor 1 $\alpha$ ; figure from Baldauf et al. 2003) showing the position of the three groups constituting most of the macroscopically visible life forms (broad triangles), and the position of myxomycetes (narrow red triangle).

However, with the growing availability of molecular data on various life forms, which stems to an increasing part from metabarcoding and next-generation sequencing (NGS), the perception of the “species-poor” unicellular groups of organisms has been questioned. Although recent refinements of NGS methods have casted doubts if all of the “hidden diversity” discovered from environmental PCR and subjected to NGS is true sequence diversity and not artifacts of the method (Medinger et al. 2010), it now became clear that many protistean groups do not only represent unique genes not found in other life forms, but display as well an astounding within-group genetic diversity.

For many, especially non-pathogenic, groups of Protista the molecular age dawned comparatively late. This is in part due to the hidden life styles and lacking economic importance of many forms, but as well due to the different level of genetic diversity. For instance, barcoding markers like the internal transcribed spacer (ITS) successfully used for barcoding especially in fungi (Schoch et al. 2012), sometimes as well in plants (Peterson et al. 2011), do not work with most protistean groups. The level of diversity in these genes is simply too high to allow meaningful alignments and thus differentiation of taxa (see Fiore-Donno et al. 2011 for an example in myxomycetes). Therefore, other genes, like the nuclear small-subunit of the ribosomal RNA gene (SSU) have to be found and tested for their suitability as barcoding markers (Pawlowski et al. 2012).

This was the first question of this dissertation, to be investigated on one of the protistean groups, the plasmodial slime molds (Myxomycetes): **Is the relative poverty in species diversity only due to a lack of accessible morphological characters which do not allow a description of taxa according to a morphological species concept?** Or, this would be the alternative hypothesis: Do we have, in spite of the often unique genetic structures found in protists, only a few, genetically uniform and ubiquitous forms in these groups, which would be in sharp contrast to the species diversity in plants or animals, which is often the product of a co-evolution with symbionts, parasites, or hosts lasting for millions of years?

### *Sexual or asexual – the paradox of maintenance of sex*

This question is closely related to the mechanisms creating genetic diversity. Beside mutations as the primary source for genetic diversity, which is an inherent feature of all life forms, in eukaryotes this concerns sexual reproduction, which is a major hallmark of the eukaryotic cell. By creating genetic diversity through recombination in a complicated process of cellular fission called meiosis, sexual reproduction ensures genetic diversity of the upcoming generation. However, sexual reproduction invokes one of the fundamental questions to biology, the paradox of maintenance of sex, arising from the fact that it has many immediate costs, compared to the advantages given by asexual reproduction (Otto et al. 2006).

This paradox of maintenance of sex does especially apply for protists, which are by nature r-strategists: fast reproduction matters more than in long-lived, macroscopic forms of life. From this reason, it is a common perception that protists spend most of their life with asexual reproduction and switch only rarely or occasionally to sexual reproduction. This constitutes the second major question of this dissertation, which was investigated in the frame of research project funded by the Deutsche Forschungsgemeinschaft (DFG): **Do natural populations of myxomycetes reproduce mainly sexual or asexual?** This involves several, more detailed questions, and the following list is in no ways complete:

Are morphospecies composed of a mixture of asexual and sexual reproducing lineages? – This would be a ready solution for the paradox of maintenance of sex: already occasional rounds of sex should ensure genetic diversity, but fast asexual reproduction will maintain a fast, cost-effective multiplication of cells.

Do asexual strains repeatedly arise from sexual ones? – As shown by Schnittler and Tesmer (2008), asexual strains of spore-dispersed organisms should have an advantage over sexual strains, regarding the colonization of terrestrial habitat islands. The typical habitats of myxomycetes (accumulations of decaying plant matter, like coarse woody debris) can be seen as such habitat islands.

Can we find evidence for cryptic allopatric speciation in species widely distributed in a continuous environment along a climatic gradient, or evidence for sympatric speciation in species growing in well-defined niches? – Such speciation processes should be closely related with sexual reproduction, since for organisms like myxomycetes, possessing an high potential for long-distance dispersal via spores (Kamono et al. 2009) geographic isolation over longer (evolutionary significant) periods of time is hard to imagine. If we have indeed a high proportion of cryptic species, sympatric speciation should be the major mechanism creating diversity.

Myxomycetes, belonging to the protistean supergroup Amoebozoa, should be, like all eukaryotes, capable of sexual reproduction. The significance of sexual reproduction of Amoebozoa was underlined by Lahr et al. (2011). However, this was questioned by a series of experiments conducted with a few cultivable species of myxomycetes (mostly belonging to the order Physarales) in the Seventies (see Collins 1979, Clark & Haskins 2013 for reviews; Fig. 2): strains raised from a single spore did either complete its life cycle in such monosporic cultures (forming fructifications releasing spores, non-heterothallic behavior) or requiring the descendants of a second spore to complete the life cycle (involving sex by amoebal syngamy, heterothallic behavior).

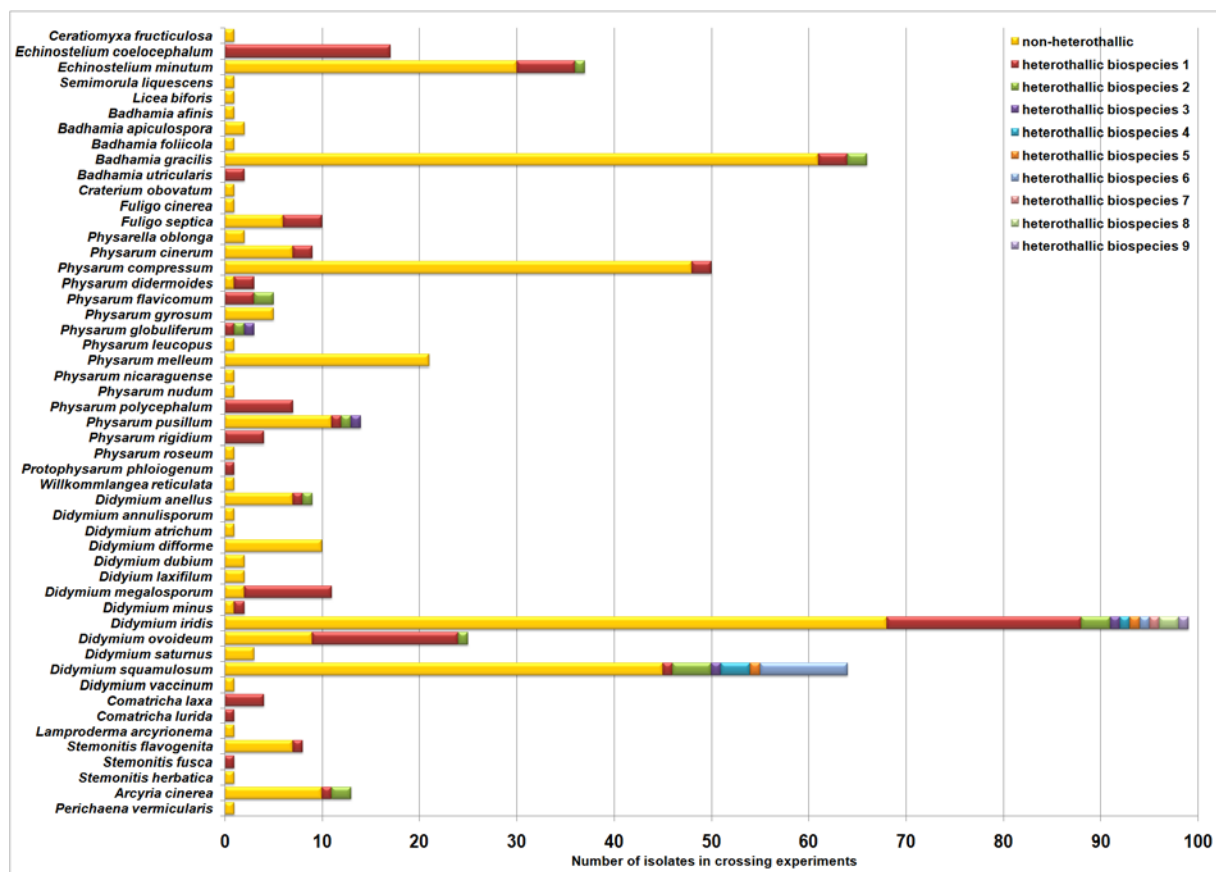


Fig. 2. Reproductive systems of myxomycetes published by various authors (compilation based on Clark & Haskins 2013). Yellow sections of the bars indicate the number of non-heterothallic (presumably asexual), sections of other colors the number of heterothallic (sexual) isolates which were investigated. The dominance of Physarales is artificial since members of this order are much easier to cultivate than all other myxomycetes. In many morphospecies sexual and asexual strains coexist; and the latter seem to be more commonly isolated from nature.

In these culture experiments, compatibility between strains was investigated as well. On one hand, this led to the discovery of mating-type genes (see below) that determine if amoebae of two strains can mate. This provides clear evidence for sexual reproduction. On the other hand, many, in most species even more, strains behaved non-heterothallic. As explained below, this lends rather evidence for asexual reproduction. However, this kind of research, being extremely laborious, ceased largely in the Nineties and afterwards, since the respective cultures are very laborious, and the majority of myxomycete species are hard to cultivate.

However, with the cheaper availability of molecular techniques, but especially with the establishment of partial sequences of the small-subunit of the ribosomal RNA gene as a barcoding marker (Fiore-Donno et al. 2008, 2011, 2012, 2013, Novozhilov et al. 2013b), natural populations of myxomycetes can be investigated for molecular markers to assess the underlying reproductive system. This is the main approach taken in this dissertation work. In contrast to all prior studies focusing on isolates from nature which were kept for several to many generations in the lab (with manifold degeneration processes reported, Mohberg 1977), this dissertation studies fruit bodies collected from natural populations with several molecular markers of different degree of variation.

Asexual reproduction in a strict sense occurs always by binary fission of amoebae, which can build huge clonal populations, furthermore called “vegetative reproduction”. Asexual reproduction as used in this dissertation refers to strains capable to complete their entire life cycle, i.e. forming as well fruiting bodies, without requiring syngamy of amoebae. Therefore, three reproductive options exist in theory. First, the non-heterothallic strains may be truly homothallic (sexuality without mating types, allowing syngamy between two amoebae originating from the same spore). Second, the non-heterothallic strains may indeed be asexual, not changing its ploidy stage throughout the life cycle (automixis by incomplete meiosis leads to diplospores releasing diploid amoebae). Third, this is the life cycle pictured in virtually all textbooks; heterothallic strains possess a mating type system, thus requiring syngamy between two non-related amoebae (Clark and Haskins 2010).

### ***Biology of the myxomycetes***

The model group chosen for this study are the plasmodial slime molds. This group of protists produces small fructifications (usually 5-10 mm in size); these sporocarps release airborne spores. This makes myxomycetes a kind of missing-link between the micro- and the macro-world. The first species have been described already by Linné (1753) in his “species Plantarum”, perceiving them as little puffballs. From this reason, the formal nomenclature of the group goes back to this date. Ecologically, Linné was right, since the spores of myxomycetes are sometimes dispersed as in puffballs (gasteromycetes) and show the same hydrophobic ornamentation, are similar in size and dispersal behavior (Tesmer & Schnittler 2007). Phylogenetically, Linné was terribly wrong, but only a century later de Bary (1861) discovered the protistean nature of these organisms: the spores that can be strikingly similar to those in puffballs (Estrado-Torres et al. 2005) germinate with amoebae or amoeboflagellates, not hyphae. In addition to the “botanical” name *Myxomycetes*, this earned the slime molds a second name, *Myxogastria*, to indicate their assignment to the realms of zoology. However, since the fructifications can be collected and stored in herbaria like fungal specimens, they are traditionally treated by mycologists. From this reason, we have a solid body of data on world-wide occurrence and distribution of the fructifications (see Stephenson et al. 2008 for review). These fructifications provide as well the starting point of this dissertation, which focuses on myxomycetes from two ecological groups: species inhabiting coarse woody debris (papers 1 and 4) and species inhabiting decaying plant matter and soil in mountains, fruiting near the edge of melting snow banks (Schnittler et al. 2015).

However, in their vegetative stages myxomycetes are part of the micro world, forming large populations of amoebae (and/or myxoflagellates) in wood and soil, especially if enriched with decaying plant matter. These amoebae reproduce asexually by fission and from therefore most likely clonal populations. Using environmental PCR, amoebae can be detected in the appropriate substrates, using barcoding markers (Kamono et al. 2013; Clissmann et al. 2015).

The myxomycete life cycle involves three dormant stages (spores can survive for decades, microcysts and sclerotia for months to years) and enables these organisms to inhabit all terrestrial ecosystems, even arid zones (Stephenson et al. 2008). Cultivation studies (Madelin 1984) revealed myxamoebae as highly abundant in most arable soils. Fructifications can be found in the field (about 60% of known species) or detected with substrate (38%) or agar cultures (2%, species with microscopic fructifications, Schnittler et al. 2012). Substrate cultures, called moist chambers, work especially well in arid zones (Schnittler et al. 2015). All kind of decaying plant matter constitutes the primary habitat



of myxamoebae. In contrast to true fungi myxamoebae are predators of other micro-organisms, including bacteria, yeasts and algae. Introductions into the natural history of myxomycetes are given in Schnittler et al. (2011, 2012), and in Stephenson and Stempen (1994). Fig. 3 pictures the life cycle of myxomycetes.

The textbook life cycle of myxomycetes involves haploid amoebae that hatch from spores and divide by binary fission. Syngamy of two haploid amoebae results in the formation of diploid plasmodium. Through subsequent mitoses not accompanied by cellular fission the multinucleate plasmodium can reach several centimeters in size. Most of the plasmodial biomass converts into sporocarpic fruiting bodies which release air-borne meiospores. Triggered by certain environmental conditions, the plasmodia start the transformation to form sporocarpic fruit bodies from which haploid meiospores are released (Clark and Haskins 2010). In contrast to this sexual pictures in most textbooks, where the syngamy of two (haploid) amoebae or amoeboflagellates is the precondition for the formation of the (diploid) plasmodium and finally the fructifications forming meiospores (solid black lines in Fig. 3); the culture experiments mentioned above suggest the existence of a second, asexual life cycle (dotted red lines). Here, all life stages are thought to be diploid. In addition, all species can form populations of unicellular amoebae and/or myxoflagellates by binary fission (solid blue lines). These two vegetative stages may convert into each other, and eventually develop unicellular but multinucleate plasmodia. Three dormant stages (microcysts, sclerotia, see thin solid lines and spores formed in fruit bodies called sporocarps) can interrupt the life cycle for unsuitable periods of time. The current knowledge about myxomycete ecology stems virtually completely from records of these fructifications, therefore data about habitat preferences must be viewed with care. First studies employing ePCR hint towards a significant proportion of “hidden diversity”: many habitats seem to be populated by amoebal populations which do not fruit. In a given region, most species are apparently rare (Schnittler et al. 2011).

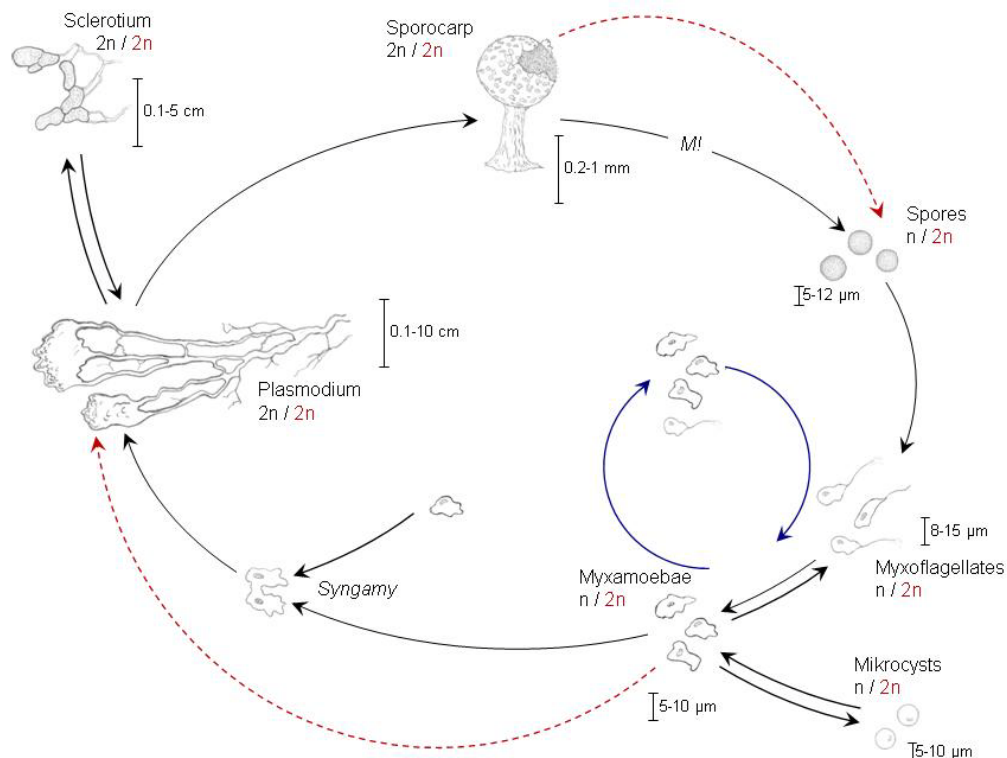


Fig. 3. Life cycle of myxomycetes. Sexual life cycle (solid black lines) including meiosis (M!) and syngamy of amoebae; vegetative multiplication of amoebae (solid blue lines) and a hypothetical asexual life cycle (dotted red lines) leave manifold options for natural occurring populations of these organisms. Scale bars show the approximate size of the life stages. Drawing adopted from Schnittler et al. (2012).

This life style, combining “zoological”, predatory behavior with “botanical” fructifications releasing airborne spores seems to be a successful innovation, since several, often non-related groups of eukaryotes developed it, which can be combined to an ecological guild of “myxomycetes and myxomycete-like organisms” (Schnittler et al. 2006). This guild comprises at least six groups of organisms. First, are the “fruiting, gliding bacteria”: the prokaryotic myxobacteria (Reichenbach 1993) include 40–60 taxa. Olive (1975) defined an eukaryotic group called Eumycetozoa, circumscribing myxomycetes (plasmodial slime molds), protostelids and dictyostelids (acellular slime molds) thought to be monophyletic (Swanson et al 2002, Fiore-Donno et al 2005). The protostelids, long seen as ancestral to myxomycetes, form minute single- to few-spored fructifications, 37 taxa are described (Spiegel et al 2004). Similar species-poor, comprising ca. 120 taxa, are the dictyostelids (Cavender 1990, Swanson et al 1999, Romeralo et al. 2010, 2011). The few species of acrasids are members of the Heterolobosa (Adl et al. 2012), a group phylogenetically distant to the eumycetozoans (Roger et al 1996, Baldauf 2003, Brown et al. 2009). Finally, the ciliate genus *Sorogena* develops fruiting bodies strikingly similar to those found in myxomycetes (Bardele et al 1991). All six groups share a number of ecological traits like (i) living as predators of other microorganisms, (ii) starting their life cycle as unicellular microorganisms forming spore-like propagules, (iii) later combining their biomass by aggregation of cells or exclusively nuclear divisions (plasmodia of most Eumycetozoans) to finally (iv) convert it to typically stalked fruit bodies which (v) develop within hours not out of a true growth process but by rearrangement of the available biomass to (vi) release air-borne propagules for long-distance dispersal (Schnittler et al. 2006).

Plasmodial slime molds (Myxomycetes, Myxogastria) are the most species-rich group in Amoebozoa (Adl et al. 2012). Primarily stalked fructifications with a complicated structure (see Fig. 4) ensure that spores are elevated above the substratum surface, which is often covered by a water film, and released one by one or at least in small portions, kept atop of the stalk by additional internal structures like the capillitium, consisting of solitary or branched threads developed out of anastomosing vacuoles (Kalyanasundaram 1973) or peridia, covering the maturing spore mass to prevent early desiccation. The key innovation of myxomycetes seems to be the long-distance dispersal (Kamono et al. 2009). Together with the often highly hydrophobic spore ornaments (Hoppe et al. 2014) this enables most species to inhabit large ranges usually determined by habitat availability (Schnittler et al. 2000), but zonal distribution patterns occur as well (Stephenson et al. 2008). The hallmark of myxomycetes is the life cycle with alternating vegetative, microscopic and motile amoebae and plasmodia but immobile macroscopical sporocarps. These free-living amoebae are abundant in soil and can live in diverse habitats (Stephenson et al. 2008, 2011; Urich et al. 2008).

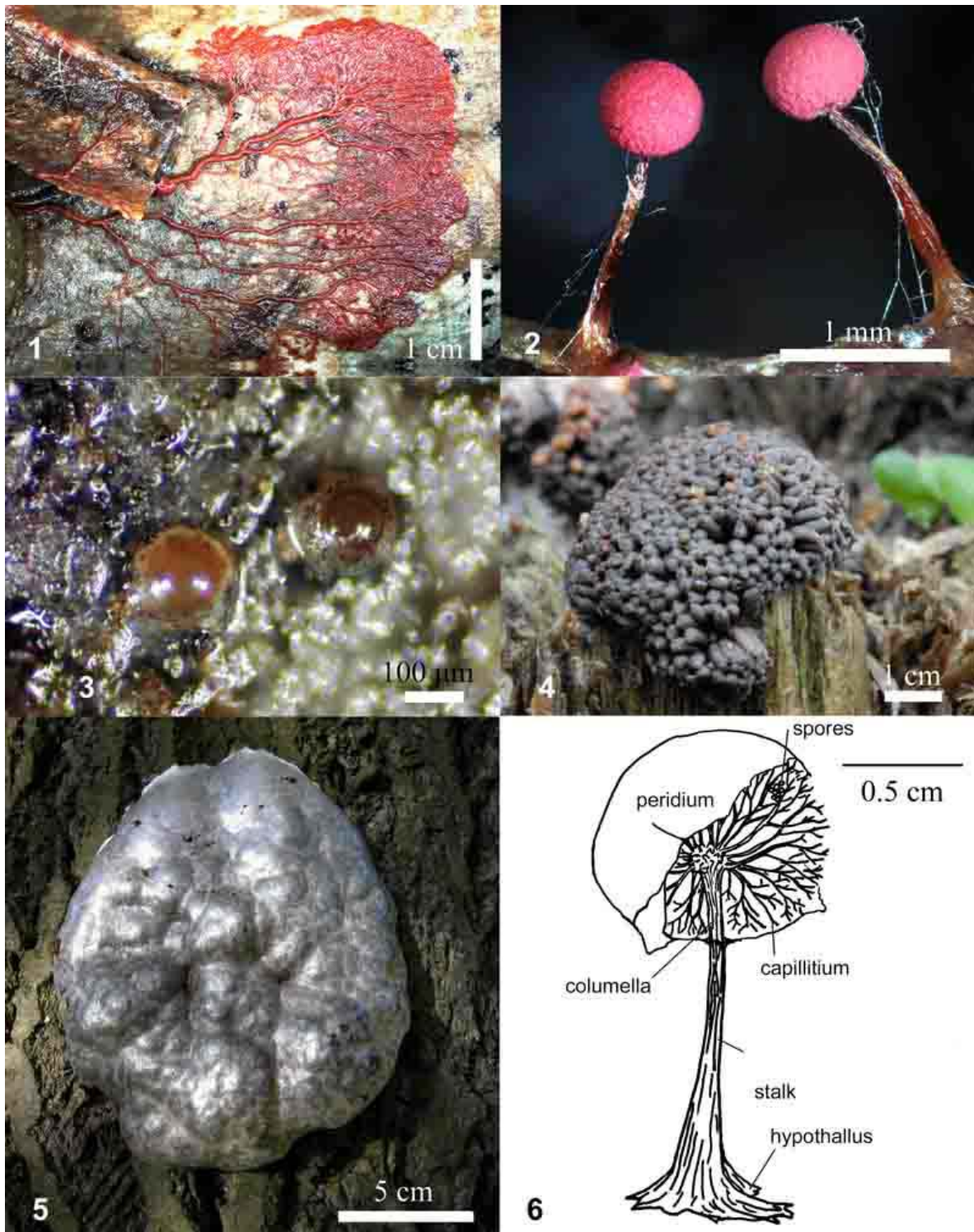


Fig. 4. Myxomycete fructifications. 1–2. Plasmodium and stalked sporocarps of *Physarum roseum*. 3. Two sessile sporangia of *Licea kleistobolus*. 4. Pseudoaethalium of *Tubifera ferruginosa*; single sporocarps can still be distinguished. 5. Aethalium of *Reticularia lycoperdon* covered by a silvery cortex; individual sporocarps cannot be distinguished. 6. Schematic drawing of *Lamproderma* spp., a typical member of the order Stemonitales, showing sporocarp morphology of. Stalk, columella and capillitium are internally secreted into anastomosing vacuoles; the hypothallus is the leftover of the plasmodium segregating into single sporocarps. In the Physarales, Trichales and Liceales, the internally secreted stalk is replaced by a secondary stalk formed by a restriction of the hypothallus. The peridium varies, according to environmental conditions and species, from completely evanescent to rather durable. Figure adopted from Schnittler et al. (2012).

## ***Myxomycete phylogeny and diversity***

Based on the morphology of the sporocarp, with morphospecies as the prevailing species concept, the number of described myxomycete species reaches about 950 (Lado 2005-2015), with numbers of described species steadily increasing (Schnittler et al. 2000). Together with the Arcellinida, myxomycetes constitute the most species-rich group of Amoebozoa (Fiore-Donno et al. 2012). Coincidentally, both groups possess structures rich in morphological characters in comparison to other Amoebozoa (thecae and sporocarps, respectively). Not surprisingly, the current myxomycete taxonomy is still entirely based on the *morphospecies concept*, even in the most recent monographs (Neubert et al. 1993, 1995, 2000; Poulain et al. 2011). However, even the traditional classification into five orders (the genus *Ceratiomyxa* plus the orders Echinosteliales, Liceales, Trichales, Physarales and Stemonitales) is in conflict with current phylogenies (Fiore-Donno et al. 2013), and the future will bring numerous amendments of this traditional classification (Schnittler et al. 2012, Eliasson 2015). This morphospecies concept has been applied as well for the recently constructed molecular phylogenies (Fiore-Donno et al. 2010, 2012, 2013), which recovered two main clades: the bright-spored clade (spores lightly colored by various pigments, orders Liceales and Trichales), and the dark-spored clade (spores dark colored by melanin, orders Stemonitales and Physarales). Still the systematic position of some genera and species remains unclear and can perhaps only be determined by molecular analyses (for instance *Kelleromyxa*, Erastova et al. 2013); and most genera are in critical need of a revision combining traditional morphology and molecular markers (see Leontyev et al. 2015 as an example).

The traditional taxonomy based on morphological characters should not necessarily coincide with a second species concept, which so far remained a largely theoretical one, since it is derived from the comparatively few species that can be cultured: the *biospecies concept*. According to this concept, groups of compatible strains (amoebae can pair with each other) form a so-called biospecies which cannot interbreed with a second biospecies due to compatibility barriers (Clark & Haskins 2013). To which extent these two species concepts coincide with each other (or can be reconciled in case of contradiction) is another problem to which this dissertation may hopefully contribute first results.

## ***Myxomycete reproductive systems***

Myxomycetes were successfully used as a model group to study the basics of nuclear division (due to the synchronic division of nuclei in plasmodia; Howard 1932) and in developmental biology (employing fructifications of the cellular slime molds, Dictyostelida, as models for cell-cell interactions, Strassman et al. 2000). Sexuality, as a hallmark of Amoebozoa (Lahr et al. 2011) was confirmed by crossing experiments on morphospecies of myxomycetes. The early experiments with cultivable model species of the genus *Physarum* and *Didymium* reveal that most isolates of a morphospecies undergo the sexual life cycle pictured in Fig. 3 with outcrossing ensured by mating types arranged in a single-locus multiallelic system (*Didymium iridis*; Betterley and Collins 1983; Clark 1993), or in three loci with multiple alleles (*Physarum polycephalum*; Clark and Haskins 2010; Collins 1975). For some cultivable species (examples) groups of isolates are compatible with each other (amoebae pair and finally sporulate) but will not pair with others in crossing experiments (Clark and Haskins 2011). Groups of compatible amoebal strains comply with a biological species concept and can be seen as biospecies (Collins 1979, 1981), providing the alternative species concept mentioned above.

As stated above, sexual myxomycete species strains from single-spore cultures should behave heterothallic: amoebal populations derived from a single spore will not sporulate if they do not come in contact with amoebae from a different and compatible clone (of the same biospecies, Collins 1981). However, crossing studies from cultivable myxomycetes revealed some morphospecies to be composed of both hetero- and non-heterothallic strains (Clark and Haskins 2010); and this does not comply with the classical life cycle. Three reproductive options may equally result in non-heterothallic behavior and cannot be distinguished in culture experiments. First, the mating system remains intact,

but multinucleate spores transport two nuclei which may show opposite mating types. Such spores were recently found in the species *Physarum pseudonotabile* (Novozhilov et al. 2013a). This should give a colonisation advantage in the sense of Schnittler & Tesmer (2008), since a multinucleate spore may include both of the original mating types segregated again during the meiosis in sporogenesis. On the other side, this option involves inbreeding (to a comparable degree as inbreeding in flowering plants).

Second, intranuclear selfing may occur due to a breakdown of the mating system, causing the mating between identical amoebae descending from the same uninucleate spore. This would mean that the descendants of one spore could mate (and would most often do so, since they are much more likely to come in closer contact with each other than descendants of two different clones). Although the colonisation advantage mentioned above applies as well, this reproductive mode would result in instant homozygosity in all loci. As such, this option which is equal to true homothally is unlikely to occur.

Third, non-heterothallic strains may be truly asexual (apomictic) and form plasmodia without mating. This option, carrying as well the colonization advantage, may be realized via automixis, which derives from an incomplete meiosis (Clark & Haskins 2013). Automixis still includes the option of recombination in meiosis I. If only meiosis II is skipped, the resulting spores will be functionally diploid. Amoebae hatching from these spores may skip syngamy and immediately form plasmodia. In this case, ancient heterozygosity is conserved. This hypothetical life cycle is pictured in Fig. 3.

### ***The approach of this dissertation***

In the first two papers of this dissertation a bright-spored myxomycete morphospecies, *Trichia varia*, and a dark-spored myxomycete genus, *Meriderma*, are used to answer three questions concerning the reproductive systems of myxomycetes. The first question is: can we detect evidence for coexisting biospecies within an accepted morphospecies with molecular markers from specimens growing in natural conditions? With the data gathered to answer the first question, a second question may be asked and answered: can we find evidence for asexual (automictic) strains in a natural population? And finally, can we make an estimate on the relative contributions of the three reproductive options to non-heterothallic behaviour in myxomycetes?

*Trichia varia* (Pers. ex J.F. Gmel.) Pers. is a common bright-spored myxomycete (Fiore-Donno et al. 2013) described by Persoon (1794). All recent monographs (Martin and Alexopoulos 1969; Nannenga-Bremekamp 1991; Neubert et al. 1993; Poulain et al. 2011) treat *T. varia* as a single, yet variable species. Based on its unique capillitium morphology (elaters with only two, not several spiral bands) *Trichia varia* was always seen as a well-defined taxon; no intraspecific taxa are currently accepted, although the taxonomic database Nomenmyx (Lado 2005–2015) lists not less than 13 heterotypic synonyms.

Using 197 *Trichia varia* specimens collected throughout Eurasia, we obtained a first dataset on three independent marker genes with partial sequences, the extrachromosomal nuclear small-subunit ribosomal RNA gene (SSU), the nuclear elongation factor 1 alpha gene (EF1A), and the mitochondrial cytochrome oxidase subunit 1 gene (COI). A second dataset containing complete SSU sequences of 66 *Trichia varia* specimens, where group I introns, sometimes with homing endonuclease genes (HEGs) inserted, could be identified. We tried to use these datasets to infer the reproductive modes and the evolutionary scenarios of group I introns and HEGs, and to identify possible biospecies or asexual strains in natural populations of *Trichia varia*. This part of the work is described in the first paper (published in *Organisms Diversity and Evolution*) of this dissertation.

A second paper deals with nivicolous myxomycetes, which are comparatively easy to collect under suitable conditions (during snow melt in mountain ranges). Our model species belongs to the dark-spored myxomycetes (Fiore-Donno et al. 2012). *Meriderma* Mar. Mey. & Poulain is a newly erected

genus proposed by Poulain et al. (2011), including several morphospecies based on morphological differences especially in spore ornamentation. Some of these morphospecies are difficult to separate based on morphological characters, although spore ornamentations vary from verrucae over spines to a more or less complete reticulum. We use an extremely variable intron found in the EF1A gene to detect putative reproductive barriers within specimens of the genus, thus effectively delimiting putative biospecies. The data set contains partial SSU sequences and partial EF1A sequences from 89 specimens. We tried to identify possible biospecies from the EF1A phylogeny, and simulate the outcomes of the shared genotypes between mountain ranges based on the mode of sexual reproduction. Combining the evidences from the marker sequences and from fluorescence labelled spores, the three possible reproductive modes for the occurrence of non-heterothallic strains were evaluated. This part of the work constitutes the second paper (published online first in *Protist*) of this dissertation.

The third paper continues to study the genus *Meriderma* with an extended data set collected mostly from five European mountain ranges. A total of 229 partial SSU sequences were obtained from these specimens. Morphological characters of 162 specimens were recorded and analysed with multivariate statistics. We compare the outcome with major clades identified in the phylogeny built from the 53 genotypes identified in the 229 partial SSU sequences, and with the classical determinations based in morphological characters according to the key of Poulain et al. (2011). These authors proposed a morphospecies concept for the genus. In addition we try to answer the question if the number of putative biospecies is limited or not, constructing a genotype accumulation curve. This part of the work is included in the third paper of this dissertation in manuscript form.

The last part of the dissertation asks the question to which extent the classical morphospecies concept is reflected by partial SSU sequences as the most promising barcode marker in myxomycetes, studying a data set of 530 specimens of mostly bright-spored myxomycetes collected in the forest Eldena located at the east of Greifswald, Germany. Using a novel approach for high throughput PCR from spores, all but 3 specimens included in this study were sequenced. Accumulation curves for morphospecies and ribotypes are constructed and compared with each other. Constructing a phylogeny including the (still very limited) number of comparison sequences in GenBank, we tried to evaluate to which extent the classical morphospecies coincide with clades in the phylogenetic trees. Due to the time chosen for collecting, the morphospecies *T. varia*, being the subject of the first paper, was most common and represented by 292 specimens. Of the remaining collections, most (216) specimens collected during this survey are bright-spored species, only 22 are dark-spored species. We obtained 527 partial SSU sequences and identified a total of 63 genotypes. This part of the work is presented as the fourth paper (published online first in *Nova Hedwigia*) of this dissertation.

## References

- Adl SM, Simpson AG, Lane CE, Lukeš J, Bass D, Bowser SS, et al. 2012. The revised classification of Eukaryotes. *Journal of Eukaryotic Microbiology* 59:429–493.
- Baldauf SL. 2003. The deep roots of eukaryotes. *Science* 300:1703–1706.
- Baldauf SL, Roger AJ, Wenk-Siefert I, Doolittle WF. 2000. A kingdom-level phylogeny of eukaryotes based on combined protein data. *Science* 290:972–977.
- Bardele CF, Foissner W, Blanton RL. 1991. Morphology, morphogenesis and systematic position of the sorocarp forming ciliate *Sorogena stoianovitchae* Bradbury & Olive, 1980. *Journal of Protozoology* 38:7–17.
- Betterley DA, Collins ONR. 1983. Reproductive systems, morphology, and genetic diversity in *Didymium iridis* (Myxomycetes). *Mycologia* 75:1044–1063.
- Brown MW, Spiegel FW, Silberman JD. 2009. Phylogeny of the "forgotten" cellular slime mold, *Fonticula alba*, reveals a key evolutionary branch within Opisthokonta. *Molecular Biology and Evolution* 12:2699–2709.
- Cavender JC. 1990. Phylum Dictyostelida. In: Margulis L, Corliss JO, Melkonian M, Chapman DJ (eds.): *Handbook of Protoctista*. Jones & Bartlett Publ., Boston, pp. 88–101.
- Clark J. 1993. *Didymium iridis* reproductive systems: additions and meiotic drive. *Mycologia* 85:764–768.
- Clark J, Haskins EF. 2010. Reproductive systems in the myxomycetes: a review. *Mycosphere* 1:337–353.
- Clark J, Haskins EF. 2011. Principles and protocols for genetic study of myxomycete reproductive systems and plasmodial coalescence. *Mycosphere* 2:487–496.
- Clark J, Haskins EF. 2013. The nuclear reproductive cycle in the myxomycetes: a review. *Mycosphere* 4:233–248.
- Clissmann F, Fiore-Donno AM, Hoppe B, Krüger D, Kahl T, Unterseher M, Schnittler M. 2013. First insight into dead wood protistan diversity: a molecular sampling of bright-spored Myxomycetes (Amoebozoa, slime-moulds) in decaying beech logs. *FEMS Microbiology Ecology* 91(6).
- Collins ONR. 1975. Mating types in five isolates of *Physarum polycephalum*. *Mycologia* 67:98–107.
- Collins ONR. 1979. Myxomycete biosystematics: some recent developments and future research opportunities. *Botanical Review* 45:145–201.
- Collins ONR. 1981. Myxomycete genetics, 1960–1981. *Journal of the Elisha Mitchell Scientific Society* 97:101–125.
- Eliasson U. 2015. Review and remarks on current generic delimitations in the myxomycetes, with special emphasis on *Licea*, *Listerella* and *Perichaena*. *Nova Hedwigia*, online first (doi: 10.1127/nova\_hedwigia/2015/0283).
- Erastova DA, Okun MV, Fiore-Donno AM, Novozhilov YK, Schnittler M. 2013. Phylogenetic position of the enigmatic myxomycete genus *Kelleromyxa* revealed by SSU rDNA sequences. *Mycological Progress* 12:599–608.
- Estrada-Torres A, Gaither TW, Miller DL, Lado C, Keller HW. 2005. The myxomycete genus *Schenella*: morphological and DNA sequence evidence for synonymy with the gasteromycete genus *Pyrenogaster*. *Mycologia* 97:139–149.
- Fiore-Donno AM, Berney C, Pawlowski J, Baldauf SL. 2005. Higher-order Phylogeny of Plasmodial Slime Molds (Myxogastria) Based on EF1A and SSU rRNA Sequences. *Journal of Eukaryotic Microbiology* 52:201–210.
- Fiore-Donno AM, Clissmann F, Meyer M, Schnittler M, Cavalier-Smith T. 2013. Two-gene phylogeny of bright-spored Myxomycetes (slime moulds, superorder Lucisporidia). *PLoS ONE* 8:e62586.
- Fiore-Donno AM, Kamono A, Meyer M, Schnittler M, Fukui M, Cavalier-Smith T. 2012. 18S rDNA phylogeny of *Lamproderma* and allied genera (Stemonitales, Myxomycetes, Amoebozoa). *PLoS ONE* 7:e35359.
- Fiore-Donno AM, Meyer M, Baldauf SL, Pawlowski J. 2008. Evolution of dark-spored Myxomycetes (slime-moulds): molecules versus morphology. *Molecular Phylogenetics and Evolution* 46:878–889.
- Fiore-Donno AM, Nikolaev SI, Nelson M, Pawlowski J, Cavalier-Smith T, Baldauf SL. 2010. Deep phylogeny and evolution of slime moulds (Mycetozoa). *Protist* 161:55–70.

- Fiore-Donno AM, Novozhilov YK, Meyer M, Schnittler M. 2011. Genetic structure of two protist species (Myxogastria, Amoebozoa) suggests asexual reproduction in sexual amoebae. *PLoS ONE* 6:e22872.
- Hoppe T, Schwippert WW. 2014. Hydrophobicity of myxomycete spores: An undescribed aspect of spore ornamentation. *Mycosphere* 5:601–606.
- Howard FL. 1932. Nuclear division in plasmodium of *Physarum*. *Annals of Botany* 46:461–477.
- Kalyanasundaram I. 1973. Capillitial development in *Stemonitis*. *Taxonomy of Fungi* 1:9–13. Madras Univ., India.
- Kamono A, Kojima H, Matsumoto J, Kawamura K, Fukui M. 2009. Airborne myxomycete spores: detection using molecular techniques. *Naturwissenschaften* 96:147–151.
- Kamono A, Meyer M, Cavalier-Smith T, Fukui M, Fiore-Donno AM. 2013. Exploring slime mould diversity in high-altitude forests and grasslands by environmental RNA analysis. *FEMS Microbiology Ecology* 84:98–109.
- Lado C. 2015. An on line nomenclatural information system of Eumycetozoa. 2005–2015. <http://www.nomen.eumycetozoa.com>. Accessed 10 July 2015.
- Lahr DJG, Parfrey LW, Mitchell EA, Katz LA, Lara E. 2011. The chastity of amoebae: re-evaluating evidence for sex in amoeboid organisms. *Proceedings of the Royal Society of London B* 278:2081–2090.
- Leontyev D, Schnittler M, Stephenson SL. 2015. A critical revision of the *Tubifera ferruginosa*-complex. *Mycologia* 107:959–985.
- Madelin MF. 1984. Myxomycete data of ecological significance. *Transactions of the British Mycological Society* 83:1–19.
- Martin GW, Alexopoulos CJ. 1969. *The Myxomycetes*. Iowa City: Iowa Univ. Press.
- Medinger R, Nolte V, Pandey RV, Jost S, Ottenwalder B, Schlotterer C, Boenigk J. 2010. Diversity in a hidden world: potential and limitation of next-generation sequencing for surveys of molecular diversity of eukaryotic microorganisms. *Molecular Ecology* 19 (Suppl. 1):32–40.
- Mohberg J. 1977. Nuclear DNA content and chromosome numbers throughout the life cycle of the *Colonia* strain of the Myxomycete, *Physarum polycephalum*. *Journal of Cell Science* 2:95–108.
- Nannenga-Bremekamp NB. 1991. *A guide to temperate Myxomycetes* (Feest A, Burgraff E: *De Nederlandse Myxomyceten*, Engl. transl.). Biopress Ltd., Bristol.
- Neubert H, Nowotny W, Baumann K. 1993. *Die Myxomyceten Deutschlands und des angrenzenden Alpenraumes unter besonderer Beruckichtigung osterreichs*. 1 Ceratiomyxales, Echinosteliales, Liceales, Trichiales. Baumann Verl., Gomaringen.
- Neubert H, Nowotny W, Baumann K. 1995. *Die Myxomyceten Deutschlands und des angrenzenden Alpenraumes unter besonderer Beruckichtigung osterreichs*. 2 Physariales. Baumann Verl., Gomaringen.
- Neubert H, Nowotny W, Baumann K. 2000. *Die Myxomyceten Deutschlands und des angrenzenden Alpenraumes unter besonderer Beruckichtigung osterreichs*. 3 Stemonitales. Baumann Verl., Gomaringen.
- Novozhilov YK, Okun MV, Erastova DA, Shchepin ON, Zemlyanskaya IV, Garca-Carvajal E, Schnittler M. 2013a. Description, culture and phylogenetic position of a new xerotolerant species of *Physarum*. *Mycologia* 105:1535–1546.
- Novozhilov YK, Schnittler M, Erastova DA, Okun MV, Schepin ON, Heinrich E. 2013b. Diversity of nivicolous myxomycetes of the Teberda State Biosphere Reserve (Northwestern Caucasus, Russia). *Fungal Diversity* 59:109–130.
- Olive LS. 1975. *The Mycetozoa*. Acad. Press, New York, San Francisco, London.
- Otto S, Gerstein A. 2006. Why have sex? The population genetics of sex and recombination. *Biochemical Society Transactions* 34:519–522.
- Pawlowski J, Audic S, Adl S, Bass D, Belbahri L, Berney C, et al. 2012. CBOL protist working group: barcoding eukaryotic richness beyond the Animal, Plant, and Fungal Kingdoms. *PLoS Biology* 10:e1001419.
- Persoon CH. 1794. *Neuer Versuch einer systematischen Eintheilung der Schwamme*. *Neues Magazin fur die Botanik in ihrem ganzen Umfange* 1:63–128.



- Peterson A, Levichev IG, Peterson J, Harpke D, Schnittler M. 2011. New insights into the phylogeny and taxonomy of Chinese species of *Gagea* (Liliaceae) – speciation through hybridization. *Organisms Diversity and Evolution* 11: 387–407.
- Poulain M, Meyer M, Bozonnet J. 2011. *Les myxomycetes*. Delémont: Féd. Mycol. Bot. Dauphiné-Savoie.
- Reichenbach H. 1993. Biology of myxobacteria: ecology and taxonomy. In: M. Dworkin M, Kaiser D (eds.), *Myxobacteria II*. American Society for Microbiology, Washington, DC, pp 13–62.
- Roger AJ, Smith MW, Doolittle RF, Doolittle WF. 1996. Evidence for the Heterolobosea from phylogenetic analysis of genes encoding glyceraldehyde-3-phosphate dehydrogenase. *Journal of Eukaryotic Microbiology* 43:475–485.
- Romeralo M, Spiegel FW, Baldauf SL. 2010. A fully resolved phylogeny of the social amoebas (*Dictyostelia*) based on combined SSU and ITS rDNA sequences. *Protist* 161:539–548.
- Romeralo M, Cavender J, Landolt J, Stephenson SL, Baldauf S. 2011. An expanded phylogeny of social amoebas (*Dictyostelia*) shows increasing diversity and new morphological patterns. *BMC Evolutionary Biology* 11:84.
- Schnittler M, Erastova DA, Shchepin ON, Heinrich E, Novozhilov YK. 2015. Four years in the Caucasus – observations on the ecology of nivicolous myxomycetes. *Fungal Ecology* 14:105–115.
- Schnittler M, Kummer V, Kuhnt A, Kriegelsteiner L, Flatau L, Müller M. 2011. Rote Liste und Gesamtartenliste der Schleimpilze (*Myxomycetes*) Deutschlands. *Schr.R. Vegetationskunde* 70:125–234.
- Schnittler M, Mitchell DW. 2000. Species diversity in *Myxomycetes* based on morphological species concept - a critical examination. *Stapfia* 73:55–62.
- Schnittler M, Novozhilov YK, Romeralo M, Brown M, Spiegel FW. 2012. *Myxomycetes* and *Myxomycete*-like organisms. In: Frey W, editor. (13th ed.) *Englers Syllabus of Plant Families*. Vol. 4. Bornträger, Stuttgart, pp 40–88.
- Schnittler M, Novozhilov YK, Shadwick JDL, Spiegel FW, García-Carvajal E, König P. 2015. What substrate cultures can reveal: *Myxomycetes* and *myxomycete*-like organisms from the Sultanate of Oman. *Mycosphere* 6:356–384.
- Schnittler M, Stephenson SL, Novozhilov YK. 2000. Ecology and world distribution of *Barbeyella minutissima* (*Myxomycetes*). *Mycological Research* 104:1518–1523.
- Schnittler M, Tesmer J. 2008. A habitat colonisation model for spore-dispersed organisms – Does it work with eumycetozoans? *Mycological Research* 112:697–707.
- Schnittler M, Unterseher M, Tesmer J. 2006. Species richness and ecological characterization of *myxomycetes* and *myxomycete*-like organisms in the canopy of a temperate deciduous forest. *Mycologia* 98:223–232.
- Schoch CL, Seifert KA, Huhndorf S, Robert V, Spouge JL, Levesque CA, Chen W; Fungal Barcoding Consortium. 2012. Nuclear ribosomal internal transcribed spacer (ITS) region as a universal DNA barcode marker for Fungi. *Proceedings of the National Academy of Sciences of the United States of America* 109:6241–6246.
- Spiegel FW, Stephenson SL, Keller HW, Moore DL, Cavender JC. 2004. *Mycetozoans*. In: Mueller GM, Bills G, Foster MS (eds.). *Biodiversity of Fungi, Inventory and monitoring methods*. Elsevier Acad. Press, Burlington, MA. pp. 547–576.
- Stephenson SL, Fiore-Donno AM, Schnittler M. 2011. *Myxomycetes* in soil. *Soil Biology and Biochemistry* 43:2237–2242.
- Stephenson SL, Schnittler M, Novozhilov Y. 2008. *Myxomycete* diversity and distribution from the fossil record to the present. *Biodiversity and Conservation* 17:285–301.
- Stephenson S, Stempen H. 1994. *Myxomycetes: Handbook of Slime Molds*. Timber Press, Portland, OR.
- Strassmann JE, Zhu Y, Queller DC. 2000. Altruism and social cheating in the social amoeba *Dictyostelium discoideum*. *Nature* 408:965–967.
- Swanson AR, Spiegel FW, Cavender JC. 2002. Taxonomy, slime molds, and the questions we ask. *Mycologia* 94:968–979.
- Swanson AR, Vadell EM, Cavender JC. 1999. Global distribution of forest soil dictyostelids. *Journal of Biogeography* 26:133–148.

- Tesmer J, Schnittler M. 2007. Sedimentation velocity of myxomycete spores. *Mycological Progress* 6:229–234.
- Urich T, Lanzén A, Qi J, Huson DH, Schleper C, Schuster SC. 2008. Simultaneous assessment of soil microbial community structure and function through analysis of the meta-transcriptome. *PLoS ONE* 3:e2527.

### 3. Publications



# Sex or no sex? Group I introns and independent marker genes reveal the existence of three sexual but reproductively isolated biospecies in *Trichia varia* (Myxomycetes)

Yun Feng<sup>1</sup> · Martin Schnittler<sup>1</sup>

Received: 17 April 2015 / Accepted: 28 July 2015  
© Gesellschaft für Biologische Systematik 2015

**Abstract** Plasmodial slime molds are members of the class Amoebozoa forming elaborate fruit bodies releasing airborne spores. Two species concepts have been developed independently: a morphological relying on fruit body characters, and a biological relying on crossing studies of a few cultivable species. In an attempt to reconcile both concepts, we obtained for 198 specimens of the common species *Trichia varia* partial sequences of three independent markers (nuclear small-subunit (SSU) ribosomal RNA gene, extrachromosomal; elongation factor 1 alpha gene, chromosomal; cytochrome oxidase subunit 1 gene, mitochondrial). The resulting phylogeny revealed 21 three-marker genotypes clustering into three groups. Combinations of the single-marker genotypes occurred exclusively within these groups, called 1, 2a, and 2b. To examine the suitability of group I introns to monitor speciation events, complete SSU sequences were generated for 66 specimens, which revealed six positions that can carry group I introns. For each of the groups 1 and 2a, five of these positions were occupied by different intron genotypes; and no genotype was shared by the two groups. Group 2b was devoid of introns. Putatively functional or degenerated homing endonuclease genes were found at different positions in groups 1 and 2a. All observations (genotypic combinations of the three markers, signs of recombination, intron patterns) fit well into a

pattern of three cryptic biological species that reproduce predominantly sexual but are reproductively isolated. The pattern of group I introns and inserted homing endonuclease genes mounts evidence that the Goddard-Burt intron life cycle model applies to naturally occurring myxomycete populations.

**Keywords** Extrachromosomal nuclear ribosomal DNA · Group I intron · Homing endonuclease · Plasmodial slime mold · Reproductive system · Speciation

## Introduction

Plasmodial slime molds (Myxomycetes, Myxogastria), sometimes called “sexual amoebae,” are the most species-rich monophyletic group of Amoebozoa (Adl et al. 2012; Lahr et al. 2011a; Smirnov et al. 2011). These free-living amoebae are abundant in soil (Urich et al. 2008) and multiply by binary fission. According to the life cycle found in many textbooks, haploid amoebae or amoebflagellates undergo syngamy, and zygotes form a diploid, syncytially organized plasmodium as the second vegetative stage. Most of the plasmodial biomass converts into sporocarpic fruit bodies which release airborne meiospores like fungi. Myxomycetes are one of the few groups of simple eukaryotes that appear to be macroscopic in dimension, which has led to a considerable body of data on distribution and ecology (Stephenson et al. 2008). Only a limited number of species, mostly of the order Physarales, will complete their life cycle in culture, even if food organisms are supplied (Clark and Haskins 2010). Well known are *Physarum polycephalum* and *Didymium iridis* as model organisms in cell physiology, developmental studies (Goodman 1980; Sauer 1982), and systems biology (Rätzel et al. 2013).

**Electronic supplementary material** The online version of this article (doi:10.1007/s13127-015-0230-x) contains supplementary material, which is available to authorized users.

✉ Martin Schnittler  
martin.schnittler@uni-greifswald.de

<sup>1</sup> Institute of Botany and Landscape Ecology, Ernst Moritz Arndt University of Greifswald, Soldmannstr. 15, 17487 Greifswald, Germany

Apart from the advanced knowledge we have about a few model species, myxomycetes in nature are poorly studied by molecular methods. Only recently were first phylogenies published (Fiore-Donno et al. 2010, 2012, 2013), which recovered two main clades: the bright-spored clade (spores lightly colored by various pigments; *Trichia varia* as the target species of this study belongs to this clade), and the dark-spored clade (spores dark colored by melanin, most of the cultivable species). Many taxa are in critical need of revision (Schnittler et al. 2012). First studies employing partial nuclear small-subunit (SSU) ribosomal RNA gene sequences as a barcode marker revealed that many morphospecies seem to be highly diverse (Novozhilov et al. 2013b), mounting evidence that the “everything is everywhere” hypothesis (Fenchel and Finlay 2004) being popular for microorganisms should be rejected, and cryptic speciation is likely to occur (Aguilar et al. 2013).

Still, the only species concept applicable for the group as a whole is entirely based on the morphology of the sporocarps (Schnittler and Mitchell 2000). However, culture experiments carried out with members of the Physarales pose a challenge for this morphospecies concept prevailing for nearly 200 years (Clark 2000). Most isolates of a morphospecies behave heterothallic: amoebal populations derived from a single spore will not sporulate if they do not come in contact with amoebae from a different clone (Collins 1981). Heterothallism is maintained via mating types which can be arranged in a single-locus multiallelic system (*Didymium iridis*; Betterley and Collins 1983; Clark 1993), or in three loci with multiple alleles (*Physarum polycephalum*; Clark and Haskins 2010; Collins 1975; Moriyama and Kawano 2010). Often, some but not all of the mating types in a morphologically defined species are compatible. Groups of compatible strains can be seen as biospecies (Clark 1995; Collins 1979), thus providing an alternative species concept. This was the first question of the study: Can we detect evidence for coexisting biospecies in nature?

If we assume that myxomycetes reproduce sexually (as it should be expected for Amoebozoa, Lahr et al. 2011b) with mating types ensuring outcrossing (Clark and Haskins 2010; Collins 1979), asexual lineages can develop via clonal populations of non-fruiting amoebae (Clark and Haskins 2011). However, in culture experiments involving multiple isolates, some strains behave non-heterothallic and form fruit bodies in single-spore cultures (Collins 1981). Automixis, i.e., incomplete meiosis and the formation of diploid instead of haploid meiospores, was invoked as the most likely reproductive system for such non-heterothallic, presumably asexual isolates (Clark and Haskins 2013). Such diploid spores should give rise to diploid amoebae which may complete the life cycle without a sexual event. If existing, these entirely asexual lineages should have an advantage over sexual lineages for the colonization of habitat islands like accumulations of plant

debris, since a single spore colonizing a new habitat island can complete the entire life cycle and disperse anew by spores (Schnittler and Tesmer 2008). A first study on a wild population of *Lamproderma* spp. (Fiore-Donno et al. 2011) suggested the existence of asexual populations, since specimens from geographical independent accessions were found to be identical in three molecular markers: the first part of SSU, its internal transcribed spacer 1 (ITS1), and the first part of the elongation factor 1 alpha gene (EF1A). Therefore, sexual and asexual biospecies may coexist within one morphologically circumscribed species. This was the second question for our study: Can we find evidence for asexual strains in a natural population?

In this study, we analyze one species for the first time with three independent marker genes: SSU (in myxomycetes located in multiple extrachromosomal DNA molecules; Torres-Machorro et al. 2010), EF1A (chromosomal), and cytochrome oxidase subunit 1 gene (COI, mitochondrial). *T. varia* (Pers. ex J.F. Gmel.) Pers. is a common myxomycete described already by Persoon (1794) based on the Linnean name *Stemonitis varia* (Linne 1792). In contrast to all established model species in myxomycetes, *T. varia* belongs to the bright-spored clade of myxomycetes (Fiore-Donno et al. 2013) and is easy to recognize by elaters within the spore mass that show only two, not several, spiral bands like the other members of this genus. This might be the reason why the name remained valid until today, although the morphological variability of the species is reflected by a rather long list of heterotypic synonyms (Lado 2014), the last one dating from 1974.

Additionally, we studied group I introns in complete SSU sequences. Perhaps caused by the lifestyle of plasmodia, which prey on various microbes (besides bacteria, also yeasts and green algae may be utilized; Haskins and Wrigley de Basanta 2008; Lazo 1961), myxomycete sequences are rich in introns (Johansen et al. 1992; Lundblad et al. 2004). As for mating types, cultivable members of the Physarales were established as a model system for the study of group I introns (Nandipati et al. 2012; Wikmark et al. 2007a, b). Ten intron insertion positions are known for SSU of myxomycetes; four of these (positions 516, 911, 959, and 1199) were reported to occur in *T. varia* (Fiore-Donno et al. 2013). Two mechanisms for intron homing are known. As the most powerful mechanism, intron homing via an intron-coded homing endonuclease (HE) is assumed, but reverse splicing through an RNA intermediate was invoked as well (Haugen et al. 2005a; Lambowitz and Belfort 1993). Although, in a strict sense, every intron poses an additional burden to the DNA replication of its host and introns can thus be seen as parasitic genes, they are selectively neutral (Edgell et al. 2011; Haugen et al. 2005a). Consequently, mutations in homing endonuclease genes (HEGs) should slowly render these genes non-functional, and according to the life cycle model of group I introns proposed by Goddard and Burt (1999), after degeneration and

complete loss of the intron at one position, a new intron homing event can take place, thus ensuring survival of the intron in the population via sexual transmission. In myxomycetes, transmission of introns can take place via syngamy and subsequent karyogamy of amoebae of different lineages (mating types) within the sexual cycle. Plasmodial fusion, controlled by a very complex set of gene loci (Clark and Haskins 2012), is limited to closely related strains and should not contribute to intron transmission, since karyogamy does not take place. Similar to findings in other groups of organisms, sexually reproducing populations of a myxomycete biospecies should display a mixture of group I introns in different stages of HEG degeneration, and their genotypes should differ from intron populations in related but reproductively isolated biospecies. As such, the intron distribution in wild populations of myxomycetes may effectively tell apart biospecies and reveal their mode of reproduction. This study presents first results on genetic variation in three independent marker genes and the distribution of group I introns for a naturally occurring metapopulation of a myxomycete.

## Methods

### Specimens

A total of 197 specimens of *T. varia* were collected throughout Eurasia, with two regions (southern Germany and southern Siberia) intensely studied. In addition, the single specimen of *T. varia* (AMFD451) used in the phylogeny of bright-spored myxomycetes (Fiore-Donno et al. 2013) was included in this study. Sequences of *Perichaena depressa* and *Trichia scabra* were used as outgroups in phylogenetic analyses. Specimens were deposited in private collections of Fiore-Donno AM, Germany (AMFD); van Hooff H, Netherlands (Hooff); Van Roy J, Belgium (JVR); de Haan M, Belgium (MdH); and Schnittler M, Germany (sc; to be deposited in M), and in the herbaria KRAM (Ronikier A, Poland) and LE (Novozhilov YK, Russia). Information about specimens and GenBank accession numbers (KM494990-KM495078) is listed in Supplementary Table S1 and a database on localities (Supplementary Database S1).

### DNA Extraction, PCR, and sequencing

About 5–20 sporocarps from each specimen were used for DNA extraction. Sporocarps were pre-cooled at  $-80\text{ }^{\circ}\text{C}$  and grounded using a ball mill (Retsch MM301) at 30 Hz for 80 s. Genomic DNA was extracted using the DNeasy Plant Mini Kit (Qiagen) or the Invisorb Spin Food Kit II (Strattec). PCR amplifications on *T. scabra* and one specimen of *T. varia* (AMFD451) were conducted with the same DNA as used for the published phylogeny (Fiore-Donno et al. 2013).

Partial SSU sequences were obtained using the primers SFATri and SR4Bright (Fiore-Donno et al. 2013), which amplify the first fragment of the gene (5'-end up to the intron insertion site 516). Partial EF1A sequences covering the first part of the gene include a short spliceosomal intron; here the primers 1FCyt and E500R were used (Fiore-Donno AM, pers. comm.). For the amplification of the first half of COI, the primers COIF1 and COIR1 were designed within reported conservative regions (Walker et al. 2011) based on gene and transcript sequences of six myxomycete species (Gott et al. 1993; Horton and Landweber 2000; Traphagen et al. 2010).

For complete SSU sequences, a single PCR product covering nearly the complete gene was obtained using the primers NUSSUF3 and NUSSUR3, which are designed within conserved regions found in the SSU alignment for bright-spored species (Fiore-Donno et al. 2013). This product was sequenced in sections, using multiple primers designed in this study. In addition, some of the partial SSU sequences were obtained using the primers NUSSUF3 and NUSSUR4.

All primers used in this study are listed in Table 1. PCR reactions were performed using the MangoTaq Kit (Bioline). Cycle sequencing reactions were performed using the BigDye Kit (ABI). In addition, Q-Solution (Qiagen) and Triton X-100 (Omnilab) were applied for PCR reactions and cycle sequencing reactions to obtain complete SSU sequences of some specimens following online protocols (Lieb 2014).

### PCR and sequencing of single spores

Single spores were isolated from *T. varia* specimens showing heterogeneities in complete SSU sequences. Under a dissecting microscope (Zeiss, Stemi SV6, magnification  $\times 50$ ), a single spore was separated with a needle from a group of spores scattered over a glass slide. Spore crushing and PCRs were conducted according to a reported protocol (Frommlet and Iglesias-Rodríguez 2008) with modifications. The single spore was transferred directly to a PCR tube containing 1  $\mu\text{l}$  TE buffer (10 mM Tris-HCl, 1 mM EDTA; pH 8.0). The PCR tube for negative control contained 1  $\mu\text{l}$  TE and a glass bead. Tubes were vortexed at 2700 rpm for 60 s; PCR reagents (MangoTaq Kit) were then added directly to the PCR tube. The first PCR was performed in a volume of 10  $\mu\text{l}$  with the primer pair NUSSUF3 and NUSSUR3. After initial denaturing at  $94\text{ }^{\circ}\text{C}$  for 2 min, we run 45 cycles of denaturing at  $94\text{ }^{\circ}\text{C}$  for 30 s, annealing at  $56\text{ }^{\circ}\text{C}$  for 30 s, elongation at  $72\text{ }^{\circ}\text{C}$  for 2 min, and a final elongation at  $72\text{ }^{\circ}\text{C}$  for 5 min. The second PCR was performed using 2  $\mu\text{l}$  from the first PCR as template, and two primer pairs (NUSSUF10 and NUSSUR6; NUSSUF16 and NUSSUR11) in separate reactions. PCR settings were identical except for a total volume of 25  $\mu\text{l}$ ; the elongation step was set at  $72\text{ }^{\circ}\text{C}$  for 1 min. Cycle sequencing reactions were performed with the reverse primer using the BigDye Kit.

**Table 1** Forward (F) and reverse (R) primers used in this study. The first three primer pairs were used to obtain partial sequences of SSU, EF1A, and COI, respectively

Locus	Primer (F/R)		Sequence (5'-3')
SSU	SFATri	F	aatctgcegaacggctccgta
SSU	SR4Bright	R	tgctggcaccagacttgt
EF1A	1FCyt	F	cagagctcgttattgncaygtngac
EF1A	E500R	R	ttggcaataaccrgcctcg
COI	COIF1	F	ctgcwtaattggtggbtttgg
COI	COIR1	R	acgtccattcckacwgrttrac
SSU	NUSSUF2	F	ggacctgtgagaaatcataagcg
SSU	NUSSUF3	F	cctgccagaatcatatgctgtcc
SSU	NUSSUF4	F	caccgagtaacaattggagga
SSU	NUSSUF5	F	taaaggaattgacggaagagcacac
SSU	NUSSUF6	F	caacacggggaactcactagg
SSU	NUSSUF8	F	gcgtccctattctgttctgc
SSU	NUSSUF9	F	gaacgccaggtacgggagc
SSU	NUSSUF10	F	gccagcaccggcggaattcc
SSU	NUSSUF11	F	ccgttgatcctgccaggtg
SSU	NUSSUF12	F	gacccttctgtttgcttgcg
SSU	NUSSUF13	F	gcttctgtgcccactgatgc
SSU	NUSSUF14	F	gcctggtgctccttccacc
SSU	NUSSUF15	F	gggtgcagttcacagactagacg
SSU	NUSSUF16	F	ctggtctattccgtaacgagcg
SSU	NUSSUF17	F	cagtgatgccttagatgctctagg
SSU	NUSSUF18	F	cggaagtccttagagcc
SSU	NUSSUF19	F	aacaaggaattctagtagtcgcc
SSU	NUSSUR1	R	aatcagaaaagcctgctggg
SSU	NUSSUR2	R	agtttcagttctgcaccatactc
SSU	NUSSUR3	R	atacctgttacgacttctcctcc
SSU	NUSSUR4	R	accagactgtctccaattgttac
SSU	NUSSUR5	R	cgcttccccgttctgctgg
SSU	NUSSUR6	R	cacctggcagagatcaacgg
SSU	NUSSUR7	R	gcaggctccactcctgtgtg
SSU	NUSSUR8	R	cgctcgttagcgggaatagacc
SSU	NUSSUR9	R	aggcggctcaaggcaggc
SSU	NUSSUR10	R	cgactgacttagactacgagc
SSU	NUSSUR11	R	agagcagggacagaatcgtcgc
SSU	NUSSUR12	R	ggctctaagggaactccec

The primers NUSSUF3 and NUSSUR3 were used to obtain a single PCR product covering nearly the whole SSU, with all remaining primers to obtain portions suitable for Sanger sequencing. Sources: primers SFATri and SR4Bright (Fiore-Donno et al. 2013); 1FCyt and E500R (Fiore-Donno AM, pers. comm.); all other primers were designed for this study

### Alignments and phylogenetic analyses of partial SSU, EF1A, and COI sequences

For a first data set, we generated 198 partial SSU sequences from *T. varia* and one sequence from *Perichaena depressa*. Together with one sequence from *T. scabra* (GenBank:

JX481314; Fiore-Donno et al. 2013), they were aligned using the multiple sequence alignment software MUSCLE (Edgar 2004) implemented in MEGA 5.05 (Tamura et al. 2011) with default settings. The resulting alignment was manually added to that of the published phylogeny of bright-spored myxomycetes (Fiore-Donno et al. 2013), resulting in 430 sites of which 272 were used for the original phylogeny (Fiore-Donno et al. 2013) plus an additional 10 sites that could be unambiguously aligned by us.

Furthermore, we obtained 58 partial EF1A sequences for *T. varia* and one sequence from *Perichaena depressa*. These and two reported sequences (*T. scabra*, GenBank: JX481343; *T. varia*, GenBank: JX481344; Fiore-Donno et al. 2013) were first aligned by MUSCLE with default settings and then manually added to the existing alignment (Fiore-Donno et al. 2013), resulting in 322 sites of which the exon part (258 sites) was used in phylogenetic analyses.

Finally, all 198 *T. varia* specimens, one *Perichaena depressa* specimen, and one *T. scabra* specimen were sequenced to obtain partial COI sequences. Sequences were aligned by MUSCLE with default settings. An alignment of 537 sites was used for phylogenetic analysis.

Phylogenetic analyses on individual genes were conducted including all single-gene genotypes identified for *T. varia*. Selected in accordance with the phylogeny of bright-spored myxomycetes (Fiore-Donno et al. 2013), specimens from *Perichaena depressa* and *T. scabra* were used as outgroups (TreeBASE: M30972, M30973, M30974). Substitution models were selected by TOPALi v2 (Milne et al. 2009) under the Bayesian information criterion (BIC) for maximum likelihood (ML) analysis and Bayesian analysis. For *T. varia* alignments, the best models were TrN (ML analysis) and HKY+G (Bayesian analysis) for partial SSU, TrNef (ML analysis) and K80 (Bayesian analysis) for partial EF1A, and HKY+G for partial COI. For alignments including additionally *Perichaena depressa* and *T. scabra*, the best models were K80+I+G for partial SSU, JC for partial EF1A, and TIM+G (ML analysis) and GTR+G (Bayesian analysis) for partial COI. ML analyses for single genes were conducted using PhyML 2.4.5 (Guindon and Gascuel 2003) implemented in TOPALi with 1000 bootstrap replications. Bayesian analyses were carried out with MrBayes 3.1.1 (Ronquist and Huelsenbeck 2003) implemented in TOPALi with two runs, one million generations, and 50 % as burn-in, sampled every 100 generations.

Sequences from all three genes were concatenated to generate a combined three-gene alignment. ML analysis was conducted on the combined three-gene alignment using PhyML with model GTR+G and 1000 bootstrap replications; Bayesian analysis with data partitions was conducted using MrBayes 3.2.2 (Ronquist et al. 2012) with two runs, one million generations, and 50 % as burn-in, sampled every 100 generations, and with three partitions each using the best model for the respective gene.



To compare genetic and geographic distances for the 197 specimens (excluding one specimen containing polymorphic sites) with partial SSU and partial COI sequences, we computed pairwise genetic distances using the maximum composite likelihood model (Tamura et al. 2004) implemented in MEGA 5.2 (Tamura et al. 2011). Geographic distances between localities of specimens were calculated using an Excel macro for the Vincenty formula (Dalglish 2014); a Mantel test including 999 iterations for the comparison of both matrices was performed with the ExtraStats function of PopTools 3.2.5 (Hood 2010).

### Alignments and phylogenetic analyses of complete SSU sequences

Our second data set includes complete SSU sequences from single PCR products of 66 specimens of *T. varia* ranging from 1835 to 5660 bp in size. Sequences with polymorphic sites were recorded using the respective IUPAC symbols.

The reported complete SSU sequence of *T. varia* specimen AMFD451 (GenBank: JX481315; Fiore-Donno et al. 2013) was inconsistent with the sequences obtained in this study. From this reason, a single PCR product was obtained with the primers NUSSUF3 and NUSSUR3 from an aliquot of the DNA from AMFD451 used by these authors and sequenced in sections directly. Comparisons revealed that the original sequence GenBank: JX481315 is most likely an artificial chimera of two origins with a breaking point near the end of the first exon. Therefore, the corrected sequence of the same specimen (GenBank: KM495017) was used for this study.

Complete SSU sequences were aligned using MUSCLE with the option “gap open –550; gap extend –3,” with manual adjustment on intron locations and within-intron alignments, resulting in a total of 9797 sites (TreeBASE: M30975). For three specimens, gaps due to incomplete sequences were recorded as missing data. The complete SSU alignment of *T. varia* was added as a block to the reported SSU alignment (supplementary alignment “journal.pone.0062586.s007” in Fiore-Donno et al. 2013, with updates based on GenBank accessions) with congruent delimitation of exon and intron borders between the two alignments. For phylogenetic analysis, the same set of 1325 sites as used by these authors was extracted. All *T. varia* specimens representing distinct genotypes within these 1325 sites were considered for a phylogeny using *Ceratiomyxa fruticulosa* as outgroup (TreeBASE: M30970). The best substitution model under the criterion BIC was SYM+I+G. Both ML (1000 bootstrap replications) and Bayesian analyses (two runs, four million generations, 50 % as burn-in, sampled every 100 generations) were conducted using PhyML and MrBayes, respectively.

Exon sequences were extracted from the *T. varia* complete SSU alignment, yielding a total of 1825 exon sites. The best substitution model for phylogenetic analyses under the criteria BIC was TrN+G for PhyML and GTR+G for MrBayes. Settings for the analyses were 1000 bootstrap replications for PhyML, and two runs, three million generations, 50 % as burn-in, and sampling every 100 generations for MrBayes. On the alignment excluding sequences containing polymorphic sites, overall mean distance was estimated by MEGA with the Tamura three-parameter substitution model and omitting gaps and missing data. Detection of recombination was performed by the pairwise homoplasy index (PHI) test (Bruen et al. 2006) implemented in SplitsTree4 (Huson and Bryant 2006).

### Analyses on intron parts of SSU sequences

Intron sequences, excluding two containing polymorphic sites, were extracted from the *T. varia* complete SSU alignment. The overall mean distance of distinct intron sequences at each insertion position was estimated by MEGA with the Tamura three-parameter substitution model, applying complete deletion of gaps and missing data. The PHI test was conducted for intron sequences at each insertion position. For the association analysis of introns across different positions, each distinct intron sequence and the state of intron-lacking were coded by numbers. Association indices  $I_A^S$  (LIAN 3.6; Haubold and Hudson 2000) and rBarD (MultiLocus 1.2.2; Agapow and Burt 2001) were computed from intron profiles, with simulated significance calculated from 10000 randomized data sets. All extrachromosomal copies of SSU in one specimen were assumed to be identical and were treated as one copy.

Known group I intron sequences of other myxomycete species were extracted from published SSU sequences (Fiore-Donno et al. 2005, 2008, 2010, 2011, 2012, 2013; Nandipati et al. 2012). The GenBank accession DQ903669 (*Meriderma aggregatum*) was replaced by the sequence named “Meriderma\_aggregatum\_DQ903669” in the supplementary alignment “journal.pone.0035359.s001” in Fiore-Donno et al. (2012) due to the inconsistency between sequences in GenBank and the publication (deletion at site 1085 in GenBank: DQ903669; sites 2280 to 5529 in *Meriderma\_aggregatum\_DQ903669* were absent in GenBank: DQ903669).

Group I intron sequences with known assignment to an intron class (classes IA, IB, IC, and ID, Michel and Westhof 1990; class IE, Li and Zhang 2005) were downloaded from the Comparative RNA Web Site (CRW; Cannone et al. 2002) and the Group I Intron Sequence and Structure Database (GISSD; Zhou et al. 2008). The reliability of intron class assignments performed with BLASTN 2.2.24 (Altschul et al. 1997) used in this study was tested by searching one of the

two databases (CRW or GISSD) against the other database or the database itself, setting an Expect value less than 0.1, and eliminating self-matching intron sequences. The results showed that regions matched by BLASTN lie within conserved regions in group I introns (Burke et al. 1987; Li and Zhang 2005; Michel and Westhof 1990), and BLASTN could be applied in group I intron class assignment. Intron classes were assigned to introns of *T. varia* and other myxomycetes by BLASTN searches against introns from databases CRW and GISSD. Direct inspection of an alignment of S956 introns in myxomycetes automatically generated by MAFFT 7.158 (Kato and Standley 2013) with the option “E-INS-i” detected two sets of sequences within S956 introns corresponding with the initial assignment to intron classes IC1 (a subclass of IC; Michel and Westhof 1990) and IE by BLASTN searches. Multiple conserved regions were identified in the MAFFT alignment of S956 introns. The conserved regions in S956 introns identified by BLASTN and MAFFT were compared with the structural alignments from GISSD, and the identified P7:P7' pairing regions were consistent with those of IC1 and IE introns, respectively. Classifications for some introns of myxomycete species not investigated by us were adopted from the literature (Lundblad et al. 2004; Wikmark et al. 2007b).

### Analyses of intron-encoded HEGs

BLASTX 2.2.24 searches were conducted on group I introns of *T. varia* and other myxomycetes against annotated HE protein sequences containing the motif His-Cys box found in nuclear ribosomal genes (Brown et al. 2012; Elde et al. 1999; Haugen et al. 1999, 2002, 2003, 2004, 2005b; Johansen et al. 1997; Machouart et al. 2004; Muscarella et al. 1990; Müller et al. 2001; Tanabe et al. 2002; Xu et al. 2013; Yokoyama et al. 2002). Intron sequences with matches to HE proteins were analyzed using StarORF 1.0 (STAR 2014). Similar to published sequences (Haugen et al. 2004), discontinued open reading frames (ORFs) were connected manually by introducing frameshifts or ignoring regions with premature stop codons. Due to low sequence similarity outside the His-Cys Box (Johansen et al. 1993), the start codon was located at the first codon for methionine in the ORF.

Eighteen putative HE protein sequences from introns of myxomycetes identified within this study, three known HE protein sequences from myxomycetes (*Physarum polycephalum*, I-*PpoI*, GenBank: AAB81102; *Didymium iridis*, I-*DirI*, GenBank: CAI83766; *Didymium iridis*, I-*DirII*, GenBank: CAI83767), and one HE protein sequence from the amoeboflagellate *Naegleria jamiesoni* (Heterolobosea, I-*NjaI*, GenBank: AAB71747) were aligned by MAFFT 7.220 with the option E-INS-i. The region from residue C131 to residue H134 of I-*PpoI* (Flick et al. 1998) was

manually adjusted based on the HE protein alignment (pfam05551, corresponding to the zinc-binding loop region of HE) from the Conserved Domain Database (Marchler-Bauer et al. 2013), and published HE protein alignments (Flick et al. 1998; Haugen et al. 2004, 2005b; Johansen et al. 1993). Thirty-seven sites spanning residues S97–H134 of I-*PpoI* (Flick et al. 1998), all not affected by frameshifts, were included in phylogenetic analyses with I-*PpoI* as the outgroup (TreeBASE: M30976). The model WAG+I+G was selected as the best substitution model under the criterion BIC for phylogenetic analyses using PhyML (performed with 1000 bootstrap replications) and MrBayes (two runs, four million generations, 50 % as burn-in, sampling every 100 generations).

## Results

### Intraspecific diversity of *T. varia* genotypes revealed by partial genes

Our first data set comprised partial sequences of three independent marker genes for 198 specimens of *T. varia* collected throughout Eurasia (Supplementary Table S1). We found 12 genotypes for partial SSU, 3 for partial EF1A, and 12 for partial COI sequences (TreeBASE: M30972, M30973, M30974). The spliceosomal intron in the first part of EF1A (sites 241–304 in the alignment TreeBASE: M30973) was 57 to 60 bp in length and distinguished three genotypes by two indels of 1 and 3 bp in length, respectively. Four genotypes contained polymorphic single nucleotides showing up as double peaks in sequence chromatograms, one in partial SSU and three in the spliceosomal intron of EF1A. If this spliceosomal intron is excluded, the heterozygous partial EF1A genotypes merged with the other homozygous genotypes into only three genotypes. The single partial SSU genotype with polymorphic single nucleotides was not treated as a separate genotype, as it comprises both nucleotides showing up in the two homogeneous genotypes. Combining the partial sequences of the three genes, 21 three-gene genotypes were identified in *T. varia* (see Supplementary Table S1 for genotype assignment and Fig. 1a for genotypic combinations of partial SSU and partial COI). Unrooted ML and Bayesian trees generated for each of the three genes separately recovered always three major clades arranged in two subsequent bifurcations (data not shown). The same clades showed up in a phylogeny constructed with the concatenated partial sequences of the three genes (Fig. 1b) and were designated as groups 1, 2a, and 2b, comprising 9, 9, and 3 three-gene genotypes, respectively.

Various associations (1:1, 1:n, and n:n) of partial SSU and partial COI genotypes were observed within but never among these three groups (Fig. 1a). In contrast, partial EF1A sequences exhibited only one genotype per group if three specimens with single-nucleotide polymorphisms in the

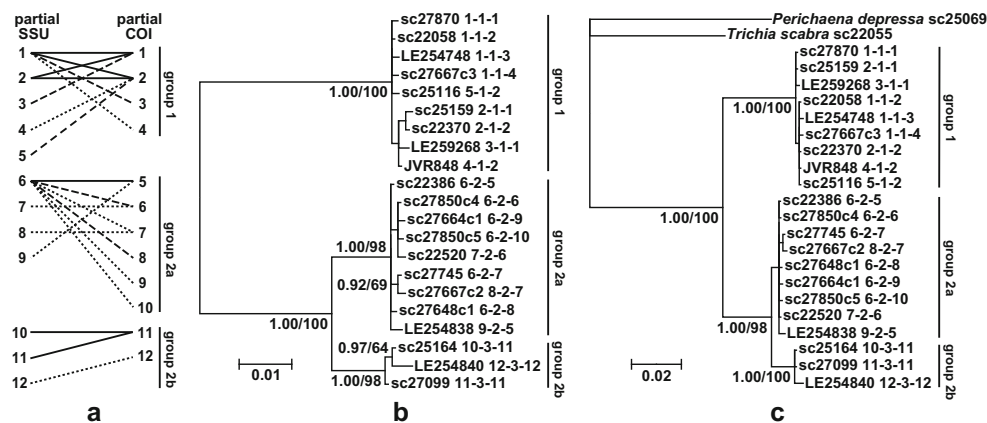


**Fig. 1** Three-gene phylogeny of *Trichia varia*. **a** Associations between partial SSU and partial COI genotypes within the three groups (1, 2a, 2b). Dotted lines indicate associations found in one specimen, dashed lines in two to five specimens, and solid lines more than five specimens. **b** Bayesian majority-rule consensus tree of combined partial sequences of

SSU, EF1A, and COI of *T. varia*. Shown is one representative specimen per three-gene genotype. **c** Bayesian majority-rule consensus tree of combined partial sequences rooted with *Perichaena depressa* and *Trichia scabra*. Bayesian posterior probabilities >0.70 and bootstrap replicates >50 are indicated

spliceosomal intron are neglected. Combining the three partial sequences to an alignment of 1282 sites, a fine-scale phylogenetic structure emerged within 21 three-gene genotypes (Fig. 1b). This structure was recovered as well in a rooted tree with *Perichaena depressa* and *T. scabra* as outgroup, where 1077 sites could be aligned (Fig. 1c). The bifurcation between groups 1 and 2a/2b is well resolved in both unrooted and rooted trees. Groups 2a and 2b receive high support only for the unrooted trees but show lower support values or unresolved structures for rooted Bayesian/ML trees (0.52/not resolved for group 2a, 1.00/100 for group 2b), most likely due to the reason that only a lower number of phylogenetically informative sites could be retained for the rooted trees.

### Geographic structure within *T. varia* three-gene genotypes

Correlation between genetic and geographic distances was extremely weak for partial SSU ( $r=-0.009$ ), partial COI ( $r=0.001$ ), and combined SSU and COI sequences ( $r=-0.005$ ), and these figures were always within the 95 % confidence intervals calculated for 999 matrix permutations. However, specimens of groups 1, 2a, and 2b were unevenly distributed among the major collection localities (Germany: Greifswald: 20/1/1; Hainich 25/0/3; Bavarian Forest 33/39/4; Russia: Caucasus, Teberda: 8/1/8; Novosibirsk 7/0/0; and Altai Mts. 12/3/3 specimens, see Supplementary Database S1). The three groups differed as well in mean elevation of the specimens (group 1, 429 m above sea level (a.s.l.),  $n=123$ ; 2a, 820 m,  $n=49$ ; 2b, 748 m,  $n=25$ ), and the differences were significant between group 1 and the two other groups ( $p=0.05$ ; unpaired non-tailed Student's *t* test).

### Phylogenetic position of *T. varia* within bright-spored myxomycetes revealed by complete SSU

Our second data set, comprising 66 complete SSU sequences (7, 35, and 24 for specimens belonging to groups 1, 2a, and 2b, respectively), was used to ascertain the position of the three groups within the phylogeny of Fiore-Donno et al. (2013) constructed for bright-spored myxomycetes. This phylogeny takes only 1325 exon sites into account which are alignable over the sampling of bright-spored myxomycete species and resulted in a fully supported monophyletic clade with seven different exon genotypes for the 66 specimens of *T. varia* (TreeBASE: M30970; three, three, and one genotype for groups 1, 2a, and 2b, respectively). Both ML and Bayesian trees showed identical topology but slightly different levels of support for each internal node (Supplementary Fig. S1). *T. varia* appeared in the clade “*Trichia* and allied genera” identified by Fiore-Donno et al. (2013) which is now better resolved than in the original phylogeny for both ML and Bayesian trees. The well-supported subclade uniting all sequences of *T. varia* was placed at the basal position, being sister to the other members of this clade which received moderate or high level of support in ML and Bayesian trees, respectively. Within the subclade *T. varia*, two sister clades were identified with high level of support, corresponding to groups 1 and 2a/2b in the three-gene phylogeny constructed with the first data set.

### Polymorphisms within complete SSU sequences of *T. varia*

Considering the complete SSU sequences of the 66 specimens from *T. varia*, we observed 33–34 genotypes (the uncertainty is due to a part of the sequence we could not obtain for three specimens of group 1) for the exon parts, but 54 genotypes if

both exon and intron parts are considered (Fig. 2). Eight genotypes were represented by more than one specimen, often from different localities (Supplementary Table S1).

Exon genotypic diversity differs strongly within groups; the relation of specimens to exon genotypes is 7:5–6 for group 1 (three sequences incomplete), 35:10 for group 2a, and 24:18 for group 2b. If introns are considered, these relations increase to 7:6, 35:30, and 24:18, respectively. Figure 2 shows within-group variations in exon sequences. Genetic distances between exons from distinct SSU genotypes are much smaller in groups 1 and 2a than in group 2b, and traces of recombination events were detected for the latter group only (Table 2). ML and Bayesian trees constructed using exon parts (Supplementary Fig. S2) recovered the same three groups (1, 2a, 2b) found for the phylogeny of three partial genes constructed with the first data set.

Four specimens displayed polymorphisms in their SSU sequences. To verify their source and to exclude the possibility of DNA contaminations caused by spores of other *T. varia* specimens, a nested PCR was performed from a single spore; with the first reaction targeting the complete SSU region and a second targeting two partial regions covering the polymorphic sites. This confirmed the heterogeneous state of SSU sequences for one specimen (sc27667c1) from group 2a in both exon and intron parts and three specimens (sc22413, sc22503, sc27657) from group 2b in exon parts: The partial sequences derived from single spores still displayed the same polymorphic patterns (double peaks in chromatograms) as seen in complete sequences from sporocarps. Nucleotides found for polymorphic sites were always identical with those occurring at corresponding sites of other homogeneous sequences from the same group (Fig. 2). In addition, homogeneous SSU sequences were obtained by single-spore PCR conducted in parallel from three of these specimens (except for sc22503).

### Introns in the SSU sequence of *T. varia*

Each investigated specimen of groups 1 and 2a contained at least one putative group I intron (Fig. 2). Altogether, six insertion positions were found (516, 529, 911, 956, 1199, and 1389; positions numbered in accordance with the *Escherichia coli* 16S ribosomal RNA gene). In group 1, introns can occur at all positions except for 1199; in group 2a, all positions except for 529 may be occupied. Group 2b was devoid of introns. PCR reactions with the primers NUSSUF6 and NUSSUR11 targeting the potential insertion position 1199 were conducted for 18 additional specimens from group 1, and gel band patterns confirmed that S1199 introns were consistently absent in this group (data not shown). Altogether, 48 distinct intron sequences could be distinguished in *T. varia*: 12 in group 1 and 36 in group 2a.

Pairwise genetic distances between S911 and S956 introns from group 2a were higher than those for the other three

positions. Traces from recombination events were detected in S911 and S956 introns but not in introns at other positions (Table 2). A set of specimens showing identical intron sequences at one position always differed in intron sequences at other positions. For 25 specimens of group 2a (excluding specimen sc27667c1 with heterogeneous intron sequences at positions S911 and S1199, and excluding specimens sc27737, sc27772c2, LE254838, and LE256579 with long introns), figures for two indices of association  $I_A^S$  and rBarD (both ranging from 0 to 1) were 0.0638 and 0.0631, respectively. The null hypothesis, assuming a complete random association, was nevertheless rejected with *p* values of 0.0087 and 0.0073, respectively.

Similarity searches on conserved motifs were used to assign group I introns in SSU of *T. varia* to classes IC1 and IE. S529 introns from group 1 could not be sequenced completely and were thus not classified. For intron-carrying groups of *T. varia*, the following pattern (group/intron class) emerged: S516: 1/IC1, 2a/IC1; S529: 1/?, 2a/none; S911: 1/IC1, 2a/IC1; S956: 1/IC1, 2a/IE; S1199: 1/none, 2a/IC1; and S1389: 1/IC1, 2a/IC1. In addition, we found both putatively functional and degenerated homing endonuclease genes at all insertion positions except for position 529 (Fig. 3).

Remarkable is the bipartite distribution of S956 introns, which was found as well for numerous species of both bright- and dark-spored myxomycetes (Fig. 4 and Supplementary Table S2). These two major phylogenetic groups possess each introns assigned to classes IC1 and IE, and their distribution does not coincide with myxomycete phylogeny. Within several genera (e.g., *Cribraria*, *Colloderma*, *Diachea*, *Lamproderma*, and *Lepidoderma*), IC1 and IE introns coexist. Similar to *T. varia* showing class IC1 introns in group 1 but class IE introns in group 2a, both intron classes were as well represented by two specimens of the dark-spored myxomycete *Lamproderma puncticulatum* (Fiore-Donno et al. 2011).

**Fig. 2** Variations in 54 genotypes of the complete SSU sequences derived from 66 specimens of *Trichia varia*. The first six columns indicate collection number, locality code, assignment to groups 1, 2a, and 2b, the SSU genotype (numbered 1–54), the exon genotype (1–33), and the number of specimens per SSU genotype (for genotypes represented by multiple specimens, see Supplementary Table S1 for all collection numbers and localities). Exon positions showing within-group variation are annotated. Intron groups are color-coded for the six insertion positions (letters A–F) and intron genotypes (numbers 1–14), with zero indicating the absence of an intron. Positions of the intron were numbered in accordance with the *Escherichia coli* 16S ribosomal RNA gene. Numbers in the table head indicate positions according to the alignment TreeBASE: M30975. Introns occupy the following positions: S516, 579–1727; S529, 1741–3046; S911, 3700–4986; S956, 5032–6313; S1199, 6624–7885; and S1389, 8081–9656. The symbols *filled square* and *open square* indicate introns with full or with remnants of putative homing endonuclease genes. Comments: <sup>a</sup>heterogeneous state, <sup>b</sup>incomplete due to missing data, <sup>c</sup>presence/absence not certain due to missing data, <sup>d</sup>abbreviation of location shown in Supplementary Table S1, and <sup>e</sup>number of specimens with identical SSU genotype



**Table 2** Analysis of complete SSU sequences of *Trichia varia*

Group	Region	Length (bp) <sup>a</sup>	ORF (bp) <sup>a</sup>	Average distance <sup>b,c</sup>	PHI test <sup>e</sup>	
					Informative sites <sup>c,d</sup>	<i>p</i> value
Exon parts (complete gene)						
1		1819/3	–	0.00124/7	1/5	–
1		>1460/1	–			
1		>1573/2	–			
2a		1809/10	–	0.00071/34	4/9	0.958
2b		1807/18	–	0.00217/21	7/15	*0.020
Intron parts (position)						
1	S516	482/1	21/1	–	–	–
1	S516	1145/2	683/2	–	–	–
1	S529	>786/1	–	–	–	–
1	S529	>1269/1	–	–	–	–
1	S529	>1305/1	–	–	–	–
1	S911	494/2	–	–	–	–
1	S956	>850/2	–	–	–	–
1	S956	1281/1	–	–	–	–
1	S1389	586/1	–	–	–	–
1	S1389	1531/1	779/1	–	–	–
2a	S516	443/4	–	0.00454/4	0/4	–
2a	S911	507/11	–	0.01051/11	8/11	*0.014
2a	S911	1265/1	675/1	–	–	–
2a	S956	450/7	47/7	0.01026/8	6/8	*0.039
2a	S956	1230/1	813/1	–	–	–
2a	S1199	531/6	–	0.00455/6	3/6	1.000
2a	S1199	1262/1	519/1	–	–	–
2a	S1389	559/4	–	0.00541/5	1/5	–
2a	S1389	1544/1	797/1	–	–	–

Length, possible open reading frames (ORFs), and average pairwise within-group distances are shown for exon and intron parts of the three major phylogenetic groups in *Trichia varia*. The number of sequences considered for the figures given is indicated after a slash

ORF open reading frame, PHI pairwise homoplasy index

\*Statistically significant with the threshold value 0.05

<sup>a</sup> Only minimum length given due to incomplete sequences; specimens with identical sequences were counted only once

<sup>b</sup> For introns, specimens with identical sequences were counted only once

<sup>c</sup> Excluding sequences containing polymorphic sites

<sup>d</sup> Excluding intron sections coding for homing endonuclease genes in specimens sc27772c2 (S911), sc27737 (S956), LE256579 (S1199), and LE253838 (S1389)

<sup>e</sup> PHI test: Bruen et al. 2006

genotype (17) differ in their COI genotypes (5 and 7, see Supplementary Table S1 and Supplementary Database S1); these are 500 km apart (French Jura/Bavarian Forest).

In seven cases, all investigated markers were identical for multiple specimens (Supplementary Table S1; Supplementary Database S1). In five cases, the two to five specimens came from the same collecting site and are separated over distances of less than 0.6 km (three cases) and 6 km (two cases). However, in two cases, identical genotypes were found over distances of 604 km (France/southern Germany) and 605 km (Netherlands/northern Germany).

### Intron-encoded homing endonuclease genes in *T. varia* and other myxomycetes

All group I introns at the six insertion positions identified for *T. varia* can carry putative full-length HEGs (Figs. 2 and 3); we only failed to detect them at position S529 (uncertain due to incomplete SSU sequences). Within introns of *T. varia*, remnants of ORF were identified in a 21-bp region of S516 introns (sites 597–618 in the alignment TreeBASE: M30975) from one specimen of group 1 and in a 47-bp region of S956 introns (sites 5089–5135 in the alignment TreeBASE: M30975) from 22

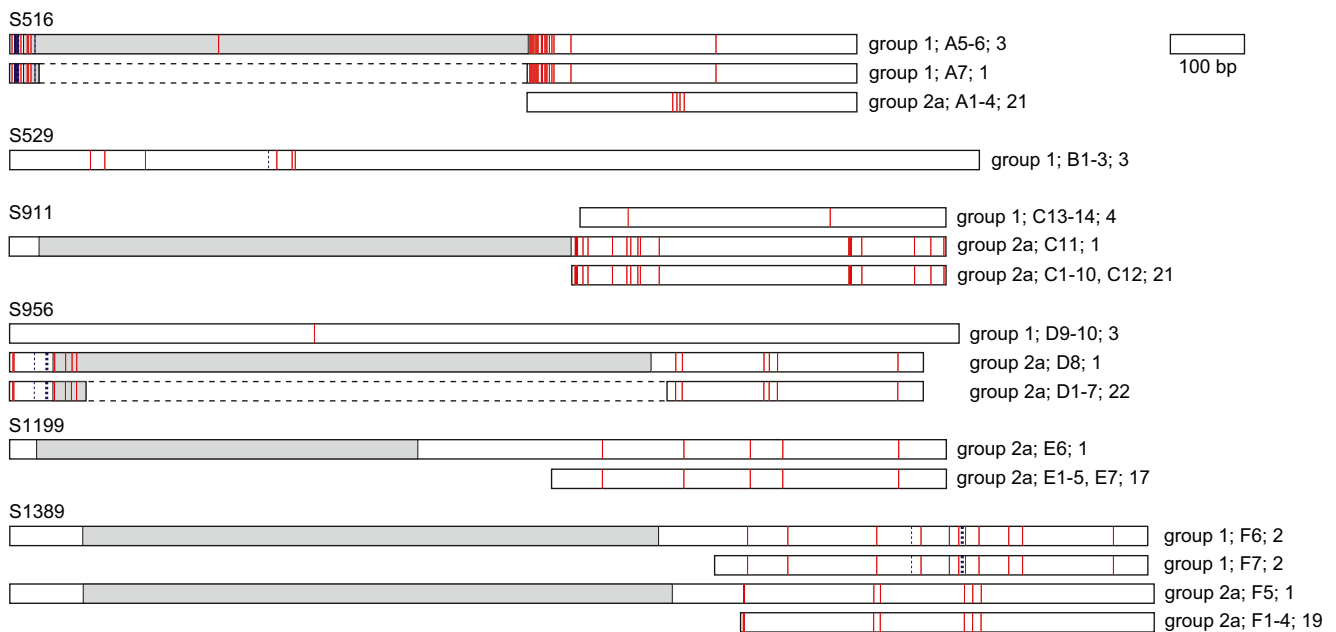


**Fig. 3** Intron types found in 66 specimens of *Trichia varia* at six insertion positions. For each of the phylogroups 1 and 2a, introns are drawn to scale as horizontal bars. *White sections* denote intron sequences and *gray sections* homing endonuclease genes. *Red/solid* and

*blue/broken vertical lines* indicate the approximate location of sites with point mutations and one-base indels, respectively. *Columns at the right* indicate the phylogroup, the intron genotype according to the codes used in Fig. 2, and the number of specimens sharing it (Color figure online)

specimens of group 2a (Fig. 2). Both ORF remnants are homologous to the first part of the corresponding HEGs found at these positions in other specimens of *T. varia*.

Using all available data, we assembled an HE protein alignment from 22 putative HEGs of Amoebozoa (Supplementary Alignment S6). We included nine HEGs found in published SSU sequences of myxomycetes (Fiore-Donno et al. 2005, 2008, 2012, 2013; Nandipati et al. 2012). Seven new sequences for HEGs were found in *T. varia*, of which the two HEGs found in S516 introns of group 1 differ by one nucleotide which translates into a different amino acid (Table 3; Supplementary Alignment S6). Existing literature reports one HEG inserted in the S1199 intron of *Diderma niveum* (Hedberg and Johansen 2013), and one in the S516 intron of *Echinostelium coelocephalum* (Brown et al. 2012). Four HEGs were already described and tested for functionality (two in the S956 intron of *Didymium iridis*, I-DirI and I-DirII, Haugen et al. 2005b; Johansen et al. 1997; one in the group I intron L1925 from the nuclear large subunit ribosomal RNA gene of *Physarum polycephalum*, I-PpoI, Muscarella et al. 1990; one in the S516 intron of *N. jamiesoni*, I-NjaI, Johansen et al. 1993). Two putative HEGs were not included in our analysis, since the high level of variation in sequences did not allow to align them. These are HEGs in the S529 intron of *Diderma niveum* (Hedberg and Johansen 2013) and in the S788 intron of *Meriderma fuscatum* (Fiore-Donno et al. 2008).

Except for HEG from L1925 of *Physarum polycephalum* and HEG from S516 of *N. jamiesoni*, 20 HEGs from SSU sequences of myxomycetes remain. Of these, 4 (all in S956

introns) were found in antisense strands while the other 16 (various insertion positions) were detected in sense strands. Their host introns classify as both IC1 (16) and IE (4). The latter were all inserted in sense strands at position 956 (see Fig. 5 for intron directions and classes). Frameshifts were observed in ten HEGs (see Table 3 for range of ORFs). Three HEGs found at position 956 (*Diderma meyeriae*, *Diachea subsessilis*, *Elaeomyxa cerifera*) have frameshifts located at the same region where in I-DirI and I-DirII nested spliceosomal introns were found (Haugen et al. 2005b; Vader et al. 1999) suggesting that spliceosomal introns might as well be nested in these HEGs. These regions were not included in protein sequences translated from ORFs, which were used for the phylogenetic analysis.

Using I-PpoI from L1925 of *Physarum polycephalum* as the outgroup, we constructed a phylogeny of the 22 alignable HE protein sequences (Fig. 5). Both the ML tree and the Bayesian tree revealed similar topologies. HEGs from antisense strands (S956 introns, class IC1) and HEGs from sense strands form two separate, strongly supported clades. HEGs from S956 introns are located within two separate clades, consistent with their differences in sense/antisense insertion and classes of the host intron (IC1/IE). Within the clade uniting all sense-inserted HEGs, two subclades are resolved with high support in the Bayesian tree but not in the ML tree, and the single HEG from S1065 shifted its position between Bayesian and ML trees. Usually, HEGs coming from one insertion position cluster together, but this is not the case, if the respective hosts come from different groups of myxomycetes (dark- or bright-spored).

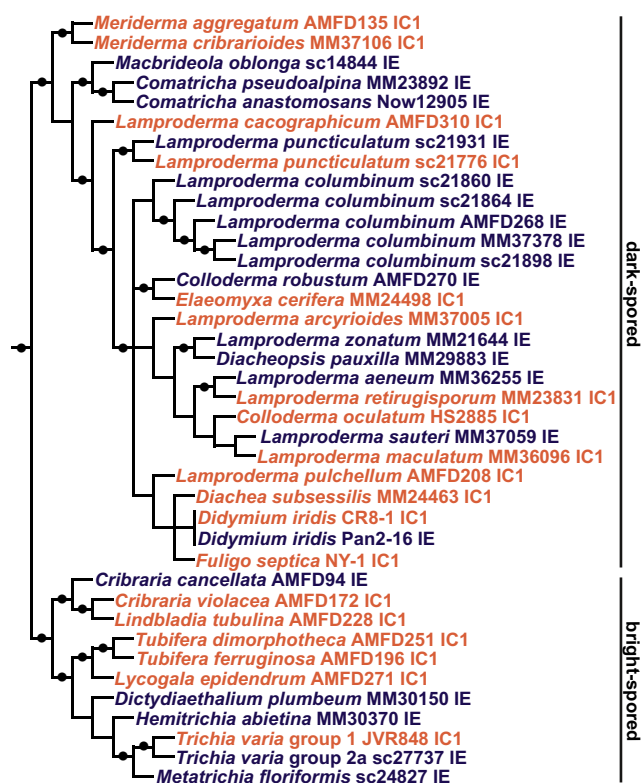


**Fig. 4** Simplified SSU phylogeny showing distribution of IC1 and IE class introns at position S956 in myxomycetes. Tree topology was derived from published SSU phylogenies (Fiore-Donno et al. 2010, 2012, 2013) and the tree presented in Supplementary Fig. S1 of this study. *Trichia varia* group 1 is represented by a specimen with an intron lacking an HEG; group 2a is represented by a specimen with a HEG-containing intron. Taxa printed in red and marked with “IC1” carry IC1 introns; those printed in blue and marked with “IE” carry IE introns. Nodes marked by dots received support of both Bayesian posterior probability >0.70 and bootstrap replicates >50 (Color figure online)

## Discussion

### Cryptic speciation in *T. varia*

Based on its unique capillitium morphology, *T. varia* was always seen as a well-defined taxon. Although the taxonomic database Nomenmyx (Lado 2005–2014) lists not less than 13 heterotypic synonyms (all but one described before 1930), based on sporocarp morphology no intraspecific taxa are currently accepted. All recent monographs (Martin and Alexopoulos 1969; Nannenga-Bremekamp 1991; Neubert et al. 1993; Poulain et al. 2011) treat *T. varia* as a single, yet variable species. This was confirmed using 1325 exon sites of complete SSU sequences (Supplementary Fig. S1): All investigated specimens of *T. varia* were united within a single clade of the phylogeny of bright-spored myxomycetes. The detailed analysis resolved three phylogenetic groups (1, 2a, 2b) occurring in both data sets assembled by us: the three-gene phylogeny of partial SSU, partial EF1A, and partial COI (Fig. 1), as

well as the exon parts of complete SSU sequences (1825 sites; Supplementary Fig. S2).

A subsample of 21 specimens from all three groups revealed no significant differences in stalk length (reaching from sessile to shortly stalked sporocarps), spore ornamentation and size, and capillitium diameter (data not shown). In-depth morphological investigations, including analyses of spore and capillitium ornamentation with scanning electron microscopy, will be needed to test for morphological differences between the three taxa, which we see as a prerequisite for their formal description.

These phylogenetic and morphological results are explained best by viewing the phylogenetic groups 1, 2a, and 2b as cryptic taxa within the morphospecies *T. varia*, a hypothesis unknowingly suggested in the choice of the basionym by Persoon (1794). Intraspecific genetic structure was found as well for north- and south-hemispheric populations of *Badhamia melanospora* (Aguilar et al. 2013), although a tree constructed of partial SSU sequences only did not resolve the respective clades. This dark-spored myxomycete occurs nearly exclusively on decayed tissues of succulent plants. For the three gene markers applied to the less specialized *T. varia*, we can clearly demonstrate cryptic speciation but did not find a clear-cut geographical structure in the investigated metapopulation. Specimens of group 1 were rarely found at higher elevations, but all three groups may share the same microhabitat: moderately to well-decayed white rotten logs, preferentially of deciduous trees. In three cases, specimens from different groups were collected on the same log (sc27648c1/2a and sc27648c2/1; sc27664c1/2a and sc27664c3/1; and sc27667c1/2a, sc27667c2/2a, and sc27667c3/1).

### Sexual biospecies in *T. varia*

For *T. varia*, we employed three virtually independent markers for the first data set of 198 specimens. SSU genes are organized in extrachromosomal units (Torres-Machorro et al. 2010); crosses between strains show a progressive increase of one parental type within the vegetative phase of the growing plasmodium (Ferris et al. 1983). The inheritance of mitochondrial DNA of *Physarum polycephalum* is mostly uniparental with the choice of donor and recipient determined by a dominance hierarchy depending on the mating type locus (Moriyama and Kawano 2010). For the nuclear single-copy gene EF1A, we assume Mendelian inheritance. Given similar relationships in *T. varia*, the three chosen markers should be independently inherited except for the point that nuclear genes expressing the mating types have some control over COI inheritance.

For partial sequences of SSU, COI, and EF1A, we recorded 5/4/3, 4/6/2, and 1/1/1 genotypes for the three groups 1, 2a, and 2b, respectively. The three groups share none of these



**Table 3** Putative homing endonuclease genes identified in myxomycetes

Species	Specimen/isolate	Intron	Class	Strand	ORF range	SSU accession number (GenBank)	Reference
<i>Echinostelium coelocephalum</i>	ATCC MYA-2964	S516	IC1	Sense	16–222, 224–262, 264–647	AY842033	Fiore-Donno et al. (2005)
<i>Lamproderma pseudomaculatum</i>	MM37354	S516	IC1	Sense	15–302, 304–636	JQ031985	Fiore-Donno et al. (2012)
<i>Trichia varia</i> (1)	sc22370	S516	IC1	Sense	19–264, 267–701	KM494993;	this study
<i>Trichia varia</i> (1)	LE259268; LE259461	S516	IC1	Sense	19–264, 267–701	KM494994; KM494995	this study
<i>Diachea subsessilis</i>	MM24463	S911	IC1	Sense	48–716	JQ031964	Fiore-Donno et al. (2012)
<i>Trichia varia</i> (2a)	sc27772c2	S911	IC1	Sense	41–715	KM495028	this study
<i>Dictydiaethalium plumbeum</i>	MM30150	S956	IE	Sense	102–848	JX481292	Fiore-Donno et al. (2013)
<i>Diderma meyeriae</i>	It-K61	S956	IE	Sense	36–338, 352–891	HE614614	Nandipati et al. (2012)
<i>Trichia varia</i> (2a)	sc27737	S956	IE	Sense	55–867	KM495020	this study
<i>Diachea subsessilis</i>	MM24463	S956	IC1	Antisense	1061–714, 691–347	JQ031964	Fiore-Donno et al. (2012)
<i>Elaeomyxa cerifera</i>	MM24498	S956	IC1	Antisense	1072–749, 722–363	JQ031967	Fiore-Donno et al. (2012)
<i>Meriderma aggregatum</i>	AMFD135	S956	IC1	Antisense	979–809, 806–465	DQ903669	Fiore-Donno et al. (2008)
<i>Colloderma robustum</i>	AMFD270	S1065	IC1	Sense	664–1689	JQ031960	Fiore-Donno et al. (2012)
<i>Diderma niveum</i>	It-K66	S1199	IC1	Sense	37–681	HE614616	Nandipati et al. (2012)
<i>Lepidoderma tigrinum</i>	AMFD192	S1199	IC1	Sense	20–676	DQ903678	Fiore-Donno et al. (2008)
<i>Trichia varia</i> (2a)	LE256579	S1199	IC1	Sense	36–554	KM495031	this study
<i>Trichia varia</i> (1)	sc22370; JVR848	S1389	IC1	Sense	98–520, 523–876	KM494993; KM494996	this study
<i>Trichia varia</i> (2a)	LE254838	S1389	IC1	Sense	99–458, 460–895	KM495030	this study

For sequences of *Trichia varia* studied by us, the assignment to group 1 or 2a is given  
ORF open reading frame, SSU small-subunit rDNA

genotypes, indicating missing gene flow and thus reproductive isolation. If association between two partial genes mediated by sexual reproduction would not be involved, mutation alone is unlikely to create the recurrent n:n association between the most common two partial SSU genotypes and two partial COI genotypes in group 1 (Fig. 1a). Only EF1A displays one genotype per group (not considering single-base heterozygosities within the short spliceosomal intron in three specimens which are likely to result from point mutations). We thus can assume that sexual reproduction is responsible for the exchange of single-marker genotypes between individuals of the same group.

The second data set with complete SSU sequences lends as well evidence for sexual reproduction. We found four heterogeneous sequences, and as well as their homogeneous counterparts, which is easier to explain by recombination between multiple genotypes mediated by sexual reproduction than by assuming simultaneous mutations. This was confirmed by single-spore PCR. Even if we assume some investigated spores to be multinucleated as recently reported for *Physarum pseudonotabile* (Novozhilov et al. 2013a), different SSU genotypes must have existed in the plasmodium giving rise to these spores. Three of the four

heterogeneous specimens displayed additionally homogeneous SSU sequences in different PCRs from single spores. Although PCR conditions occasionally favor one SSU genotype over the other, a model of selective replication of a single SSU genotype is likely to be the best explanation for the coexistence of spores with heterogeneous and homogeneous SSU sequences in *T. varia*. This selection process takes place in each individual nucleus of the growing plasmodium but continues during meiosis (where only one of the four nuclei survives; Clark and Haskins 2013; Gray and Alexopoulos 1968), and even in germinating spores (Ferris et al. 1983). Our results of single-spore PCR in *T. varia* were not in conflict with this model and suggested further that one parental genotype seems to be completely eliminated in spores showing homogeneous sequences. In spores displaying heterogeneous sequences, elimination still continues. Individual spores of one specimen are not synchronized regarding this elimination process. Therefore, the occurrence of heterogeneous SSU sequences can be seen as a trace of recent sexual events.

In addition, variation in both group I introns and exon parts of complete SSU sequences points toward sexual reproduction within each of three phylogroups of *T. varia*. The seven

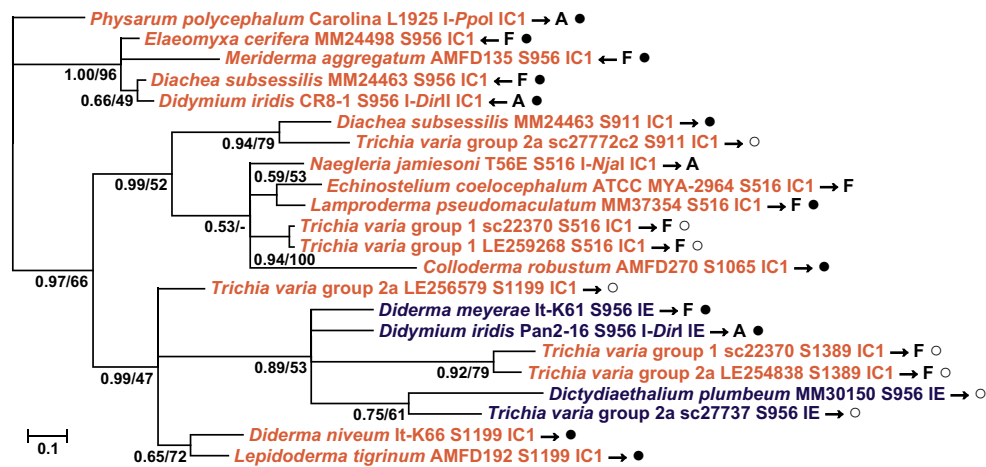


**Fig. 5** Bayesian majority-rule consensus tree of protein sequences from homing endonuclease genes of myxomycetes. The tree is rooted with I-PpoI from the L1925 intron of *Physarum polycephalum*. Support values are indicated for nodes with either Bayesian posterior probability >0.50 or bootstrap replicates >50, with the symbol “-” indicating topologies with branches deviating between Bayesian and ML trees. Taxa printed in red

carry IC1, and those printed in blue IE introns as HEG hosts. Additional symbols: IC1=IC1 introns as HEG hosts, IE=IE introns as HEG hosts, rightward arrow sense strand, leftward arrow antisense strand, A=protein with experimentally confirmed enzymatic activity, F=frameshift, open circle bright-spored myxomycetes, filled circle dark-spored myxomycetes (Color figure online)

specimens of group 1 constitute a small sample not sufficient to test for recombination, although the introns appear to be randomly distributed (Fig. 2). For the 35 specimens from group 2a, the near-random association of HEG-lacking introns in group 2a specimens (low values of both the  $I_A^S$  and rBarD indices) indicates that within-group homologous recombination between extrachromosomal ribosomal DNAs mediated by sexual reproduction effectively breaks down associations among intron sequences. Another possible cause for the near-random association of HEG-lacking introns is intron homing via reverse splicing, which as well requires different SSU genotypes being brought together by sexual reproduction. Signals of recombination were detected in the entire introns of this group (positions 911 and 956), indicating that homologous recombination between extrachromosomal ribosomal DNAs mediated by sexual reproduction had occurred. Specimens of group 2b uniformly lack introns, but exon regions of the complete SSU show as well signals of recombination (Table 2).

Furthermore, patterns of SSU group I intron distribution provide convincing evidence for reproductive isolation between the three groups. Although all groups possess identical recognition sequences for intron insertion at all six insertion positions, groups 1 and 2a lack introns at different positions (529 vs 1199), none of the intron sequences found at the commonly occupied positions (516, 911, 956, and 1389) occurs in both groups, and group 2b is devoid of any introns (Fig. 2). The HEGs in the single position (1389) common to both intron-bearing groups of *T. varia* cluster as well together but are highly divergent from each other (Fig. 3; TreeBASE: M30976). We thus assume that reproductive isolation prevents inter-group intron homing among three groups of *T. varia*.

Summarizing, the patterns of partial SSU and COI genotypes, heterogeneities and recombination signals in complete SSU sequences, and group I intron distribution provide strong evidence that the three groups (1, 2a, 2b) of *T. varia* represent three biospecies which reproduce predominantly sexual. Similarly, a rapid decay of linkage disequilibrium was found for single-nucleotide polymorphisms from 137 gene fragments of wild North American strains of the cellular slime mold *Dictyostelium discoideum*, pointing to frequent sexual reproduction (Flowers et al. 2010). These results fit into the pattern of postulated widespread sexuality in Amoebozoa (Lahr et al. 2011b).

Our study demonstrates that the biospecies concept derived from case studies with cultivable myxomycetes is applicable in nature. Crossing experiments with several dark-spored myxomycetes (Clark and Haskins 2013) indicated the existence of several biospecies within a single morphospecies, as it was the single crossing experiment targeting a bright-spored species (*Arcyria cinerea*; Clark et al. 2002).

#### Asexual strains in *T. varia*?

A recent study investigating partial SSU, ITS1, and partial EF1A sequences in natural populations of the dark-spored myxomycetes *Lamproderma columbinum* and *L. puncticulatum* (Fiore-Donno et al. 2011) found groups showing identical sequences in all three markers which can be interpreted as evidence for missing or rare sexual reproduction. However, only exon sequences of SSU were considered for this study, and SSU and ITS1 markers are not independently inherited since both are linked together in one extrachromosomal molecule (Torres-Machorro et al. 2010). In

addition, genotypic diversity for partial SSU sequences in *Lamproderma* (with a relation of specimens to genotypes of 52:11) was lower than for complete SSU in this study (66:54). When the resolution of markers is low, the observation of identical sequences in independently inherited markers is conformable with, but does not prove complete absence of recombination. Due to the lower genotypic diversity of the three (effectively two) independent markers in *Lamproderma*, this study may have failed to detect recombination; thus, the observed identical sequences in these markers evidence but do not prove asexual reproduction.

In the first data set composed of partial SSU, COI, and EF1A sequences of *T. varia*, we found among 198 specimens only 21 multilocus genotypes. With 66 specimens and 54 genotypes, our second data set of complete SSU sequences is much more polymorphic. Adding non-overlapping sequences from the first data set would only marginally enhance resolution: two specimens with the same complete SSU genotype displayed different COI sequences. Similar to the study of Fiore-Donno et al. (2011), we found as well seven cases with multiple specimens identical in all investigated markers (Supplementary Table S1; Supplementary Database S1). Two of these cases involved two identical specimens collected at distances exceeding 600 km. Therefore, the question remains if asexual strains, completing their life cycle without syngamy, occur in natural myxomycete populations of *T. varia*.

We must assume that amoebae divide by fission and can form large clonal populations. According to the sexual life cycle depicted in most textbooks, amoebal syngamy is a prerequisite for entering the next life stage, the diploid plasmodium, and finally the formation of fruit bodies. If this holds true, haploid amoebal clones cannot be detected by a study based on sequences from fruit bodies, since plasmodia and fruit bodies require prior syngamy of amoebae. With this approach, including whole cohorts of spores, all paternal alleles will be resampled. In theory, heterogeneous sequences can occur if different alleles coexist in one fruit body. However, extrachromosomal SSU and mitochondrial COI will quickly become uniform, since one genotype will be eliminated (Ferris et al. 1983; Moriyama and Kawano 2010), and EF1A alone was found to be monomorphic in each of the three groups found within *T. varia*. This explains why we found only exceptional heterogeneous (SSU) or heterozygous (EF1A) sequences in *T. varia*.

Nevertheless, panmictic sexual reproduction should result in different genotypic combinations of multiple marker genes if they are (i) sufficiently polymorphic and (ii) independently inherited. Even then, repeated pairings within two widespread amoebal clones will produce the same multilocus genotype. The same holds true for the separation of a plasmodium into multiple parts, which migrate and fruit at different places. The five cases involving distances below 6 km with identical

multiple markers may be explained by migrating amoebae or microcysts (mating repeatedly and thus producing the same genotype) and/or plasmodia (which may segregate and migrate independently). As such, this may as well be explained without assuming the existence of a second, asexual life cycle proposed in Clark and Haskins (2010) to explain the occurrence of non-heterothallic isolates.

The two cases of identical multilocus genotypes in *T. varia* occurring more than 600 km apart are difficult to explain by assuming migration of amoebae, microcysts, or plasmodia. But, we only found one extremely polymorphic marker, complete SSU sequences with their introns. In this marker, one of two different SSU genotypes which may be combined via amoebal syngamy is subsequently eliminated. Spores, which may bridge large distances, usually transport only one SSU genotype. Given the much lower variation in the other two markers (COI and EF1A), this increases the probability that identical multilocus genotypes occur by chance at two distant locations. We thus hesitate to take the two cases of identical multilocus genotypes involving specimens from distant locations as proof for the existence of asexual strains in nature. Viewing these results from the other side (different genotypic combinations of multiple markers, signs of recombination, intron patterns), we can conclude that sexual reproduction is at least the prevailing mode of reproduction in natural populations of *T. varia*.

### Intron evolution in *T. varia*

Why do species of group 2b lack any group I introns but assume an intermediate position in all intraspecific phylogenies constructed for *T. varia*? Similar to the “intron early” and “intron late” scenarios proposed for red and brown algae (Bhattacharya et al. 2001), group 2b may represent either a lineage with empty insertion sites after precise intron loss or it has yet not encountered any intron-homing event. Changes in reproductive strategy (conversion from sexual to asexual reproduction) would fit with the “intron early” scenario: group 2a and 2b share an ancestor being sister to group 1, and both groups 1 and 2a still maintain HEGs and their host introns in various states. In this case, intron sequence variation between groups 1 and 2a should be interpreted as divergence after speciation. In non-heterothallic isolates, selfing (theoretically possible if the mating system collapses) or automixis can occur; such an asexual cycle was proposed by Clark and Haskins (2010). This should disfavor the preservation of HEGs and host introns, in contrast to outcrossing that increases frequency of HEGs in populations (Goddard et al. 2001). However, the observation of heterogeneous SSU sequences in three specimens of group 2b points toward outcrossing (intact sexual cycle controlled by mating types). The alternative scenario (intron late, no intron homing has yet occurred) is as well supported by S956 intron classification.

Our phylogeny of HE proteins known from myxomycetes (Fig. 5) displays two separate clades for S956 HEGs hosted in antisense strand of IC1 introns and HEGs hosted in sense strand of IE introns (the HEG at S956 from group 2a locates in the latter clade). HEGs in myxomycetes display a conserved His-Cys box, whereas free-standing HEGs (capable of moving without their host introns) from bacteria and phages show the motifs GIY-YIG or H-N-H (Hafez and Hausner 2012). We thus assume that myxomycete HEGs move together with their host introns, although exceptions were discussed (Haugen et al. 2005a, b). Joint evolution of HEGs and intronic hosts is as well suggested by the HEG phylogeny: S956 IE introns with HEG in sense strand of group 2a, and HEG-lacking S956 IC1 introns of group 1 were likely acquired from different sources, even if we did not find an example for an S956 HEG in group 1. Thus, the intron late scenario appears to be most likely: At least for insertion position 956, HEGs and host introns were not vertically inherited from the common ancestor of *T. varia* to groups 1 and 2a, but independently acquired by these groups after the divergence into groups 1, 2a, and 2b, and intron homing was not yet successful in group 2b.

### HEG and intron transmission in *T. varia*

Group I introns in *T. varia* belong to three categories: introns with full-length HEGs (with putatively functional HEGs at positions 911, 956, and 1199, or with putatively non-functional HEGs at positions 516 and 1389), introns with partial HEGs (with putative HEG remnants at positions 516 and 956), and introns without HEGs (Fig. 3). For several organisms, coexisting introns of several categories have been found, while additional specimens lack introns (Goddard et al. 2006; Haugen et al. 2005a; Koufopanou et al. 2002; Nielsen and Johansen 2009), which corroborates the intron life cycle model (Goddard and Burt 1999; Gogarten and Hilario 2006). All five intron positions found to be occupied by HEGs in *T. varia* groups 1 and 2a would fit into this model.

Except for their HEG sequences in different stages of degeneration, all introns occurring in group 1 and 2a specimens can be unambiguously aligned for each group and insertion position, since only point mutations generate differences in intron sequences. This suggests that introns were acquired independently for each group and position from one common ancestor by lateral transfer from lineages outside the population of *T. varia* investigated herein.

If two amoebae mate, transmission of introns may be accomplished via sexual events by intron homing at the DNA level mediated by HE or at the RNA level through reverse splicing (Haugen et al. 2005a; Lambowitz and Belfort 1993). In accordance with published hypotheses about group I intron transmission routes (Bhattacharya et al. 1996; Hibbett 1996; Johansen et al. 1992; Milstein et al. 2008; Nikoh and

Fukatsu 2001), HE-mediated intron homing via sexual events may have led to the current distribution of group I introns within natural populations for each of the groups 1 and 2a of *T. varia*. Identical or near-identical introns carrying HEGs at positions 516 and 1389 in multiple specimens of group 1 point toward HE-mediated transmission via sexual events.

Specimens of *T. varia* group 1 contain introns with HEGs at two positions, and for group 2a at four positions. Considering each position separately, the loss of HEG together with uniform deletion sites in the intron is unlikely to occur individually for each specimen. Most probably, HEGs were lost before introns spread vertically through inheritance within the population. Consequently, the transmission of introns was not mediated by HEGs. The same argument holds true for the lateral transfers of group I introns mediated by multiple reverse splicing instead of HEG within lineages in green algae and the fungal subphylum Pezizomycotina (Bhattacharya et al. 1996, 2005). Reverse splicing can as well be involved to explain sexually mediated transmission of introns to intronless individuals of group 2a. However, compared to HE-mediated intron homing, reverse splicing was suggested to work less efficient (Bhattacharya et al. 2005; Haugen et al. 2005a). For introns without putatively functional HEGs of *T. varia* group 2a, both mutation and recombination might have led to the current distribution pattern of introns. Recombination as one of the mechanisms shaping the distribution of group I introns had been discussed for lichens (DePriest 1993). In group 2a, recombination is likely to contribute: Recombination signals were detected in introns S911 and S956, and intron sequences assume a near-random association among all five insertion positions. Introns might first have spread by vertical inheritance within individuals of group 2a; later mutations accumulated and created multiple intron genotypes at each position (Fig. 3). Subsequently, introns might be gained via reverse splicing or be lost in a precise way by resuming the original insertion recognition sequences through reverse transcription of spliced RNAs (Dujon 1989), and simultaneously, recombination events may have led to individuals with a different set of intron sequences across all five positions. The current distribution of HEG-lacking group I introns in *T. varia* group 2a might be a result of dynamic interactions involving mutation and recombination but involves less likely intron homing and loss through reverse splicing.

### S956 introns in myxomycetes

A published phylogeny of group I introns sampled from various organisms (Haugen et al. 2005b) reveals that S956 introns in dark-spored myxomycete species belong to either the IC1 clade (*Didymium iridis*, *Fuligo septica*) or the IE clade (*Didymium iridis*, *Diderma meyeriae*). S956 introns from two isolates of the myxomycete *Didymium iridis* (CR8-1 from

Costa Rica and Pan2-16 from Panama) belong to classes IC1 and IE, respectively, but their SSU genes are identical in all exon parts. It was suggested that both introns have different evolutionary histories and were most likely acquired from different sources. Our phylogeny of all hitherto known S956 introns from myxomycetes (Fig. 4) demonstrates that distribution of IC1 and IE introns is not completely lineage-specific for both bright- and dark-spored myxomycetes, suggesting multiple acquisitions through lateral transmission during hybridization events in addition to vertical inheritance attributable to the spreading of IC1 and IE S956 introns, respectively. The HE protein phylogeny shown in Fig. 5 divided HEGs at S956 introns into two clades (inserted antisense in an IC1 intron, or sense in an IE intron). We found the division between HEGs with different reading directions (sense and antisense) to be deeper than the division between HEGs inserted into IC1 and IE introns, respectively. We thus can assume that two ancestral HEGs repeatedly and sporadically invaded different myxomycete lineages. Considering the more extensive sampling of HEG sequences done by us, the two HEGs reported for *Didymium iridis*, an antisense-IC1 in isolate CR8-1 and a sense-IE in isolate Pan2-16 (Haugen et al. 2005b), appear now to be distantly related.

Group I intron insertion recognition sequences in SSU are rather conserved across myxomycete lineages (see SSU alignments in Fiore-Donno et al. 2012, 2013), which may facilitate intron homing via lateral transmission between distantly related species, especially if given the tolerance of HE proteins against degeneracy within the recognition sequence (Hafez and Hausner 2012). In comparison to the relatively frequent lateral transmissions in S956 introns, as inferred from their assignment to classes IC1 and IE, introns at other positions might be as motile, but we lack a signature comparable to the IC1 and IE class assignment.

Intron homing events may result in the transfer of exon sections adjacent to the intron, as it was shown for the intron L1925 of *Physarum polycephalum* (Muscarella and Vogt 1989, 1993). In addition to possible homologous recombination in SSU during hybridization as inferred from the IC1/IE distribution in S956 introns of myxomycetes, the transfer of flanking exons by intron homing might be recorded as evolutionary history and introduce homoplasies into flanking exons that affect as well the resolution for SSU phylogenies of myxomycetes.

## Conclusions

Perhaps for their lacking economic importance, but as well due to the high variation in usually conserved markers which is common for protists (Pawlowski et al. 2012), the molecular age for myxomycetes dawned comparatively late. This is the first population genetic study targeting

a natural metapopulation of a myxomycete species with three independent markers and exploring group I intron distribution in SSU as a tool to elucidate speciation processes. For the investigated species *T. varia*, the most likely scenario is the existence of three reproductively isolated, yet predominantly or entirely sexual, biospecies. The comparatively low variation in EF1A sequences, and as well the absence of obvious morphological traits that distinguish these biospecies, point towards a recent speciation event. Patterns of intron distribution underline the reproductive isolation of these biospecies, and their homing endonuclease genes in various stages of decay point towards the existence of the Goddard-Burt cycle. As suggested by various authors (Hafez and Hausner 2012; Hausner et al. 2014), these genes may be universally distributed among eukaryotes.

**Acknowledgments** This research was supported by the Deutsche Forschungsgemeinschaft (DFG) to MS (SCHN 1080/2-1). The authors owe thanks for technical support to Anja Klahr, Greifswald. Fieldwork in the Bavarian Forest National Park was supported by Claus Bässler from the research unit of the park administration. We wish to thank Anna Maria Fiore-Donno for suggesting four primer sequences. For loans of specimens of *T. varia*, we are indebted to A.M. Fiore-Donno, Germany; Myriam de Haan, Belgium; Hans van Hooff, Netherlands; Yuri K. Novozhilov, Russia; Anna Ronikier, Poland; and Jos Van Roy, Belgium.

## References

- Adl, S. M., Simpson, A. G., Lane, C. E., Lukeš, J., Bass, D., Bowser, S. S., et al. (2012). The revised classification of eukaryotes. *Journal of Eukaryotic Microbiology*, 59, 429–493.
- Agapow, P. M., & Burt, A. (2001). Indices of multilocus linkage disequilibrium. *Molecular Ecology Notes*, 1, 101–102.
- Aguilar, M., Fiore-Donno, A. M., Lado, C., & Cavalier-Smith, T. (2013). Using environmental niche models to test the ‘everything is everywhere’ hypothesis for *Badhamia*. *The ISME Journal*, 8, 737–745.
- Altschul, S. F., Madden, T. L., Schäffer, A. A., Zhang, J., Zhang, Z., Miller, W., et al. (1997). Gapped BLAST and PSI-BLAST: a new generation of protein database search programs. *Nucleic Acids Research*, 25, 3389–3402.
- Betterley, D. A., & Collins, O. N. R. (1983). Reproductive systems, morphology, and genetical diversity in *Didymium iridis* (Myxomycetes). *Mycologia*, 75, 1044–1063.
- Bhattacharya, D., Friedl, T., & Damberger, S. (1996). Nuclear-encoded rDNA group I introns: origin and phylogenetic relationships of insertion site lineages in the green algae. *Molecular Biology and Evolution*, 13, 978–989.
- Bhattacharya, D., Cannone, J. J., & Gutell, R. R. (2001). Group I intron lateral transfer between red and brown algal ribosomal RNA. *Current Genetics*, 40, 82–90.
- Bhattacharya, D., Reeb, V., Simon, D. M., & Lutzoni, F. (2005). Phylogenetic analyses suggest reverse splicing spread of group I introns in fungal ribosomal DNA. *BMC Evolutionary Biology*, 5, 68.
- Brown, M. W., Silberman, J. D., & Spiegel, F. W. (2012). A contemporary evaluation of the acrasids (Acrasidae, Heterolobosea, Excavata). *European Journal of Protistology*, 48, 103–123.
- Bruen, T. C., Philippe, H., & Bryant, D. (2006). A simple and robust statistical test for detecting the presence of recombination. *Genetics*, 172, 2665–2681.

- Burke, J. M., Belfort, M., Cech, T. R., Davies, R. W., Schweyen, R. J., Shub, D. A., Szostak, J. W., & Tabak, H. F. (1987). Structural conventions for group I introns. *Nucleic Acids Research*, *15*, 7217–7221.
- Cannone, J. J., Subramanian, S., Schnare, M. N., Collett, J. R., D'Souza, L. M., Du, Y., et al. (2002). The Comparative RNA Web (CRW) Site: an online database of comparative sequence and structure information for ribosomal, intron, and other RNAs. *BMC Bioinformatics*, *3*, 2.
- Clark, J. (1993). *Didymium iridis* reproductive systems: additions and meiotic drive. *Mycologia*, *85*, 764–768.
- Clark, J. (1995). Myxomycete reproductive systems: additional information. *Mycologia*, *87*, 779–786.
- Clark, J. (2000). The species problem in the myxomycetes. *Stapfia*, *73*, 39–53.
- Clark, J., & Haskins, E. F. (2010). Reproductive systems in the myxomycetes: a review. *Mycosphere*, *1*, 337–353.
- Clark, J., & Haskins, E. F. (2011). Principles and protocols for genetical study of myxomycete reproductive systems and plasmidial coalescence. *Mycosphere*, *2*, 487–496.
- Clark, J., & Haskins, E. F. (2012). Plasmidial incompatibility in the myxomycetes: a review. *Mycosphere*, *3*, 131–141.
- Clark, J., & Haskins, E. F. (2013). The nuclear reproductive cycle in the myxomycetes: a review. *Mycosphere*, *4*, 233–248.
- Clark, J., Schnittler, M., & Stephenson, S. L. (2002). Biosystematics of the myxomycete *Arcyria cinerea*. *Mycotaxon*, *82*, 343–346.
- Collins, O. N. R. (1975). Mating types in five isolates of *Physarum polycephalum*. *Mycologia*, *67*, 98–107.
- Collins, O. N. R. (1979). Myxomycete biosystematics: some recent developments and future research opportunities. *Botanical Review*, *45*, 145–201.
- Collins, O. N. R. (1981). Myxomycete genetics, 1960–1981. *Journal of the Elisha Mitchell Scientific Society*, *97*, 101–125.
- Dalgleish, D. (2014). Contexture. Excel tips, tutorials, and videos. Excel latitude and longitude calculations. <http://www.contextures.com/excellatitudelongitude.html>. Accessed 2 Jan 2014.
- DePriest, P. T. (1993). Small subunit rDNA variation in a population of lichen fungi due to optional group-I introns. *Gene*, *134*, 67–74.
- Dujon, B. (1989). Group I introns as mobile genetic elements: facts and mechanistic speculations—a review. *Gene*, *82*, 91–114.
- Edgar, R. C. (2004). MUSCLE: multiple sequence alignment with high accuracy and high throughput. *Nucleic Acids Research*, *32*, 1792–1797.
- Edgell, D. R., Chalamcharla, V. R., & Belfort, M. (2011). Learning to live together: mutualism between self-splicing introns and their hosts. *BMC Biology*, *9*, 22.
- Elde, M., Haugen, P., Willassen, N. P., & Johansen, S. (1999). I-NjaI, a nuclear intron-encoded homing endonuclease from *Naegleria*, generates a pentanucleotide 3' cleavage-overhang within a 19 base-pair partially symmetric DNA recognition site. *European Journal of Biochemistry*, *259*, 281–288.
- Fenchel, T., & Finlay, B. J. (2004). The ubiquity of small species: patterns of local and global diversity. *BioScience*, *54*, 777–784.
- Ferris, P. J., Vogt, V. M., & Truitt, C. L. (1983). Inheritance of extrachromosomal rDNA in *Physarum polycephalum*. *Molecular and Cellular Biology*, *3*, 635–642.
- Fiore-Donno, A. M., Berney, C., Pawlowski, J., & Baldauf, S. L. (2005). Higher-order phylogeny of plasmidial slime molds (Myxogastria) based on elongation factor 1-A and small subunit rRNA gene sequences. *Journal of Eukaryotic Microbiology*, *52*, 201–210.
- Fiore-Donno, A. M., Meyer, M., Baldauf, S. L., & Pawlowski, J. (2008). Evolution of dark-spored Myxomycetes (slime-molds): molecules versus morphology. *Molecular Phylogenetics and Evolution*, *46*, 878–889.
- Fiore-Donno, A. M., Nikolaev, S. I., Nelson, M., Pawlowski, J., Cavalier-Smith, T., & Baldauf, S. L. (2010). Deep phylogeny and evolution of slime moulds (Mycetozoa). *Protist*, *161*, 55–70.
- Fiore-Donno, A. M., Novozhilov, Y. K., Meyer, M., & Schnittler, M. (2011). Genetic structure of two protist species (Myxogastria, Amoebozoa) suggests asexual reproduction in sexual amoebae. *PLoS ONE*, *6*, e22872.
- Fiore-Donno, A. M., Kamono, A., Meyer, M., Schnittler, M., Fukui, M., & Cavalier-Smith, T. (2012). 18S rDNA phylogeny of *Lamproderma* and allied genera (Stemonitales, Myxomycetes, Amoebozoa). *PLoS ONE*, *7*, e35359.
- Fiore-Donno, A. M., Clissmann, F., Meyer, M., Schnittler, M., & Cavalier-Smith, T. (2013). Two-gene phylogeny of bright-spored Myxomycetes (slime moulds, superorder Lucisporidia). *PLoS ONE*, *8*, e62586.
- Flick, K. E., Jurica, M. S., Monnat, R. J., Jr., & Stoddard, B. L. (1998). DNA binding and cleavage by the nuclear intron-encoded homing endonuclease I-PpoI. *Nature*, *394*, 96–101.
- Flowers, J. M., Li, S. I., Stathos, A., Saxer, G., Ostrowski, E. A., Queller, D. C., et al. (2010). Variation, sex, and social cooperation: molecular population genetics of the social amoeba *Dictyostelium discoideum*. *PLoS Genetics*, *6*, e1001013.
- Frommlet, J. C., & Iglesias-Rodríguez, M. D. (2008). Microsatellite genotyping of single cells of the dinoflagellate species *Lingulodinium polyedrum* (Dinophyceae): a novel approach for marine microbial population genetic studies. *Journal of Phycology*, *44*, 1116–1125.
- Goddard, M. R., & Burt, A. (1999). Recurrent invasion and extinction of a selfish gene. *Proceedings of the National Academy of Sciences of the United States of America*, *96*, 13880–13885.
- Goddard, M. R., Greig, D., & Burt, A. (2001). Outcrossed sex allows a selfish gene to invade yeast populations. *Proceedings of the Royal Society of London B*, *268*, 2537–2542.
- Goddard, M. R., Leigh, J., Roger, A. J., & Pemberton, A. J. (2006). Invasion and persistence of a selfish gene in the Cnidaria. *PLoS ONE*, *1*, e3.
- Gogarten, J. P., & Hilario, E. (2006). Inteins, introns, and homing endonucleases: recent revelations about the life cycle of parasitic genetic elements. *BMC Evolutionary Biology*, *6*, 94.
- Goodman, E. M. (1980). *Physarum polycephalum*: a review of a model system using a structure-function approach. *International Review of Cytology*, *63*, 1–58.
- Gott, J. M., Visimirski, L. M., & Hunter, J. L. (1993). Substitutional and insertional RNA editing of the cytochrome c oxidase subunit I mRNA of *Physarum polycephalum*. *The Journal of Biological Chemistry*, *268*, 25483–25486.
- Gray, W. D., & Alexopoulos, C. J. (1968). *Biology of the Myxomycetes*. New York: The Ronald Press Co.
- Guindon, S., & Gascuel, O. (2003). A simple, fast, and accurate algorithm to estimate large phylogenies by maximum likelihood. *Systematic Biology*, *52*, 696–704.
- Hafez, M., & Hausner, G. (2012). Homing endonucleases: DNA scissors on a mission. *Genome*, *55*, 553–569.
- Haskins, E. F., & Wrigley de Basanta, D. (2008). Methods of agar culture of Myxomycetes: an overview. *Revista Mexicana de Micología*, *27*, 1–7.
- Haubold, B., & Hudson, R. R. (2000). LIAN 3.0: detecting linkage disequilibrium in multilocus data. *Bioinformatics*, *16*, 847–848.
- Haugen, P., Huss, V. A. R., Nielsen, H., & Johansen, S. (1999). Complex group-I introns in nuclear SSU rDNA of red and green algae: evidence of homing-endonuclease pseudogenes in the Bangiophyceae. *Current Genetics*, *36*, 345–353.
- Haugen, P., De Jonckheere, J. F., & Johansen, S. (2002). Characterization of the self-splicing products of two complex *Naegleria* LSU rDNA group I introns containing homing endonuclease genes. *European Journal of Biochemistry*, *269*, 1641–1649.
- Haugen, P., Coucheron, D. H., Rønning, S. B., Haugli, K., & Johansen, S. (2003). The molecular evolution and structural organization of self-

- splicing group I introns at position 516 in nuclear SSU rDNA of myxomycetes. *Journal of Eukaryotic Microbiology*, 50, 283–292.
- Haugen, P., Reeb, V., Lutzoni, F., & Bhattacharya, D. (2004). The evolution of homing endonuclease genes and group I introns in nuclear rDNA. *Molecular Biology and Evolution*, 21, 129–140.
- Haugen, P., Simon, D. M., & Bhattacharya, D. (2005a). The natural history of group I introns. *Trends in Genetics*, 21, 111–119.
- Haugen, P., Wikmark, O. G., Vader, A., Coucheron, D. H., Sjøttem, E., & Johansen, S. D. (2005b). The recent transfer of a homing endonuclease gene. *Nucleic Acids Research*, 33, 2734–2741.
- Hausner, G., Hafez, M., & Edgell, D. R. (2014). Bacterial group I introns: mobile RNA catalysts. *Mobile DNA*, 5, 8.
- Hedberg, A., & Johansen, S. D. (2013). Nuclear group I introns in self-splicing and beyond. *Mobile DNA*, 4, 17.
- Hibbett, D. S. (1996). Phylogenetic evidence for horizontal transmission of group I introns in the nuclear ribosomal DNA of mushroom-forming fungi. *Molecular Biology and Evolution*, 13, 903–917.
- Hood, G. M. (2010). PopTools version 3.2.5. <http://www.poptools.org>. Accessed 1 April 2014.
- Horton, T. L., & Landweber, L. F. (2000). Evolution of four types of RNA editing in myxomycetes. *RNA*, 6, 1339–1346.
- Huson, D. H., & Bryant, D. (2006). Application of phylogenetic networks in evolutionary studies. *Molecular Biology and Evolution*, 23, 254–267.
- Johansen, S., Johansen, T., & Haugli, F. (1992). Structure and evolution of myxomycete nuclear group I introns: a model for horizontal transfer by intron homing. *Current Genetics*, 22, 297–304.
- Johansen, S., Embley, T. M., & Willassen, N. P. (1993). A family of nuclear homing endonucleases. *Nucleic Acids Research*, 21, 4405.
- Johansen, S., Elde, M., Vader, A., Haugen, P., Haugli, K., & Haugli, F. (1997). In vivo mobility of a group I twintron in nuclear ribosomal DNA of the myxomycete *Didymium iridis*. *Molecular Microbiology*, 24, 737–745.
- Katoh, K., & Standley, D. M. (2013). MAFFT multiple sequence alignment software version 7: improvements in performance and usability. *Molecular Biology and Evolution*, 30, 772–780.
- Koufopanou, V., Goddard, M. R., & Burt, A. (2002). Adaptation for horizontal transfer in a homing endonuclease. *Molecular Biology and Evolution*, 19, 239–246.
- Lado, C. (2014). An on line nomenclatural information system of Eumycetozoa. 2005–2014. <http://www.nomen.eumycetozoa.com>. Accessed 8 April 2014.
- Lahr, D. J. G., Grant, J., Nguyen, T., Lin, J. H., & Katz, L. A. (2011a). Comprehensive phylogenetic reconstruction of Amoebozoa based on concatenated analyses of SSU rDNA and actin genes. *PLoS ONE*, 6, e22780.
- Lahr, D. J. G., Parfrey, L. W., Mitchell, E. A., Katz, L. A., & Lara, E. (2011b). The chastity of amoebae: re-evaluating evidence for sex in amoeboid organisms. *Proceedings of the Royal Society of London B*, 278, 2081–2090.
- Lambowitz, A. M., & Belfort, M. (1993). Introns as mobile genetic elements. *Annual Review of Biochemistry*, 62, 587–622.
- Lazo, W. R. (1961). Growth of green algae with myxomycete plasmidia. *The American Midland Naturalist Journal*, 65, 381–383.
- Li, Z., & Zhang, Y. (2005). Predicting the secondary structures and tertiary interactions of 211 group I introns in IE subgroup. *Nucleic Acids Research*, 33, 2118–2128.
- Lieb, B. (2014). PCR Additives. <http://www.staff.uni-mainz.de/lieb/additiva.html>. Accessed 6 March 2014.
- Linne, C. (1792). *Systema Naturae. Tom. II. Pars II.* listed under the name *Stemonitis*. 1467–1470.
- Lundblad, E. W., Einvik, C., Rønning, S., Haugli, K., & Johansen, S. (2004). Twelve group I introns in the same pre-rRNA transcript of the myxomycete *Fuligo septica*: RNA processing and evolution. *Molecular Biology and Evolution*, 21, 1283–1293.
- Machouart, M., Lacroix, C., Bui, H., Feuillade de Chauvin, M., Derouin, F., & Lorenzo, F. (2004). Polymorphisms and intronic structures in the 18S subunit ribosomal RNA gene of the fungi *Scytalidium dimidiatum* and *Scytalidium hyalinum*. Evidence of an IC1 intron with an His-Cys endonuclease gene. *FEMS Microbiology Letters*, 238, 455–467.
- Marchler-Bauer, A., Zheng, C., Chitsaz, F., Derbyshire, M. K., Geer, L. Y., Geer, R. C., et al. (2013). CDD: conserved domains and protein three-dimensional structure. *Nucleic Acids Research*, 41, D348–D352.
- Martin, G. W., & Alexopoulos, C. J. (1969). *The Myxomycetes*. Iowa City: Iowa Univ. Press.
- Michel, F., & Westhof, E. (1990). Modelling of the three-dimensional architecture of group I catalytic introns based on comparative sequence analysis. *Journal of Molecular Biology*, 216, 585–610.
- Milne, I., Lindner, D., Bayer, M., Husmeier, D., McGuire, G., Marshall, D. F., & Wright, F. (2009). TOPALi v2: a rich graphical interface for evolutionary analyses of multiple alignments on HPC clusters and multi-core desktops. *Bioinformatics*, 25, 126–127.
- Milstein, D., Oliveira, M. C., Martins, F. M., & Matioli, S. R. (2008). Group I introns and associated homing endonuclease genes reveals a clinal structure for *Porphyra spiralis* var. *amplifolia* (Bangiales, Rhodophyta) along the eastern coast of South America. *BMC Evolutionary Biology*, 8, 308.
- Moriyama, Y., & Kawano, S. (2010). Maternal inheritance of mitochondria: multipolarity, multiallelism and hierarchical transmission of mitochondrial DNA in the true slime mold *Physarum polycephalum*. *Journal of Plant Research*, 123, 139–148.
- Müller, K. M., Cannone, J. J., Gutell, R. R., & Sheath, R. G. (2001). A structural and phylogenetic analysis of the group IC1 introns in the order Bangiales (Rhodophyta). *Molecular Biology and Evolution*, 18, 1654–1667.
- Muscarella, D. E., & Vogt, V. M. (1989). A mobile group I intron in the nuclear rDNA of *Physarum polycephalum*. *Cell*, 56, 443–454.
- Muscarella, D. E., & Vogt, V. M. (1993). A mobile group I intron from *Physarum polycephalum* can insert itself and induce point mutations in the nuclear ribosomal DNA of *Saccharomyces cerevisiae*. *Molecular and Cellular Biology*, 13, 1023–1033.
- Muscarella, D. E., Ellison, E. L., Ruoff, B. M., & Vogt, V. M. (1990). Characterization of I-Ppo, an intron-encoded endonuclease that mediates homing of a group I intron in the ribosomal DNA of *Physarum polycephalum*. *Molecular and Cellular Biology*, 10, 3386–3396.
- Nandipati, S. C., Haugli, K., Coucheron, D. H., Haskins, E. F., & Johansen, S. D. (2012). Polyphyletic origin of the genus *Physarum* (Physarales, Myxomycetes) revealed by nuclear rDNA minichromosome analysis and group I intron synapomorphy. *BMC Evolutionary Biology*, 12, 166.
- Nannenga-Bremekamp, N. B. (1991). *A guide to temperate Myxomycetes* (Feest A, Burgraff E: *De Nederlandse Myxomyceten*, Engl. transl.). Bristol: Biopress Lim.
- Neubert, H., Nowotny, W., & Baumann, K. (1993). *Die Myxomyceten Deutschlands und des angrenzenden Alpenraumes unter besonderer Berücksichtigung Österreichs. Band 1. Ceratiomyxales, Echinosteliales, Liceales, Trichiales*. Gomaringen: Baumann Verl.
- Nielsen, H., & Johansen, S. D. (2009). Group I introns: moving in new directions. *RNA Biology*, 6, 375–383.
- Nikoh, N., & Fukatsu, T. (2001). Evolutionary dynamics of multiple group I introns in nuclear ribosomal RNA genes of endoparasitic fungi of the genus *Cordyceps*. *Molecular Biology and Evolution*, 18, 1631–1642.
- Novozhilov, Y. K., Okun, M. V., Erastova, D. A., Shchepin, O. N., Zemlyanskaya, I. V., García-Carvajal, E., & Schnittler, M. (2013a). Description, culture and phylogenetic position of a new xerotolerant species of *Physarum*. *Mycologia*, 105, 1535–1546.

- Novozhilov, Y. K., Schnittler, M., Erastova, D. A., Okun, M. V., Schepin, O. N., & Heinrich, E. (2013b). Diversity of nivicolous myxomycetes of the Teberda State Biosphere Reserve (Northwestern Caucasus, Russia). *Fungal Diversity*, *59*, 109–130.
- Pawlowski, J., Audic, S., Adl, S., Bass, D., Belbahri, L., Berney, C., et al. (2012). CBOL protist working group: barcoding eukaryotic richness beyond the Animal, Plant, and Fungal kingdoms. *PLoS Biology*, *10*, e1001419.
- Persoon, C. H. (1794). Neuer Versuch einer systematischen Eintheilung der Schwämme. *Neues Magazin für die Botanik in ihrem ganzen Umfange*, *1*, 63–128.
- Poulain, M., Meyer, M., & Bozonnet, J. (2011). *Les myxomycetes*. Delémont: Féd. Mycol. Bot. Dauphiné-Savoie.
- Rätzel, V., Ebeling, B., Hoffman, X. K., Tesmer, J., & Marwan, W. (2013). *Physarum polycephalum* mutants in the photocontrol of sporulation display altered patterns in the correlated expression of developmentally regulated genes. *Development Growth and Differentiation*, *55*, 247–259.
- Ronquist, F., & Huelsenbeck, J. P. (2003). MrBayes 3: Bayesian phylogenetic inference under mixed models. *Bioinformatics*, *19*, 1572–1574.
- Ronquist, F., Teslenko, M., van der Mark, P., Ayres, D. L., Darling, A., Höhna, S., et al. (2012). MrBayes 3.2: efficient Bayesian phylogenetic inference and model choice across a large model space. *Systematic Biology*, *61*, 539–542.
- Sauer, H. W. (1982). *Developmental Biology of Physarum*. Cambridge: Cambridge University Press.
- Schnittler, M., & Mitchell, D. W. (2000). Species diversity in Myxomycetes based on the morphological species concept—a critical examination. *Stapfia*, *73*, 55–62.
- Schnittler, M., & Tesmer, J. (2008). A habitat colonisation model for spore-dispersed organisms—does it work with eumycetozoans? *Mycological Research*, *112*, 697–707.
- Schnittler, M., Novozhilov, Y. K., Romeralo, M., Brown, M., & Spiegel, F. W. (2012). Myxomycetes and Myxomycete-like organisms. In F. W. Stuttgart (Ed.), *Englers Syllabus of Plant Families. Volume 4. 13th edition* (pp. 40–88). Bornträger.
- Smirnov, A. V., Chao, E., Nassonova, E. S., & Cavalier-Smith, T. (2011). A revised classification of naked lobose amoebae (Amoebozoa: Lobosa). *Protist*, *162*, 545–570.
- STAR. (2014). StarORF. Software Tools for Academics and Researchers. <http://star.mit.edu/orf>. Accessed 25 March 2014.
- Stephenson, S. L., Schnittler, M., & Novozhilov, Y. K. (2008). Myxomycete diversity and distribution from the fossil record to the present. *Biodiversity and Conservation*, *17*, 285–301.
- Tamura, K., Nei, M., & Kumar, S. (2004). Prospects for inferring very large phylogenies by using the neighbor-joining method. *Proceedings of the National Academy of Sciences of the United States of America*, *101*, 11030–11035.
- Tamura, K., Peterson, D., Peterson, N., Stecher, G., Nei, M., & Kumar, S. (2011). MEGA5: molecular evolutionary genetics analysis using maximum likelihood, evolutionary distance, and maximum parsimony methods. *Molecular Biology and Evolution*, *28*, 2731–2739.
- Tanabe, Y., Yokota, A., & Sugiyama, J. (2002). Group I introns from Zygomycota: evolutionary implications for the fungal IC1 intron subgroup. *Journal of Molecular Biology*, *54*, 692–702.
- Torres-Machorro, A. L., Hernández, R., Cevallos, A. M., & López-Villaseñor, I. (2010). Ribosomal RNA genes in eukaryotic microorganisms: witnesses of phylogeny? *FEMS Microbiology Reviews*, *34*, 59–86.
- Traphagen, S. J., Dimarco, M. J., & Silliker, M. E. (2010). RNA editing of 10 *Didymium iridis* mitochondrial genes and comparison with the homologous genes in *Physarum polycephalum*. *RNA*, *16*, 828–838.
- Urich, T., Lanzén, A., Qi, J., Huson, D. H., Schleper, C., & Schuster, S. C. (2008). Simultaneous assessment of soil microbial community structure and function through analysis of the meta-transcriptome. *PLoS ONE*, *3*, e2527.
- Vader, A., Nielsen, H., & Johansen, S. (1999). In vivo expression of the nucleolar group I intron-encoded I-*DirI* homing endonuclease involves the removal of a spliceosomal intron. *The EMBO Journal*, *18*, 1003–1013.
- Walker, L. M., Dewsbury, D. R., Parks, S. S., Winsett, K. E., & Stephenson, S. L. (2011). The potential use of mitochondrial cytochrome c oxidase I for barcoding myxomycetes. In *VII International Congress on Systematics and Ecology of Myxomycetes: 11–16 September 2011; Recife, Brazil* (pp. 138).
- Wikmark, O. G., Haugen, P., Haugli, K., & Johansen, S. D. (2007a). Obligatory group I introns with unusual features at positions 1949 and 2449 in nuclear LSU rDNA of Didymiaceae myxomycetes. *Molecular Phylogenetics and Evolution*, *43*, 596–604.
- Wikmark, O. G., Haugen, P., Lundblad, E. W., Haugli, K., & Johansen, S. D. (2007b). The molecular evolution and structural organization of group I introns at position 1389 in nuclear small subunit rDNA of myxomycetes. *Journal of Eukaryotic Microbiology*, *54*, 49–56.
- Xu, C., Wang, C., Sun, X., Zhang, R., Gleason, M. L., Eiji, T., & Sun, G. (2013). Multiple group I introns in the small-subunit rDNA of *Botryosphaeria dothidea*: implication for intraspecific genetic diversity. *PLoS ONE*, *8*, e67808.
- Yokoyama, E., Yamagishi, K., & Hara, A. (2002). Group-I intron containing a putative homing endonuclease gene in the small subunit ribosomal DNA of *Beauveria bassiana* IFO 31676. *Molecular Biology and Evolution*, *19*, 2022–2025.
- Zhou, Y., Lu, C., Wu, Q. J., Wang, Y., Sun, Z. T., Deng, J. C., & Zhang, Y. (2008). GISSD: group I intron sequence and structure database. *Nucleic Acids Research*, *36*, D31–D37.



## ORIGINAL PAPER

# What an Intron May Tell: Several Sexual Biospecies Coexist in *Meriderma* spp. (Myxomycetes)



Yun Feng<sup>a</sup>, Anja Klahr<sup>a</sup>, Paulina Janik<sup>b</sup>, Anna Ronikier<sup>b</sup>, Thomas Hoppe<sup>a</sup>, Yuri K. Novozhilov<sup>c</sup>, and Martin Schnittler<sup>a,1</sup>

<sup>a</sup>Institute of Botany and Landscape Ecology, Ernst Moritz Arndt University of Greifswald, Soldmannstr. 15, D-17487 Greifswald, Germany

<sup>b</sup>Institute of Botany, Polish Academy of Sciences, Lubicz 46, 31-512 Krakow, Poland

<sup>c</sup>V.L. Komarov Botanical Institute of the Russian Academy of Sciences, Prof. Popov St. 2, 197376 St. Petersburg, Russia

Submitted July 5, 2015; Accepted March 23, 2016  
Monitoring Editor: Sandra L. Baldauf

**Specimens of the snowbank myxomycete *Meriderma atrosporum* agg. from five European mountain ranges were sequenced for parts of the nuclear small subunit ribosomal RNA gene (SSU) and the protein elongation factor 1 alpha gene (EF1A). A phylogeny of the EF1A gene, including a very variable spliceosomal intron, resulted in seven phylogroups, and this topology was confirmed by SSU sequences. Two thirds of all specimens were heterozygous for the EF1A gene, and the two haplotypes of these specimens occurred always in the same phylogroup. Except for two cases in closely related phylogroups all ribotypes were as well limited to one phylogroup. This pattern is consistent with the assumption of reproductively isolated sexual biospecies. Numbers of EF1A-haplotypes shared between mountain ranges correlate with geographical distance, suggesting relative isolation but occasional long-distance dispersal by spores. Most subpopulations (divided by putative biospecies and mountain ranges) were in Hardy-Weinberg equilibrium. A simulation assuming panmixis within but not in between subpopulations suggested that similar numbers of shared genotypes can be created by chance through sexual reproduction alone. Our results support the biospecies concept, derived from experiments with cultivable members of the Physarales. We discuss the results on the background of possible reproductive options in myxomycetes.**

© 2016 Elsevier GmbH. All rights reserved.

**Key words:** Protein elongation factor 1 alpha; nuclear small subunit ribosomal RNA; plasmodial slime molds; reproductive system; spliceosomal intron; speciation.

## Introduction

Myxomycetes, known as well under the name Myxogastria since de Bary (1859) recognized their

protistan nature, belong to the supergroup Amoebozoa (Adl et al. 2012) and possess a sexual life cycle: From spores typically 7–12 μm in diameter (Schnittler and Tesmer 2008) haploid myxoflagellates or myxamoebae hatch. These amoebae divide by binary fission, which leads to clonal populations (Clark and Haskins 2010) that can reach high densities in soil (Feest and Madelin

<sup>1</sup>Corresponding author; fax +49 3834 864114  
e-mail [martin.schnittler@uni-greifswald.de](mailto:martin.schnittler@uni-greifswald.de) (M. Schnittler).

1985, 1988; Stephenson et al. 2011; Urich et al. 2008). Syngamy of two haploid amoebae starts the next life stage, the plasmodium. Through subsequent mitoses not accompanied by cellular fission these multinucleate structures can reach several centimeters in size and move by protoplasmic streaming (Guttes et al. 1961), ingesting other microorganisms. If environmental conditions deteriorate, these plasmodia typically segregate into many small portions which typically form colonies of fruit bodies 0.2–10 mm tall (Clark and Haskins 2015). Within this transformation, meiosis takes place, and the resulting meiospores complete the life cycle. Airborne spores (Kamono et al. 2009) enable myxomycetes to colonize habitat islands like accumulations of decaying plant material. The group comprises currently ca. 980 species (Lado 2005–2015) as recognized by a morphospecies concept based on the elaborate characters of the fructifications that facilitate spore dispersal (Schnittler et al. 2012a). In addition, three dormant stages work as a back-insurance against sudden environmental changes: myxamoebae can form microcysts, plasmodia may convert to multinucleate sclerotia, and finally spores can persist up to several decades (Erbisch 1964). For these reasons, myxomycetes are able to colonize some of the driest habitats on earth, like parts of Central Asia (Schnittler 2001; Novozhilov and Schnittler 2008; Schnittler et al. 2012b) or the Atacama desert (Lado et al. 2012).

According to this life cycle, myxomycetes can be called sexual amoebae, and sex seems indeed to be a hallmark of all eukaryotes, including Amoebozoa (Lahr et al. 2011; Spiegel 2011). Experiments with cultivable model species like *Physarum polycephalum* Schwein. and *Didymium iridis* (Ditmar) Fr. confirmed this: single spore cultures do often not fruit before descendants of a second spore are given to the culture. Such experiments revealed groups of isolates that are compatible with each other (amoebae may pair and finally sporulate) but not with others (Clark and Haskins 2011). For fusion of diploid plasmodia, barriers are even higher (Clark and Haskins 2012). Groups of compatible amoebal strains comply with a biological species concept and can be seen as biospecies (Collins 1979, 1981). Outcrossing within a biospecies is ensured by mating types, which can be realized via a single-locus multiallelic system (*Didymium iridis*: Betterley and Collins 1983; Clark 1993), or by three loci with multiple alleles (*Physarum polycephalum*: Clark and Haskins 2010; Collins 1975). Thus, myxamoebae derived from single-spore cultures should behave heterothallic, requiring descendants from a

second spore to mate and complete the life cycle (Fig. 1 A1). Beside the syngamy of spores from different plasmodia (true outcrossing) amoebae with genetically different nuclei but originating from the same colony can mate. This internuclear selfing is comparable to selfing in vascular plants: within a few generations the degree of homozygosity for any given locus should sharply increase (Fig. 1A2).

However, experiments with cultivable Physarales revealed in several cases morphospecies to be composed of both hetero- and non-heterothallic strains (see Clark 1995 and references therein; ElHage et al. 2000). This applies for many of the ca. 50 species screened in cultures (Clark and Haskins 2010) and does not comply with the classical life cycle. For these non-heterothallic strains (single-spore cultures sporulate), several reproductive options are conceivable. First, the sexual life cycle with outcrossing ensured by mating types remains intact, but multinucleate spores transport two nuclei which may show opposite mating types (Fig. 1B). This pseudohomothallism (Merino et al. 1996) should strongly increase the probability of internuclear selfing. Karyogamy may occur prior to, during germination, or after it; in the latter case two compatible amoebae with genetically different nuclei hatch at the same place and can mate. Multinucleate spores were detected in the newly described *Physarum pseudonotabile* (Novozhilov et al. 2013a), and older literature reports this as well (see review in Gray and Alexopoulos 1968). If meiosis would take place prior to spore cleavage, multinucleate spores can develop if more than one nucleus is enclosed in a spore. Aldrich (1967) found synaptonemal complexes within spores, consistent with meiosis after spore cleavage, but Clark and Haskins (2013) discuss both possibilities. For post-cleavage meiosis, three of the four nuclei must degenerate to create a haploid uninucleate spore, but accidental survival of more than one nucleus would as well result in multinucleate spores. Second, a breakdown of the mating system may cause true homothallism via intranuclear selfing: now identical amoebae descending from the same uninucleate spore can mate (Fig. 1C). This life cycle is still sexual but would instantly lead to fully homozygous offspring. Third, automixis may occur if meiosis remains incomplete, either by coalescence of products of meiosis II (which is comparable to internuclear selfing) or by suppression of meiosis II (Clark and Haskins 2013). In the first case, karyogamy still occurs. Both cases produce spores with a single diploid nucleus; the resulting amoebae will not undergo syngamy. Depending on the extent of recombination,

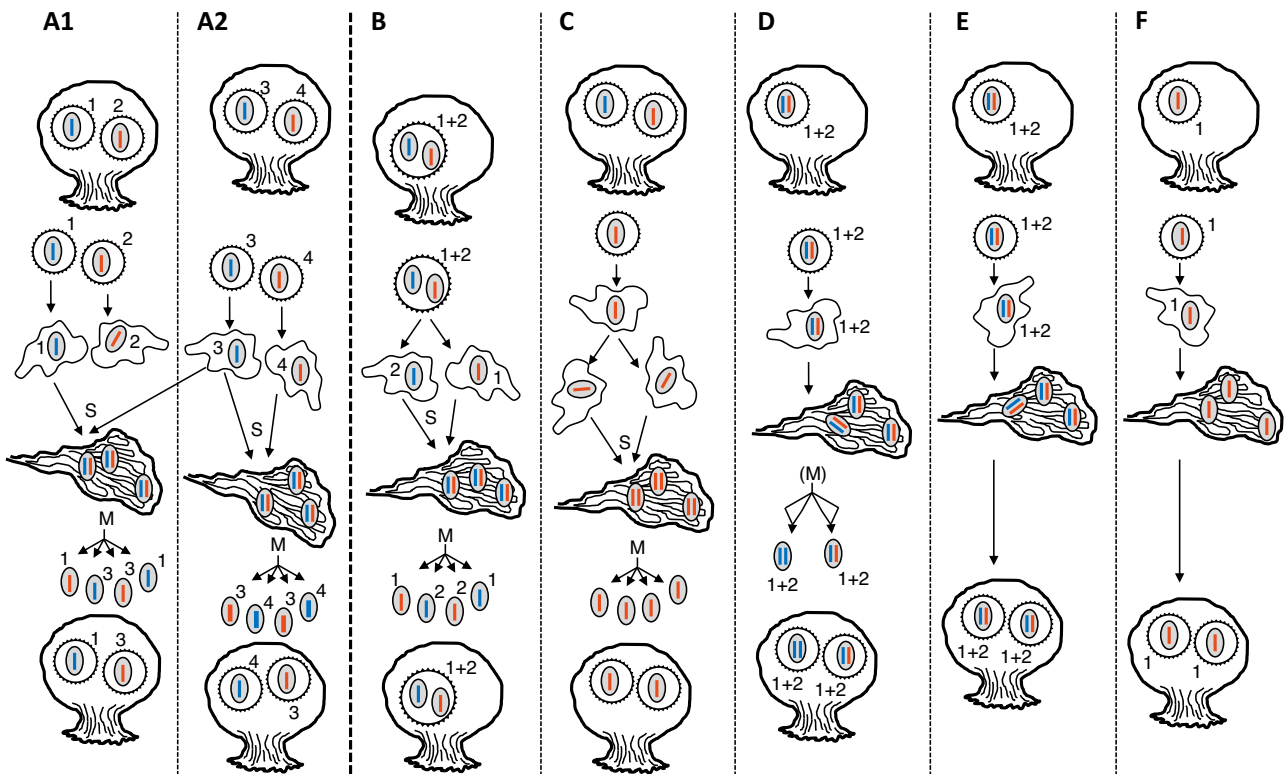


**Figure 1.** Reproductive options in myxomycetes. **A** Sexual life cycle with 1, 2, . . . ,  $n$  mating types (numbers). Fruit bodies (above) contain meiotic spores (one or two are pictured) with different somatic alleles for a given locus (red and blue bars). Amoebae descending from spores of different sporocarps (A1; mating types 1 and 3, true outcrossing) or from one sporocarp (A2; mating types 3 and 4, internuclear selfing) may undergo syngamy (S). During fruit body formation meiosis (M) takes place; mating types and somatic alleles can recombine. **B** Pseudohomothallism via multinucleate spores increases the chance for internuclear selfing, since one spore carries both mating types. **C** The breakdown of mating types would allow intranuclear selfing: amoebae of the same clone mate. **D** Automixis allows still for recombination, but meiosis remains incomplete due to either coalescence of the products of meiosis II (pictured) or suppression of meiosis II. Spores and hatching amoebae are diploid and fail to mate via syngamy. Diploid (**E**) or haploid (**F**) apomictic strains skip completely meiosis and syngamy. Single spore cultures will behave heterothallic for option A, but non-heterothallic for options C–F.

inherited heterozygosity is partially or completely preserved in such a subsexual life cycle (Fig. 1D). Fourth, non-heterothallic strains may be truly asexual (apomictic, skipping completely meiosis and karyogamy) and form plasmodia without mating. Consequently, such apomictic strains do not show nuclear phases. Notwithstanding mutations, inherited heterozygosity will be fully preserved for diploid apomicts (Fig. 1E), whereas haploid apomicts appear homozygous (Fig. 1F). If this reproductive mode is common, we can expect a few diploid (and maybe heterozygous) genotypes to be very common and widespread, or again a homozygote excess for haploid apomicts (like the Colonia strain of *Physarum polycephalum*, Mohberg 1977). All reproductive options mentioned above equally result in non-heterothallic

behavior and cannot be distinguished in culture experiments.

For the non-heterothallic life cycle, some lines of evidence point towards automixis: non-heterothallic isolates usually do not crossbreed (Betterley and Collins 1983) and measurements of DNA contents in myxamoebae and plasmodia are identical and appear to be  $2n$  (Therrien et al. 1977). This complies as well with apomixis, but cytological studies revealed regularly the occurrence of synaptonemal complexes (Aldrich and Mims 1970). In theory, changes in ploidy level between amoebae and plasmodia should occur in the case of cryptic sexuality (Fig. 1B, C); but not with automixis or apomixis (Fig. 1D, E). In practice, such investigations are hampered by several problems. Plasmodia can, at least in culture, become polyploid (Koevenig and

Jackson 1966; Mohberg 1977; Werenskjold et al. 1988). Only a few studies on ploidy levels were conducted (Therrien and Yemma 1975; Therrien et al. 1977), and due to the very small chromosomes meiosis is difficult to observe (Aldrich and Mims 1970), although chromosome numbers seem to be limited (Hoppe et al. 2014). Finally, amoebae itself can be multinucleated and are hard distinguish from microplasmidia (Mohberg 1977; Yemma et al. 1972).

Non-heterothallic strains should carry a short-term advantage in comparison to heterothallic strains: descendants of the first spore colonizing a new habitat can complete the life cycle and disperse again (Schnittler and Tesmer 2008). For heterothallic strains, two spores with compatible mating types must independently arrive so that their descendant amoebae can mate. In the presence of selective forces causing different fitness in different genotypes, for all conceivable options with non-heterothallic strains (internuclear selfing via multinucleate spores, intranuclear selfing, automixis, apomixis) genetic diversity of the respective populations should decline sooner or later, since recombination between descendants of different sporocarps will not take place, and genotypes with lower fitness will die off. This trade-off can be seen as another expression of the often discussed paradox of sex (Maynard Smith 1978): a short-term advantage (increasing colonization ability) is counterbalanced by a long-term disadvantage (decreasing genetic diversity), which becomes detrimental with changing environmental conditions. The compromise between maximum colonizing ability and maximum genetic diversity would be a mixed reproductive system (for instance, combining internuclear selfing / true outcrossing and automixis), as realized in many species of algae, plants and fungi. In a certain sense, this is already realized in myxomycetes: The sexual life cycle can be delayed by theoretically immortal, clonal populations of amoebae which can convert to microcysts. However, the main propagules for the group are the (meiotic) spores born in specialized fructifications to become airborne. Therefore, the question is with Spiegel (2011) if strains exist which complete their entire life cycle without a sexual event, thus effectively dispersing mitotic spores.

Virtually all myxomycete species used for crossing experiments belong to the dark-spored myxomycetes (synthesizing melanin, Rakoczy and Panz 1994); one of the two major groups including the traditional, yet not monophyletic orders Stemonitales and Physarales (Fiore-Donno et al. 2012). A molecular investigation of the myxomycete

genus *Meriderma* (Stemonitales), initiated to revise its taxonomy, revealed a highly variable marker that gave an unexpected opportunity to study population genetics to see (i) if different biospecies coexist in nature, (ii) if there is a homozygote excess or if some genotypes dominate the population, and (iii) if some genotypes appear to have a colonization advantage (a wider distribution range than that to be expected by spread via amoebae only). In a panmictic population, neutral alleles for populations with a sexual life cycle and a high degree of outbreeding (Fig. 1A1) should be in Hardy-Weinberg equilibrium (HWE) and show a fairly high proportion of heterozygotes. Dominant internuclear selfing (1A2), pseudohomothallism with multinucleate spores (1B) or automixis (1D) by coalescence of meiosis II products would lead to an increase in homozygosity. True homothallism (1C) or a haploid apomictic life cycle (1F) cause instant homozygosity, whereas for automixis by suppression of meiosis II or diploid apomixis (1E) a few hetero- or homozygous genotypes will be very widespread, since they can disperse via spores. Two marker genes, partial sequences of the nuclear small subunit ribosomal RNA gene (SSU) and of the protein elongation factor 1 alpha gene (EF1A), were studied, and the latter sequences turned out to be often heterozygous due to an extremely variable spliceosomal intron. Both markers are independently inherited: SSU as a multi copy gene is located in extrachromosomal units with a non-Mendelian inheritance (Ferris et al. 1983); EF1A as a nuclear gene displays Mendelian inheritance (see discussion in Feng and Schnittler 2015).

*Meriderma* spp. belongs to the nivicolous myxomycetes, an ecological group fruiting in spring in mountaneous areas where a high and long-lasting snow cover creates stable conditions for amoebal growth under the snow (Schnittler et al. 2015). Poulain et al. (2011) proposed a morphospecies concept for the genus based on differences especially in spore ornamentation. We found two morphotypes to be well distinguishable from all others: the rare *M. fuscatum* (Meyl.) Mar. Mey. & Poulain (described earlier as *Lamproderma fuscatum* Meyl., the only taxon with brown spore mass) and a taxon not yet formally named: *M. aggregatum* ad int. (the only taxon in the genus developing always sessile sporocarps). The other taxa proposed by Poulain et al. (2011) are difficult to separate based on morphological characters, although spore ornamentations vary from verrucae over spines to a more or less complete reticulum. This group, with five morphospecies proposed, forms the focus of the present study.

Acknowledging the problems in species differentiation we treat this group here under the preliminary name *Meriderma atrosporum* agg. (81 specimens studied; see Supplementary Material Database S1).

Whereas the correlations between molecular phylogenies and morphological characters will be discussed in a separate paper, this study presents data on the molecular diversity of the genus and its consequences for reproduction and dispersal, investigating specimens from five European mountain ranges.

## Results

### Phylogenies Based on Exon Sequences

In both the ML/Bayesian phylogenies of partial SSU sequences (Supplementary Material Figs S1, S2) and of exon sections of EF1A sequences (Supplementary Material Figs S3, S4) the morphologically visible division into three groups, representing *Meriderma fuscatum*, *M. aggregatum* and *M. atrosporum* agg. was recovered (Fig. 2). The clade of *M. aggregatum* comprises the most diverging sequences within *Meriderma* if seen by branch lengths, but is always clearly separated, as it is the case for *M. fuscatum*.

All specimens assigned by an initial morphological examination to *M. atrosporum* agg. form a single large clade in SSU phylogenies. The phylogeny constructed from the concatenated alignment (partial SSU and EF1A exon parts, Figure 2, Supplementary Material Figs S5, S6) confirms this, and displays additionally an internal structure of the *M. atrosporum* agg. clade. Five phylogroups, here numbered A to E, can be differentiated (Fig. 2). Two specimens form solitary branches. Specimen s020 appears outside all phylogroups in both SSU and EF1A trees, whereas specimen s068 clusters in the SSU phylogenies with phylogroup B and in EF1A phylogenies with phylogroup C. The SSU sequences (21 ribotypes among 81 specimens sequenced) are slightly less diverse than the EF1A sequences (25 exon genotypes). Neither SSU or EF1A alone recovers clearly all five phylogroups; these are resolved best in the two-gene phylogeny. Several specimens show identical SSU and EF1A exon genotypes.

The analyzed part of the EF1A gene comprises an upstream section with 78 amino acids (positions 40–273 in the alignment, see Supplementary Material Alignment S2), a spliceosomal intron and a downstream section with another 77 amino acids

(positions 436–666 in the alignment). Compared with the sequence of *M. fuscatum*, a taxon being sister to all other investigated species of *Meriderma*, the seven sequences of *M. aggregatum* vary in 47 positions, nearly all concerning the third base of a triplet (Supplementary Material Fig. S7), but this leads to only four changes in amino acids (Ala/Ser, Gly/Ala, Tyr/Phe, Lys/Arg/Gln). The 81 investigated specimens of *M. atrosporum* agg. deviate in 52 positions and four amino acids (Ala/Ser, Phe/Leu, one specimen only, Ala/Asp, Asp/Asn).

To see if the data set of the 81 partial SSU sequences from *M. atrosporum* agg. is spatially structured, we performed a Mantel test based on p-distance values. In most of the five clades, sequences from one of the five mountain ranges dominate. This coincides with a weak correlation between genetic and geographical distances ( $R=0.198$ ); and this value is significant if compared with the 5/95% confidence interval for the mean correlation from 999 randomized runs ( $R5\%=0.043$ ,  $R_{\text{mean}}=0.002$ ,  $R95\%=0.062$ ). The exon section of the EF1A gene yielded similar results ( $R=0.244$ , randomized runs gave  $R5\%=0.019$ ,  $R_{\text{mean}}=0.003$ ,  $R95\%=0.025$ ).

### EF1A Phylogeny

The data set providing the highest genetic diversity are the EF1A sequences. Due to the deviating intron sequences of *M. aggregatum* which cannot be aligned with those of *M. atrosporum* agg. we had to exclude this species and rooted the tree with *M. fuscatum*. For *M. atrosporum* agg. the 25 genotypes found for exon parts increase to 54 if the spliceosomal intron is considered as well. A phylogeny of EF1A sequences including the intron places all but one specimen in the same phylogroups (Fig. 3, Supplementary Material Figs S8, S9) as it is the case for the concatenated phylogeny of partial SSU and EF1A exon sequences (Fig. 2). Now, the five phylogroups A–E appear with high support (bootstrap 100/posterior probability 1.00) in ML/Bayesian trees, and the phylogroups B and C are differentiated into two subgroups (called B1, B2 and C1, C2, Fig. 3). The two haplotypes of a specimen that is heterozygous for the EF1A marker appear always within one of the seven phylogroups. Similarly, all ribotypes occur in one phylogroup only, with the exception of r09 (occurring in B1 and B2) and r15/r16 (occurring in C1 and C2). Specimen 020 cannot be clearly assigned to a phylogroup, and specimen 068 appears between groups B and C in the concatenated tree, but within group C in the EF1A tree.

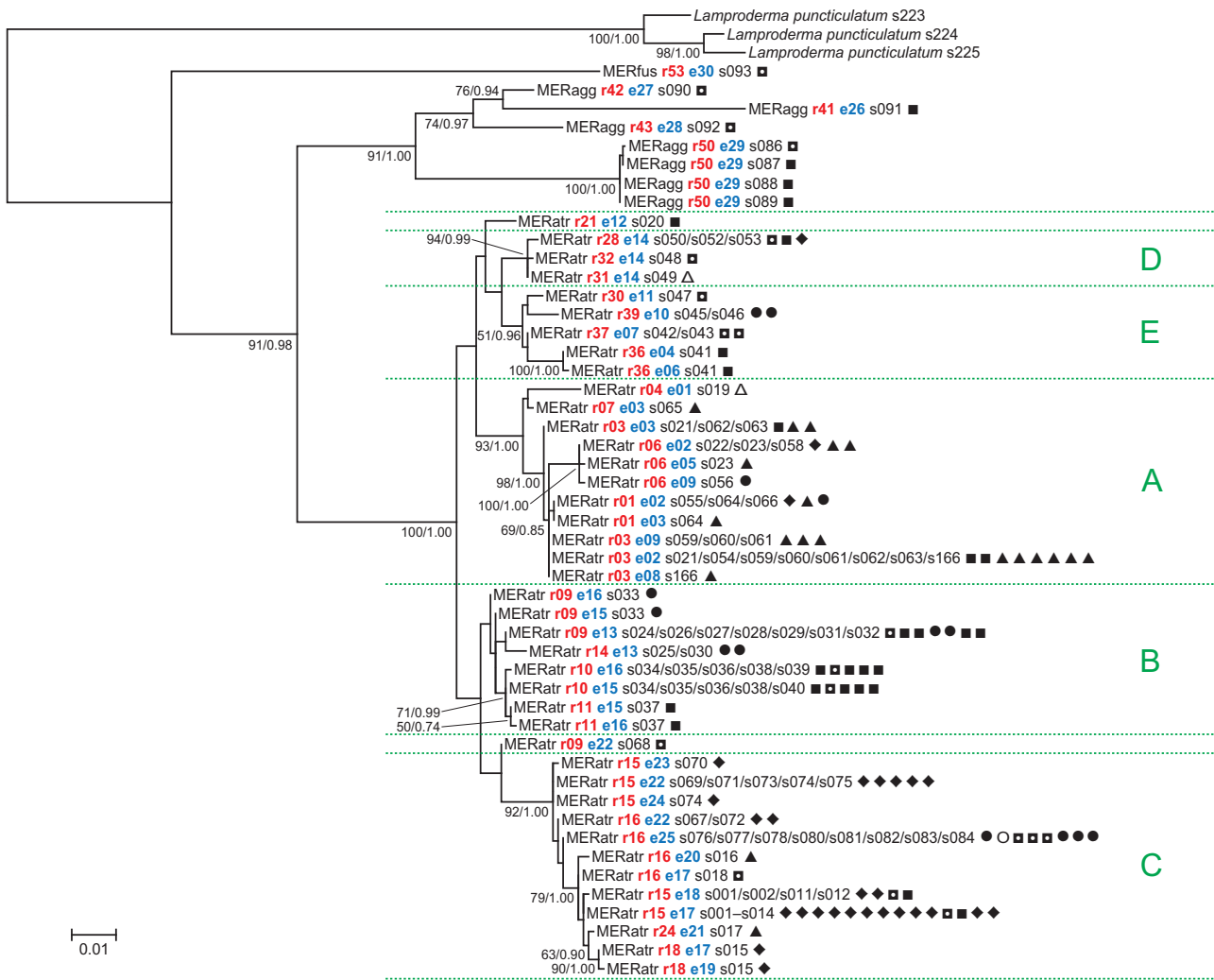


**Figure 2.** ML tree of concatenated partial SSU sequences and EF1A exon sequences for 81 specimens of *Meriderma atrosporum* agg., 7 specimens of *M. aggregatum*, and 1 specimen of *M. fuscatum*, rooted with 3 genotypes of *L. puncticulatum*. Labels include the ribotypes (r, not contiguous), the EF1A exon haplotypes (e), the specimen number (s) according to Supplementary Database S1, and the morphological determination according to the concept of Poulain et al. (2011). Specimens with identical SSU/EF1A genotypes are listed subsequently for a branch. The origin of the specimens is indicated by symbols (five intensely investigated mountain ranges: ▲Khibine Mts., ■ German Alps, □ French Alps, ● Carpathians, ◆ Caucasus, and single specimens from: ○ Black Forest, △ British Colombia). Shown is the topology of the ML tree. Bootstrap / posterior probability values which are both above 50/0.5 are indicated.

### Patterns in the EF1A Spliceosomal Intron

The spliceosomal intron in EF1A sequences seems to be obligatory for myxomycetes, occurring in all 15 genera of bright-spored myxomycetes investigated by Fiore-Donno et al. (2013), in *Physarum polycephalum* (Baldauf and Doolittle 1997) and in 5 other dark-spored genera investigated by us (data not shown). The intron starts after the amino acid Gln (triplet CAA, IUPAC nucleic acid notation) followed by donor site excision sequence GTRAGT

(Roy and Gilbert 2006). In *Meriderma*, the starting sequence is usually GTATG (Supplementary Material Alignment S2). The most likely branching point, which should include an adenine (sequence CTR[A]Y) is represented ca. 54 positions upstream by the sequence CTGCAT present in most but not all specimens. The end of the intron, usually characterized by a Y-rich core and the sequence NCAG, is in all *Meriderma* spp. marked by the sequence TTAG (except for GTAG in *M. fuscatum*). Intron patterns differ between taxa: *M. fuscatum* has a

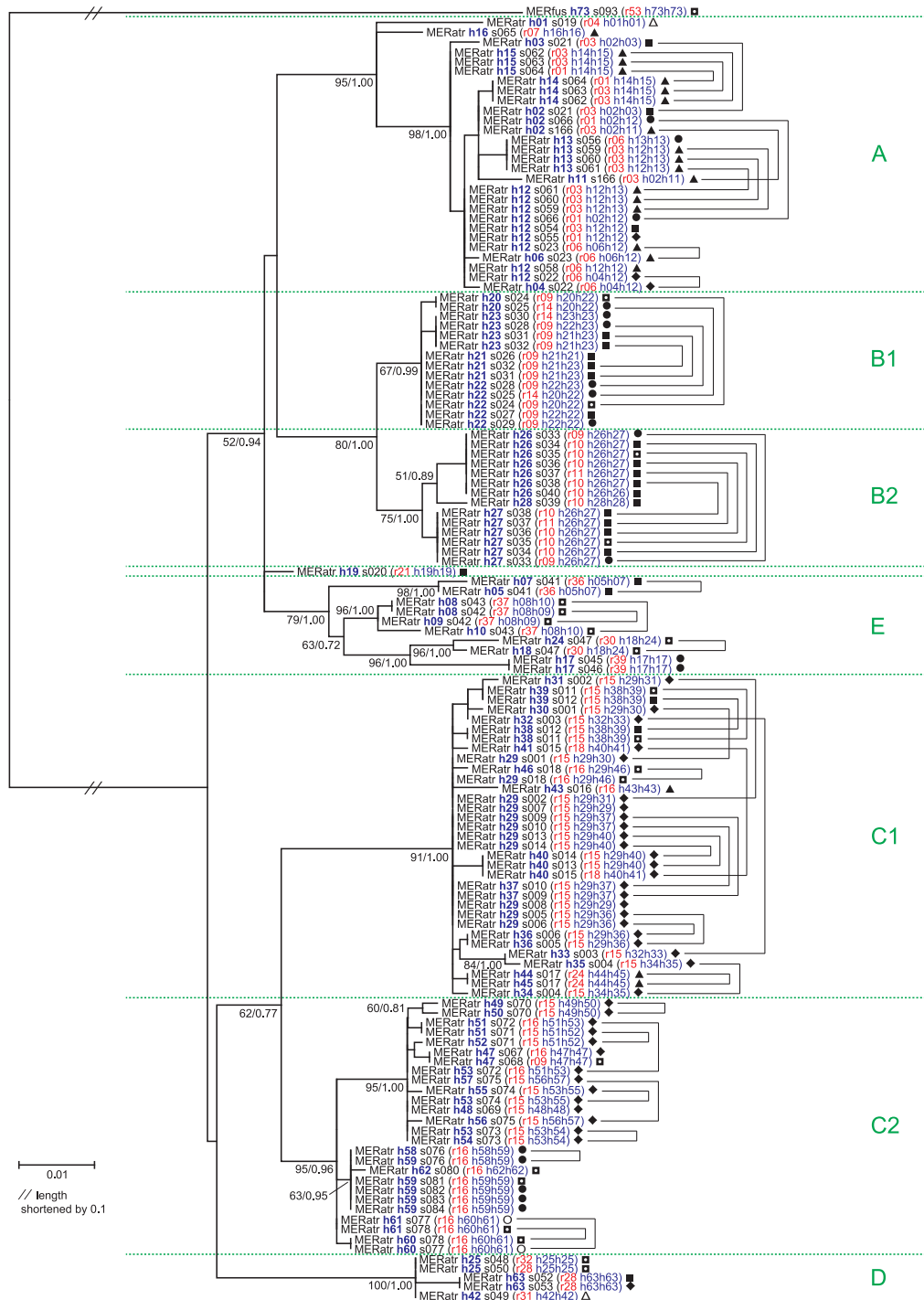


**Figure 3.** ML tree of partial EF1A sequences for 81 specimens of *Meriderma atrosporum* agg. rooted with *M. fuscatum* (fus); 607 contiguous positions (465 in exon part, 142 in intron part) were analyzed. The two alleles of specimens showing heterozygous sequences are treated separately and were connected by a loop. Labels include haplotypes (h), ribotypes (r, not contiguous), specimen number (s), and the morphological determination according to the concept of Poulain et al. (2011). Symbols for the origin of the specimens are the same as in Figure 2. Shown is the topology of the ML tree. Bootstrap / posterior probability values both above 50/0.5 are indicated.

**Table 1.** Statistics for EF1A geno- and haplotypes of the seven phylogroups of *Meriderma atrosporum* agg. recorded in five European mountain ranges.

Phylogroup	All	A	B1	B2	C1	C2	D	E
Specimens investigated	77	16	9	8	18	16	4	6
Genotypes found	51	10	5	3	13	12	2	5
Proportion of heterozygous genotypes	0.67	0.70	0.50	0.33	0.85	0.67	0.00	0.80
Genotypes to expect								
Chao2	93.6	29.7	6.7	3.9	17.4	33.1	2.0	7.5
SD	16.3	16.2	1.3	1.9	4.0	15.2	0.2	3.4
Asymptote (hyperbolic regression)	151.9	24.6	15.0	4.4	41.0	49.9	3.1	24.0
SD	0.2	0.3	0.6	0.4	0.8	1.7	0.5	0.6
Haplotypes found	60	10	4	3	17	16	2	8
Haplotypes to expect								
Chao2	108.9	19.4	4.0	3.0	27.4	36.6	2.0	12.2
SD	18.3	9.6	0.1	0.3	7.4	13.6	0.2	4.3
Asymptote (hyperbolic regression)	122.1	15.3	5.0	3.2	41.3	48.6	3.1	31.7
SD	0.9	0.2	0.2	0.1	1.3	1.3	0.5	1.0

T-rich intron (86 bases). In *M. aggregatum* two intron types can be found: first a T-rich intron (3 specimens, all homozygous, 74–94 bases); second a C-rich intron with a C-homopolymer (11–16 bases) followed by a AC dinucleotide microsatellite motif (up to 12 repeats). This sequence is extremely difficult to obtain, and we succeeded for only four specimens (all heterozygous, length 103–107 bases, see Supplementary Material Alignment S2). In both SSU and EF1A exon phylogenies and the concatenated tree (Fig. 2), the specimens with these two intron patterns form separate clades. In *M. atrosporum* agg. the intron belongs as well to the T-rich type.

Supplementary Material Figure S10 shows a scheme of the alleles found for EF1A sequences, including the intron. This simplified alignment visualizes the seven phylogroups named A, B1, B2, C1, C2, D and E. The phylogeny rooted with *M. fuscatum* (Fig. 3) shows the two alleles (EF1A haplotypes) of one specimen connected by loops. The haplotypes of one specimen always cluster within a single phylogroup. All together, 50 (61.7%) of the 81 investigated specimens of *M. atrosporum* agg. are heterozygous. Length differences between intron sequences are moderate (104–122 bases); since most heterozygosities are caused by 1–2 substitutions and one, more rarely two, indels per sequence (Supplementary Material Alignment S2). We recorded a total of 54 EF1A genotypes (exon and intron) composed of 63 haplotypes. All specimens except s020 (Bavarian Alps) can be assigned to one of the phylogroups A–E. All groups, with the exception of group D represented by five

specimens, contain both homo- and heterozygous specimens.

To test for the completeness of sampling within the five mountain ranges, we calculated accumulation curves for both EF1A geno- and haplotypes and computed two estimators for the completeness of sampling (Chao2 and the constant  $a$  for a hyperbolic regression following the formula  $y = ax / (b + x)$ , Table 1). The sample included 77 specimens (specimen s020 not assignable to one of the phylogroups and three more originating from other areas were omitted). For all phylogroups together, we found about half of the geno- and haplotypes to be expected according to the Chao2 estimator (54% and 55%, respectively). Figures for the hyperbolic regression were lower (34% and 49%, respectively). Genetic diversity varied strongly between phylogroups, with E, C2, and C1 being most diverse (ratio specimens to haplotypes).

In all five mountain ranges we found a high proportion of individuals with heterozygous EF1A sequences (Khibine, 3/9 homozygous/heterozygous specimens; French Savoie 5/8; Bavarian Alps 6/9; Polish Carpathians 8/5; northern Caucasus, Russia, 6/18). Figure 4 shows numbers of geno- / haplotypes found for the respective mountain ranges. In total the 77 specimens from five mountain ranges included 60 alleles (46 private, 14 shared) and 51 genotypes (43 private, 8 shared). From the eight genotypes shared between mountain ranges, five are homozygous. The number of alleles shared between subpopulations from the five mountain ranges, weighted by the number of possible combinations of two specimens,



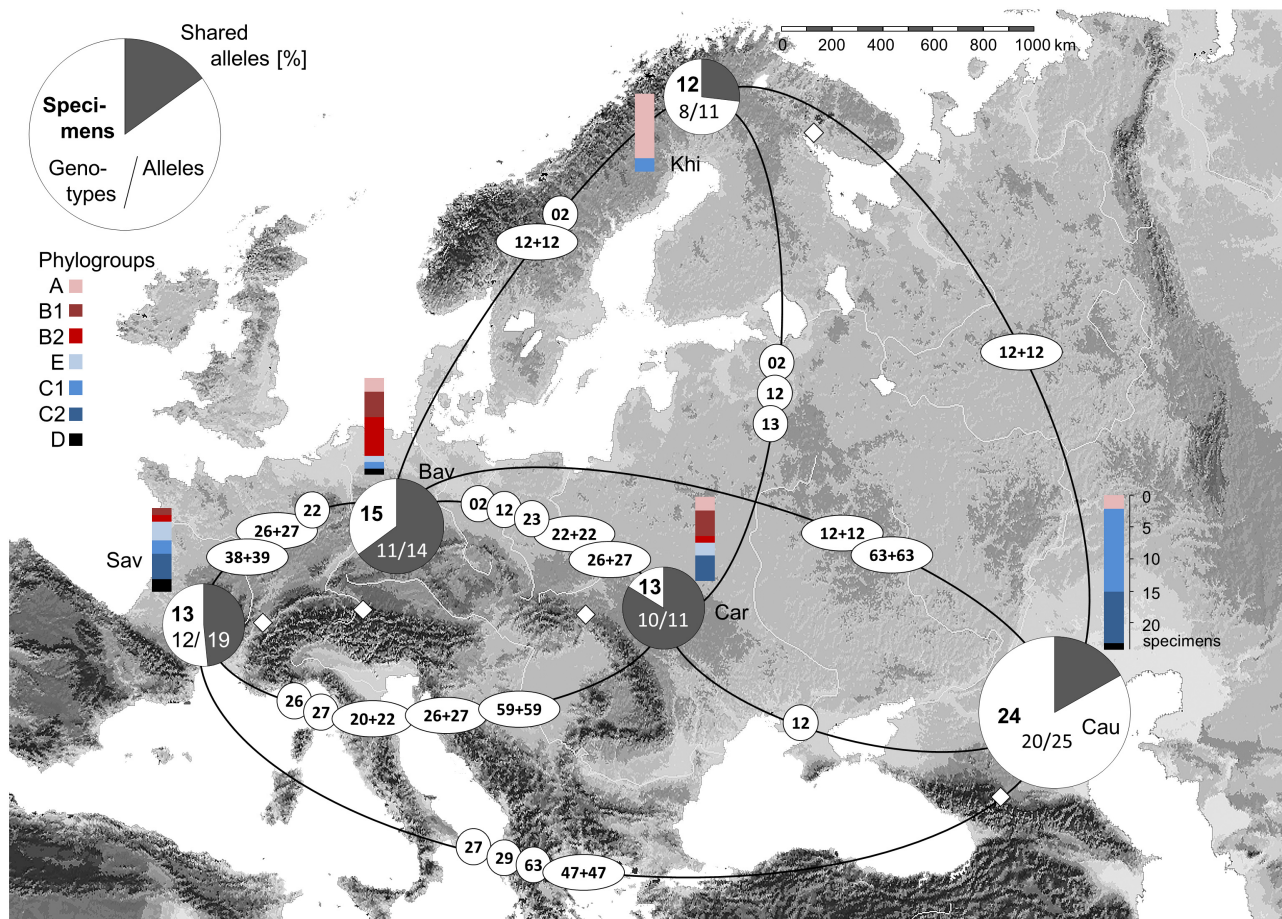


**Figure 4.** EF1A haplotypes of *Meriderma atrosporum* agg. from five European mountain ranges (study areas indicated by diamonds). Pie diagrams (scaled according to the number of specimens sequenced) denote the proportion of alleles shared with other regions (dark grey); numbers of specimens, genotypes and alleles for the respective region are given. Single alleles (circles) and genotypes (ellipses) shared between mountain ranges are indicated by lines. Colored bars show the number of specimens belonging to phylogroups A–E for each of the mountain ranges (Bav: Bavarian Alps, Car: Carpathians, Cau: Caucasus, Khi: Khibine Mts., Sav: Savoie, French Alps). Maps: Microsoft Encarta Reference Library, 2003 and Google Earth (modified).

is inversely correlated with the distance between these subpopulations (linear regression:  $R = 0.806$ , Figure 5).

In all mountain ranges except for the French Savoie, where we received most of the specimens from a large existing collection (MM), we found a considerable proportion of genotypes represented by more than one specimen (Khibine: 3 of 8 genotypes; French Savoie 1 of 12; Bavarian Alps 2 of 11; Polish Carpathians 2 of 10; northern Caucasus, Russia, 4 of 20). Most but not all of these specimens with identical genotypes were sampled within short distances (12: < 1 km, 3: < 10 km, 7: < 100 km), but some specimens from different mountain ranges displayed as well identical genotypes (12: 250–3000 km).

Exact tests for deviations from HWE were performed for four models (Table 2). A model with one panmictic population resulted in a much higher expected heterozygosity than the observed figure (0.64). Assuming first isolation between mountain ranges, second isolation between phylogroups (according to a model with seven reproductively isolated biospecies), and third isolation between phylogroups and mountain ranges, the deviation gradually decreased. For the last model, the majority of subpopulations is in HWE.

In addition, a simulation with a heterothallic sexual cycle was computed (equivalent to Fig. 1A1). The model defines subpopulations that are isolated by mountain ranges and across phylogroups but allows for amoebae from all spores of a

**Table 2.** Exact tests for deviation from Hardy-Weinberg equilibrium assuming different degrees of isolation (within mountain ranges, within phylogroups, and within mountain ranges and phylogroups). Shown are the ID's of the subpopulations, the observed ( $H_{obs}$ ) and expected ( $H_{exp}$ ) degree of heterozygosity, the test statistics (asterisks marking significance at  $p=0.05$ ), and the weighted average degree of heterozygosity ( $\hat{H}_{exp}$ ) for the whole population.

ID	n=	$H_{obs}$	$H_{exp}$	P	$\hat{H}_{exp}$
<i>Panmixis</i>					<b>0.97</b>
All	77	0.64	0.97	0.001	
<i>Isolated mountain ranges</i>					<b>0.92</b>
Khi	12	0.75	0.91	0.002	
Sav	13	0.62	0.97	0.000	
Bav	15	0.60	0.93	0.000	
Car	13	0.38	0.89	0.000	
Cau	24	0.75	0.93	0.000	
<i>Isolated phylogroups</i>					<b>0.81</b>
A	16	0.69	0.83	0.007	
B1	9	0.56	0.75	0.171*	
B2	8	0.75	0.63	0.022	
E	6	0.67	0.89	0.028	
C1	18	0.83	0.86	0.098*	
C2	16	0.50	0.90	0.000	
D	4	0.00	0.57	0.087*	
<i>Isolated mountain ranges and phylogroups</i>					<b>0.73</b>
Khi_A	10	0.80	0.87	0.002	
Bav_A	2	0.50	0.83	0.333*	
Car_A	2	0.50	0.83	0.331*	
Cau_A	2	0.50	0.50	1.000*	
Bav_B1	4	0.50	0.71	0.317*	
Sav_B1	1	1.00	1.00	1.000*	
Car_B1	4	0.50	0.68	1.000*	
Sav_B2	1	1.00	1.00	1.000*	
Bav_B2	6	0.67	0.67	0.882*	
Cau_B2	1	1.00	1.00	1.000*	
Sav_E	3	1.00	0.93	1.000*	
Bav_E	1	1.00	1.00	1.000*	
Car_E	2	0.00	0.00	monomorphic	
Khi_C1	2	0.50	0.83	0.333*	
Sav_C1	2	1.00	1.00	1.000*	
Bav_C1	1	1.00	1.00	1.000*	
Cau_C1	13	0.85	0.78	0.494*	
Sav_C2	4	0.25	0.89	0.010	
Car_C2	4	0.25	0.25	1.000*	
Cau_C2	8	0.75	0.95	0.066*	
Sav_D	2	0.00	0.00	monomorphic	
Bav_D	1	0.00	0.00	monomorphic	
Cau_D	1	0.00	0.00	monomorphic	

subpopulation to mate with equal probability. To counteract the effect of loss of rare alleles by genetic drift from the small sample ( $n=77$ ), for a second simulation every genotype was replicated ten times ( $n=770$ ). For the first offspring generation both simulations result in only slight changes for the degree of heterozygosity in comparison to

the figure observed for the whole real population (Table 3). The proportion of private genotypes in all genotypes found was slightly higher, and the observed figures were slightly outside the computed confidence intervals. As to expect from the effects of genetic drift in small populations, the number of haplotypes decreased significantly in the

**Table 3.** Results of simulation for the first offspring generation assuming panmictic sexual subpopulations with reproductive isolation between phylogroups and between mountain ranges. Shown are numbers of private (unique for one mountain range) and shared EF1A haplo- and genotypes for the real sample and a tenfold increased population (each genotype was replicated ten times). Figures are the mean  $\pm$  SD of 999 simulations. An asterisk indicate values where observed values lie within the 95% confidence range of the simulation results (see Supplementary Databases S2, S3).

	Sample Observed	Sample Expected	Sample x10 Expected
Sample size	77	77	770
Number of haplotypes	60	48.5 $\pm$ 2.4	*60.0 $\pm$ 0.0
- private haplotypes	46	37.1 $\pm$ 2.7	*46.0 $\pm$ 0.0
- shared haplotypes	14	11.4 $\pm$ 1.2	*14.0 $\pm$ 0.0
Number of Genotypes	51	*53.8 $\pm$ 2.8	170.0 $\pm$ 5.0
- proportion of homozygote genotypes	0.36	*0.39 $\pm$ 0.0	*0.37 $\pm$ 0.0
- private genotypes	43	48.6 $\pm$ 3.4	151.8 $\pm$ 5.2
% of all	84.3	90.8 $\pm$ 2.9	89.3 $\pm$ 0.8
- shared genotypes	8	5.2 $\pm$ 1.3	18.2 $\pm$ 1.3
- shared and heterozygous	3	*2.0 $\pm$ 1.0	6.7 $\pm$ 0.5
% of shared	37.5	74.9 $\pm$ 18.5	*37.1 $\pm$ 3.2
- shared and homozygous	5	3.3 $\pm$ 1.1	11.5 $\pm$ 1.3
% of shared	62.5	25.1 $\pm$ 18.5	*62.9 $\pm$ 3.2

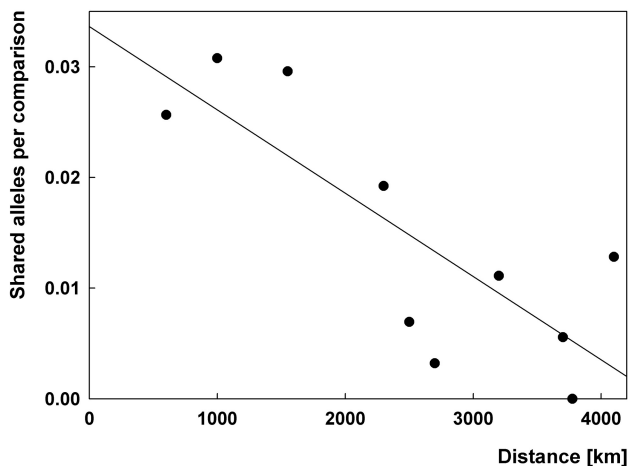


**Figure 5.** Shared EF1A haplotypes vs distance between mountain ranges for 77 specimens of *Meriderma atrosporum* agg. The distance between the each of the five investigated mountain ranges ( $\pm$ 50 km) was plotted against the number of shared haplotypes weighted by the number of possible combinations between any two specimens from two mountain ranges.

simulation with  $n=77$ , but all haplotypes were retained for a tenfold sample size ( $n=770$ ). In the latter case, the higher sample size resulted in many more genotypes than observed (170 compared to 51 observed), which led to higher numbers for shared genotypes (18.2 vs 8.0 observed). However, the proportions of homo- and heterozygous

genotypes in all shared genotypes remained nearly the same as observed.

### Number of Nuclei in Spores

Both TEM images but especially counts of DAPI-stained spores revealed uniformly a single nucleus per spore (Supplementary Fig. S11). Four specimens were counted (s005, phylogroup C, 11 spores; s024, B, 39; s042, E, 42; s080, C, 10). The single nucleus is well visible in TEM, but invisible in LM images.

## Discussion

Until now myxomycetes were largely neglected by molecular biologists, most likely since they do not carry any economic importance and do not include pathogenic species. Only in recent years first phylogenies of the group were constructed (Fiore-Donno et al. 2012, 2013). The prevailing species concept is still based on the morphological characters of the fructifications, and only a few of the latest papers (e.g., Hoppe et al. 2010; Leontyev et al. 2014; Novozhilov et al. 2013a, b) on myxomycete taxonomy employ molecular markers, especially partial sequences for the nuclear small subunit ribosomal RNA gene (SSU). This gene is widely accepted as a barcode marker for other groups of protists (Pawlowski et al. 2012; Adl et al. 2014). In myxomycetes, its first ca. 600 bases, seen

from the 5'-end, are free of introns and informative but can still be aligned due to the alteration of highly variable and rather conservative sections (see fig. 4 in [Fiore-Donno et al. 2012](#)). This marker was successfully used to show geographic differentiation within the morphospecies *Badhamia melanospora* Speg. ([Aguilar et al. 2013](#)).

From another direction of research, being especially popular in the decades 1960–1980, a second species concept evolved. This was based on crossing experiments with single-spore cultures of the model species *Physarum polycephalum* and *Didymium iridis* (both Physarales). These species can be kept in axenic media, and compatible amoebal strains were identified as biospecies ([Collins 1979](#)). However, rarely different biospecies could be linked with differences in fruit body morphology (*D. iridis*; [Clark 1993, 2000](#)). Since most myxomycetes were never or only with high efforts cultivated, the biospecies concept remained a theoretical approach and was never applied to natural populations.

This was the starting point for this study. In the genus *Meriderma* a second marker, the gene coding for the protein elongation factor 1 alpha (EF1A), turned out to be extremely variable due to a spliceosomal intron in the first part of the gene. In myxomycetes this intron is very different in length, reaching from 40 bases in *Trichia alpina* (R.E. Fr.) Meylan to 719 bases in *Lycogala epidendrum* (L.) Fr. ([Fiore-Donno et al. 2013](#)). Not a lot is known about intraspecific diversity of the intron: in the bright-spored myxomycete *Trichia varia* (Pers. ex J.F. Gmel.) Pers. it is about 60 bases long and showed differences in between, but not within three intraspecific groups, most likely biospecies ([Feng and Schnittler 2015](#)). In the case of *Meriderma* reported herein, the same intron is much longer and extremely diverse (Supplementary Material Fig. S10).

### Geographic Differentiation in *M. atrosporum* agg.

We first used partial SSU sequences to study the internal structure of the genus. Both markers, partial SSU sequences (Supplementary Material Figs S1, S2) and the exon sections of the EF1A gene (Supplementary Material Figs S3, S4), but as well the concatenated phylogeny ([Fig. 2](#), Supplementary Material Figs S5, S6), clearly separated two taxa which can be morphologically distinguished as well, *M. fuscatum* and *M. aggregatum*. For the remaining specimens which cannot be easily distinguished by morphology (*M. atrosporum*

agg.) we found a less pronounced geographical differentiation between the five studied mountain ranges in comparison to the trans-continental separation found by [Aguilar et al. \(2013\)](#) for *Badhamia melanospora*. The dark-spored species *B. melanospora* is a succulenticolous myxomycete ([Lado et al. 2007](#)) and shows therefore another kind of geographical restriction, tracing the geographical distribution of succulent plants whose decaying tissues, infected with yeasts and bacteria, provide the substrate. For *M. atrosporum* agg. geographical differentiation is present but not complete ([Fig. 4](#)). A Mantel test confirmed the presence of a spatial genetic structure for both markers. In the phylogeny constructed from exon and intron sections of the EF1A gene ([Fig. 3](#)) most sequences of a phylogroup origin from one of the mountain ranges (A: Khibine Mts., B: German Alps and Carpathians, C: Caucasus, E: French Alps), although all included sequences from several ranges (A: 3, B: 3, C: 5, D: 3 and E: 3). The number of ribotypes is large (21 in 81 investigated specimens) but seems to be limited: Two ribotypes of published sequences from three specimens of *M. atrosporum* agg. (French Alps; [Fiore-Donno et al. 2008, 2012](#)) re-occurred in the specimens investigated by us.

### Phylogroups in *M. atrosporum* agg.

The phylogeny constructed from exon parts of the EF1A gene (Supplementary Material Figs S3, S4) is not in contradiction with the SSU phylogeny (Supplementary Material Figs S1, S2). Although the genetic variation in both markers is not sufficient to resolve the phylogroups as clearly as revealed by the EF1A phylogeny constructed from exon plus intron sections, only two specimens assume uncertain (s020) or contradictory (s068) positions.

Since our sampling is not exhaustive (only about half of the geno- and haplotypes to expect according to accumulation curves were found, [Table 1](#)), specimen s020 may be simply a representative of another rare phylogroup, where we found a single specimen only. Specimen s068 is the only contradictory case: it falls clearly into phylogroup C2 according to the EF1A-phylogeny, but the SSU phylogeny places it in group B. In this case, a crossing between groups cannot be ruled out. A primary hybrid between two groups is likely to display different alleles in the EF1A marker, but can be expected to have a homogenous SSU sequence, since this extrachromosomal multi-copy gene shows a non-Mendelian inheritance. EF1A as a nuclear single-copy gene can be expected to follow Mendelian inheritance. However, already

second-generation offspring may show a homogeneous EF1A (as it is the case for specimen s068) but inherited the SSU genotype that originated in the other phylogroup.

### Patterns in the EF1A Spliceosomal Intron

For *Meriderma*, the intron included in the first part of the EF1A gene exhibits a degree of variation hitherto not found within myxomycetes. We found 54 geno- and 63 haplotypes within 81 investigated specimens. This diversity is only comparable with that found for a study of the bright-spored species *Trichia varia* (Feng and Schnittler 2015) for the complete SSU sequences with six intron insertion positions that may carry different group I introns. Since SSU is expected to be homogeneous for myxomycetes, sequences can be obtained without cloning. In contrast, alleles (haplotypes) in the EF1A spliceosomal intron will be maintained and should thus effectively witness sexual events, but for heterozygous specimens the sequences can only be obtained by cloning.

For the cellular slime mold *Dictyostelium discoideum* with a well annotated genome (Eichinger et al. 2005), a duplication of the EF1A gene located on chromosome 1 is reported (efaAI, gene ID: 8616922; efaAII, gene ID: 8616783), whereas for the myxomycete model species *Physarum polycephalum* (no annotated genome available) only one sequence is known (tef1, AF016243). In a tree constructed from the complete exon part (1140 positions, Supplementary Material Alignment S4, Fig. S12) of the EF1A genes of 50 myxomycetes, 5 other protists and the two EF1A copies from *D. discoideum*, the latter two formed a separate cluster and did not group individually with our sequences, pointing towards a duplication event occurring within the evolution of *D. discoideum*. This holds true as well for the exon part of partial EF1A sequences (as done by us, 465 positions) with additional 30 exon haplotypes of *Meriderma* and 3 exon haplotypes of *Lamproderma puncticulatum* (Supplementary Material Alignment S4, Fig. S13). Together with the results of cloning (which showed always the same two alleles except for a few randomly distributed one-base mutations) this lends strong evidence that the two alleles of the *Meriderma* EF1A gene originate from a single copy of this gene.

Even with the allelic diversity shown in this study we cannot assume a single marker to be sufficiently variable to allow genotyping to the individual level of the plasmodium or the resulting colony of fruit bodies, and this is confirmed by the

accumulation curves constructed for haplo- and genotypes, whose analyses let to expect about 100–150 geno- and 110–120 haplotypes for *M. atrosporum* agg. for the five investigated mountain ranges (Table 1). The world-wide diversity for the intron marker is probably much higher. The three additional specimens not coming from one of the five mountain ranges contributed three new EF1A-genotypes and four new haplotypes, but did not repeat a haplotype already found in the five intensely studied mountain ranges. The host gene of the spliceosomal EF1A-intron follows Mendelian inheritance; variation may accumulate by either mutations or recombination events. As for SSU and EF1A exon sequences, different phylogroups are visible already by a visual inspection of the intron patterns (Supplementary Material Fig. S10). Two of the five major phylogroups show an additional bifurcation (B1, B2 and C1, C2, see Fig. 3). Most remarkable is the haplotype pattern within the EF1A phylogeny constructed from combined exon and intron sections (loops in Fig. 3). Crosses between phylogroups (which should show up as the two haplotypes of a specimen found in two different groups) are seemingly absent, which indicates reproductive isolation. In addition, all seven phylogroups delimited by us have exclusive ribotypes (with the exception of B1/B2 and C1/C2 where the separation is incomplete for 1 and 2 ribotypes, respectively). This pattern is explained best by assuming seven reproductively isolated biospecies, since except for specimen 068 no apparent crossings between phylogroups occurred, and not a single haplotype reoccurs in a second phylogroup. Each of these putative biospecies represents a gene pool of its own, and recombination will produce fruit bodies with diverse combinations of haplotypes. In the presence of mating types a high proportion of heterozygous sequences can be expected. As such, our trees give evidence for the existence of at least seven biospecies within *M. atrosporum* agg., being identical with the phylogroups A, B1, B2, C1, C2, D and E. Our sampling is in no way exhaustive and largely limited to the five investigated mountain ranges. A larger extent of sampling may add more putative biospecies: specimen s020 from Bavaria, not fitting into one of the seven groups and showing a unique homozygous EF1A genotype, may be a representative of such an undersampled biospecies. In a similar way, a group like C2 and E may turn out to consist of more than one reproductively isolated units, if sampling is extended.

These putative biospecies are largely but not entirely restricted to one of the mountain ranges.

This relative geographical isolation may have influenced speciation, as it is indicated by the fact that for every biospecies one, rarely two of the mountain ranges comprise at least 50% of all specimens (A: Khibine, B1: Fench and German Alps, B2: German Alps, C1: German Alps, C2: Caucasus, D: Caucasus and E: French Alps). This pattern is more consistent with the moderate endemism model found as well for other groups of protists (e.g., Ciliata, Foissner et al. 2008) than the ubiquist model of Fenchel and Finlay (2004). Spores of *Meriderma* are between 10 and 20  $\mu\text{m}$  in diameter and are thus larger than for most fungi (terminal sedimentation velocity to expect between 2 and 10 mm/s, compare Tesmer and Schnittler 2007). As indicated by the relationship between distance and shared haplotypes (Fig. 5), we must assume limited dispersal across mountain ranges, with gene flow to expect over longer periods of time. Long-distance dispersal in myxomycetes was detected by sequencing spores from aerial samples (Kamono et al. 2009). Consistent with this, a study from lowlands in Germany, employing environmental PCR, detected sequences assignable to *Meriderma* (Fiore-Donno et al. 2016), but fruit bodies are known only from montaneous regions (Schnittler et al. 2011). Therefore, lowlands should be sink populations for this genus. Our results for *Meriderma atrosporum* agg. are explained best by assuming nearly complete isolation between phylogroups (putative biospecies) and fairly complete isolation between mountain ranges.

Within a phylogroup and a mountain range, sex should regularly occur, creating different genotypes of fruit bodies. This is indicated by the high proportion of specimens heterozygous for the spliceosomal EF1A-intron (and sometimes for exon positions). The respective haplotypes will be separated again during another meiosis and spore formation, but in this study they appear heterozygous, since the DNA for one specimen originates from multiple spores of a fruit body which were sequenced. Meiotic recombination and mutation events may create new haplotypes. Recombination happens only in rare cases for the comparatively short intron, but the haplotypes h57 and h58 in group C2 may be an example (see Supplementary Material Alignment S2, Fig. S10).

### Do other Reproductive Options Exist?

The high diversity in the EF1A intron marker, together with a fairly high overall degree of heterozygosity (0.64) in the studied metapopulation

across five mountain ranges suggests regular sexual events, as depicted in Figure 1A, but does not rule out the presence of the other reproductive options. Pseudohomothallism via multinucleate spores (complying with the life cycle in Fig. 1B) seems not to occur in *Meriderma* spp., as indicated by TEM analyses of DAPI-stained spores (Supplementary Material Fig. S11). In addition, pseudohomothallism as the dominating life cycle in a population would make mating type genes superfluous.

If occurring frequently, several other reproductive options would result in a homozygote excess and deviation from HWE. These are internuclear selfing (Fig. 1A2), pseudohomothallism via multinucleate spores (1B) or automixis with coalescing products of meiosis II (1D). True homothallism (1C) or a haploid apomictic life cycle (1F) would even result in instant homozygosity. Looking at deviations from HWE for the entire metapopulation, the exact test gives a clear picture: for the population as a whole, the observed heterozygosity (0.64) is much lower than the expected (0.97). However, this difference decreases gradually, if we take the isolation between phylogroups (putative biospecies) and mountain ranges into account (Table 2). In the last case, most of the subpopulations are in HWE (but the number of individuals becomes very small), and the overall expected heterozygosity drops to 0.73.

As a second approach, we simulated the fate of these subpopulations over ten generations with a purely sexual cycle, assuming complete isolation between phylogroups and mountain ranges (Supplementary Material Databases S2, S3). On one hand, these assumptions may overestimate the degree of heterozygosity, since all spores of a subpopulation is given equal mating probability (in nature, spores from one colony where amoebae hatch in close vicinity may have a higher chance of mating than those coming from different colonies). On the other hand, the real degree of heterozygosity may be underestimated by assuming complete isolation between mountain ranges (in nature, there should be limited gene flow). In accordance with the test for HWE, the degree of heterozygosity for the first offspring generation is still comparable to the observed values (Table 3). However, heterozygosity will decrease after 10 generations due to loss of alleles by genetic drift. If this effect is (at least in part) outbalanced by increasing the population size ( $n=770$ , replicating each of the observed genotypes ten times), the overall degree of heterozygosity remains fairly stable (observed: 0.64, first generation:  $60 \pm 0.0$  haplotypes,  $h_e = 0.64 \pm 0.02$ , tenth

generation:  $55.9 \pm 1.8$  haplotypes,  $h_e = 0.57 \pm 0.03$ ; means  $\pm$  SD for 999 simulations).

From these analyses it becomes unlikely, that one of the alternative reproductive options outlined above is very common (in addition, a loss in heterozygosity may be explained as well by assuming repeated mating events of the same large amoebal populations, see below). However, for one alternative reproductive option, diploid apomixis (Fig. 1E) the degree of heterozygosity should not immediately decrease, if heterozygosity will be inherited from sexual ancestors. Since apomictic genotypes will disperse via diploid spores, a few dominant and/or widely distributed genotypes would indicate a fitness advantage for diploid apomicts. Identical genotypes may thus be created by three ways: a) diploid apomixis, b) by chance via independent sexual events involving genetically different amoebae, and c) by repeated matings between amoebae of the same two clonal populations.

Repeated matings may be not rare: in myxomycetes, a single spore should be able to build up an entire, clonal amoebal population by binary fission of amoebae. Amoebae of myxomycetes can encyst (Shchepin et al. 2014) to survive inhospitable conditions, like frost (winters with low to missing snow cover) or drought (summer); therefore we can expect amoebal populations to persist and give rise to multiple, genetically identical fructifications when mating repeatedly with each other. Consistent with this assumption, 12 of 34 cases of specimens with identical genotypes involved specimens collected less than 1 km apart. These distances are well within the range amoebae may be able to bridge, especially if moved passively by melt water from snow banks or as microcysts by dust.

But the survey involves as well specimens with identical genotypes found within a mountain range but separated by larger distances (1–100 km, 10 of 34), sometimes between mountain ranges (250–3000 km, 12 of 34), which would comply with the assumption of an additional diploid apomictic life cycle. Therefore the question arises, if the repeated occurrence of genotypes shared between mountain ranges, with many of them (5 of 8) including homozygous genotypes, lends evidence for this second, asexual life cycle. To explore if such identical genotypes can be created independently from each other by chance, we constructed the simulation routine outlined above. Interestingly, under these assumptions the proportion of homozygous specimens obtained by the simulations does not significantly deviate from the sample obtained by us (Table 3). If simulations were run with only the 77

specimens that were investigated, rare alleles will be quickly lost due to genetic drift, and such haplotypes become extinct already in the first offspring generation. Simulations with a tenfold increased sample (creating a population of 770 by multiplying each genotype ten times) suffered much less from loss of rare alleles. With this larger sample we obtained  $170 \pm 5$  genotypes. This is in the range of genotypes to be expected for a tenfold increased sample size, if a genotype accumulation curve would have been constructed and extrapolated with a hyperbolic function (Table 1). We observed 8 of the 51 existing genotypes to be shared between mountain ranges (15.6%); the simulations results in proportions of 9.6% and 10.7% (models with  $n = 77$  and  $n = 770$ , respectively, see Table 3). Therefore, most of the observed genotypes that are common between mountains can be created by chance. However, long-distance dispersal between mountain ranges (not considered in the simulation) may increase the proportion of shared genotypes.

We thus conclude that the pattern of EF1A genotypes found by us can well be explained by assuming exclusively reproduction following sexual events, therefore alternative reproductive options should be at least rare. These results challenge the conclusions of a study on *Lamproderma* (dark-spored myxomycetes), where numerous specimens were found to be identical in three marker genes (SSU, ITS, and EF1A). This was interpreted as evidence for the existence of asexual strains (Fiore-Donno et al. 2011). However, in this genus the EF1A spliceosomal intron is rather short (ca. 90 bp) and seems to be much less variable. In contrast, our results are in agreement with a recent study on the bright-spored species *Trichia varia* (Feng and Schnittler 2015) that revealed three, most likely reproductively isolated biospecies for which a total of 18 partial SSU ribotypes were found (Feng and Schnittler 2015, 2016). In both cases our data do not hint towards an asexual life cycle, but do as well not prove its complete absence.

It cannot be ruled out, that the more frequent occurrence of non-heterothallic samples in early culture experiments was caused by a degeneration of the strains, which often were kept over a long time in the laboratory. For instance, multiple cases of degeneration are known for the most widely cultivated *Physarum polycephalum* (Laffler and Dove 1977), including strains with haploid plasmodia (Mohberg 1977), such that lost the ability to fruit, or older plasmodia becoming polyploid (Werenskiold et al. 1988). For the study of natural populations in myxomycetes, markers allowing individual level

genotyping of fructifications, or strains, need to be developed. This would definitely exclude or confirm the existence of other reproductive modes than sexual heterothallism.

## Conclusions

The results of this study on *Meriderma atroporum* agg. are explained best by the assumption of several biospecies (seven were detected in this study). These are reproductively isolated from each other but predominantly exchange genes within a biospecies by sexual events. This confirms the results obtained with numerous crossings for cultivable Physarales (like *Didymium iridis*), where at least a large proportion of specimens behaves heterothallic.

If the hypothesis holds true, that the non-heterothallic strains found in many cultured species (Clark and Haskins 2010) do not reflect the natural conditions in all or most myxomycetes, but result at least in part from a degeneration of these strains, we need (i) studies including “wild” populations and (ii) markers allowing true genotyping to settle the question about the biological importance of alternative reproductive options in myxomycetes.

This study shows further that the biospecies concept is, at least in theory, applicable to natural populations of myxomycetes to overcome the short-cuts of the morphospecies concept (Clark 2000; Schnittler and Mitchell 2000) if sufficiently polymorphic markers can be found. However, it might be difficult to link reproductively isolated biospecies with differences in morphological characters, to make them visible for taxonomists.

## Methods

**Specimens:** Specimens of *Meriderma* spp. were systematically collected in five European mountain ranges: the Khibine Mountains (Kola peninsula, Russia, see Erastova et al. 2015), the Bavarian Alps (Germany), the French Alps (Dept. Haute Savoie, France), the Carpathians (southern Poland) and the Northern Caucasus (Teberda State Biosphere Reserve, Russia, see Novozhilov et al. 2013b). In addition, singular specimens obtained by loan from several other parts of the world, e.g. the American Rocky Mountains, were considered. Specimens were deposited in herbaria KRAM (A. Ronikier, Cracow, Poland), LE (Y.K. Novozhilov, St. Petersburg, Russia) and in the collections BW (B. Woerly, France), HK (A. Kuhn, Germany), MM (M. Meyer, France), sc (M. Schnittler, Germany, to be deposited in M). Information about specimens and GenBank accession numbers is found in Supplementary Material Database S1.

**DNA Extraction, PCR and sequencing:** About 2–3 sporocarps per specimen were pre-cooled at  $-80^{\circ}\text{C}$  and grounded

using a ball mill (Retsch MM301) at 30 Hz for 80 seconds. Genomic DNA was extracted using the Invisorb Spin Food Kit II (Stratec). Partial sequences of the first part of the SSU (5'-end until the first known intron insertion site) were obtained using the primer pair S1 (AACCTGGTTGATCCTGCC) and SU19R (GACTTGCTCTAATTGTTACTCG, Fiore-Donno et al. 2008, 2012), which amplifies a partial SSU sequence for most dark-spored myxomycetes.

Partial EF1A sequences covering the first part of the gene include a spliceosomal intron; here the primers 1FPhy (GCAAGTCCACCACCACTGG; Fiore-Donno et al. 2011) and E800R (CTTGTCGGTCGGGCGCTTGGGCT; Fiore-Donno et al. 2005) were used for an initial screening. The latter was replaced by a new primer called EMerR1b which was designed to work best with *Meriderma* spp. (GGGGTTGTATC-CGATCTTC, all primers written in 5'-3' direction). The primer pair 1FPhy and EMerR1b was used throughout the study and amplifies triplet codes of the amino acids 14–91 and 92–168 (numbering according to the sequence AF016243, *Physarum polycephalum*, Baldauf and Doolittle 1997). Between the codes for amino acids 91 and 92 a spliceosomal intron of ca. 100 bases in length is located.

PCR reactions were performed using the MangoTaq DNA Polymerase (Bioline) with the following conditions: initial denaturing at  $94^{\circ}\text{C}$  / 2 min, followed by 40 cycles of denaturing ( $94^{\circ}\text{C}$  / 30 s), annealing ( $58^{\circ}\text{C}$  / 30 s) and elongation ( $72^{\circ}\text{C}$  / 60 s), plus a final elongation at  $72^{\circ}\text{C}$  / 5 min. Cycle sequencing reactions were performed using the BigDye Terminator v3.1 Cycle Sequencing Kit (Applied Biosystems, Thermo Fisher Scientific). Since many EF1A sequences showed heterozygosities with frequent short indels, the respective alleles were cloned with the NEB PCR Cloning Kit (New England Biolab). PCR amplicons were purified by using SureClean Plus (Bioline). The concentration of the resuspended PCR pellet was photometrically measured (Nanodrop Lite, Thermo Scientific). Ligation was assembled via calculating the amount of the insert to be added by relative length calculation. Ligation and transformation were done according to the manufacturer instructions. Best results in terms of an even distribution and a sufficient number of colonies were obtained by plating 100  $\mu\text{l}$  transformed *E. coli* strain DH5 $\alpha$  outgrowth on one LB-agar plate. A colony PCR was carried out with the vector-specific primers provided by the supplier. Amplicons were purified by SureClean Plus and used for cycle sequencing (BigDye Terminator v3.1 Cycle Sequencing Kit, Applied Biosystems, Thermo Fisher Scientific).

**Phylogenetic and population genetic analyses:** Partial SSU sequences were free of heterogeneities and were aligned using MAFFT 7.215 (Katoh and Standley 2013) with the iterative refinement method “X-INS-i” under the option “-scarnapair” that considered secondary structure information of RNA. The partial EF1A sequences turned out to be often heterozygous by several substitutions and short indels. From this reason, the sequences were cloned, and between 2 and 11 clones were sequenced to obtain both alleles. The partial EF1A sequences were aligned by MAFFT 7.215 with the option “E-INS-i” and then manually adjusted. Exon parts of EF1A sequences were determined according to the known protein and nucleotide EF1A sequence of *Physarum polycephalum* (Genbank AF016243; Baldauf and Doolittle 1997). Two alignments were constructed: first an alignment of exon sections with 465 bases including 155 (78 + 77) triplet codes, here the intron was cut out. The second alignment included the intron which comprises ca.  $110 \pm 20$  bases. Since heterozygosities occurred not only in the spliceosomal intron, but as well in several positions of the exon section (typically the third base of a triplet code), for both alignments the respective alleles were treated separately.



The SSU alignment (Supplementary Alignment S1) consists of 593 exon positions, of which 569 contiguous positions were used in phylogenetic analyses. The EF1A alignment includes 465 exon positions (equaling 155 triplet codes) plus 142 intron positions (Supplementary Material Alignment S2). Substitution models for Maximum likelihood (ML) analysis and Bayesian analysis were selected using TOPALi 2.5 (Milne et al. 2009) under the Bayesian information criterion. For SSU and the exon sections of the EF1A gene the best models were TrNef+G (ML analysis) and K80+G (Bayesian analysis), respectively. For EF1A exon part and intron part, the best models were TrNef+G (ML analysis) and SYM+G (Bayesian analysis). ML analyses were conducted using PhyML 2.4.5 (Guindon and Gascuel 2003) implemented in TOPALi with 1000 bootstrap replications. Bayesian analyses were carried out with MrBayes 3.1.1 (Ronquist and Huelsenbeck 2003) implemented in TOPALi with 2 runs, 10 million generations, 50% as burnin, sampled every 100 generations. Both SSU and EF1A exon phylogenies were rooted with three genotypes of *L. puncticulatum* Härkönen (Fiore-Donno et al. 2011). In addition, a concatenated alignment of the SSU and EF1A exon part (Supplementary Alignment S3) was used for a two-gene phylogeny.

A Mantel test including 999 iterations for the comparison of geographical and genetic distance matrices (SSU sequences) was performed with the ExtraStats function of PopTools 3.2.5 (Hood 2010). It calculates a confidence interval from the permutations of the two matrices. If the real correlation is outside the 5/95% confidence intervals, a significant spatial structure of the data set must be assumed. Geographic distances between localities of specimens were calculated using an Excel macro for the Vincenty formula (Dalglish 2014).

The EF1A intron sections aligned sufficiently well only within *Meriderma atrosporum* agg. (several specimens of *M. aggregatum* displayed a completely deviating intron type); we therefore rooted this phylogeny with *Meriderma fuscatum* (MM38934). For partial SSU sequences from 81 specimens of *Meriderma atrosporum* agg. p-distances (Nei and Kumar 2000) were computed with MEGA 5.2 (Tamura et al. 2011). Due to many heterozygote specimens the same data set for partial EF1A sequences included 131 sequences; here only the exon part was considered to compute p-distances. In the rare cases of heterozygosities in the EF1A exon parts we selected one of the alleles at random.

Considering both exon and intron parts, EF1A haplotypes (alleles) for the 81 investigated specimens of *M. atrosporum* agg. were identified. Haplotype accumulation curves were constructed according to the Hubert formula, employing the program EstimateS (50 randomizations; Version 7, Colwell 2004), which computes also a number of estimators of species richness. The Chao2 estimator (Chao et al. 2006) was chosen as most reliable (Unterseher et al. 2008) and calculated with the "classical settings" of estimateS. In addition, a hyperbolic regression according to the Michaelis-Menten formula  $y = ax/(b + x)$ , resulting in a curve shape coming very close to a broken-stick model (Magurran 2004, compare Schnittler 2001) was applied to the data, with the parameter a giving an estimate for the maximum number of haplotypes to be expected if sampling would be continued indefinitely.

For the 77 specimens of *Meriderma atrosporum* agg. an exact test for the deviation from HWE (accounting for multi-allelic loci) was computed with Arlequin 3.5.2 (Excoffier and Lischer 2010) on base of the EF1A haplotypes (exon and intron parts), assuming different degrees of isolation within subpopulations. Four models were tested: a single panmictic population, and subpopulations isolated by mountain ranges (assuming no long-distance dispersal of spores), by phylogroups (assuming reproductively isolated biospecies), and by

mountain ranges and phylogroups. In addition, two simulation runs were programmed in Excel to calculate the average degree of heterozygosity and the number of geno- and haplotypes shared between mountains over ten generations. We assumed panmixis within a biospecies (defined as a clade recovered in the combined SSU and EF1A phylogeny and including all alleles of the heterozygous specimens belonging to it) and within a mountain range, but not in between biospecies and mountain ranges (Supplementary Material Databases S2, S3). We randomly paired gametes (equal to haploid meiospores) for each generation, and monitored the outcome with respect to the number of geno- and haplotypes shared between the populations. A total of 999 model runs were performed with the tool "Monte Carlo Simulation" of the Excel PlugIn Poptools (Hood 2010). Confidence intervals (95%) were calculated for model parameters for a Mantel test to see if the observed values are still within their limits. The first model comprised the 77 investigated specimens from the five mountain ranges. To minimize loss of rare alleles due to genetic drift, the genotype of each specimen was replicated ten times, resulting in 770 genotypes in the second model.

**Transmission electron microscopy and fluorescence labeling of spores:** For TEM preparation, whole sporocarps were transferred into an Eppendorf tube, vortexed and stored in glutaraldehyde-paraformaldehyde buffer for 21 days (685  $\mu$ l ddH<sub>2</sub>O, 5  $\mu$ l HEPES, 20  $\mu$ l NaN<sub>3</sub>, 40  $\mu$ l glutaraldehyde and 250  $\mu$ l paraformaldehyde). Spores were microwaved for 5 min and kept in 5 mM HEPES-buffer (containing 1% glutaraldehyde, 4% paraformaldehyde and 50 mM NaN<sub>3</sub>) for 28 days at 4 °C. The spores were centrifuged (5 min, 3000 rpm), embedded in agarose and subsequently fixed with 0.5% glutaraldehyde and 1% osmium tetroxide in 0.1 M cacodylate buffer (CCP) containing 0.01 M CaCl<sub>2</sub> for 1 h at 4 °C. Agarose gels were stored in CCP containing 2% osmium tetroxide for 90 min at room temperature and stained with 0.5% uranyl acetate overnight. After dehydration in an increasing series of ethanol, the gels were embedded in Epon and cut by an ultramicrotome (Reichert Ultracut, Leica UK). The spores were contrasted with uranyl acetate and lead citrate and studied using a transmission electron microscope LEO 906 (Carl Zeiss Microscopy).

For nuclear staining, fruiting bodies were vortexed and stored in glutaraldehyde-paraformaldehyde buffer for 21 days. The spores were microwaved for 5 min and fixed with 5 mM HEPES for 25 min at room temperature, embedded in agarose, dehydrated in an increasing series of ethanol, and finally embedded in Epon. Subsequent slices of 120 nm diameter were produced with the ultramicrotome and transferred to coated slides. Spores were stained with DAPI (4,6-Diamidin-2-phenylindol). Individual spores were followed through every fifth over 100 slices to ascertain if one or several nuclei occurred in a spore, using 1000x magnification with a fluorescence microscope (Leica, Germany).

## Acknowledgements

This work was carried out in the frame of an application for the Research Training Group RESPONSE (RTG 2010), now supported by the Deutsche Forschungsgemeinschaft (DFG). Funding was provided by grants for MS (SCHN 1080/2-1, DFG; Forschungsnetzwerk Ostseeraum, Univ. Greifswald), YKN (Russian Foundation for

Basic Research 13-04-00839a, 15-29-02622 ofim and an institutional grant of the Komarov Botanical Institute RAS No. 01201255604), PJ (“Młodzi Naukowcy” no. 6/2015, W. Szafer Institute of Botany, Polish Acad. Sci.) and AR (N N303 799440, Polish Nat. Sci. Centre; statutory fund, W. Szafer Institute of Botany). For loans of specimens we owe thanks to M. Meyer and B. Woerly, France; S.L. Stephenson, USA; and A. Kuhnt, Germany; R. Schlüter (Greifswald) helped with electron microscopy. The authors owe thanks to A.M. Fiore-Donno, Cologne, for fruitful discussions in an early phase of this research; and to F.W. Spiegel, Univ. of Arkansas, who helped to formulate the theoretical framework for the study. We are especially grateful to J. Clark and E. Haskins, who put together most of their achievements, forming the background triggering this research, in a series of reviews published in *Mycosphere* (2010–2015).

## Appendix A. Supplementary Data

Supplementary data associated with this article can be found, in the online version, at <http://dx.doi.org/10.1016/j.protis.2016.03.003>.

## References

- Aldrich HC** (1967) The ultrastructure of meiosis in three species of *Physarum*. *Mycologia* **59**:127–148
- Aldrich HC, Mims CW** (1970) Synaptonemal complexes and meiosis in myxomycetes. *Am J Bot* **57**:935–941
- Adl SM, Habura A, Eglit Y** (2014) Amplification primers of SSU rDNA for soil protists. *Soil Biol Biochem* **69**:328–342
- Adl SM, Simpson AGB, Lane CE, Lukeš J, Bass D, Bowser SS, Brown MW, Burki F, Dunthorn M, Hampl V, Heiss A, Hoppenrath M, Lara E, le Gall L, Lynn DH, McManus H, Mitchell EAD, Mozley-Stanridge SE, Parfrey LW, Pawlowski J, Rueckert S, Shadwick L, Schoch CL, Smirnov A, Spiegel FW** (2012) The revised classification of eukaryotes. *J Eukaryot Microbiol* **59**:429–493
- Aguilar M, Fiore-Donno A-M, Lado C, Cavalier-Smith T** (2013) Using environmental niche models to test the ‘everything is everywhere’ hypothesis for *Badhamia*. *The ISME Journal* **8**:737–745
- De Bary A** (1859) Die Mycetozoen. *Ein Beitrag zur Kenntnis der niedersten Thiere. Zeitschr Wiss Zool* **10**:88–175
- Baldauf SL, Doolittle WF** (1997) Origin and evolution of the slime molds (Mycetozoa). *Proc Natl Acad Sci USA* **94**:12007–12012
- Betterley DA, Collins ONR** (1983) Reproductive systems, morphology, and genetic diversity in *Didymium iridis* (Myxomycetes). *Mycologia* **75**:1044–1063
- Chao A, Chazdon RL, Colwell RK, Shen T-J** (2006) Abundance-based similarity indices and their estimation when there are unseen species in samples. *Biometrics* **62**:361–371
- Clark J** (1993) *Didymium iridis* reproductive systems: additions and meiotic drive. *Mycologia* **85**:764–768
- Clark J** (1995) Myxomycete reproductive systems: additional information. *Mycologia* **87**:779–786
- Clark J** (2000) The species problem in the myxomycetes. *Staphia* **73**:39–53
- Clark J, Haskins EF** (2010) Reproductive systems in the myxomycetes: a review. *Mycosphere* **1**:337–353
- Clark J, Haskins EF** (2011) Principles and protocols for genetic study of myxomycete reproductive systems and plasmodial coalescence. *Mycosphere* **2**:487–496
- Clark J, Haskins EF** (2012) Plasmodial incompatibility in the myxomycetes: a review. *Mycosphere* **3**:131–141
- Clark J, Haskins EF** (2013) The nuclear reproductive cycle in the myxomycetes: a review. *Mycosphere* **4**:233–248
- Clark J, Haskins EF** (2015) Myxomycete plasmodial biology: a review. *Mycosphere* **6**:643–658
- Collins ONR** (1975) Mating types in five isolates of *Physarum polycephalum*. *Mycologia* **67**:98–107
- Collins ONR** (1979) Myxomycete biosystematics: some recent developments and future research opportunities. *Bot Rev* **45**:145–201
- Collins ONR** (1981) Myxomycete genetics, 1960–1981. *J Elisha Mitch Sci Soc* **97**:101–125
- Colwell RK** (2004) EstimateS: Statistical estimation of species richness and shared species from samples. Version 7. User’s Guide and application published at <http://purl.oclc.org/estimates>. Accessed Dec 2007.
- Dagleish D** (2014) Contexture. Excel tips, tutorials, and videos. Excel latitude and longitude calculations. <http://www.contextures.com/excellatitudelongitude.html>. Assessed 10 Dec 2014.
- Eichinger L, Pachebat JA, Glöckner G, Rajandream MA, Sucgang R, et al.** (2005) The genome of the social amoeba *Dictyostelium discoideum*. *Nature* **435**:43–57
- EIHage N, Little C, Clark J** (2000) Biosystematics of the *Didymium squamulosum* complex. *Mycologia* **92**:54–64
- Erastova DA, Novozhilov YK, Schnittler M** (2015) Nivicolous myxomycetes of the Khibiny Mountains, Kola Peninsula, Russia. *Nova Hedwigia*, online first (doi: 10.1127/nova\_hedwigia/2015/0274)
- Erbisch FE** (1964) Myxomycete spore longevity. *The Michigan Botanist* **3**:120–121
- Excoffier L, Lischer HEL** (2010) Arlequin suite ver 3. 5: A new series of programs to perform population genetic analyses under Linux and Windows. *Mol Ecol Res* **10**:564–567
- Feest A, Madelin MF** (1985) Methods for the enumeration of myxomycetes in soils and its application to a wide range of soils. *FEMS Microbiol Ecol* **31**:103–109

- Feest A, Madelin MF** (1988) Seasonal population changes of myxomycetes and associated organism in four woodland soils. *FEMS Microbiol Ecol* **53**:133–140
- Fenchel T, Finlay BJ** (2004) The ubiquity of small species: patterns of local and global diversity. *BioScience* **54**:777–784
- Feng Y, Schnittler M** (2015) Sex or no sex? Independent marker genes and group I introns reveal the existence of three sexual but reproductively isolated biospecies in *Trichia varia* (Myxomycetes). *Org Div Evol* **15**:631–650
- Feng Y, Schnittler M** (2016) Molecular or morphological species? Myxomycete diversity in a deciduous forest in northeastern Germany. *Nova Hedwigia*, [http://dx.doi.org/10.1127/nova\\_hedwigia/2016/0326](http://dx.doi.org/10.1127/nova_hedwigia/2016/0326)
- Ferris PJ, Vogt VM, Truitt CL** (1983) Inheritance of extra-chromosomal rDNA in *Physarum polycephalum*. *Mol Cell Biol* **3**:635–642
- Fiore-Donno AM, Berney C, Pawlowski J, Baldauf SL** (2005) Higher-order phylogeny of plasmodial slime molds (Myxogastria) based on elongation factor 1-A and small subunit rRNA gene sequences. *J Eukaryot Microbiol* **52**:201–210
- Fiore-Donno AM, Meyer M, Baldauf SL, Pawlowski J** (2008) Evolution of dark-spored myxomycetes (slime-molds): molecules versus morphology. *Mol Phylogenet Evol* **46**:878–889
- Fiore-Donno AM, Novozhilov YK, Meyer M, Schnittler M** (2011) Genetic structure of two protist species (Myxogastria, Amoebozoa) suggests asexual reproduction in sexual amoebae. *PLoS ONE* **6**:e22872
- Fiore-Donno AM, Weinert J, Wubet T, Bonkowski M** (2016) Metacommunity analysis of amoeboid protists in grassland soils. *Sci Reports* **6**:19068
- Fiore-Donno AM, Clissmann F, Meyer M, Schnittler M, Cavalier-Smith T** (2013) Two-gene phylogeny of bright-spored myxomycetes (slime moulds, superorder Lucisporidia). *PLoS ONE* **8**:e62586
- Fiore-Donno AM, Kamono A, Meyer M, Schnittler M, Fukui M, Cavalier-Smith T** (2012) 18S rDNA phylogeny of *Lamproderma* and allied genera (Stemonitales, Myxomycetes, Amoebozoa). *PLoS ONE* **7**:e35359
- Foissner W, Chao A, Katz LA** (2008) Diversity and geographic distribution of ciliates (Protista: Ciliophora). *Biodivers Conserv* **17**:345–363
- Gray W, Alexopoulos CJ** (1968) *Biology of the Myxomycetes*. The Ronald Press Company, New York, 288p
- Guindon S, Gascuel O** (2003) A simple, fast, and accurate algorithm to estimate large phylogenies by maximum likelihood. *Syst Biol* **52**:696–704
- Guttus E, Guttus S, Rusch HP** (1961) Morphological observations on growth and differentiation of *Physarum polycephalum* grown in pure culture. *Dev Biol* **3**:588–614
- Hood GM** (2010) PopTools version 3.2.5. Available on the internet. <http://www.poptools.org>. Accessed 17. August 2014.
- Hoppe T, Kutschera U** (2014) Chromosome numbers in representative myxomycetes: a cytogenetic study. *Mycol Prog* **13**:189–192
- Hoppe T, Mueller H, Kutschera U** (2010) A new species of *Physarum* (Myxomycetes) from a boreal pine forest in Thuringia (Germany). *Mycotaxon* **114**:7–14
- Kamono A, Kojima H, Matsumoto J, Kawamura K, Fukui M** (2009) Airborne myxomycete spores: detection using molecular techniques. *Naturwissenschaften* **96**:147–151
- Katoh K, Standley DM** (2013) MAFFT multiple sequence alignment software version 7: improvements in performance and usability. *Mol Biol Evol* **30**:772–780
- Koevenig JL, Jackson RC** (1966) Plasmodial mitoses and polyploidy in the myxomycete *Physarum polycephalum*. *Mycologia* **58**:662–667
- Lado C** (2005–2015) An on line nomenclatural information system of Eumycetozoa. <http://www.nomen.eumycetozoa.com>. Accessed 2 December 2015.
- Lado C, Wrigley de Basanta D, Estrada-Torres A, Stephenson SL** (2012) The biodiversity of myxomycetes in central Chile. *Fungal Divers* **59**:3–32
- Lado C, Mosquera J, Estrada A, Beltrán E, Wrigley de Basanta D** (2007) Description and culture of a new succulenticolous *Didymium* (Myxomycetes). *Mycologia* **99**:602–611
- Laffler TG, Dove WF** (1977) Viability of *Physarum polycephalum* spores and ploidy of plasmodial nuclei. *J Bacteriol* **131**:473–476
- Lahr DJG, Parfrey LW, Mitchell EA, Katz LA, Lara E** (2011) The chastity of amoebae: re-evaluating evidence for sex in amoeboid organisms. *Proc R Soc B* **278**:2081–2090
- Leontyev D, Schnittler M, Moreno GH, Stephenson LS, Mitchell DW, Rojas C** (2014) The genus *Alwisia* (Myxomycetes) revalidated, with two species new to science. *Mycologia* **106**:936–948
- Magurran AE** (2004) *Measuring Biological Diversity*. Blackwell Publ., Oxford, UK, 264p
- Maynard Smith J** (1978) *The Evolution of Sex*. Cambridge University Press, Cambridge, UK, 236p
- Merino ST, Nelson MA, Jacobson DJ, Natvig DO** (1996) Pseudohomothallism and evolution of the mating-type chromosome in *Neurospora tetrasperma*. *Genetics* **143**:789–799
- Milne I, Lindner D, Bayer M, Husmeier D, McGuire G, Marshall DF, Wright F** (2009) TOPALi v2: a rich graphical interface for evolutionary analyses of multiple alignments on HPC clusters and multi-core desktops. *Bioinformatics* **25**:126–127
- Mohberg J** (1977) Nuclear DNA content and chromosome numbers throughout the life cycle of the Colonia strain of the myxomycete *Physarum polycephalum*. *J Cell Sci* **24**:95–108
- Nei M, Kumar S** (2000) *Molecular Evolution and Phylogenetics*. Oxford University Press, New York, 333p
- Novozhilov YK, Schnittler M** (2008) Myxomycete diversity and ecology in arid regions of the Great Lake Basin of western Mongolia. *Fungal Divers* **59**:97–119
- Novozhilov YK, Schnittler M, Erastova DA, Okun MV, Schepin ON, Heinrich E** (2013b) Diversity of nivicolous myxomycetes of the Teberda State Biosphere Reserve (North-western Caucasus, Russia). *Fungal Divers* **59**:109–130

- Novozhilov YK, Okun MV, Erastova DA, Shchepin ON, Zemlyanskaya IV, García-Carvajal E, Schnittler M** (2013a) Description, culture and phylogenetic position of a new xerotolerant species of *Physarum*. *Mycologia* **105**:1535–1546
- Pawlowski J, Audic S, Adl S, Bass D, Belbahri L, Berney C, Bowser SS, Cepicka I, Decelle J, Dunthorn M, Fiore-Donno AM, Gile GH, Holzmann M, Jahn R, Jirku M, Keeling PJ, Kostka M, Kudryavtsev A, Lara E, Lukes J, Mann DG, Mitchell EAD, Nitsche F, Romeralo M, Saunders GW, Simpson AGB, Smirnov AV, Spouge JL, Stern RF, Stoeck T, Zimmermann J, Schindel D, de Vargas C** (2012) CBOL protist working group: barcoding eukaryotic richness beyond the animal, plant, and fungal kingdoms. *PLoS Biol* **10**:e1001419
- Poulain M, Meyer M, Bozonnet J** (2011) Les Myxomycètes. *Fédération mycologique et botanique Dauphiné-Savoie, Delémont*, 556p
- Rakoczy L, Panz T** (1994) Melanin revealed in spores of the true slime moulds using the electron spin resonance method. *Acta Protozoologica* **33**:227–231
- Ronquist F, Huelsenbeck JP** (2003) MrBayes 3: Bayesian phylogenetic inference under mixed models. *Bioinformatics* **19**:1572–1574
- Roy SW, Gilbert W** (2006) The evolution of spliceosomal introns: patterns, puzzles and progress. *Nat Rev Genet* **7**:211–221
- Schnittler M** (2001) Ecology of Myxomycetes of a winter-cold desert in western Kazakhstan. *Mycologia* **93**:653–669
- Schnittler M, Mitchell DW** (2000) Species diversity in myxomycetes based on the morphological species concept – a critical examination. *Stapfia* **73**:55–62
- Schnittler M, Tesmer J** (2008) A habitat colonisation model for spore-dispersed organisms – does it work with eumycetozoans? *Mycol Res* **112**:697–707
- Schnittler M, Novozhilov YK, Carvajal E, Spiegel FW** (2012b) Myxomycete diversity in the Tarim basin and eastern Tian-Shan, Xinjiang Prov. , China. *Fungal Divers* **59**:91–108
- Schnittler M, Erastova DA, Shchepin ON, Heinrich E, Novozhilov YK** (2015) Four years in the Caucasus – observations on the ecology of nivicolous myxomycetes. *Fungal Ecol* **14**:105–115
- Schnittler M, Novozhilov YK, Romeralo M, Brown M, Spiegel FW** (2012a) Myxomycetes and Myxomycete-like Organisms. In Frey W (ed) *Englers Syllabus of Plant Families Vol. 4*, 13th edn Bornträger, Stuttgart, pp 40–88
- Schnittler M, Kummer V, Kuhnt A, Krieglsteiner L, Flatau L, Müller M** (2011) Rote Liste und Gesamtartenliste der Schleimpilze (Myxomycetes) Deutschlands. *Schriftenreihe Vegetationskunde* **70**:125–234
- Shchepin O, Novozhilov YK, Schnittler M** (2014) Nivicolous myxomycetes in agar culture: some results and open problems. *Protistology* **8**:53–61
- Spiegel FW** (2011) Commentary on the chastity of amoebae: re-evaluating evidence for sex in amoeboid organisms. *Proc R Soc B* **278**:2096–2097
- Stephenson SL, Fiore-Donno AM, Schnittler M** (2011) Myxomycetes in Soil. *Soil Biol Biochem* **43**:2237–2242
- Tamura K, Peterson D, Peterson N, Stecher G, Nei M, Kumar S** (2011) MEGA5: molecular evolutionary genetics analysis using maximum likelihood, evolutionary distance, and maximum parsimony methods. *Mol Biol Evol* **28**:2731–2739
- Tesmer J, Schnittler M** (2007) Sedimentation velocity of myxomycete spores. *Mycol Prog* **6**:229–234
- Therrien CD, Yemma JJ** (1975) Nuclear DNA content and ploidy values in clonally developed plasmodia of the myxomycete *Didymium iridis*. *Caryologia* **28**:313–320
- Therrien CD, Bell WR, Collins ONR** (1977) Nuclear DNA content of myxamoebae and plasmodia in six non-heterothallic isolates of a myxomycete *Didymium iridis*. *Am J Bot* **64**:286–291
- Unterseher M, Schnittler M, Dormann C, Sickert A** (2008) Fungal diversity on attached dead wood in forest canopies. *FEMS Microbiol Lett* **282**:205–213
- Urich T, Lanzén A, Qi J, Huson DH, Schleper C, Schuster SC** (2008) Simultaneous assessment of soil microbial community structure and function through analysis of the metatranscriptome. *PLoS ONE* **3**:e2527
- Werenskiold AK, Schreckenbach T, Valet G** (1988) Specific nuclear elimination in polyploid plasmodia of the slime mold *Physarum polycephalum*. *Cytometry* **9**:261–265
- Yemma JJ, Therrien DC** (1972) Quantitative microspectrophotometry of nuclear DNA in selfing strains of the myxomycete *Didymium iridis*. *Am J Bot* **59**:828–835

Available online at [www.sciencedirect.com](http://www.sciencedirect.com)

**ScienceDirect**

## Morphological or biological species? A revision of *Meriderma* spp. (Myxomycetes)

Martin Schnittler<sup>1\*</sup>, Yun Feng<sup>1</sup>, Eva Heinrich<sup>1</sup>, Paulina Janik<sup>2</sup>, Anna Ronikier<sup>2</sup>, Anja Klahr<sup>1</sup>, Daria A. Erastova<sup>3</sup>, Yuri K. Novozhilov<sup>3</sup>, Marianne Meyer<sup>4</sup>

<sup>1</sup>*Institute of Botany and Landscape Ecology, Ernst Moritz Arndt University of Greifswald, Soldmannstr. 15, D-17487 Greifswald, Germany*

<sup>2</sup>*Institute of Botany, Polish Academy of Sciences, Lubicz 46, 31-512 Krakow, Poland*

<sup>3</sup>*V.L. Komarov Botanical Institute of the Russian Academy of Sciences, Prof. Popov St. 2, 197376 St. Petersburg, Russia*

<sup>4</sup>*Maison forestière, F-73730 Rognaix, France*

\*Corresponding author. Tel.: +49 3834 864123; fax: +49 3834 864114. E-mail address: martin.schnittler@uni-greifswald.de (M. Schnittler)

### Abstract

Using partial sequences of the small subunit of the rRNA gene (SSU) as a barcode marker, we found 53 ribotypes among 227 accessions of the nivicolous myxomycete genus *Meriderma*. A ribotype accumulation curve levels off, indicating  $68.4 \pm 14.5$  ribotypes to expect according to the Chao2 estimator. Except for one specimen, the topology of the SSU phylogeny confirms results from a prior study employing the protein elongation factor 1 alpha (EF1A), where several putative biospecies could be recognized. A novel method for automated analyses of SEM images allows deriving quantitative descriptors for spore ornamentation, which were subjected to multivariate analyses. Spore ornamentation provided traits with the highest explanatory power in a multivariate statistics, whereas spore size and stalk length were much less significant. For some but not all putative biospecies a unique combination of morphological characters was found, which is in accordance with the hypothesis of instant sympatric speciation via mutations creating incompatible strains splitting from existing biospecies. The morphologically recognizable taxa of the genus are described and a key for the genus *Meriderma* is given.

### Keywords

automated analysis of spore ornamentation, nuclear small subunit ribosomal RNA, plasmodial slime molds, speciation, species concepts, species differentiation

### Introduction

In contrast to most fungi, where nomenclature starts with Fries (1821), the time of origin for the nomenclature in myxomycetes is Linné's *Species Plantarum* (1753), as discussed in Demoulin et al. (1981). This demonstrates that the minute fruit bodies of myxomycetes have always attracted the attention of botanists, later mycologists and, since Anton de Bary's (1859) report about their protistean nature, zoologists. The number of taxa described seems to grow in a non-linear fashion (Schnittler & Mitchell 2000), with currently about 945 described species (Lado 2005–2015).

Except for taxonomists, the few species of myxomycetes which can easily be maintained in axenic culture (mostly members of one order, Physarales) are of interest for cytologists due to their unique life cycle: From spores that are typically between 7 and 12  $\mu\text{m}$  in diameter (Schnittler & Tesmer 2008) flagellate or amoeboid cells hatch, which can form clonal populations and prey on other microorganisms. Syngamy between these cells produces a zygote which forms a unique multinucleate structure, called plasmodium, by subsequent mitoses that are not accompanied by cellular division. These syncytial plasmodia reach macroscopic dimensions in most species, and will typically segregate again into smaller protions which form stalked or sessile fructifications dispersing meiospores. The ecological hallmarks of this life cycle, predatory life style of amoeboid cells on terrestrial but wet substrates, forming sessile, typically stalked fruit bodies that disperse spores are shared by several groups of non-related organisms which can be seen as an ecological guild (myxomycetes and myxomycete-like organisms, Schnittler et al. 2006).

The key feature for myxomycete taxonomy is the sporocarpic fructification with its intricate morphological characters (Schnittler et al. 2012). The manifold structures ensuring proper dispersal of the airborne spores (stalk, columella, peridium, capillitium) plus the spores themselves make a morphological species concept applicable. Not surprising in this context, myxomycetes constitute the most species-rich group in Amoebozoa, rivaled only by the Arcellinida (thecamoebae), the only other group in this phylum developing morphological structures beyond the amoebal cell (Lahr et al. 2011a; Smirnov et al. 2011; Adl et al. 2012).

Experiments with amoebae raised from single spore cultures (Collins 1979) have led to a completely different species concept, based on the compatibility of amoebal strains. Most widely used were *Physarum polycephalum* and *Didymium iridis* (Clark & Haskins 2010). Typically, an isolate from a single spore behaves heterothallic in culture, sporulating only after contact with amoebae of another spore (i.e. another clone, Collins 1981). This heterothallism is maintained via mating types, described as a single-locus multiallelic system (*Didymium iridis*; Betterley and Collins 1983; Clark 1993), or a three-locus system, as well including multiple alleles (*Physarum polycephalum*; Collins 1975; Clark and Haskins 2010). In the more extensively investigated morphospecies with numerous available isolates, groups of strains that compatible to each other, but not to strains of another group, emerge (Collins 1979; Clark 1995). Therefore, this experimental approach provides a second species concept, called with Clark (2000) biospecies concept. It is based on reproductive isolation, recognizable by compatibility with other isolates.

In spite of the postulate that sex is an universal feature of Amoebozoa (Lahr et al. 2011b) some isolates, called non-heterothallic, can complete their life cycle in single-spore cultures. Selfing (two amoebae from the same clone fuse) or, more likely, automixis is invoked as an explanation, with more evidence for the latter (Clark & Haskins 2013). In addition, multinucleate spores may exist (Novozhilov et al. 2013a). If such spores carry nuclei with multiple mating types, they may as well behave non-heterothallic. In all three cases, these non-heterothallic isolates may or may not mate with others – culture experiments alone cannot give an answer. Among the much more common heterothallic isolates, compatibility groups constitute putative biospecies.

We thus have the uncomfortable situation that two species concepts exist parallel to each other. The morphospecies concept prevailing since Linné for over 250 years (Clark 2000) is still the only applicable concept for the study of naturally occurring myxomycete populations. Virtually all formal descriptions of species are based solely on morphological characters of the fructification; only a (still insignificant) number of the latest papers tried to back up these descriptions with phylogenies constructed from marker genes (e.g., Leontyev et al. 2015). However, these marker genes do not tell anything about compatibility of strains and, in a strict sense, add only more, yet molecular, traits (which are in contrast to morphological traits not directly influenced by environmental conditions, i.e. lack the plasticity component of trait expression). The biospecies concept requires extremely labor-intensive cultivations (Clark & Haskins 2011) and is therefore hard to apply for larger series of specimens. In addition, only a small fraction of species (mostly litter-inhabiting members of the Physarales) can be cultivated from spore to spore.

This is the starting point of this study: is there any way to link the two species concepts to each other? And, more precisely: if biospecies exist not only in laboratory studies but as well in “wild” populations, reproductive isolation between them should have led to subtle morphological differences. Therefore an in-depth analysis should be able to find morphological differences between reproductively isolated groups, if the biospecies are reproductively isolated for a longer period of time and if the investigated characters are not extremely plastic, i.e. show extreme variation within one genotype.

A study on the myxomycete genus *Meriderma* carried out with two marker genes (Feng et al. 2015) provides a chance to study the relationships between putative biospecies and an independently proposed morphological species concept. Recent advances in molecular investigations (see Stephenson et al. 2011 for review) produced the first phylogenies for myxomycetes, splitting the class into two major groups: the bright-spored myxomycetes (Fiore-Donno et al. 2013) and the dark-spored myxomycetes (Fiore-Donno et al. 2012). The genus *Meriderma* was recovered as a basal clade of the latter group. *Meriderma* belongs to the nivicolous (snowbank) myxomycetes. This ecological group, first discovered by Meylan (1908) preys most likely on microbes of undersnow microbial communities

(Schmidt et al. 2012) and requires a long-lasting, continuous snow cover for vegetative life (Schnittler et al. 2015). Mountains provide primary but not exclusive habitats for nivicolous myxomycetes (Ronikier and Ronikier 2009). Probably due to the intense UV radiation in mountains, nearly all of the nivicolous myxomycetes are dark-spored, accumulating melanin in spore coats. A very prominent example is *Meriderma*, where most species have a charcoal-black spore mass (resembling that of smut fungi). This genus illustrates as well the progress with the application of the morphological species concept. Meylan (1910) treated nearly the whole genus as a single variable species, *Lamproderma atrosporum* Meyl. This species was later recognized as very variable, and for all these forms a new genus *Meriderma* was erected by Poulain et al. (2011). All species of *Meriderma* possess a peridium that is firmly connected with the capillitium by funnel-shaped ends and fragments into pieces, whereas all species of *Lamproderma* have a capillitium with free ends and a contiguous peridium, which often detaches in large flakes. This separation was confirmed by a phylogeny based on complete SSU sequences (Fiore-Donno et al. 2012). With the separation of *Meriderma* from *Lamproderma*, a second species described already by Meylan (1932), *Lamproderma fuscatum*, was as well transferred to the new genus. It is the only morphospecies that can be easily distinguished from all other species of *Meriderma* by its brown, not black, spore mass. However, spore ornamentations are extremely variable in all specimens of *Meriderma* with black spore mass, reaching from verrucae over spines to a more or less complete reticulum of elevated ridges. Mainly based on differences in spore ornamentation, Poulain et al. (2011) proposed a morphological concept for the new genus and distinguished eight taxa. However, transitional forms seem to appear frequently, therefore several of these taxa were not yet described formally.

Two marker genes were studied for the genus *Meriderma*. Partial sequences of the nuclear small subunit ribosomal RNA gene (SSU) are established as barcoding gene for other protists (Pawlowski et al. 2012), and the first ca. 600 bp can be obtained in a single PCR step and are free of introns (Fiore-Donno et al. 2012, Novozhilov et al. 2013b). SSU genes occur in one to several copies of extrachromosomal units and are not inherited according to the Mendelian rules. In crosses between ribotypes, one of the two will be gradually eliminated in the progeny (Ferris et al. 1983). In addition, the protein-elongation factor EF1A was studied, a nuclear single copy gene displaying Mendelian inheritance. In *Meriderma* spp. the latter gene includes an extremely variable spliceosomal intron, and most of the 89 specimens investigated by Feng et al. (2015) are heterozygous for it. Both, independently inherited, marker genes resulted in very similar phylogenies which differentiated the same groups within the genus. Most interesting, the two alleles for one of the many specimens that are heterozygous for the EF1A gene clustered without exception always in one of these phylogroups, thus demonstrating the existence of reproductively isolated biospecies. In this study, we present an extended sampling for an SSU phylogeny and combine this with a quantitative analysis of morphological characters. For this purpose, we developed an algorithm to analyse patterns of spore ornamentation recognizable in SEM micrographs which may be of general interest for the analysis of spores from fungi, mosses, or ferns. Using an extended sampling including 227 specimens, this study compares morphological characters with the position of a specimen in the SSU phylogeny and links the phylogenetic groups (putative biospecies) to groups similar in morphological characters (morphospecies).

## Material and methods

### *Investigated specimens*

Specimens of *Meriderma* spp. were systematically collected in five European mountain ranges: the Khibine Mountains (Kola peninsula, Russia, Erastova et al. 2015), the Bavarian Alps (Germany), the French Alps (Dept. Haute Savoie, France), the Carpathians (southern Poland) and the Northern Caucasus (Teberda State Biosphere Reserve, Russia, Novozhilov et al. 2013b, Schnittler et al. 2015). In addition, specimens obtained by loan from several other parts of the world, e.g. the American Rocky Mountains, were considered. Specimens were deposited in herbaria KRAM (A. Ronikier, Cracow, Poland), LE (YK. Novozhilov, St. Petersburg, Russia), the personal collections of M. Schnittler (Greifswald, Germany, to be deposited in M) and M. Meyer (Rognaix, France, to be

deposited in P). A total of 227 specimens was sequenced; 162 were subjected to morphological analyses. Since not all specimens were available, we were only able to obtain from 135 specimens both sequences and morphological traits. Information about specimens and GenBank accession numbers are listed in Supplementary File 1 (data base with locality information, Microsoft Excel 2013).

#### ***DNA Extraction, sequencing and phylogenetic trees***

Procedures were carried out as described in Feng et al. (2015), grinding 2–3 sporocarps with a ball mill (Retsch MM301) at 30 Hz for 80 seconds and using the Invisorb Spin Food Kit II (Stratec). Partial sequences of the first part of the SSU (5'-end until the first known insertion site for a group I intron) were obtained using the primer pair S1 and SU19RSp (Fiore-Donno et al. 2008); and the MangoTaq Kit (Bioline). Conditions included initial denaturing at 94°C / 2 min, followed by 40 cycles of denaturing (94°C / 30 s), annealing (58°C / 30 s) and elongation (72°C / 60 s), plus a final elongation at 72°C / 5 min. Cycle sequencing reactions were performed using the BigDye Terminator v3.1 Cycle Sequencing Kit (Applied Biosystems, Thermo Fisher Scientific, Cat No. 4337455); sequencing was carried out with the BigDye Kit on an ABI 3130 Sequencer.

All partial SSU sequences were free of heterogeneities and were aligned using MAFFT 7.215 (Katoh and Standley 2013) with the iterative refinement method “X-INS-i” under the option “–scarnapair” that considered the secondary structure information of RNA. The SSU alignment (Supplementary Alignment S1) consists of 600 positions, of which 576 contiguous positions were used in phylogenetic analyses. Substitution models were selected using TOPALi 2.5 (Milne et al. 2009) under the Bayesian information criterion, with TrN+G (Maximum Likelihood analysis) and K80+G (Bayesian analysis) turning out as best models. Maximum Likelihood analysis was conducted using PhyML 2.4.5 (Guindon and Gascuel 2003) implemented in TOPALi with 1000 bootstrap replications. Bayesian analysis was carried out with MrBayes 3.1.1 (Ronquist and Huelsenbeck 2003) implemented in TOPALi with 2 runs, 20 million generations, 50% as burnin, sampled every 100 generations. The SSU phylogeny was rooted with several specimens of *Lamproderma* (*L. ovoideum* AK06022, JQ031984; *L. puncticulatum* sc21931, HQ687194; *L. pseudomaculatum* MM37354, JQ031985; *L. retirugisporum* MM23831, JQ031989, see Fiore-Donno et al. 2011, 2012).

#### ***Ribotype analyses***

To estimate the extent to which the molecular component of the survey was exhaustive, a ribotype accumulation curve (RAC) was constructed using the program EstimateS version 8.2 (Colwell 2009). The Chao2 incidence-based estimator of species richness (Chao et al. 2006, Colwell et al. 2012) and the expected richness function “Mao Tau” were used to construct the RAC. In addition, a hyperbolic regression according to the Michaelis-Menten formula  $y = ax/(b+x)$ , resulting in a curve shape approaching the broken-stick model (Magurran 2004; Unterseher et al. 2008) was applied to the data, with the parameter  $a$  giving an estimate for the maximum number of species to be expected.

To detect possible spatial genetic structure among the 227 specimens investigated, we computed pairwise genetic distances using the Maximum Composite Likelihood model (Tamura et al. 2004) implemented in MEGA 5.2 (Tamura et al. 2011). Geographic distances between localities of specimens were calculated using an Excel macro for the Vincenty formula (Dalglish 2014); a Mantel test including 999 iterations for the comparison of both matrices was performed with the ExtraStats function of PopTools 3.2.5 (Hood 2010).

#### ***Determination and morphological analyses***

All 227 investigated specimens (see Supplementary File 1) were determined to species level according to the key published in Poulain et al. (2011). Sporocarps were first examined with a Stemi DV4 from Zeiss including an ocular scale. Microscopic measurements were carried out in a semi-automated mode with a Leica DM 2500 microscope equipped with a Leica DFC450 C camera and the Leica Application Suite software (Version 4.1.0). For illustration, 3–5 spore images (100x) taken from the top of the spore to the equator were stacked using the freeware program CombineZP (Hadley 2010). Colors were noted according to the ISCC-NBS color name charts illustrated with centroid colors (Anonymous 1976). SEM micrographs were prepared with the critical-point drying technique;



specimens were examined with a Hitachi S-3000N scanning electron microscope at 10 kV to provide images rich in contrast that are suitable for an automated analysis.

A suite of morphological characters was recorded for a set of 162 specimens where we had available collections with sufficiently large colonies. First, the shape of the sporotheca was measured by examining 5–10 sporocarps of average size under a dissecting microscope: stalk height (1, Sta\_1), sporotheca height (2, Spt\_h), and relation stalk height to sporotheca height (3, StaSpt, to account for the often large size differences between individual sporocarps). Spore diameter (4, Sp\_d1, including ornaments) was measured first under oil immersion (1000x) in fresh slides prepared with polyvinyl lactophenol; the mean of 25 spores was used for analysis. Second, we calculated spore diameter (5, Sp\_d2, excluding ornaments) from 5–10 spores in SEM micrographs, measuring each spore in two directions perpendicular to each other and taking the mean as measure. Similarly, the height of ornamentations (6, Spi\_1) was measured directly from the SEM micrographs (5 measurements per spore, 3–5 spores per specimen).

A suite of quantitative descriptors for spore ornamentation was derived from SEM micrographs of spores, employing the image analysis language ImageJ (Rasband 2011) to analyse spore ornamentation patterns. Two macros were programmed in ImageJ (Supplementary File 3). The first macro prepares a black and white image of  $6 \times 6 \mu\text{m}$  diam from the central part of the spore (see Fig. 4). After keying in the magnification of the SEM micrograph, a circular section appears on the screen and can be dragged to the central part of a spore. In a next step, a threshold for separating spore ornaments from the background has to be chosen by the user in a way, that the background appears white, elevated ornaments like warts, spines or ridges appear black. To minimize edge effects, the macro repeats the procedure automatically eight times more moving the centre of the selection by  $0.5 \mu\text{m}$  in eight directions, producing a total of nine black and white images per spore. These images are used for analysis by a second, fully automated macro, which analyses a circular section of  $6 \mu\text{m}$  diameter for each image to derive seven quantitative descriptors for spore ornamentation. The proportion of surface covered with ornaments (7, Or) is calculated by comparing the black proportion of the image (ornaments) with its entire area ( $28.27 \mu\text{m}^2$ ). Similarly, the proportion of surface covered by the largest contiguous ornament (8, OrMax) is calculated. Ornament density was counted as the number of contiguous ornaments per  $\mu\text{m}^2$  (9, OrD); here a threshold was set and all speckles below  $0.03 \mu\text{m}^2$  were excluded. These may result from pollution or the gradual change in background color, resulting in scattered false positive pixels. The mean circularity of these ornaments (10, OrCirc) was calculated, using the circularity index (0–1) of ImageJ. Since ornaments in *Meriderma* vary from clearly separated warts to ridges, a “reticulation index” (11, Re) was calculated, using the watershed algorithm of imageJ: ornaments were counted as contiguous and after separation by this algorithm, and an index  $1 - \text{contiguous/separated ornaments}$  was calculated. This index approaches 0 for round and separated warts but 1 for contiguous ridges. The proportion of surface covered by the largest contiguous mesh (12, MeMax) was derived from the largest contiguous area of background, resulting in a high value for small separated ornaments, but a small one for a reticulum, cutting the background into small meshes. Similar to ornament density, mesh density (13, MeD) as the mean number of meshes per  $\mu\text{m}^2$  and mesh circularity (14, MeCirc) was calculated. A last descriptor was the evenness of ornaments (15, Tes), measuring how evenly the ornaments are distributed on the spore surface. The algorithm for the Dirichlet tessellation built into ImageJ was employed to assign an “influence sphere” for each single contiguous ornament, and the standard deviation of the size of these spheres was taken as a parameter. All spore parameters were computed for each of the nine black and white images of one spore (level 1), than the mean for a spore was taken (level 2), and finally the mean of 3–6 spores per specimen analyzed in this way (level 3) was used as input data for a multivariate analysis.

The means of all 15 characters were subjected to a Detrended Correspondence Analysis (DCA) carried out with the software PC-ORD 5 (McCune and Mefford 1999), using the option “rescale axis” and 50 segments. Plots of the sample scores were overlaid with (i) the determinations according to the key of Poulain et al. (2011) and (ii) the major clades in the phylogenetic tree built from partial SSU sequences. In addition, we performed NMS with Sørensen distances (slow mode).

## Results

### Phylogeny

Within 227 specimens we recorded a total of 53 ribotypes (different partial SSU sequences). A ribotype accumulation curve levels off (Fig. 1), resulting in  $68.4 \pm 14.5$  ribotypes to be expected according to the Chao2 estimator if sampling would continue for an infinite number of specimens. Values for a hyperbolic curve fit are comparable ( $85.4 \pm 0.7$  ribotypes, fit with  $R=0.997$ ). This equals 77 and 62% of the overall ribotype diversity sampled according to the Chao2 or hyperbolic curve estimator, respectively. Figures for the five intensely sampled mountain ranges (37 ribotypes from 175 specimens, data not shown) are not much different, for this part of the survey 57 and 66% of the overall ribotype diversity in the five regions would have been sampled. These results are in accordance with the virtually absent spatial genetic structure of the data set (correlation between genetic and geographical distances  $-0.021$ , for 999 randomized runs the mean correlation was  $0.003$  with 5/95% confidence intervals of  $-0.017/0.021$ ).

A phylogeny of partial SSU sequences 227 specimens of *Meriderma* spp. is shown in Fig. 2. The extended sampling recovered essentially the same topology as found in the phylogenies (partial SSU and partial EF1A sequences) constructed from 89 specimens presented in Feng et al. (2015). *Meriderma* appears as a monophyletic clade clearly separated from the species of *Lamproderma*. Within the *Meriderma* clade several groups can be differentiated. The uppermost group, here named G, belongs to four specimens determined as *M. fuscatum* (ribotypes r52, r53) or the very similar *M. atrofuscatum* (r51). One specimen of ribotype r53 was sequenced for EF1A and displayed a T-rich spliceosomal intron in this gene (see supplementary file S1 and Feng et al. 2015). All specimens of the next group (F) were determined as *M. aggregatum*. This group is well supported but divides into two subgroups, which were retrieved as well in the EF1A phylogeny of Feng et al. (2015). The ribotypes r40–r46 include specimens with a T-rich spliceosomal intron in the EF1A, whereas ribotypes r47–r50 include specimens with an entirely different EF1A intron, characterized by a C-homopolymer and a CA dinucleotide microsatellite (Feng et al. 2015). Remarkable are the rather high genetic distances within ribotypes r40–r46.

All remaining specimens form a clade with rather low genetic distances to each other, and these correspond to the clade with all specimens tentatively named *Meriderma atrosporum* agg. in Feng et al. (2015). Within this clade five groups (A–E) can be identified; and these groups correspond with putative biospecies defined by EF1A haplotypes, including the very variable spliceosomal intron (Feng et al. 2015). With one exception all 81 specimens investigated by Feng et al. (2015) reappear in the same groups in the SSU phylogeny with enlarged specimen sampling presented herein. An independent determination, employing the morphospecies concept proposed by Poulain et al. (2011), resulted in five morphospecies coinciding mostly (six exceptions within 199 specimens) with the clades A–E (Fig. 1). All but two specimens of phylogroup A were determined as *M. spinulisporum*; exceptions are specimens s019 and s102 (see Supplementary File 1). This group shows taller, spine-like, somewhat irregularly scattered warts. Phylogroup C displays the morphology of *M. echinulatum* with spines coalescing to short ridges; three specimens (s016, s067, and s115) fit better the morphology of other groups. Phylogroup B corresponds to *M. carestiae*: the spines coalesce to low ridges forming an incomplete (var. *carestiae*) to nearly complete (var. *retisporum*) reticulum (exception: specimen s039). Group D shows uniformly the morphology of *M. verrucosporum*: spores are adorned with small, sense and rather shallow warts. Phylogroup E corresponds completely to *M. cribrarioides*, showing a coarse and virtually complete reticulum of tall ridges.

However, morphology and phylogeny do coincide in all cases. Very likely, *M. aggregatum* (ribotypes r40–r46 and r47–r50 in group F) includes two different biospecies, as indicated by the very different introns found in the specimens sequenced for EF1A. Similarly, in the EF1A phylogeny of Feng et al. 2015, groups B and C of the clade named tentatively *M. atrosporum* agg. include at least two putative biospecies (named clades B1, B2 and C1, C2 in this study). Here, morphology does not help to differentiate between biospecies: the specimens of groups B1 and B2 investigated for EF1A in Feng et al. (2015) determine nearly all as *M. carestiae* var. *carestiae* or var. *retisporum* (B1: 7/2, B2: 4/3 specimens). Specimens of the groups C1 and C2 determine nearly all as *M. echinulatum* (C1: 17, C2:15 specimens). In addition, some specimens (mostly not investigated by Feng et al. 2015) do not assign clearly to one of the groups (all ribotypes not underlaid with grey in Fig. 2). Most conspicuous

is ribotype r29 (sc24929, determined as *M. spinulisporum*). Ribotypes r21–23 (all determined as *M. cribrarioides*) are placed between clades A and C. One specimen of the latter group (HK110423-30) was investigated by Feng et al. 2015 and was as well not assigned to one of the clades A–E. The last group, placed between clades B and C, includes four ribotypes (r08, r12, r13, r35), with the first three ribotypes determined as *M. cribrarioides*, the latter as *M. verrucosporum*.

### **Morphology**

Within the genus *Meriderma*, the most distinct phylogroup G includes all specimens determined as *M. fuscatum* (Meyl.) Mar. Mey. & Poulain or *M. atrofuscatum* ad. int. The first taxon was already recognized as distinct before the genus *Meriderma* was separated from *Lamproderma*. Specimens of this clade possess two clear-cut taxonomic characters separating it from all other taxa: the spore mass is not completely black but brown (s.Br 55) to dark brown (d.Br 59), and the spores tend to be smaller than in all other species ( $12.1 \pm 7.0 \mu\text{m}$ ,  $n=6$ ). The ornamentation consists of small and rather dense blunt warts (Fig. 3). One specimen with a longer branch (genotype r51) was determined as *M. atrofuscatum* due to its darker spore (d.Br 59) mass. Supplementary Table S1 shows figures and standard deviations for the recorded morphological traits for all clades marked in Fig. 1.

All specimens of phylogroup F correspond with *M. aggregatum*. This taxon appears to be composed of several divergent ribotypes, as indicated by the comparatively long branches in the SSU phylogeny (Fig. 2) and two very different patterns in the EF1A sequences (Feng et al. 2015). Morphologically the taxon can be defined clearly by two prominent characters telling it apart from all other morphotypes: the sporocarps are always sessile with a broad base and grow in dense groups, usually touching each other. Spores tend to be rather large ( $14.73 \pm 7.41 \mu\text{m}$ ,  $n=22$ ). The two subgroups with very different types of EF1A introns reappear as well in the SSU phylogeny (Fig. 2): among the upper, very diverse subgroup with seven ribotypes were three specimens with a T-rich EF1A intron. The lower subgroup (four ribotypes) includes four specimens displaying the C-rich intron (see Fig. 2 in Feng et al. 2015).

The phylogroups A–E include all specimens assigned by Feng et al. (2015) to *M. atosporum* agg. Although the determination according to the species concept proposed by Poulain et al. (2011) is not unambiguous, in each clade the majority of species keys out as one of the taxa proposed by these authors. Spore size ranges between  $12.7 \pm 1.0 \mu\text{m}$  for specimens determined as *M. verrucosporum* ( $n=13$ ) and  $14.4 \pm 4.8$  for specimens determined as *M. spinulisporum* ( $n=53$ , see Supplementary Table S1).

An initial DCA of all 15 morphological traits resulted in 0.106, 0.031 and 0.007 as eigenvalues for the three ordination axes. If the regression coefficients of trait values for each specimen with the respective axes are taken as a measure for the discriminative power of the recorded traits, most descriptors for spore ornamentation derived from SEM images (traits 7–14 in Table 1) perform better than measurements of sporocarp dimensions and spore diameter. However, the descriptive traits derived from SEM images (9) are often correlated with each other. A second DCA carried out with these 9 descriptors showed eigenvalues of 0.240, 0.017 and 0.004 for the three axes.

In a third run we reduced the number of characters from 15 to 10; only those traits were the sum of the two regression coefficients exceeds 0.8 were selected, which excluded traits 2 (Spt\_h), 4 and 5 (Sp\_D1, Sp\_D2), 14 (MeCirc) and 15 (Tes). Now the eigenvalues improve to 0.192, 0.044, 0.016 for the three axes. Further reduction of the number of traits did not improve the eigenvalues any more (data not shown).

The NMS ordination produced a meaningful solution for all 15 traits after 97 iterations (final stress for a two-dimensional solution 10.858, final instability 0.000). With the reduction to 10 traits, values improved (84 iterations, final stress 8.581, final instability 0.000, Fig. 4). The reduction to only the 9 descriptive traits from the analysis of SEM images did not lead to a meaningful solution.

A pattern of several clusters emerges if the positions for each specimen in the two-dimensional projection of the NMS overlaid with determination results (Fig 4A) or the respective phylogroups A–G from the phylogenetic analysis (Fig 4B). With the exception of a few specimens, clusters defined by morphological determination of taxa coincide with these defined by SSU-phylogroups. Most variable is phylogroup B: since the degree of reticulation in these specimens reaches from a rather incomplete to a nearly complete reticulum, 38 specimens were determined as *M.*

*caestiae* var. *caestiae*, 8 more as *M. caestiae* var. *retisporum* (Fig. 2). In the corresponding EF1A phylogeny of Feng et al. (2015), this clade separates into two subclades (putative biospecies), but these are not resolved in the SSU phylogeny. The same situation was found for clade C, where EF1A results indicated two putative biospecies but virtually all specimens key out as only one taxon (*M. echinulatum*). Clade D corresponds morphologically with *M. verrucosporum*, but seems not to be very well circumscribed.

If one looks at the standard deviations for the centroids of the species scores of the two-dimensional NMS plot (Fig. 4), the determination results do not necessarily define more coherent clusters than the phylogenetic analyses. A comparison of the standard error of means of the specimen scores for the two axes for each cluster shows, that some clusters are more narrowly circumscribed by classical determination, some by the corresponding clades from phylogenetic analysis (grey crosshairs in Fig. 4).

Summarizing these results, we found correlations between morphological traits and ribotypes. However, in at least three cases putative biospecies (corresponding to subgroups in the SSU phylogeny, Fig. 2) cannot be separated by morphological characters: two different subgroups appear in groups F (*M. aggregatum*, different EF1A introns), B (*M. caestiae* / *caestiae* var. *retisporum*) and C (*M. echinulatum*, in the latter two cases the subgroups do not share EF1A haplotypes based on the spliceosomal intron, Feng et al. 2015). In addition, eleven specimens with eight ribotypes cannot be assigned to any of the groups A–E and show different morphologies (Fig. 2).

## Discussion

Although myxomycetes were one of the last larger groups of organisms to be explored with molecular markers, with the first part of the SSU there seems now a reliable barcoding marker to be available for the group. Partial SSU sequences were successfully applied in other Protistean groups (Pawlowski et al. 2012). In myxomycetes, the first ca. 600 bases of the SSU are free of introns and roughly comparable in lengths throughout the group (Fiore-Donno et al. 2012, 2013); and its sequence shows an alteration of conservative and variable sections which allows an easy alignment. Partial SSU sequences were employed to trace geographical variation in *Badhamia melanospora* (Aguilar et al. 2013), to elucidate the internal structure of the complex species *Tubifera ferruginosa* (Leontyev et al. 2015), or to differentiate three cryptic species in *Trichia varia* (Feng & Schnittler 2015). Therefore, SSU became the marker of choice for this study, trying to link the biospecies concept (theoretically sound but never applied in practice) with the morphospecies concept (completely empirical but practically applicable) at the example of the genus *Meriderma*.

Most interesting in this context is that (i) the number of ribotypes in *Meriderma* is high but not indefinitely high, as suggested by the statistical evaluation of the ribotype accumulation curve (Fig. 1), and (ii) that the phylogeny based on ribotypes shows essentially the same topology as the phylogeny based on a nuclear gene like EF1A (Feng et al. 2015). The selection of specimens used for this study centers around the European Alps. Many (84 of 227 specimens) come from this region, another 41 from the northern Caucasus. Enlarging the geographical area of sampling is likely to enlarge the number of both putative biospecies and morphological forms. This holds especially true for the few accessions from North America (14). Four North American specimens cluster with the rather heterogeneous clade D which morphologically corresponds to *M. verrucosporum*; found to be a rare species in the European Alps. Two other specimens from North America belong to the 11 specimens that could not be assigned to any of the SSU phylogroups. We cannot rule out that the ribotypes not clustering with one of the phylogroups represent new biospecies, which we currently cannot define due to their apparent rarity.

Nivicolous myxomycetes like *Meriderma* occur often in large colonies of well matured sporocarps, and all structures, sporocarps and spores, are usually larger than in many other myxomycetes (Schnittler & Tesmer 2008). In addition, most nivicolous genera possess elaborated capillitial and peridial structures. Nevertheless, this ecological group has a reputation as difficult to determine. Only at the first glance this appears to be a contradiction, since it may be exactly the better accessibility of morphological characters enabling taxonomists to distinguish more morphotypes than in other groups of myxomycetes. From this reason, we should have higher chances to find

morphological correlates for biospecies in nivicolous genera. Indeed, since the days of Meylan, who described 26 species and varieties of nivicolous myxomycetes in a series of subsequent papers (1908–1937, see Kowalski 1975), the number of species described as new to science has grown steadily, with about 108 species currently known as at least preferentially nivicolous (Bozonnet et al. 1992, Schnittler et al. 2015). The genus *Meriderma*, growing from a single species (*Stemonitis carestiae*, 1879), than two (with *Lamproderma fuscatum*, 1932) to eight taxa proposed in the monograph of Poulain et al. (2011), is a prominent example.

If the biospecies concept which was worked out in laborious experiments from cultivable members of the Physarales (Collins 1981, Clark & Haskins 2010) holds true for many or even most myxomycete groups, reproductive isolation, disrupting gene flow, may have led via genetic drift or adaptive selection to different niches to slightly differing morphological characters, which may be recognized as separate taxa by a morphological species concept. From this reason, we should expect both species concepts to coincide at least partially. In contrast to the famous examples of allopatric speciation in plants (i.e. the genus *Aeonium*, Jorgensen & Oleson 2001, Mort et al. 2002, Thiv et al. 2010) or animals (*Geospiza*, Farrington et al. 2014, but see de Leon et al. 2010), myxomycetes may show a more effective geneflow between geographically isolated populations via long-distance dispersal of spores (Kamono et al. 2009). Indeed, the number of private alleles of each population of *Meriderma* from the five intensely investigated mountain ranges is low for EF1A sequences (Feng et al. 2015). The same holds true for partial SSU sequences: all eight ribotypes represented by five or more specimens came at least from two different regions. However, sympatric speciation may play a more important role, as suggested by (non-compatible) biospecies found in early cultivation studies (Clark & Haskins 2010) or the pattern of heterozygous EF1A genotypes recorded for *Meriderma* spp. (Feng et al. 2015). For hypothetical mutations founding a new, reproductively isolated biospecies there is a principal problem: the first carrier of such a mutation will not find a mating partner. This, in theory, would hold true if the mutation occurs in a haploid amoeba. But if we assume such a mutation to occur in the diploid plasmodium, via recombination during spore formation the spores arising from the progeny of the mutated nucleus might acquire both mating type alleles present in the plasmodium, which should lead to a new biospecies with two mating type alleles which is capable of sexual reproduction. Via frequency-dependent selection, the new biospecies should quickly acquire more mating type alleles, since the carrier of a new mating type allele has an advantage, as long as the new allele is still rare in the population: it will find a compatible partner with a higher probability than the carrier of an established (and frequent) allele. The genes responsible for such incompatibilities, defining a biospecies, may be different from mating type genes, as suggested by investigations on plasmodial incompatibility (Clark & Haskins 2012).

However, these mutations founding a new biospecies do not affect all the genes responsible for visible characters. From this reason, a morphological approach must fail, even with the most sophisticated analyses, to witness very recent speciation events if we assume that most morphological characters are under selective pressure, i.e. their phenotypic expression is fairly uniform for a biospecies. In contrast, in genes not under strong selective pressure, as it seems to be the case for the hypervariable loops of the SSU (see Fig. 4 in Fiore-Donno et al. 2012) differences might accumulate faster via initial founder effects connected with a new biospecies and subsequent independent mutations. We therefore assume morphologically recognizable speciation to lag behind biological speciation. Indeed, in a similar case where a combination of three independent marker genes (SSU, EF1A, and mitochondrial cytochrome oxidase, COI) detected three putative biospecies in the bright-spored myxomycete *Trichia varia* (Feng & Schnittler 2015), partial SSU genes allowed clearly to tell the three biospecies apart, but a first approach to detect morphological differences between these failed. Accelerated diversification rates in comparison to other members of the Amoebozoa have been found for myxomycetes (Fiz-Palacios et al. 2013), which points to a co-evolution between myxomycetes and terrestrial plants. If we assume that the instant emergence of new biospecies by reproductive isolation is one of these mechanisms, it is likely that differences in morphological characters will emerge much more slowly, requiring different selective forces.

In the case of *Meriderma*, the morphological concept of Poulain et al. (2011), which was developed prior to the molecular analyses presented in this study, seems indeed to track differences between putative biospecies later established by analyses of a hypervariable intron in the EF1A gene

(Feng et al. 2015) and confirmed by the SSU phylogeny presented in this study. Clearly, differences in morphological characters reflect the separation into putative biospecies, defined by EF1A into haplotypes (Feng et al. 2015) and expressed as phylogroups in the SSU phylogeny. However, the suite of morphological characters analyzed by us does not allow distinguishing all putative biospecies. Except for the problem of recent speciation explained above, there are more conceivable reasons.

First, we have measurement errors and methodical shortcomings in our analyses. The automated approach to calculate quantitative descriptors of spore ornamentation from SEM micrographs makes this complex of characters, which was given high weight in the concept presented by Poulain et al. (2011) accessible for a statistical evaluation. However, it is not free of errors. If the SEM micrographs are rich in contrasts (therefore the voltage should be on the upper end of the feasible range), false recognition of ornaments can be largely excluded. More important are edge effects in complex, especially reticulated, ornaments. Only a comparatively small area of the spores (with the spores in *Meriderma* ranging from 12–16  $\mu\text{m}$  in diameter we are limited to a circle of 6  $\mu\text{m}$  diameter) allows to view ornaments from the top. However, the rather coarse reticulum in *M. cribrarioides* displays meshes with up to 3  $\mu\text{m}$  diameter (Fig. 3), therefore the number of meshes caught completely in the 6  $\mu\text{m}$  circle fluctuates between 0 and 4 in one and the same specimen. This edge effect could only be minimized but not eliminated by averaging the descriptors from not one but nine selections, shifted by 0.5  $\mu\text{m}$  in eight directions from the manually chosen one.

Second, we have only a comparatively low number of morphological traits analysed. For instance, the capillitium, caused by a network of anastomosing vacuoles which will be filled with secreted compounds (Kalyanasundaram 1973), may be as well provide valuable traits. However, we are still not able to find appropriate quantitative descriptors for the three-dimensional, richly branched network of capillitial threads resembling a miniature tree. A first examination found no differences between taxa in easily accessible measures like the diameter of capillitial threads. More characters may enhance resolution in the multivariate analyses, but may as well add noise if extremely variable traits are added to the analysis. Stalk length (see Fig. 5) as an extremely variable character provides an example.

Third, the characters taken by us may have a strong plastic component beside its genetic determination. For instance, the weather conditions in the short time of fruit body formation (which mostly takes place when the snow is still covering the spot, Schnittler et al. 2015) may influence the ontogenesis of spore characters, like the height of the ornaments (which turned out to be of lesser explanatory value than assumed by us). Another example is spore size, found to be rather variable in most phylogroups and/or proposed morphospecies (see Supplementary Table S1). Except for *M. fuscatum*, which seems to have consistently smaller spores than all other taxa, no significant differences were found between the other taxa. Especially the conspicuous large-spored forms found in some morphotypes (compare descriptions in Poulain et al. 2011) seem to lack taxonomic importance.

Fourth, the reproductive isolation between biospecies may not be complete; and still rare cases of crosses between putative biospecies occur. The genes investigated in the study of Feng et al. (2015, EF1A) and this study (SSU) are completely independent, and at least in the latter case our marker is definitely not linked with genes responsible for morphological traits. Therefore, genes coding for a deviating spore ornament may “trickle” via crossbreds into a biospecies usually forming another type of spore ornamentation. We found one possible example: specimen s068 of the SSU-phylogroup B (morphologically determined as *M. carestiae* and therefore complying with this phylogroup) belongs to the putative biospecies C2 in the EF1A phylogeny presented in Feng et al. (2015).

From all these reasons we should find only for some but not all biospecies a unique combination of morphological characters that allows “visualizing” them as morphospecies. Nevertheless, this study demonstrates that the morphological concept proposed by Poulain et al. (2011) has a sound biological foundation. To facilitate further biogeographic and biodiversity research, we therefore describe in the following taxonomic treatment the forms proposed *ad interim* formally, being well aware that further analyses, including more specimens and more sophisticated analyses, may split these taxa even further. However, an important aspect of taxonomy is practicability: the entities described by taxonomists should be applicable for field research, which means that determinations can be achieved with reasonable efforts and accessible equipment for trait analysis. We therefore mention

frequently traits visible best in SEM micrographs but will relate to the appearance in images from compound microscopes (compare Fig. 3).

### Taxonomic treatment

The following taxonomic treatment splits the genus *Meriderma* first into three aggregates; these entities can usually be differentiated by examining specimens with a dissecting microscope (DM). The taxa itself can only be determined by the use of a compound microscope (LM, 1000x times). SEM micrographs are extremely helpful (Fig. 2). Taxa proposed in Poulain et al. (2011) but not formally described are indicated as “ad. int.” (ad interim). The symbols  $\equiv$  and  $=$  denote homo- and heterotypic synonymes, respectively,  $-$  indicates taxa not seen as distinct. Spore sizes are given including ornaments and based on measurements of 25 spores of a specimen, based on the 162 specimens investigated by us.

***Meriderma*** Mar. Mey. & Poulain, Poulain et al. 2011: 551

Nivicolous myxomycetes with crowded to aggregated, rarely scattered sporocarps and spherical to elongated sporothecae. Peridium fresh silvery shining but soon fragmenting into small portions that remain attached to the capillitium, translucent pale brown to nearly colorless in transmitted light. Stalk, absent or reaching height of the sporotheca, stout, widened at the base, furrowed, round to irregular in cross-section, based on an irregular broad hypothallus which sometimes connects aggregated sporocarps, tapering into a columella reaching the center of the sporotheca. Capillitium arising over the whole length of the columella, internally branched and anastomosing, black to ferruginous brown, free ends stout and usually expanded into a funnel-shaped structure connecting to the peridium. Spore mass concolorous, spores very variable in size (10.5–)12–16(–21.5)  $\mu\text{m}$ , ornaments ranging from scattered blunt spines to a complete reticulum of elevated ridges.

*Type: M. carestiae* (Ces. & de Not.) Mar. Mey. & Poulain, Poulain et al. 2011, Les Myxomycetes I: 517, II: 488

$\equiv$  *Stemonitis carestiae* Ces & De Not. 1879, Erb. Critt. Ital. series II, fasc. 18, no. 888

*Notes:* The fragmenting peridium with its funnel-shaped capillitial ends tells this genus apart from *Lamproderma*. In contrast to this genus, *Meriderma* tends to fruit at lower elevations, often in upper montane forests. Stalks may be absent in untypically developed stalked species. In all taxa single specimens occur where most spores are extremely large, and single large spores occur as well occasionally in otherwise typical material (these are not included in figures for spore measurements). We hypothesize that these specimens possess unreduced spores. Until the biological reasons are known, we do not see it as useful to maintain varieties based on spore size.

*Meriderma fuscatum* agg.: Sporocarps ferruginous brown (s.Br 55) to dark brown (d.Br 59), short stalked, spores smaller than in all other species, usually not exceeding 12  $\mu\text{m}$  in diam. Spores with distinct but not very evenly distributed warts.

***M. fuscatum*** (Meyl.) Mar. Mey. & Poulain, Poulain et al. 2011, Les Myxomycetes I: 515, II: 481

$\equiv$  *L. fuscatum* Meyl. 1932, Bull. Soc. Vaud. Sci. Nat. 57: 372; see Kowalski 1968, Mycologia 60(4): 764

Sporocarps ferruginous (coffee) brown (s.Br 55–deep Br 56), grouped (together but not always touching each other), 1.5–1.8 mm tall, stalk 1/4–1/3 of sporotheca height, sporotheca globose to subglobose, 0.6–1.4 mm in diam. Capillitium with many and paler ends and therefore lesser funnel-shaped structures than in the other species. Peridium grey, sometimes iridescent blue, pale ferruginous brown to translucent (LM). Spores (9.5–)9.8–11.0(–12.5)  $\mu\text{m}$  in size, ornamented with irregularly distributed warts, density (SEM) 2–3 per  $\mu\text{m}^2$ , warts 0.25–0.35  $\mu\text{m}$  tall, rounded in shape, appearing blunt, with a slightly broadened base, nearly always separated but irregularly distributed, very rarely forming small groups but never short ridges.

*Notes:* This taxon seems to fruit much rarer than all other species of the genus.

*Type:* MM24907

*var. atrofuscatum*

= *M. atrofuscatum* ad. int., Poulain et al. 2011, Les Myxomycetes I: 515, II: 482

Sporocarps dark brown (d.Br 59, rarely d.gy.Br 62), capillitium ends somewhat more stout, spores slightly larger (9.5–)10.0–11.5(–13.5)  $\mu\text{m}$  in size, warts more regularly distributed.

*Notes:* Characters are approaching those of *M. atrosporum* agg., but the single sequenced specimen (MM29232) clustered clearly within *M. fuscatum* agg., although displaying a deviating ribotype (r51).

*Meriderma aggregatum* agg.: Sporocarps aggregated (in dense colonies touching each other), always sessile on a rather broad base, even not single sporocarps stalked, obovate (taller than wide) in shape, charcoal-black (br Black 65). Spores warted.

***M. aggregatum*** (see Poulain et al. 2011, Les Myxomycetes I: 516, II: 484)

– *M. aggregatum* fo. *macrosporum* ad. int., Poulain et al. 2011, Les Myxomycetes I: 516

Sporocarps aggregated, always sessile, charcoal-black, rarely very dark brown, 1.3–1.7 mm tall and 0.8–1.0 mm wide. Capillitium dark, paler towards the ends which often develop funnel-shaped structures. Peridium grey to silvery, fragmenting into rather small pieces, pale violaceous grey to translucent (LM). Spores (12.0–)12.5–14.0(–14.5)  $\mu\text{m}$  in size, ornamented with rather regularly distributed short spines, density (SEM) 1.5–2.5 per  $\mu\text{m}^2$ , spines 0.35–0.80  $\mu\text{m}$  tall, usually two times taller than wide but much lower in specimens from western North America, ends often with irregular outgrowths, with a slightly broadened base, nearly always separated.

*Notes:* In molecular analyses, this taxon forms two clearly separated clusters, which are most likely reproductively isolated. We did not find corresponding morphological differences with the material investigated by us. We anticipate that further studies may succeed in distinguishing the two putative biospecies, but in this study we name only this taxon within *M. aggregatum* agg.

*Type:* MM32487

*Meriderma atrosporum* agg. Sporocarps gregarious but nearly always separated from each other by typically one sporocarp diameter, at least single sporocarps, in well developed material most sporocarps clearly stalked, sporotheca globose to subglobose, charcoal-black (br Black 65). Spore ornamentation variable, warted to spiny to reticulate. In older collections, the material is usually found under the name *Lamproderma atrosporum*.

***M. carestiae*** (Ces. & de Not.) Mar. Mey. & Poulain, Poulain et al. 2011, Les Myxomycetes I: 517, II: 488

= *Stemonitis carestiae* Ces & De Not. 1879, Erb. Critt. Ital. series II, fasc. 18, no. 888

= *L. violaceum* var. *carestiae* (Ces. & de Not.) Lister 1894: Monogr. Mycetoza 1: 130

= *L. sauteri* var. *carestiae* (Ces. & de Not.) Meyl. 1917, Bull. Soc. Vaud. Sci. Nat. 51: 264

= *L. carestiae* (Ces. & de Not.) Meyl. 1932, Bull. Soc. Vaud. Sci. Nat. 57: 368

= *L. cribrarioides* var. *carestiae* (Ces. & de Not.) G. Moreno & H. Singer, Sanchez et al. 2007, Bol. Soc. Micol. Madrid 31:182

= *L. atrosporum* var. *atrosporum* Meyl. pro parte

– *M. carestiae* fo. *microsporum* ad. int., Poulain et al. 2011, Les Myxomycetes I: 517

– *M. carestiae* fo. *macrosporum* ad. int., Poulain et al. 2011, Les Myxomycetes I: 517

(see Sanchez et al. 2007, Bol. Soc. Micol. Madrid 31:182)

Sporocarps gregarious to scattered, globose to subglobose, stalked, charcoal-black, 1.5–2.5 mm tall and 0.8–1.2 mm wide. Stalk usually well-developed, reaching 0.6–1.2 times sporotheca height. Capillitium dark, paler towards the ends which develop many funnel-shaped structures. Peridium grey to silvery, fragmenting into larger pieces, pale violaceous grey to translucent (LM). Spores (10.0–)12.5–13.2(–14.5)  $\mu\text{m}$  in size, ornamented with ridges forming a very incomplete net, a clear majority of meshes usually open (convex outline), resembling a labyrinth, density (SEM) 0.1–0.3 elements per  $\mu\text{m}^2$ , ridges



0.45–0.60(–0.7)  $\mu\text{m}$  tall, upper surface of ridges rounded, rarely with irregular outcrops, ridges mostly massive, rarely perforated.

*Notes:* In molecular analyses, this taxon forms two clearly separated clusters, and these do not correspond to the varieties *caestiae* and *retisporum*. In analyses of SEM images the degree of reticulation, providing the most valuable distinguishing characters, overlaps (typically 0.8–0.9 in var. *caestiae*, 0.9–0.95 in var. *retisporum*). Due to the lack of clearly distinguishing characters, but as well the missing coincidence with phylogenetically defined groups we describe the var. *retisporum* only as a *forma*.

*Type:* Ron401

fo. *retisporum* (see Poulain et al. 2011, Les Myxomycetes I: 517)

Spores ornamented with a minority of incomplete (open, concav outline) and a majority of complete (closed, convex outline) meshes, the latter very different in size, 0.3–2.0  $\mu\text{m}$  diameter.

*Type:* MM33193

***M. cribrarioides*** (Fr.) Mar. Mey. & Poulain, Poulain et al. 2011, Les Myxomycetes I: 517, II: 489

≡ *Stemonitis cribrarioides* Fr. 1829, Syst. Mycol. 3:163

≡ *L. cribrarioides* (Fr.) R.E. Fr. 1911, Svensk. Bot. Tidskr. 4: 259

= *L. atrosporum* Meyl. 1910, Bull. Soc. Vaud. Sci. Nat. 46: 51

= *L. cribrarioides* var. *atrosporum* (Meyl.) G. Moreno, H. Singer, Illana & A. Sanchez, Singer et al. 2003: Oesterr. Z. Pilzk. 12:18

= *L. atrosporum* fo. *subcylindricum* Meyl. 1932, Bull. Soc. Vaud. Sci. Nat. 57: 368

= *L. atrosporum* var. *pseudocribrarioides* Mar. Mey., G. Moreno, A. Sanchez, H. Singer & Illana, Moreno et al. 2002: Fungi non Delineati 19: 22

(see Sanchez et al. 2007, Bol. Soc. Micol. Madrid 31:182; Singer et al. 2003, Oesterr. Z. Pilzk. 12:16, Kowalski 1975, Mycologia 67(3): 467)

Sporocarps gregarious to scattered, globose to subglobose, short-stalked, charcoal-black, 1.0–1.5 mm tall and 0.8–1.0 mm wide. Stalk short, sometimes not developed, reaching up to one fourth of the sporotheca height. Capillitium dark, paler towards the ends which develop many funnel-shaped structures. Peridium grey to silvery, fragmenting into larger pieces, pale violaceous grey to translucent (LM). Spores (12.0–)13.0–14.1(–15.5)  $\mu\text{m}$  in size, ornamented with ridges forming a complete net, density (SEM) around 0.1 elements per  $\mu\text{m}^2$ , ridges (0.50–)0.70–1.20  $\mu\text{m}$  tall, upper surface of ridges rounded to even, ridges often perforated, small (down to 0.25  $\mu\text{m}$  wide) and large (1.5–2.5  $\mu\text{m}$  wide) meshes coexist.

*Notes:* Although one phylogroup (E) unambiguously coincides with *M. cribrarioides*, not all specimens displaying this morphology belong to this phylogroup. We thus must assume the existence of different biospecies within this morphologically circumscribed taxon.

*Type:* MM33287

***M. echinulatum*** (Meyl.) Mar. Mey. & Poulain., Poulain et al. 2011, Les Myxomycetes:I: 516, II: 485

≡ *L. atrosporum* var. *echinulatum* Meyl. 1932, Bull. Soc. Vaud. Sci. Nat. 57: 368

– *M. echinulatum* var. *macrosporum* (Meyl.) Mar. Mey. & Poulain, Poulain et al. 2011, Les Myxomycetes I: 516, II: 485

– *L. atrosporum* var. *macrosporum* Meyl. 1932, Bull. Soc. Vaud. Sci. Nat. 57: 372

(see Kowalski 1975, Mycologia 67(3): 467; Singer et al. 2003, Oesterr. Z. Pilzk. 12:16)

Sporocarps gregarious, subglobose to obovoid, short-stalked, charcoal-black, 0.9–1.4 mm tall and 0.8–1.2 mm wide. Stalk short, rarely not developed, reaching up to ¼ times sporotheca height. Capillitium dark, paler towards the ends which develop many funnel-shaped structures. Peridium grey to silvery, fragmenting into larger pieces, pale violaceous grey to translucent (LM). Spores (10.0–)12.2–13.8(–14.5)  $\mu\text{m}$  in size, ornamented with spines typically coalescing to short, irregularly formed crests, density (SEM) 0.5–0.8 elements per  $\mu\text{m}^2$ , spines (0.5–)0.6–0.9  $\mu\text{m}$  tall, with sharp and rough outgrowths, the short ridges connecting (2–)5–8 spines are somewhat lower and are much more

conspicuous in SEM than in LM (Fig. 2). Due to then short labyrinthiform connections between the spines, the spore ornamentation appears somewhat irregular.

*Notes:* The molecular analysis using SSU and EF1A sequences revealed at least two putative biospecies (named groups C1 and C2 in Feng et al. 2015) with a morphology that fits this description.

*Type:* MM33291

***M. spinulisporum*** (see Poulain et al. 2011, Les Myxomycetes I: 517, II: 487)

non *Lamproderma spinulisporum* Mar. Mey., Nowotny & Poulain, Les Myxomycetes I: 514, II: 480

– *M. spinulisporum* fo. *intermedium* ad int., Poulain et al. 2011, Les Myxomycetes I: 517

– *M. spinulisporum* fo. *gigasporum* ad int., Poulain et al. 2011, Les Myxomycetes I: 517

Sporocarps gregarious to scattered, subglobose to obovoid, stalked, charcoal-black, 1.5–1.9 mm tall and 0.8–1.1 mm wide. Stalk usually well developed, assuming one fourth to one half of sporotheca height. Capillitium dark, paler towards the ends which develop many funnel-shaped structures. Peridium grey to silvery, fragmenting into larger pieces, pale violaceous grey to translucent (LM). Spores (11.5–)12.0–15.5(–16.5)  $\mu\text{m}$  in size, ornamented with short spines that mostly clearly separated from each other, density (SEM) (1.0–)1.5–2.0 per  $\mu\text{m}^2$ , spines (0.45–)0.5–0.7(–0.9)  $\mu\text{m}$  tall, with rough outgrowths letting them appear bacculate, small and larger spines coexist, only rarely 2–4 spines are connected to short crests.

*Notes:* Macrosporus specimens with spores up to 20  $\mu\text{m}$  in diam. seem to occur most often in this taxon (compare Fig. 2).

*Type:* Ron680

***M. verrucosporum*** (see Poulain et al. 2011, Les Myxomycetes I: 516, II: 483)

Sporocarps gregarious to scattered, subglobose, rarely obovoid, stalked, charcoal-black, 0.8–1.2 mm tall and 0.8–1.0 mm wide. Stalk usually well developed, reaching  $\frac{1}{2}$  or more times sporotheca height. Capillitium dark, with paler but stout ends and many, sometimes large, funnel-shaped structures. Peridium grey to silvery, fragmenting into larger pieces, pale violaceous grey to translucent (LM). Spores (11.5–)12.0–14.0(–15.5)  $\mu\text{m}$  in size, ornamented with warts, density (SEM) 0.5–2.0 per  $\mu\text{m}^2$ , warts 0.3–0.5  $\mu\text{m}$  tall, rounded or with rough outgrowths near the tips, sometimes 3–5 warts are connected to short crests.

*Notes:* Specimens with this set of morphological characters may belong to several putative biospecies (clade D in Feng et al. 2015). This taxon seems to be more common in western North America.

*Type:* MM34478

### Key to the taxa

The following key should work for typically developed specimens, but the considerable variation in stalk length and spore ornamentation (Fig. 5) does not allow the determination of every specimen with certainty. Especially maldeveloped specimens of usually stalked specimens may fruit with sessile sporocarps. Spore size is especially variable, the occasionally occurring macrosporous forms are not considered in the figures for spore size given in the key.

- 1 Sporocarps usually stalked, brown to dark brown, gregarious to scattered, capillitium with thin ends, funnel-shaped structures present but not very frequent, spores <12.5 $\mu\text{m}$  in diam., (SEM) with blunt, irregularly distributed but usually separated spines (*M. fuscatum* agg.)..... 2
- 1\*Sporocarps sessile to stalked, charcoal-black, , aggregated to scattered, capillitium with rather stout ends, often broadened into funnel-shaped structures, spores nearly always >12.5  $\mu\text{m}$  in diam. .... 3
- 2 Sporocarps clearly ferruginous brown, spores typically 8–11 $\mu\text{m}$  in diam. .... ***M. fuscatum***
- 2\* Sporocarps dark brown but never completely black, spores typically 10–11.5 $\mu\text{m}$  in diam. .... ***M. fuscatum* var. *atrofuscatum***
- 3 Sporocarps always sessile with a rather broad base, aggregated (touching each other), clearly elongated, spores with rather regularly distributed separate spines (rarely 2–3 connected), these (SEM) 0.35–0.80  $\mu\text{m}$  tall ..... ***M. aggregatum***

- 3\* Sporocarps stalked (but stalk may be short, exceptionally sessile), gregarious to scattered (but usually not touching each other), subglobose to obovoid, spore ornamentation varying from warts over spines connected to crests to a complete reticulum (*M. atrosporum* agg.)..... 4
- 4 Sporocarps long stalked (ca. 1/2 sporotheca height), spores with dense and rather evenly distributed small warts (SEM) 0.3–0.5 µm tall, these rounded or ragged, very rarely forming short crests .... *M. verrucosporum*
- 4\* Sporocarps short to long stalked, spores with spines or crests which are usually (SEM) >0.5 µm tall ..... 5
- 5\* Sporocarps clearly stalked (1/4–1/2 sporotheca height), spores with separated spines (rarely very short crests), these (SEM) ragged, 0.5–0.7 µm tall but uneven in size, very rarely forming short crests ..... *M. spinulisporum*
- 5\* Sporocarps short to long stalked, spores with conspicuous longer crests or a (nearly) complete reticulum ..... 6
- 6 Sporocarps short stalked (<=1/4 sporotheca height), spores with irregularly distributed spines connected to labyrinthiform crests, but these never form complete meshes, crests (SEM) 0.6–0.9 µm tall, ragged ..... *M. echinulatum*
- 6\* Sporocarps short to long stalked, spores with at least some closed meshes formed of ridges, these in transmitted light often appearing paler than the spines itself..... 7
- 7 Sporocarps long stalked (1/2 –1x sporotheca height), spores with ridges forming an incomplete net, but most meshes open, these (SEM) 0.45–0.6 µm tall, crests mostly massive ..... *M. carestiae*
- 7\* Sporocarps long to short stalked, spores with a reticulum, where most of the meshes are closed (with concav outline) ..... 8
- 8 Sporocarps long stalked (1/2 –1 sporotheca height), spores with a nearly complete net, ridges (SEM) 0.45–0.6 µm tall, mostly massive ..... *M. carestiae* var. *retisporum*
- 8\* Sporocarps short stalked (<=1/4 sporotheca height), spores with a complete net of small and large meshes (virtually all concav in outline), ridges (SEM) 0.7–1.2 µm tall, in ransmitted light clearly visible as a frame around the spore, in SEM often but not always with perforations. ...*M. cribrarioides*

### Acknowledgements

This work was carried out in the frame of an application for the Research Training Group RESPONSE (RTG 2010), now supported by the Deutsche Forschungsgemeinschaft (DFG). Funding was provided by grants for MS (SCHN 1080/2-1, DFG; Forschungsnetzwerk Ostseeraum, Univ. Greifswald), YKN (RFBR 10-04-00536a, 13-04-00839a, 12-04-33018 mol\_a\_ved, Russian Foundation for Basic Research; FNCP N 16.518.11.7071, Ministry of Education and Science of the Russian Federation), PJ ("Młodzi Naukowcy" no. 6/2015, W. Szafer Institute of Botany, Polish Acad. Sci.) and AR (N N303 799440, Polish Nat. Sci. Centre; statutory fund, W. Szafer Institute of Botany). For loans of specimens we owe thanks to M. Meyer and B. Woerly, France; S.L. Stephenson, USA; and A. Kuhnt, Germany. We are especially grateful to J. Clark and E. Haskins, who put together most of their achievements, forming the background triggering this research, in a series of four reviews published in *Mycosphere* (2010–2013).

### References

- Adl SM, Simpson AG, Lane CE, Lukeš J, Bass D, Bowser SS, Brown MW, Burki F, Dunthorn M, Hampl V, et al. 2012. The revised classification of eukaryotes. *J Eukaryot Microbiol.* 59:429–493.
- Aguilar M, Fiore-Donno AM, Lado C, Cavalier-Smith T. 2013. Using environmental niche models to test the ‘everything is everywhere’ hypothesis for *Badhamia*. *ISME J.* 8:737–745.
- Anonymous. 1976. ISCC-NBS Color name charts illustrated with centroid colors. Inter-Society Color Council. National Bureau of Standards. Washington, D.C. <http://tx4.us/nbs-iscc.htm> (accessed 10.10.2014).
- Betterley DA, Collins ONR. 1983. Reproductive systems, morphology, and genetical diversity in *Didymium iridis* (Myxomycetes). *Mycologia* 75:1044–1063.

- Bozonnet JM, Meyer M, Poulain M, 1992. Special Myxomycetes. *Bulletin Trimestriel de la Fédération Mycologique et Botanique Dauphiné-Savoie* 125:1–5.
- Chao A, Chazdon RL, Colwell RK, Shen TJ. 2006. Abundance-based similarity indices and their estimation when there are unseen species in samples. *Biometrics* 62:361–371.
- Clark J. 1993. *Didymium iridis* reproductive systems: additions and meiotic drive. *Mycologia* 85:764–768.
- Clark J. 1995. Myxomycete reproductive systems: additional information. *Mycologia* 87:779–786.
- Clark J. 2000. The species problem in the myxomycetes. *Stappia* 73:39–53.
- Clark J, Haskins EF. 2010. Reproductive systems in the myxomycetes: a review. *Mycosphere* 1:337–353.
- Clark J, Haskins EF. 2011. Principles and protocols for genetical study of myxomycete reproductive systems and plasmodial coalescence. *Mycosphere* 2:487–496.
- Clark J, Haskins EF. 2012. Plasmodial incompatibility in the myxomycetes: a review. *Mycosphere* 3:131–141.
- Clark J, Haskins EF. 2013. The nuclear reproductive cycle in the myxomycetes: a review. *Mycosphere* 4:233–248.
- Collins ONR. 1975. Mating types in five isolates of *Physarum polycephalum*. *Mycologia* 67:98–107.
- Collins ONR. 1979. Myxomycete biosystematics: some recent developments and future research opportunities. *Bot Rev.* 45:145–201.
- Collins ONR. 1981. Myxomycete genetics, 1960–1981. *J Elisha Mitch Sci Soc.* 97:101–125.
- Colwell RK. 2009. EstimateS: Statistical estimation of species richness and shared species from samples. Version 8.2. User's Guide and application. <http://purl.oclc.org/estimates> (accessed 12.04.2012).
- Colwell RK, Chao A, Gotelli NJ, Lin S-Y, Mao CX, Chazdon RL, Longino JT. 2012. Models and estimators linking individual-based and sample-based rarefaction, extrapolation and comparison of assemblages. *J Plant Ecol.* 5:3–21.
- Dalgleish D. 2014. Contexture. Excel tips, tutorials, and videos. Excel latitude and longitude calculations. <http://www.contextures.com/excellatitudelongitude.html> (accessed 17.08.2014).
- de Leon LF, Bermingham E, Podos J, Hendry AP. 2010. Divergence with gene flow as facilitated by ecological differences: within-island variation in Darwin's finches. *Phil Trans R Soc B* 365:1041–1052.
- De Bary A. 1859. Die Mycetozen. Ein Beitrag zur Kenntnis der niedersten Thiere. *Zeitschr Wiss Zool.* 10:88–175.
- Demoulin V, Hawksworth DL, Korf RP, Pouzar Z. 1981. A solution of the starting point problem in the nomenclature of fungi. *Taxon* 30: 52–63.
- Erastova DA, Novozhilov YK, Schnittler M. 2015. Nivicolous myxomycetes of the Khibiny Mountains, Kola Peninsula, Russia. *Nova Hedwigia*, online first (doi: 10.1127/nova\_hedwigia/2015/0274).
- Farrington HL, Lawson LP, Clark CM, Petren K. 2014. The evolutionary history of Darwin's finches: speciation, gene flow, and introgression in a fragmented landscape. *Evolution* 68:2932–2944.
- Feng Y, Schnittler M. 2015. Sex or no sex? Independent marker genes and group I introns reveal the existence of three sexual but reproductively isolated biospecies in *Trichia varia* (Myxomycetes). *Org Divers Evol.* 15:631–650.
- Feng Y, Klahr A, Janik P, Ronikier A, Hoppe T, Novozhilov YK, Schnittler M. 2015. What an intron may tell: several sexual biospecies coexist in *Meriderma* spp. (Myxomycetes). *Protist*, online first (doi: 10.1016/j.protis.2016.03.003).
- Ferris PJ, Vogt VM, Truitt CL. 1983. Inheritance of extrachromosomal rDNA in *Physarum polycephalum*. *Mol Cell Biol.* 3:635–642.
- Fiore-Donno AM, Clissmann F, Meyer M, Schnittler M, Cavalier-Smith T. 2013. Two-gene phylogeny of bright-spored myxomycetes (slime moulds, superorder Lucisporidia). *PLoS ONE* 8:e62586.
- Fiore-Donno AM, Kamono A, Meyer M, Schnittler M, Fukui M, Cavalier-Smith T. 2012. 18S rDNA phylogeny of *Lamproderma* and allied genera (Stemonitales, Myxomycetes, Amoebozoa). *PLoS ONE* 7:e35359.

- Fiore-Donno AM, Meyer M, Baldauf SL, Pawlowski J. 2008. Evolution of dark-spored myxomycetes (slime-molds): molecules versus morphology. *Mol Phylogenet Evol.* 46:878–889.
- Fiore-Donno AM, Novozhilov YK, Meyer M, Schnittler M. 2011. Genetic structure of two protist species (Myxogastria, Amoebozoa) suggests asexual reproduction in sexual amoebae. *PLoS ONE* 6:e22872.
- Fiz-Palacios O, Romeralo M, Ahmadzadeh A, Weststrand S, Ahlberg PA, Baldauf S. 2013. Did terrestrial diversification of amoebas (Amoebozoa) occur in synchrony with land plants? *PLoS ONE* 8:e74373.
- Fries ME. 1821. *Systema mycologicum*, vol 1. Lund. 520 p.
- Guindon S, Gascuel O. 2003. A simple, fast, and accurate algorithm to estimate large phylogenies by maximum likelihood. *Syst Biol.* 52:696–704.
- Hadley A. 2010. CombineZP. <http://www.hadleyweb.pwp.blueyonder.co.uk> (accessed 22.07.2015).
- Hood GM. 2010. PopTools version 3.2.5. <http://www.poptools.org> (accessed 17.08.2014).
- Jorgensen TH, Olesen JM. 2001. Adaptive radiation of island plants: evidence from *Aeonium* (Crassulaceae) of the Canary Islands. *Persp Plant Ecol Evol Syst.* 4:29–42.
- Kalyanasundaram I. 1973. Capillitial development in *Stemonitis*. In: Subramanian C (ed.) *Taxonomy of Fungi I*. University of Madras, India. pp. 9–13.
- Kamono A, Kojima H, Matsumoto J, Kawamura K, Fukui M. 2009. Airborne myxomycete spores: detection using molecular techniques. *Naturwissenschaften* 96:147–151.
- Katoh K, Standley DM. 2013. MAFFT multiple sequence alignment software version 7: improvements in performance and usability. *Mol Biol Evol.* 30:772–780.
- Kowalski DT. 1975. The myxomycete taxa described by Charles Meylan. *Mycologia* 67:448–494.
- Lado C. 2005–2015. An on line nomenclatural information system of Eumycetozoa. <http://www.nomen.eumycetozoa.com> (accessed 28.07.2015).
- Lahr DJG, Grant J, Nguyen T, Lin JH, Katz LA. 2011a. Comprehensive phylogenetic reconstruction of Amoebozoa based on concatenated analyses of SSU rDNA and actin genes. *PLoS ONE* 6:e22780.
- Lahr DJG, Parfrey LW, Mitchell EA, Katz LA, Lara E. 2011b. The chastity of amoebae: re-evaluating evidence for sex in amoeboid organisms. *Proc R Soc B* 278:2081–2090.
- Leontyev D, Schnittler M, Stephenson SL 2015. A critical revision of the *Tubifera ferruginosa*-complex. *Mycologia* 107:959–985.
- Linné C. 1753. *Species Plantarum*. Uppsala.
- Magurran AE. 2004. *Measuring biological diversity*. Blackwell Publishing, Malden, Massachusetts.
- McCune B, Mefford MJ. 1999. PC-ORD. Multivariate analysis of ecological data. Version 4. MjM Software Design. Gleneden Beach, Oregon. 237 p.
- Meylan, Ch. 1908. Contributions à la connaissance des Myxomycètes du Jura. *Bull Soc Vaud Sc Nat.* 44:285–302.
- Meylan, Ch. 1910. Myxomycètes du Jura (Suite). *Bull Soc Vaud Sci Nat.* 46:49–57.
- Meylan, Ch. 1932. Les espèces nivales du genre *Lamproderma*. *Bull Soc Vaud Sci Nat.* 57:359–373.
- Milne I, Lindner D, Bayer M, Husmeier D, McGuire G, Marshall DF, Wright F. 2009. TOPALi v2: a rich graphical interface for evolutionary analyses of multiple alignments on HPC clusters and multi-core desktops. *Bioinformatics* 25:126–127.
- Mort ME, Soltis DE, Soltis PS, Francisco-Ortega J, Santos-Guerra A. 2002. Phylogenetics and evolution of the Macaronesian clade of Crassulaceae inferred from nuclear and chloroplast sequence data. *Syst Bot.* 27:271–288.
- Novozhilov YK, Okun MV, Erastova DA, Shchepin ON, Zemlyanskaya IV, García-Carvajal E. 2013a. Description, culture and phylogenetic position of a new xerotolerant species of *Physarum*. *Mycologia* 105:1535–1546.
- Novozhilov YK, Schnittler M, Erastova DA, Okun MV, Schepin ON, Heinrich E. 2013b. Diversity of nivicolous myxomycetes of the Teberda State Biosphere Reserve (Northwestern Caucasus, Russia). *Fungal Divers.* 59:109–130.
- Pawlowski J, Audic S, Adl S, Bass D, Belbahri L, Berney C, Bowser SS, Cepicka I, Decelle J, Dunthorn M, et al. 2012. CBOL protist working group: barcoding eukaryotic richness beyond the Animal, Plant, and Fungal Kingdoms. *PLoS Biol.* 10:e1001419.

- Poulain M, Meyer M, Bozonnet J. 2011. Les Myxomycètes. Sevrier: Federation mycologique et botanique Dauphiné-Savoie. 556 p.
- Rasband WS. 1997–2012. ImageJ. U.S. National Institutes of Health. Bethesda, Maryland. <http://imagej.nih.gov/ij> (accessed 10.07.2015).
- Ronikier A, Ronikier M, 2009. How 'alpine' are nivicolous myxomycetes? A worldwide assessment of altitudinal distribution. *Mycologia* 101:1–16.
- Ronquist F, Huelsenbeck JP. 2003. MrBayes 3: Bayesian phylogenetic inference under mixed models. *Bioinformatics* 19:1572–1574.
- Schmidt SK, Naff CS, Lynch RC. 2012. Fungal communities at the edge: Ecological lessons from high alpine fungi. *Fungal Ecol.* 5:443–452.
- Schnittler M, Erastova DA, Shchepin ON, Heinrich E, Novozhilov YK. 2015. Four years in the Caucasus – observations on the ecology of nivicolous myxomycetes. *Fungal Ecol.* 14:105–115.
- Schnittler M, Mitchell DW. 2000. Species diversity in myxomycetes based on the morphological species concept – a critical examination. *Stappia* 73:55–62.
- Schnittler M, Novozhilov YK, Romeralo M, Brown M, Spiegel FW. 2012. Myxomycetes and Myxomycete-like organisms. In: Frey W, editor. (13th ed.) Englers Syllabus of Plant Families. Vol. 4. Bornträger, Stuttgart. pp. 40–88.
- Schnittler M, Tesmer J. 2008. A habitat colonisation model for spore-dispersed organisms – does it work with eumycetozoans? *Mycol Res.* 112:697–707.
- Schnittler M, Unterseher M, Tesmer J. 2006. Species richness and ecological characterization of myxomycetes and myxomycete-like organisms in the canopy of a temperate deciduous forest. *Mycologia* 98:223–232.
- Smirnov AV, Chao E, Nassonova ES, Cavalier-Smith T. 2011. A revised classification of naked lobose amoebae (Amoebozoa: Lobosa). *Protist* 162:545–570.
- Stephenson SL. 2011. From morphological to molecular: studies of myxomycetes since the publication of the Martin and Alexopoulos (1969) monograph. *Fungal Divers.* 50:21–34.
- Tamura K, Nei M, Kumar S. 2004. Prospects for inferring very large phylogenies by using the neighbor-joining method. *Proc Natl Acad Sci USA.* 101:11030–11035.
- Tamura K, Peterson D, Peterson N, Stecher G, Nei M, Kumar S. 2011. MEGA5: molecular evolutionary genetics analysis using maximum likelihood, evolutionary distance, and maximum parsimony methods. *Mol Biol Evol.* 28:2731–2739.
- Thiv M, Esfeld K, Koch M, 2010. Studying adaptive radiation at the molecular level: a case study in the Macaronesian Crassulaceae-Sempervivoideae. In: Glaubrecht M (ed.) Evolution in action - Adaptive radiations and the origins of biodiversity. Springer, Heidelberg. pp. 35–59.
- Unterseher M, Schnittler M, Dormann C, Sickert A. 2008. Application of species richness estimators for the assessment of fungal diversity. *FEMS Microbiol Lett.* 282:205–213.

## Tables and Figures

Table 1. Correlation coefficients for 15 morphological traits from 162 specimens of *Meriderma* spp. with the first two axes of a Detrended Correspondence Analysis.

No.	Trait	Axis1	Axis2
1	Stalk length (Sta_l)	-0.072	0.944
2	Sporotheca height (Spt_h)	-0.179	0.046
3	Ratio stalk length : sporotheca height (StaSpt)	-0.074	0.935
4	Spore diameter, transmitted light (Sp_d1)	-0.075	-0.295
5	Spore diameter, SEM (Sp_d2)	-0.177	-0.184
6	Spine length, SEM (Spi_l)	0.493	-0.422
7	Proportion of surface covered by ornaments (Or)	0.502	-0.322
8	Size of largest ornament (OrMax)	0.926	-0.132
9	Ornament density (OrD)	-0.943	0.213
10	Mean circularity of ornaments (OrCirc)	-0.928	0.169
11	Reticulation index (0-1, Re)	0.950	-0.171
12	Size of largest mesh (MeMax)	-0.890	0.104
13	Density of meshes (MeD)	0.885	0.001
14	Mean circularity of meshes (MeCirc)	0.354	0.183
15	Evenness of ornamentaion (Tes)	0.421	-0.164

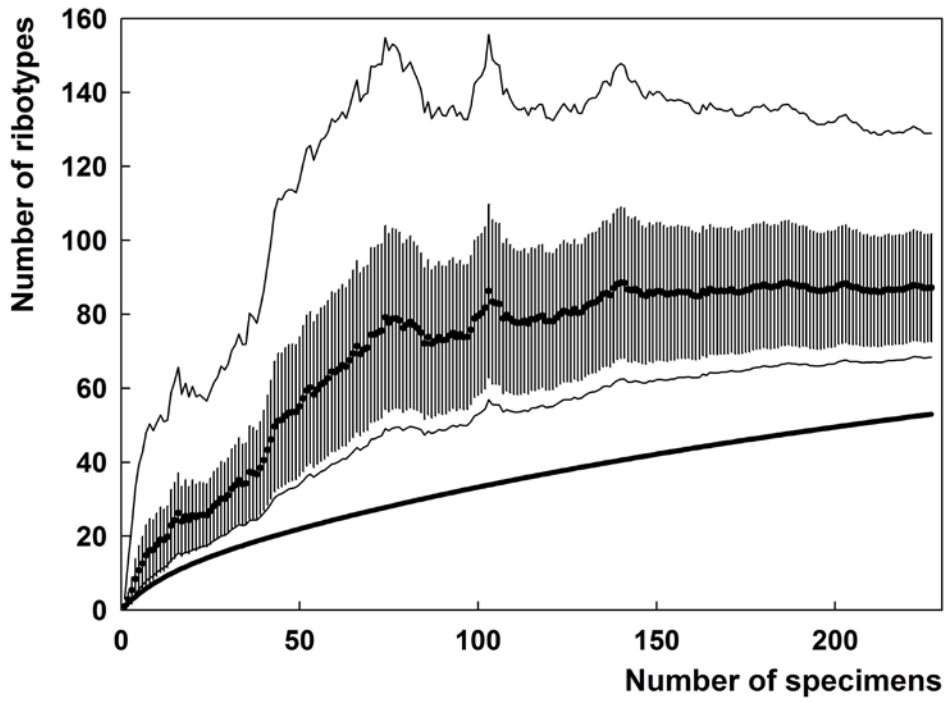


Fig. 1. Ribotype accumulation curve (thick solid line) for 227 specimens of *Meriderma* spp., showing the behavior of the Chao2 richness estimator with 95% confidence intervals (solid thin lines) and standard deviation (error bars).



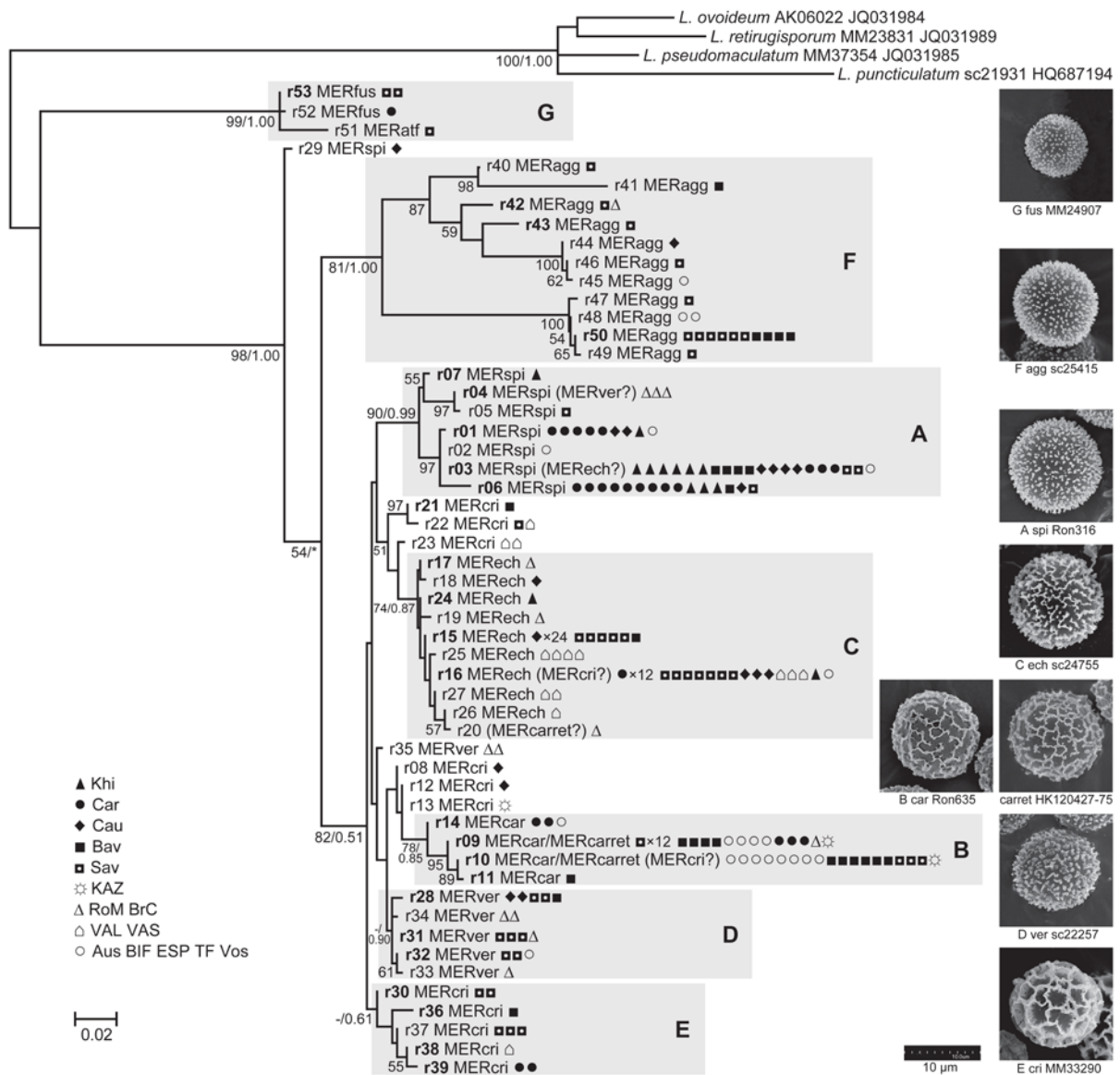


Fig. 2. Phylogeny of partial SSU sequences constructed from 229 specimens of *Meriderma* spp. Shown are the ribotypes (r01–r54), often represented by several identical sequences from more than one specimen. In the maximum likelihood tree bootstrap / posterior probability values >50 percent / >0.5 are indicated; a hyphen (–) indicates bootstrap value < 50, a star (\*) indicates a conflicting topology of the respective Bayesian tree. For each of the major clades A–G SEM micrographs of typical spore ornamentations are shown. Symbols indicate the origin of investigated specimens, with Khi – Khibine Mts., Kola peninsula, Russia; Car – Polish Carpathians; Cau – northern Caucasus, Teberda Reserve, Russia; Bav – German Alps; Sav – French Alps, Savoie; KAZ – Ili Alatau Mts. near Almaty, southern Kazakhstan, RoM –Rocky Mountains, Colorado, US; BrC – Coastal Mountains around Whistler, British Columbia, Canada; VAL – Valamo island, VAS Vaskelevo, both N of St. Petersburg, Russia; Aus – Austrian Alps; BIF – Black Forest, Germany; ESP – Sierra Nevada, Spain; TF – Thuringian Forest, Germany; Vos – Vosges Mts., eastern France. Abbreviations for species names show the result of determinations according to the morphological species concept of Poulain et al. (2011): agg – *M. aggregatum*, atf – *M. atrofuscatum*, car – *M. carestiae*, carret – *M. carestiae* var. *retisporum*, cri – *M. cribrarioides*, ech – *M. echinulatum*, fus – *M. fuscatum*, spi – *M. spinulisporum*, ver – *M. verrucosporum*. Names in parentheses denote single specimens with a morphology deviating from that of the other specimens in the clade.

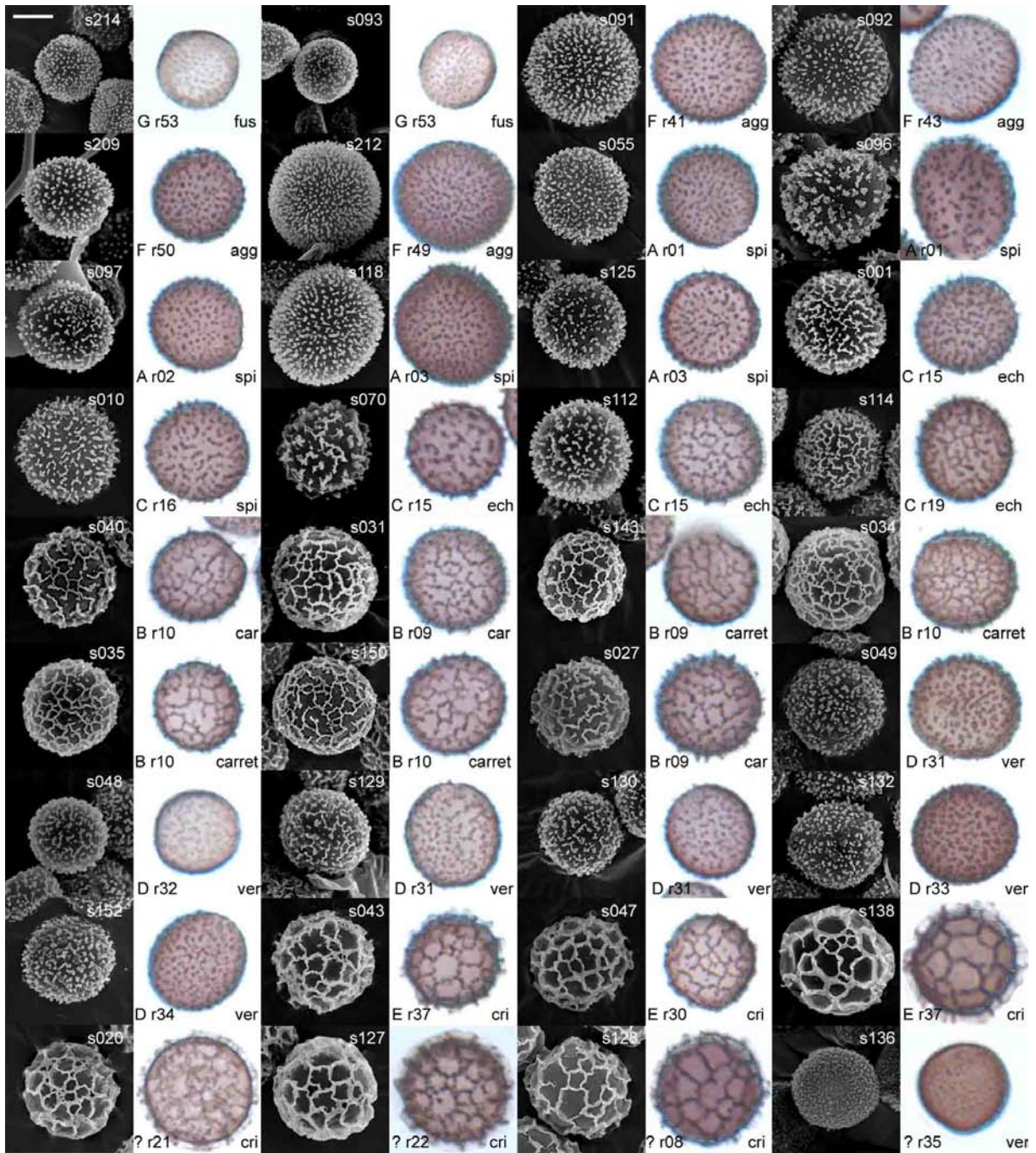


Fig. 3. Spore morphologies in *Meriderma* spp. Shown are SEM micrographs and the corresponding images from the same specimen in a compound microscope (1000x, stacked image). For each pair of images the specimen number (upper left), the clade / ribotype in the SSU phylogeny and the result of a morphological determination is given (lower right, see Fig. 2 for abbreviation of taxon names). A question mark denotes specimens which could not be assigned to any of the clades A–G. Bar: 5µm.

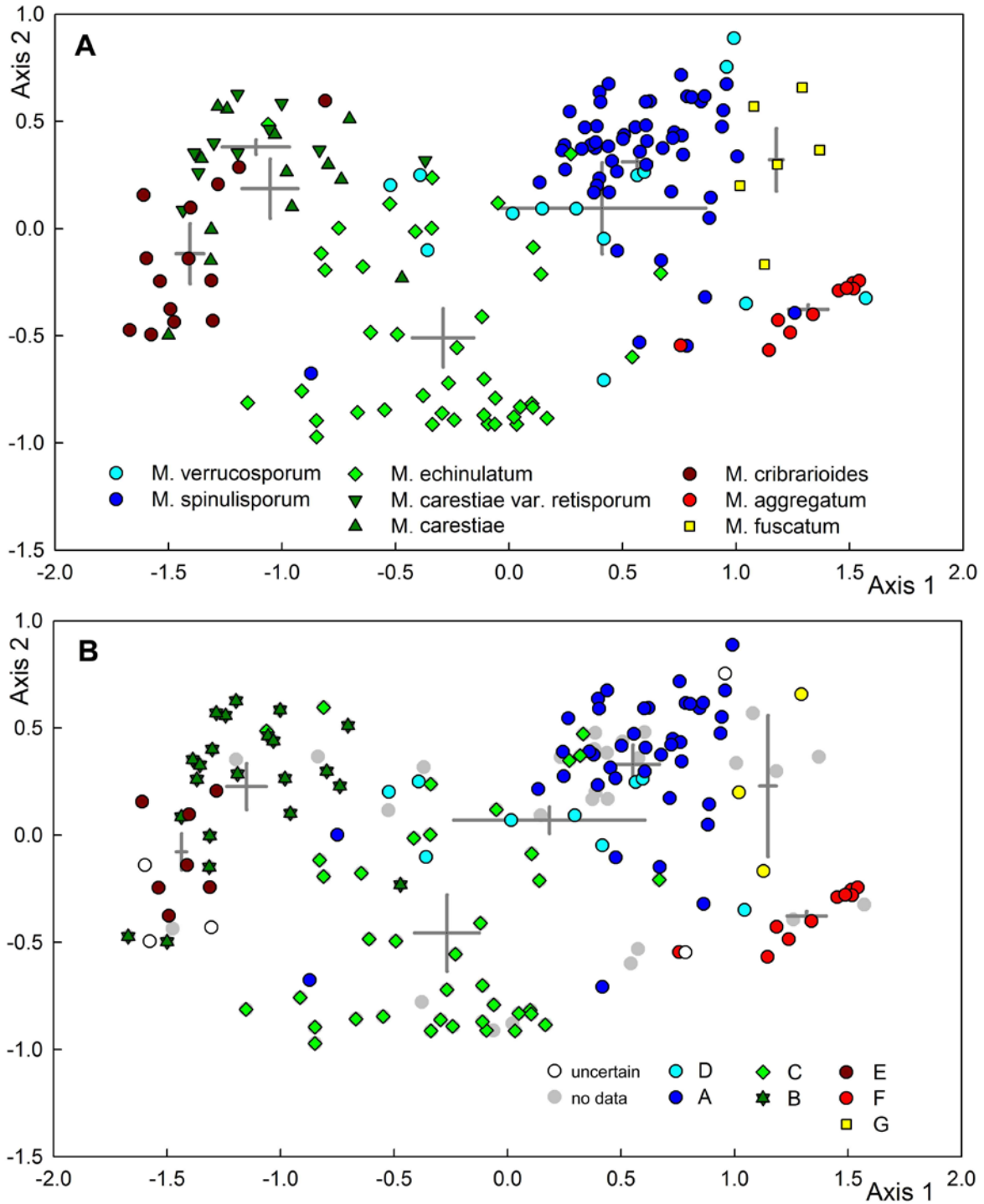


Fig. 4. Nonmetric multidimensional scaling considering 10 morphological characters measured in 162 specimens. A Species scores overlaid with determination results. B species scores overlaid with the assignment to major groups in the SSU phylogeny (130 specimens assigned to groups, 5 of uncertain position, 27 specimens not sequenced). Grey crosshairs denote the centroids (means of axis1 and axis2 coordinates of species scores) of the clusters (A: specimens belonging to the same morphotype and B: specimens showing the same phylogroup); centroids are scaled according to the standard error (enlarged fivefold).

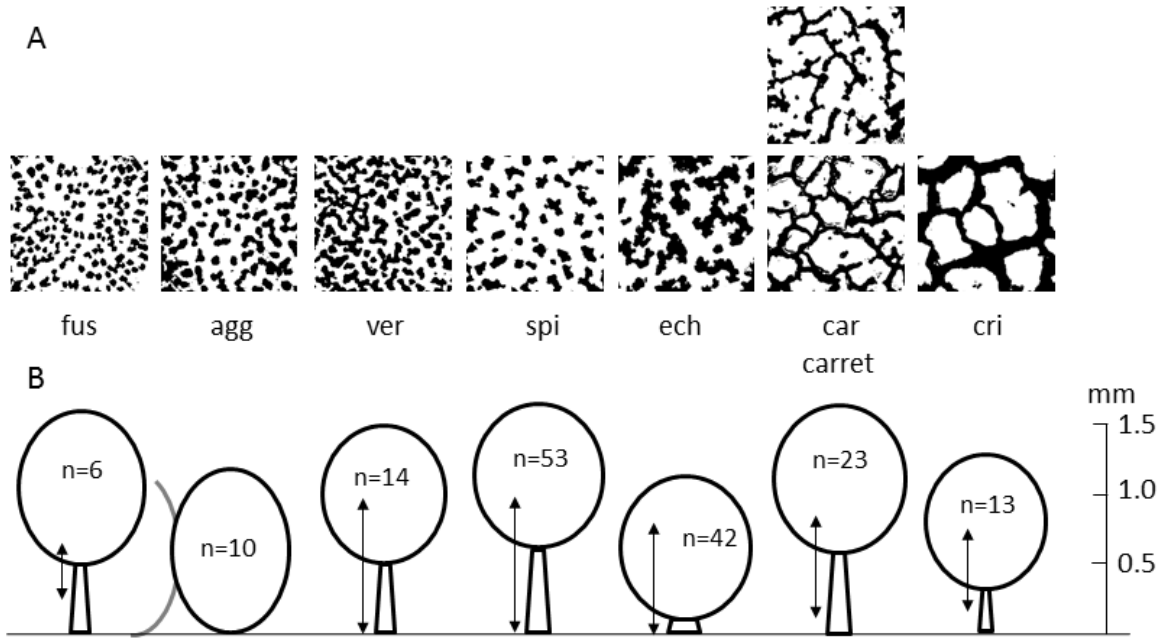


Fig. 5. A Comparison of typical spore ornaments for the species of *Meriderma*, shown are black and white images of a 6x6  $\mu\text{m}$  section from SEM micrographs as used for automated analysis in ImageJ. B Average shapes of sporocarps, shown are the median values of stalk length and sporotheca height for the investigated specimens (see Supplementary data base S1). Arrows beside the sporocarps indicate the minimum and maximum values encountered for stalk length. Abbreviations for taxa are as in Fig. 2.



## Molecular or morphological species? Myxomycete diversity in a deciduous forest in northeastern Germany

Yun Feng and Martin Schnittler\*

Institute of Botany and Landscape Ecology, Ernst Moritz Arndt University of Greifswald, Soldmannstr. 15, 17487 Greifswald, Germany

With 3 figures and 1 table

**Abstract:** To compare morphological and molecular diversity for lignicolous myxomycetes, DNA samples of all specimens found within a survey covering the late-autumn aspect of myxomycete fructifications on coarse woody debris were sequenced, using partial sequences of the nuclear small-subunit ribosomal RNA gene (SSU) as a barcode marker. A total of 161 logs, mostly from European beech (*Fagus sylvatica*) in the old-growth forest of Eldena in northeastern Germany, was surveyed from early October to early December 2012, resulting in 530 collections representing 27 morphospecies (26 species and one variety) from 14 genera. Bright-spored taxa were far more abundant (508 records / 17 taxa / 50 ribotypes) than dark-spored ones (22 records / 10 taxa / 15 ribotypes). Accumulation curves constructed from morphospecies and ribotypes both converged, resulting in figures of  $32.6 \pm 4.9 / 90.0 \pm 11.1$  for taxon / ribotype diversity to be expected according to the Chao2 estimator. A phylogeny based on partial SSU sequences for bright-spored myxomycetes revealed morphospecies to be largely consistent with phylogenetic groups. Most but not all intensely sampled morphospecies contain multiple ribotypes that cannot be differentiated by light microscopy. The study demonstrates that SSU sequences can function as reliable barcode markers for myxomycetes, but these also reveal a significant, yet not infinite, amount of hidden diversity.

**Key words:** Amoebozoa, barcoding, plasmodial slime molds, morphospecies diversity, genotypic diversity, nuclear small-subunit ribosomal RNA gene.

### Introduction

Due to their fructifications achieving macroscopic dimensions, the plasmodial slime molds (myxomycetes or myxogastrids) were one of the few protistean groups attracting the attention of early botanists. The first species were mentioned in Linné's *Species Plantarum* (1753) and Persoon's *Illustrations of the Fungi* (1791–1793). Later, Anton de Bary (1859) discovered that these organisms are protists, not fungi. The fruiting

---

\*Corresponding author: martin.schnittler@uni-greifswald.de

bodies are the reason why we have a solid body of data on distribution and (phenology-based) ecology of myxomycetes (Stephenson et al. 2008). Nearly 1000 species have been described (Lado 2015), with ever growing numbers (Schnittler & Mitchell 2000), making the myxomycetes one of the most species-rich groups in Amoebozoa.

In contrast to these achievements in classical taxonomy, the molecular taxonomy of myxomycetes is lagging behind that of other groups of protists, since these organisms are neither parasitic nor pathogenic, nor of any economic importance. The first phylogenies of the group were published only recently (Fiore-Donno et al. 2008, 2012, 2013) and are based mainly on sequences of the nuclear small-subunit ribosomal RNA gene (SSU), which was successfully used as a barcode marker for other protistean groups (Pawlowski et al. 2012). This changed the traditional taxonomy of the myxomycetes considerably, since the five orders (Echinosteliales, Liceales, Trichiales, Physarales and Stemonitales) are not all monophyletic. Now widely accepted is the division into a dark-spored (spores containing melanin) group and a bright-spored (spores containing other pigments) group instead of the division Stemonitales (forming fructifications with an internal stalk, epihypothallic developmental type; Ross 1973, Clark & Haskins 2014) versus the other orders (external stalk, subhypothallic developmental type). As already expected (Eliasson 1977, 2015), the Liceales are not a natural group, with the genus *Cribraria* clearly separated from all other bright-spored myxomycetes (the classical orders Liceales and Trichiales; Fiore-Donno et al. 2013), whereas within the dark-spored myxomycetes, the Physarales are nested within Stemonitales (Fiore-Donno et al. 2012).

SSU sequences from myxomycetes are extremely rich in introns (Lundblad et al. 2004), and as many as ten insertion sites are now known (Feng & Schnittler 2015, Fiore-Donno et al. 2013). This makes entire SSU sequences, varying in length between 2000 and 8000 bases, difficult to obtain. However, the first ca 600 bases of the SSU are free of introns and can be obtained by Sanger sequencing with a single primer pair. Such partial SSU sequences were used for a first estimate of molecular diversity in niviculous myxomycetes (Novozhilov et al. 2013b), to explore geographic differentiation in the species *Badhamia melanospora* (Aguilar et al. 2013), to determine the systematic position of the genus *Kelleromyxa* (Erastova et al. 2013), the phylogeny of the species complex *Physarum notabile* (Novozhilov et al. 2013a), and to revise the genus *Tubifera* (Leontyev et al. 2015).

Nevertheless, the more than 1000 published surveys exploring the myxomycete biota of a particular region are still all based on morphological differentiation of the species present. This paper presents the first survey to include a full secondary barcoding component, based on SSU sequences obtained from the spores of collected specimens. Objectives of the study were (1) to compare the morphological diversity of myxomycetes with the genetic diversity of the respective partial SSU ribotypes, using a limited assemblage of species, (2) to obtain a first estimate of the extent of hidden diversity in myxomycetes, and (3) to construct a phylogeny of bright-spored myxomycetes with partial SSU sequences to prove their suitability as a barcode marker for this group of organisms.

## Materials and methods

**STUDY SITE:** The nature reserve Eldena, located in northeastern Germany (state of Mecklenburg-Western Pomerania), is a partly old-growth forest encompassing approximately 427 ha, formerly in the possession of the Cistercian monastery Eldena since reformation times of the University of Greifswald. The area has been wooded, yet with different intensities of human use, since historic times. The climate is cool subcontinental, with annual mean figures for temperature and precipitation 8°C and 566 mm, respectively (Spangenberg 2003). The dominant tree species is *Fagus sylvatica* L. (beech), accompanied by *Fraxinus excelsior* L. (ash), *Carpinus betulus* L. (hornbeam) and *Quercus robur* L. (oak). During autumn 2012, a total of 161 logs, mostly in progressive stages of decay, were surveyed. Most of these logs came from beech, with a minor component from oak.

**SPECIMENS:** Myxomycete specimens were collected by the first author from 161 dead logs in the forest Eldena from October 1 to December 3 in 2012. For each log examined, all colonies of the morphospecies *Trichia varia* that differed by morphology, degree of maturation, and location of the colony were collected separately as individual specimens for microsatellite genotyping; these results will be published in a separate paper. For all other morphospecies, mostly one specimen per log and morphospecies was collected. Sporocarps were preserved in polyvinyl lactophenol as semipermanent slides. Specimens were deposited in the personal collection of M. Schnittler (Greifswald, Germany, to be deposited in M). Information about all specimens collected in this survey and their ribotypes with GenBank accession numbers (KT358640–KT358702) is listed in Supplementary Databases S1 and S6, respectively. In addition, 24 bright-spored myxomycete specimens not collected in this survey were used for sequencing as comparison material for phylogenetic analyses. Supplementary Database S2 contains information on these 24 specimens and their respective GenBank accession numbers (KT358703–KT358726).

**DNA EXTRACTION, PCR AND SEQUENCING:** Partial sequences of the nuclear small subunit ribosomal RNA gene (SSU) were obtained from 527 specimens collected in this survey and the 24 bright-spored specimens not collected in this survey. The partial SSU sequences obtained in this study cover the first part of SSU that is free of introns.

For specimens from different sources and collected at different times, two commercially available kits (Invisorb Spin Food Kit II, Stratec; DNeasy Plant Mini Kit, Qiagen) were used for extraction of genomic DNA with good results. For *Trichia varia*, 5–20 sporocarps were treated with the Invisorb kit, quantified using Nanodrop Lite (Thermo Scientific), and diluted to a concentration of 5 µg/µl. For *Lycogala epidendrum* DNA was extracted from a small portion of the aethalium with the DNeasy kit. The 24 bright-spored specimens were treated as well with the DNeasy kit.

For all other specimens collected in this survey, a small amount of spores was directly transferred with a toothpick to an empty PCR tube and used as template like in the single-spore two-step PCR procedure modified from Frommlet et al. (2008) and described in Feng & Schnittler (2015). Our preliminary studies showed that this procedure can be applied to myxomycetes as a multiplex PCR described in Frommlet et al. (2008), with a small number of spores targeting simultaneously two marker genes, partial SSU and partial mitochondrial cytochrome oxidase subunit I gene. For this study we applied the method as direct-spore PCR and used the same primer pair in both steps, since we targeted only a single marker.

As the main primer pair for all specimens of bright-spored myxomycetes NUSSUF3 (CCTGCCAGAATCATATGCTTGTC; Feng & Schnittler 2015; all primers written in 5'–3' direction) and NUSSUR4 (ACCAGACTTGTCCTCCAATTGTTAC; Feng & Schnittler 2015) was used. For specimens of *Lycogala epidendrum* the reverse primer was replaced by SR4Bright (TGCTGGCACCAGACTTGT; Fiore-Donno et al. 2013). For dark-spored myxomycetes, a pair of primers was designed based on the complete SSU alignment in Fiore-Donno et al. (2012), called NUSSUF20 (TCGACAACCTGGTTGATCCTG) and NUSSUR13 (ACCAGACTTGTCCTCTAATTGTTAC). All these primers amplify the first part of SSU that is free of introns. The end of the primer sequences NUSSUR4 and NUSSUR13 overlap with the upstream recognition sequence for intron S516 if seen from the inserted intron (Feng & Schnittler 2015). In species possessing the S516 intron, the primer SR4Bright may cause problems, since in this case it covers two regions flanking the intron.

For PCR using extracted DNA of *Trichia varia* the annealing temperature was set to 56°C; for all specimens of *Lycogala epidendrum* and the 24 accessions from comparison material of bright-spored myxomycetes the annealing temperature was 52°C. For direct-spore PCR the annealing temperature of the first PCR was 52°C and of the second PCR 52°C or 55°C. PCR reactions were performed using the MangoTaq Kit (Bioline). Cycle sequencing reactions were performed using the BigDye Kit (ABI).

**MORPHOSPECIES DIVERSITY ASSESSMENT:** Myxomycetes were determined according to Martin & Alexopoulos (1969) and Neubert et al. (1993, 1995, 2000); nomenclature follows Lado (2015). The abundance of morphospecies was classified according to Stephenson et al. (1993), based on the proportion of a morphospecies in relation to the total number of records: R, rare (<0.5% of all records); O, occasional (>0.5–1.5% of all records); C, common (>1.5–3% of all records); A, abundant (>3% of all records). To ensure comparability with other surveys, the number of 318 records served as a baseline, counting only record per log for each morphospecies.

**IDENTIFICATION OF PARTIAL SSU RIBOTYPES:** Partial SSU sequences were aligned separately for bright- and dark-spored myxomycetes using MUSCLE (Edgar 2004) implemented in MEGA 5.05 (Tamura et al. 2011) with default settings. From these alignments (TreeBASE: M34158, M34159), the number of unique ribotypes for each morphospecies was identified. The overall mean genetic distance between ribotypes was computed for each morphospecies containing multiple ribotypes using the maximum composite likelihood model (Tamura et al. 2004) implemented in MEGA, applying complete deletion of gaps.

**MORPHOSPECIES AND PARTIAL SSU RIBOTYPE ACCUMULATION CURVES:** To estimate the extent to which both the morphological and the molecular component of the survey was exhaustive, individual-based ribotype accumulation curves (RAC) were constructed using the program EstimateS version 8.2 (Colwell 2009). The Chao2 incidence-based estimator of species richness (Chao et al. 2006, Colwell et al. 2012) and the expected richness function "Mao Tau" were used to construct the RAC. In addition, a hyperbolic regression according to the Michaelis-Menten formula  $y = ax/(b+x)$ , resulting in a curve shape approaching the broken-stick model (Magurran 2004; Unterseher et al. 2008) was applied to these data, with the parameter *a* giving an estimate for the maximum number of species to be expected. For *Cribraria rufa* and *Stemonitis fusca*, both represented by single specimens, sequences could not be obtained using the primers listed above. For the construction of the RAC, we included both species with one genotype each. The third specimen where sequencing failed belonged to *Hemitrichia clavata*; here we assumed the same genotype to occur as for the 10 specimens whose DNA was successfully sequenced. For two records of *Trichia favoginea* and *T. scabra* that gave multiple (heterogeneous) ribotypes, we randomly selected one ribotype, which is the first listed in Supplementary Database 1.

**PHYLOGENETIC ANALYSES:** For comparison, all published sequences of myxomycetes that cover the first part of SSU that is free of introns and vouchers specimens determined to the species level were downloaded from GenBank on 8 June 2015. The section of the first part of SSU was extracted separately for bright-spored and dark-spored myxomycetes from the preliminary alignments generated using MAFFT 7.245 (Kato & Standley 2013) with the progressive method "FFT-NS-2".

Of the usable sequences (complete for partial SSU, voucher determined, BLAST search indicating myxomycetes), 63 represent bright-spored myxomycetes (Fiore-Donno et al. 2005, 2010, 2013, Leontyev et al. 2014a, 2014b, Shadwick et al. 2009; see Supplementary Database S3 for information about GenBank accessions). In addition, 12 SSU sequences of the bright-spored morphospecies *Trichia varia* were included in the analysis (Feng & Schnittler 2015; Supplementary Database S3). For sequences of dark-spored myxomycetes, the partial SSU alignment was refined by Cd-hit (Li & Godzik 2006) with a threshold to exclude 100% identical sequences and resulted in 270 unique and complete sequences with determined vouchers (Aguilar et al. 2013, Erastova et al. 2013; Fiore-Donno et al. 2005, 2008, 2009, 2011, 2012; Haugen et al. 2005; Hoppe & Schnittler 2015, Horton & Landweber 2000, Johansen et al. 1988, Kamono et al. 2013, Lundblad et al. 2004, Nandipati et al. 2012, Novozhilov et al. 2013a, 2013b, 2014, Shchepin et al. 2014, Wikmark et al. 2007; see Supplementary Database S4 for information about GenBank accessions).

The final alignments for bright-spored and dark-spored taxa (TreeBASE: M34158 and M34159) were generated separately using MAFFT 7.215 with the iterative refinement method "X-INS-i" under



the option "scarnapair" that considered secondary structure information of RNA. All unique partial SSU sequences identified from bright-spored myxomycetes collected in this survey were aligned with the 75 published sequences of bright-spored myxomycetes and the 24 sequences of bright-spored myxomycetes not belonging to the survey but generated within this study. This alignment contains 1802 nucleotide positions (TreeBASE: M34158). A continuous section of 308 bp, representing a relatively reliably aligned region of the alignment, was extracted from positions 1482 to 1789 and used for phylogenetic analysis. The alignment including dark-spored representatives contains all unique partial SSU sequences identified from dark-spored specimens collected in this survey and 270 published sequences of dark-spored myxomycetes. This alignment contains 1666 nucleotide positions (TreeBASE: M34159), of which a continuous section of 1546 bp extracted from positions 93 to 1638 covering most of the alignment was included to construct a phylogenetic tree of dark-spored myxomycetes.

Substitution models for Maximum Likelihood (ML) analysis and Bayesian analysis were selected using TOPALi 2.5 (Milne et al. 2009) under the Bayesian information criterion. The best model was SYM+G for both ML analysis and Bayesian analysis, and as well for both bright-spored and dark-spored myxomycetes. For both, bright-spored and dark-spored myxomycetes, ML analyses were conducted using PhyML 2.4.5 (Guindon & Gascuel 2003) implemented in TOPALi with 1000 replications. Bayesian analyses were carried out only for the relatively reliably aligned data set compiled for bright-spored species, using MrBayes 3.1.1 (Ronquist & Huelsenbeck 2003) implemented in TOPALi with 2 runs, 20 million generations, 50% as burn-in, sampled every 100 generations.

## Results

### Morphospecies diversity

The late-autumn survey in the forest Eldena yielded 530 specimens of myxomycetes from 161 logs, representing 27 morphospecies (16 species and one variety for bright-spored, 10 species for dark-spored myxomycetes) belonging to 14 genera (see Table 1 and Supplementary Database S1 for morphological determinations). Three specimens could not be unambiguously determined by sporocarp morphology and microscopic characters (sc22698, *Trichia* cf. *persimilis*; sc22968 and sc22914, *Physarum* cf. *notabile*). Of the 27 morphospecies 9 were classified as rare, 6 as occasionally occurring, 3 as common, and 9 as abundant (Table 1). The morphospecies classified as abundant provide 88% of all the specimens in the survey. *Trichia varia* was collected with multiple specimens per log on 92 logs for the study of Feng & Schnittler (2015) and thus accounted for 292 specimens. For the remaining species, only occasionally more than one specimen per log was collected. Of the remaining 238 specimens from 134 logs, 216 are bright-spored myxomycetes and 22 are dark-spored myxomycetes. Considering only the 318 records obtained on a log-base (92 for *T. varia* and 226 from other taxa), bright-spored myxomycetes represented 93% of all records. Based on all 530 records, a total of 19 taxa (13 bright-spored and 6 dark-spored) were represented by more than one specimen, whereas 8 taxa were found as singletons (4 bright-spored and 4 dark-spored). Of the 161 logs being surveyed, 75 were found to harbor a single morphospecies only. The remaining 86 logs yielded more than one morphospecies, with log L139 displaying six morphospecies, the highest number of taxa per log (see Supplementary Database S5 for distribution of morphospecies on logs).

The individual-based accumulation curve computed from morphologically recognizable taxa (26 species and one variety, see Table 1) clearly converged (Fig. 1A). The Chao2

Table 1. Morphospecies and ribotype diversity of the assemblage of myxomycetes characterizing the late-autumn aspect of the deciduous forest Eldena.

Group <sup>1</sup>	Species	Records		ACOR <sup>2</sup>	Ribotypes			Average distance	Indel (No.) length
		No.	%		Code	No.	Length		
bright	<i>Arcyria denudata</i>	18	5.66	A	AD	6	537	0.01405	1 (3-bp)
bright	<i>Arcyria stipata</i>	1	0.31	R	AS	1	524	–	–
bright	<i>Cribraria rufa</i>	1	0.31	R	–	–	–	–	–
bright	<i>Hemitrichia calyculata</i>	50	15.7	A	HA	1	528	–	–
bright	<i>Hemitrichia clavata</i>	11	3.46	A	HL	1	510	–	–
bright	<i>Hemitrichia imperialis</i>	6	1.89	C	HI	2	506	0.00198	–
bright	<i>Lycogala epidendrum</i>	25	7.86	A	LE	3	852	0.26563	numerous
bright	<i>Metatrichia floriformis</i>	18	5.66	A	MF	2	514	0.07051	3 (1-bp), 2 (2-bp)
bright	<i>Metatrichia vesparium</i>	13	4.09	A	MV	2	552	0.00364	–
bright	<i>Trichia contorta</i>	1	0.31	R	TC	1	527	–	–
bright	<i>Trichia decipiens</i>	4	1.26	O	TD	3	548	0.29661	numerous
bright	var. <i>hemitrichoides</i>	1	0.31	R	TD	1	531	–	–
bright	<i>Trichia favoginea</i>	17	5.35	A	TF	4	493	0.00407	–
bright	<i>Trichia persimilis</i> / <i>Trichia</i> cf. <i>persimilis</i>	8	2.52	C	TP	4	501	0.02242	1 (1-bp), 3 (2-bp)
bright	<i>Trichia scabra</i>	29	9.12	A	TS	6	500	0.04336	1 (1-bp)
bright	<i>Trichia varia</i>	92	28.9	A	TV	11	530	0.05542	1 (1-bp)
bright	<i>Tubifera ferruginosa</i>	1	0.31	R	TU	1	731	–	–
dark	<i>Brefeldia maxima</i>	1	0.31	R	BM	1	587	–	–
dark	<i>Diderma montanum</i>	1	0.31	R	DM	1	568	–	–
dark	<i>Fuligo leviderma</i>	1	0.31	R	FL	1	571	–	–
dark	<i>Fuligo septica</i>	4	1.26	O	FS	1	561	–	–
dark	<i>Lamproderma arcyrioides</i>	2	0.63	O	LA	2	550	0.05637	3 (1-bp), 1 (5-bp)
dark	<i>Physarum album</i>	3	0.94	O	PA	1	589	–	–
dark	<i>Physarum</i> cf. <i>notabile</i>	2	0.63	O	PN	2	604	0.14409	numerous
dark	<i>Physarum robustum</i>	2	0.63	O	PR	2	604	0.15833	numerous
dark	<i>Stemonitis fusca</i>	1	0.31	R	–	–	–	–	–
dark	<i>Stemonitopsis typhina</i>	5	1.57	C	ST	3	717	0.00186	–

<sup>1</sup> Systematic position of the taxon, differentiating bright- and dark-spored myxomycetes.

<sup>2</sup> Abundance scale according to Stephenson (1993): R (rare, <0.5% of all records), O (occasionally occurring, >0.5–1.5% of all records), C (common, >1.5–3% of all records), A (abundant, >3% of all records).

richness estimator depicted  $32.6 \pm 4.9$  taxa to expect, a hyperbolic curve fit resulted in  $30.5 \pm 0.1$  taxa. With only one record per taxon and log counted, these figures do hardly change (Chao2:  $36.0 \pm 7.1$ , hyperbolic regression:  $30.8 \pm 0.2$ , data not shown).

### Molecular diversity: partial SSU ribotypes

For all but three specimens we obtained partial SSU sequences (PCR failed for sc22624, *Stemonitis fusca*; sc22788, *Hemitrichia clavata*; and sc27079, *Cribraria*

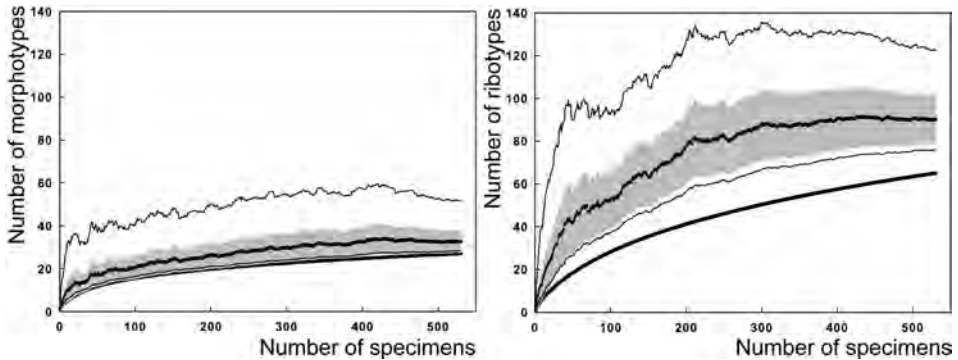


Fig. 1. Individual-based accumulation curves (solid smooth line, 530 records) for morphospecies (A) and ribotypes (B). The solid jagged line depicts the Chao2 estimator with SD (grey range) and 5/95% confidence intervals (thin jagged lines).

*rufa*). This resulted in 63 unique ribotypes (49 from bright-spored, 14 from dark-spored myxomycetes). Two specimens (sc22570, *Trichia scabra*; sc27055, *T. favoginea*) showed heterogeneous sequences that combined two ribotypes (Supplementary Database S1). The direct-spore PCR of some specimens possessing a unique ribotype or displaying heterogeneous sequences was repeated and the results confirmed either ribotype uniqueness or heterogeneity of these specimens. Fig. 1B shows the individual based accumulation curve for genotypic diversity (RAC), resulting in  $90.0 \pm 11.1$  and  $90.8 \pm 0.4$  ribotypes to expect for the Chao2 and hyperbolic curve fit estimators, respectively.

Within the morphospecies containing multiple ribotypes identified in this survey, average genetic distances range from 0.002 to 0.343 in 10 bright-spored morphospecies and 0.002 to 0.182 in 4 dark-spored species (see Table 1 for average genetic distance and length of alignment for each morphospecies). Among the 10 bright-spored morphospecies with multiple ribotypes, *Hemitrichia imperialis*, *Metatrichia vesparium*, and *Trichia favoginea* each comprised 2–4 ribotypes with variations caused by point mutations only, while the other 7 morphospecies, each including 2–11 ribotypes, had a higher intraspecific diversity made up by both point mutations and indels (Table 1; see alignment TreeBase: M34158). Three of the four dark-spored morphospecies with multiple ribotypes each comprised 2 ribotypes differing by both point mutations and indels; the remaining morphospecies *Stemonitopsis typhina* contained 3 ribotypes differing by point mutations only (Table 1; see alignment TreeBase: M34159).

Genotypic diversity seems to differ between bright-spored and dark-spored myxomycetes. In general, dark-spored specimens (22 records of 15 ribotypes with 10 morphological taxa) seem to be more diverse than bright-spored specimens (508 records of 50 ribotypes with 17 taxa; or 216 records of 39 ribotypes with 16 taxa, if the more intensely sampled *Trichia varia* is not included). Although RACs could be constructed for both bright- and dark-spored myxomycetes, the extremely different

extent of sampling would not allow a safe conclusion about overall genotypic diversity between the two groups.

For the exhaustively collected morphospecies *Trichia varia*, partial SSU ribotypes of 14 specimens collected in this survey were already published in Feng & Schnittler (2015). The 292 specimens from 92 logs accounted for 11 ribotypes. Two ribotypes dominated (TV1 with 184 and TV2 with 80 specimens), whereas the other nine ribotypes identified in this study were represented by only 28 specimens. Compared to the ribotypes (TV1 to TV12, Feng & Schnittler 2015) already found and assigned to three phylogenetic groups preliminary named group 1, 2a, and 2b (Fig. 3), four new ribotypes (TV13 to TV16) were identified in this survey and assigned preliminary to group 1 based on the phylogenies presented in Figs 3 and S1. The partial SSU alignment in this study has an extension at the beginning in comparison with the partial SSU alignment published in Feng & Schnittler (2015). Two of the ribotypes (TV10, TV11) identified in Feng & Schnittler (2015) showed an additional mutation (A vs C) within this extended region; we, therefore, further divided the original ribotype TV10 into two ribotypes, TV10 with variation A and TV17 with variation C. Similarly, the original ribotype TV11 was divided into TV11 with variation A and TV18 with variation C. This results in a total of 18 ribotypes known for the morphospecies *T. varia*. Co-occurrence of several ribotypes in one log is not uncommon: 63 logs yielded one, but 27 two, 1 three, and 1 four ribotypes.

Although a study from a single area will never reveal the whole extent of ribotype variation within a morphospecies, our data set allows us to safely to state that genotypic diversity varies significantly among morphospecies (Fig. 2). In contrast to the situation in *Trichia varia*, two bright-spored taxa (*Hemitrichia calyculata* and *H. clavata*) and one dark-spored taxon (*Fuligo septica*) displayed uniformly one ribotype shared by multiple specimens. One extreme case is the single ribotype shared by 52 specimens of *H. calyculata*. For morphospecies with multiple ribotypes, often one or two ribotypes are dominant, such as *Metatrichia vesparium* (ribotype MV1, 12 records; ribotype MV2, 1 record).

### **Phylogenetic relationships of partial SSU ribotypes**

The Bayesian and ML trees of 148 aligned partial SSU sequences of bright-spored myxomycetes, including 49 ribotypes identified in this survey, are shown in Figs 3 and S1, respectively. Using the conserved region at the end of the alignment that could be aligned with high confidence compared to other parts of the alignment, all multiple ribotypes for each of the ten molecularly diverse bright-spored morphospecies found in this survey cluster together. Of the 24 bright-spored specimens not collected in this survey but used for DNA sequencing for comparison purposes, 6 specimens share identical ribotypes with specimens recorded in this survey. These are sc22243 (AD4), sc22247 (MV1), sc22252 (MF1), and sc22253 (AD1) collected in Saxony; sc22536 (TD1) collected in the Bavarian Forest National Park; and sc25173 (TS1) collected in the National Park "Hainich-Dün". The other 18 specimens represented different ribotypes which clustered together with their counterparts from Genbank or coming from this survey.

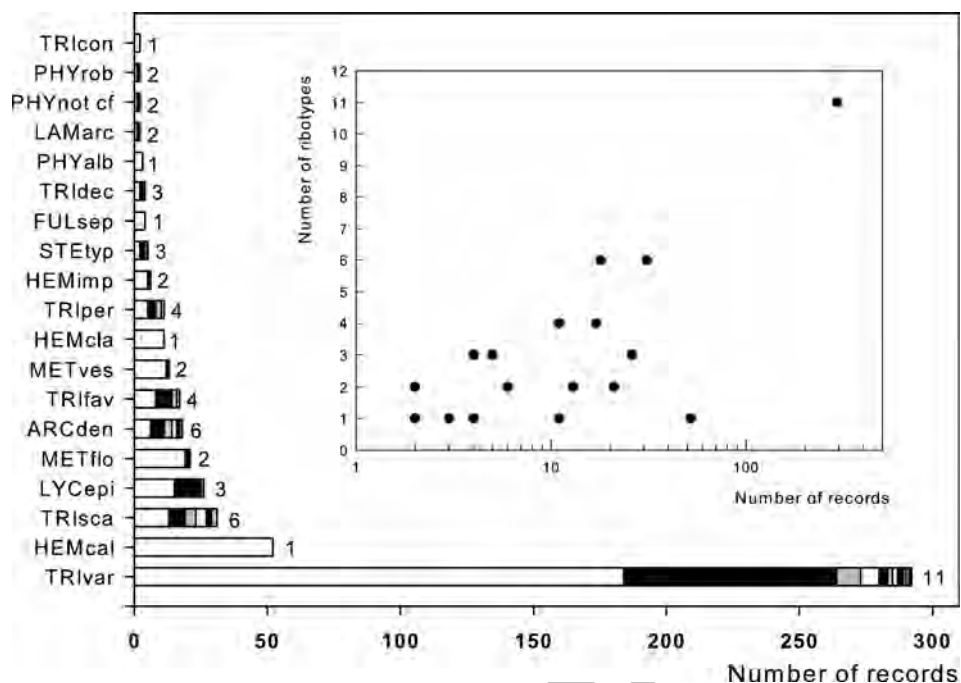


Fig. 2. Records (horizontal bars) and the respective proportions of different ribotypes (sections in different grayshades) for all species of myxomycetes (indicated by abbreviations of GENus and species names) represented by more than one record. For each bar, the number of ribotypes per taxon is indicated (*Trichia decipiens* var. *hemitrichioides* is treated as a taxon on its own). Inset: Relationship between the number of records (log scale) and the number of ribotypes found per taxon.

Rooted with the two closely related genera *Cribraria* and *Lindbladia*, the phylogenies split all other bright-spored myxomycetes into two groups consistent with the complete SSU phylogeny in Fiore-Donno et al. (2013). One group consisting of all four genera of the Reticulariaceae (*Alwisia*, *Lycogala*, *Reticularia*, *Tubifera*, compare Fiore-Donno et al. 2013, Leontyev et al. 2014a) appeared with high support in the Bayesian tree but low support in the ML tree, and another group mostly including taxa of the classical order Trichiales (13 genera: *Arcyodes*, *Arcyria*, *Calomyxa*, *Cornuvia*, *Dianema*, *Dictydiaethalium*, *Hemitrichia*, *Licea*, *Metatrichia*, *Oligonema*, *Perichaena*, *Prototrichia* and *Trichia*) appeared with moderate support in the Bayesian tree but received no support in the ML tree. Within these two groups, the phylogenetic relationships above the species level, however, are not resolved for most of the morphospecies, possibly due to the limited characters included in the analysis, except for the robust clade containing *Hemitrichia calyculata*, *H. clavata*, and *Trichia decipiens*, which is similar to the "New clade 2" in Fiore-Donno et al. (2013) except for *Hemitrichia abietina* located in a robust clade mostly with species of *Arcyria* in the Bayesian tree and of unresolved position in the ML tree.

Fig. 3. Bayesian majority-rule consensus tree for 148 partial SSU sequences of bright-spored myxomycetes. Bayesian posterior probabilities >0.5 are indicated. Labels written in bold indicate the 49 ribotypes found in this survey (listing taxon name, ribotype, location, and number of records sharing this ribotype).





Below the species level, both Bayesian and ML phylogenies indicated possible cryptic taxa within some morphospecies. One remarkable case is represented by the three ribotypes of *Lycogala epidendrum* (LE1 and LE2/3), which divide into two groups in both Bayesian and ML phylogenies. We found that these groups can be differentiated by the color and texture of the aethalia (group LE1 bears more pronounced and darker ornamentations on the surface than group LE2/LE3). Another case is *Metatrichia floriformis*, where the two specimens with the ribotype MF2 (sc22856 and sc27076) always show single scattered sporocarps which never share a common stalk as usually observed in this species (and in all of the 19 specimens sharing ribotype MF1). However, in all other cases the ribotypes of genetically diverse morphospecies could not be differentiated by morphological characters viewed by light microscopy. The morphospecies *Trichia varia* was highly supported as one monophyletic clade that contains two strongly supported subclades, which is consistent with the phylogenies in Feng & Schnittler (2015). Phylogenetic structure shows that the four new ribotypes (TV13–16) found in this survey belong to *Trichia varia* group 1 as named in Feng and Schnittler (2015). While all three groups (1, 2a, 2b) of *Trichia varia* were found in this survey, morphological characters have not yet been identified to differentiate among them (Feng & Schnittler 2015). In addition, four other morphospecies (*Arcyria denudata*, *Trichia decipiens*, excluding the variety *hemitrichoides*, *T. persimilis*, and *T. scabra*) also showed variations, including both point mutations and indels, and in parallel a high level of diversification in the phylogenies. Within the morphospecies *Trichia decipiens*, the ribotype of the morphologically clearly distinguished variety *hemitrichoides* (TD2) is as well clearly separated on the phylogenies from the other three ribotypes. However, the specimens belonging to the ribotypes TD1, 3 and 4 could not be told apart by sporocarp morphology. Similarly, the ribotypes of *Trichia scabra* cannot be distinguished morphologically, but the phylogenies show two subclades (TS1–2/TS3–6) with moderate to high support, consistent with the patterns of indel variation. For *Arcyria denudata* (AD1–4, 6/AD5), and *Trichia persimilis*/*T. cf. persimilis* (TP1–3/TP4), sporocarp morphology as seen by light microscopy does as well not reflect the major divisions within each morphospecies in the phylogenies. The same holds true for the three morphospecies (*Hemitrichia imperialis*, *Metatrichia vesparium*, and *Trichia favoginea*) with multiple ribotypes differing by point mutations only.

Due to the overall lower genetic diversity in partial SSU sequences for dark-spored myxomycetes, longer sections of the partial SSU alignment were aligned automatically. To avoid any arbitrary decisions, all of the amplicon except for its ends was chosen for analysis. As it was also the case for the bright-spored group, a ML phylogeny (Supplementary Fig. S2) rooted with the two genera *Barbeyella* and *Echinostelium* shows a high but not maximum level of coincidence between morphospecies determination and phylogenetic relationships of ribotypes at the species level. The positions of the 14 dark-spored ribotypes found in this survey on the phylogeny are generally consistent at genus level, including four morphospecies with multiple ribotypes. Multiple ribotypes of *Stemonitopsis typhina*, showing variation of point mutations only, clustered together in a robust clade. Two ribotypes of *Lamproderma arcyrioides*, which differed by both point mutations and indels, also grouped together within a robust clade but showed deep divergence. The four specimens determined as



*Physarum cf. notabile* and *Physarum robustum* showed an intermingled pattern, with one specimen from each morphospecies grouping together, reflecting the ambiguous determination results.

## Discussion

Myxomycetes have been determined according to fruit body morphology for nearly 250 years, but none of the currently used monographs includes any information on molecular characters (e.g., Nannenga-Bremekamp 1991, Neubert et al. 1993, 1995, 2000, Poulain et al. 2011). In contrast, barcoding is already well established for several groups of protists (see Pawlowski et al. 2012, Adl et al. 2014 and references listed herein). Model organisms like *Tetrahymena* (Chantangsi et al. 2007), or pathogenic groups like *Plasmodium* (Ogedengbe et al. 2011) are especially well studied, but barcoding is now gaining importance as well for free-living protists such as the ciliates (Gentekaki & Lynn 2009). To close the striking gap between the well-established body of data on fruit-body (morphological) diversity and the rather limited knowledge about molecular diversity of myxomycetes, a workable barcoding approach would seem to be extremely worthwhile.

This was the purpose of this study, being the first for myxomycetes that included in addition to the morphological species determination a full barcoding component: checking the suitability of the hitherto most widely applied marker, partial sequences of the small-subunit ribosomal RNA (SSU) gene, for barcoding. A good barcode marker should coincide with a morphological species concept as close as possible, showing a maximum of variation between but a minimum of variation within a morphospecies (Hebert et al. 2003, Schoch et al. 2012).

SSU sequences are very diverse in eukaryotic microorganisms, witnessing their long evolutionary history. In myxomycetes, they are organized in linear extrachromosomal units with one to many repeats (Torres-Machorro et al. 2010). The SSU genes will be homogenized within plasmodial development (Ferris et al. 1983), therefore all copies of the gene usually display an uniform sequence (see discussion in Feng & Schnittler 2015). SSU genes were used to construct the first phylogenies for myxomycetes (Fiore-Donno et al. 2012, 2013). To avoid the sometimes very long intron insertion sites (see e.g., Nandipati et al. 2012), the first part of the gene that is free of introns was chosen as a barcoding marker. This section of 500–600 bases in length (Table 1) shows alternating conserved and variable sections (see Fig. 4 in Fiore-Donno et al. 2012), which helps to align sequences. A first study using partial SSU sequences in a survey of nivicolous myxomycetes (Novozhilov et al. 2013b) showed that these sequences could differentiate between species, but often a morphospecies was represented by more than one ribotype. In this study, we used these sequences throughout a diversity-directed survey, to compare directly morphospecies and ribotype diversity.

However, not all published sequences appear to originate truly from myxomycetes, and in not all cases does the species seem to have been determined correctly. Especially problematic is the situation in dark-spored myxomycetes, the first group becoming accessible for molecular analyses. For this group, 890 sequences containing some

part(s) of the SSU were downloaded from GenBank. Of these, 331 sequences with missing data at the first part of SSU and 7 sequences not representing myxomycetes were excluded. The remaining 552 sequences included several identical ones (which were not necessarily assigned to the same taxon), or vouchers not determined to the species level, or some from environmental samples (no determination possible), or unpublished sequences, leaving 270 unique and species-level determined sequences, which formed the backbone of the tree presented in Supplementary Fig. S2. However, we were unable to check the correct identification for these sequences and can rely on the published names only. Misidentification and/or cross-amplification of other myxomycete sequences is likely to be responsible for the appearance of a genus in multiple clusters (for example *Fuligo* spp.). For bright-spored myxomycetes primers for SSU sequences were developed later; and the situation is somewhat better regarding consistency between taxonomic identification and SSU sequences. Of the 156 sequences downloaded from GenBank containing some part(s) of the SSU, 6 with missing data at the first part of SSU, 15 not representing myxomycetes, 29 sequences from environmental samples (no determinations available), and 31 unpublished or vouchers not determined to the species level were excluded.

It should be noted, that partial SSU sequences seem to be a valuable tool for myxomycete barcoding, but one cannot expect that phylogenies constructed from these rather short sequences will properly reflect relationships between higher taxonomic ranks, or that these markers alone allow to trace back speciation events.

### **Relationships between morphospecies and clades in the phylogenetic trees**

The number of described myxomycete species has reached approximately 950 (Lado 2015). Currently, myxomycete taxonomy is still based entirely on the morphospecies concept, using light and recently scanning electron microscopy to examine characters of sporocarps and spores (see Neubert et al. 1993, 1995, 2000). This morphospecies concept has been applied as well for the recently constructed molecular phylogenies (Fiore-Donno et al. 2010, 2012, 2013). The species described in the classical monograph of Lister (1894, 1911, 1925) have been continuously revised during the past hundred years, and the number of taxa described as new to science has steadily increased (Schnittler & Mitchell 2000). However, only recently has the description of new and the delimitation of established taxa been augmented by molecular evidence from gene markers and phylogenetic analyses (Erastova et al. 2013, Leontyev et al. 2014a, 2014b, 2015, Novozhilov et al. 2013a, 2014).

This study focused on the diversity of myxomycetes collected in a two-month period within a deciduous forest comprising ca four square kilometers. The relatively uniform mesoclimate in the small collecting area and the rather short collecting period, covering the late-autumn aspect of myxomycetes only, should limit the variation of morphological characters and hopefully cause a maximum level of consistency in them. This helps to achieve a safe morphological determination to match morpho- and ribotypes. The chosen substrate (deciduous, mostly white-rotten wood) and the time of the year (late autumn to early winter) clearly favored bright-spored myxomycetes, which comprise 95.8% of all records. Therefore, this discussion focuses on the bright-spored species, where we have enough material to visualize within-species variation. Looking at

partial SSU sequences, the most promising barcode marker in myxomycetes thus far, we showed for this survey that the morphospecies concept is generally consistent with the phylogenetic clades of ribotypes, since most morphospecies with multiple ribotypes clustered in the same clade. Ribotypes help to differentiate species, as shown by the example of the morphologically differentiable variety *Trichia decipiens* var. *hemitrichoides*: a clearly deviating ribotype for this variety, supports the separation of this variety (and perhaps elevating it to species level, as it was treated for the counts herein) from the typical form of this species. For some morphospecies that are taxonomically difficult to determine, such as *Physarum* cf. *notabile* and *Ph. robustum*, the conflict between morphological determination and ribotype clustering pattern may reflect real difficulties to find discernible characters for morphospecies determination. In such cases, molecular markers may be of crucial importance to achieve a refined and consistent delimitation of taxa.

### Cryptic taxa in myxomycetes

Below the taxonomic level of morphospecies, 14 of the 27 morphospecies identified in this survey display multiple ribotypes with various levels of average genetic distance and patterns of indels (Table 1). However, in a only a few cases were consistent morphological characters accessible by light microscopy found that could be linked to ribotype variation. An example is the complex species *Lycogala epidendrum*, here represented by three ribotypes. Already, the late Nannenga-Bremekamp mentioned this high level of variety in her monograph (1991) and worked on a morphological concept for the delimitation of taxa within *Lycogala*, which was unfortunately never published. *Lycogala epidendrum* is also one of the two morphospecies that possess the highest level of genetic distance (0.266); the other morphospecies is *Trichia decipiens* (0.297; or 0.362 if the most distant ribotype of var. *hemitrichoides* is included). Beside these two morphospecies, six others (*Arcyria denudata*, *Lamproderma arcyrioides*, *Metatrichia floriformis*, *Trichia persimilis*/*T. cf. persimilis*, *T. varia* and *T. scabra*), together with the two morphologically confused *Physarum* species (*Physarum* cf. *notabile* and *Ph. robustum*, after their determination being corrected based on partial SSU ribotypes), possess a higher level of average genetic distance ranging from 0.014 to 0.158. Among them, only the two ribotypes of *M. floriformis* could be linked to a morphological trait (MF1 with fascicled sporocarps; MF2 with scattered solitary sporocarps). All of these ten morphospecies mentioned above show ribotypic variation not only by point mutations, but as well by indels. In contrast, the remaining four morphospecies with the lowest levels of average genetic distance (ranging from 0.002 to 0.004) contain only point mutations.

Especially intensely investigated was the common morphospecies *Trichia varia*, where the name chosen by Persoon actually indicates a certain degree of morphological variation. For this taxon, three cryptic biospecies (most likely reproducing sexually but reproductively isolated), represented by three phylogroups named 1, 2a, and 2b, were identified based on partial sequences of three markers (SSU, and genes coding for the elongation factor 1 alpha and mitochondrial cytochrome oxidase subunit 1; Feng & Schnittler 2015). The difference between the deeply diverging group 1 and groups 2a/2b is reflected in partial SSU sequences, showing a 1-bp indel in addition to point

mutations, whereas the more closely related groups 2a and 2b differ only by point mutations. Similarly, a study of the dark-spored genus *Meriderma* revealed several putative biospecies (unpublished data); and indels in partial SSU sequenced can be used to tell them apart, whereas within a biospecies most ribotypes differ by point mutations only. More studies are needed to show if the presence of indels in partial SSU sequences is a useful preliminary indication for the existence of separate biospecies within a morphologically circumscribed taxon (even if reproductive isolation of these biospecies remains to be demonstrated). In diversity studies, the presence of indels in partial SSU sequences may indicate the existence of multiple cryptic taxa within a morphospecies, but this marker alone is insufficient to demonstrate reproductive isolation between those cryptic taxa, as shown by a study including several markers for the morphospecies *Trichia varia* (Feng & Schnittler 2015). If the criterion of the presence of indels is applied to the 14 morphospecies possessing multiple ribotypes found in this survey, ten of them might include multiple cryptic taxa, but four seem to represent a single biological species. Therefore, the statement of Adl et al. (2014) that determination at the microscopic (morphological) level hugely under-describes the true diversity in protists (see as well Bass et al. 2007 and Adl et al. 2007) applies for myxomycetes as well.

### **Primer availability**

The identification of conserved regions within marker genes and the design of universal or broadly applicable PCR primers are crucial components of DNA barcoding. Primers targeting the nuclear small-subunit ribosomal RNA gene (SSU) have been systematically designed for eukaryotic organisms (Hugerth et al. 2014). Adl et al. (2014) evaluated the published primers targeting the SSU of soil protists, including myxomycetes. For partial SSU sequences located upstream of the group I intron insertion position 516 (numbered in accordance with the *Escherichia coli* 16S rRNA gene), the forward primer S1 (Fiore-Donno et al. 2008, SSU\_PF6 in Adl et al. 2014) is a nearly universal forward primer for both bright-spored and dark-spored myxomycetes, but recognizes as well numerous other protists, as shown in Adl et al. 2014. Reverse primers for partial SSU sequences are not as universal as this forward primer and may include several candidates from published primers (Fiore-Donno et al. 2008, 2010, 2012, 2013).

The primers used in this study for bright-spored myxomycetes (NUSSUF3, NUSSUR4) were initially designed for *Trichia varia* (Feng & Schnittler 2015). A comparison with the bright-spored SSU alignment of Fiore-Donno et al. (2013) shows that this primer pair would perform well for most but not all taxa of bright-spored myxomycetes (e.g., excluding *Cribraria*). For dark-spored myxomycetes, the primers used in this study (NUSSUF20 and NUSSUR13) were specifically designed for universal usage based on the SSU alignment representing dark-spored taxa (Fiore-Donno et al. 2012). All five primers used in this study lack degenerate nucleotides. For sole purposes of barcoding degenerate primers may be designed to achieve a maximum taxonomic coverage within myxomycetes. For example, the primers NUSSUR4 (bright) and NUSSUR13 (dark) are nearly identical in sequence and cover the same region, but have one different position (C vs T). A degenerate primer with Y(C/T) would work

for most bright-spored and virtually all dark-spored myxomycetes. However, with near-universal primers the risk to cross-amplify contaminants (non-target myxomycete species or other organisms) increases with the proportion of contaminant DNA and the number of non-matching positions in the primer. Primers with several degenerate sites (especially near the 3'-end) are more likely to match with contaminant DNA, increasing the risk of contaminant amplification.

## Conclusions

Barcoding is currently used for many groups of organisms, and this study demonstrated the feasibility of such an approach for myxomycetes. The phylogeny constructed for the bright-spored species, which are common in the investigated late autumn aspect of lignicolous myxomycetes, showed that a grouping according to partial SSU sequences (which represents essentially a phylogenetic species concept) is usually not in conflict with the traditional morphospecies concept (see Figs 3 and S1). However, only exceptionally (*Hemitrichia calyculata* and *H. clavata* can serve as examples) a morphospecies is genetically uniform, at least for this survey and the employed marker. More often, one morphospecies is represented by several ribotypes, and cryptic speciation, as shown in detail for the case of *Trichia varia* by Feng & Schnittler (2015), might be the rule rather than the exception. As such, a revision of myxomycetes with molecular markers can be expected to increase the number of known taxa by a factor we estimate as between two and ten. More studies, combining molecular and morphological approaches, are needed to derive exact estimates for the extent of cryptic speciation for myxomycetes.

## Acknowledgements

This research was supported by the Deutsche Forschungsgemeinschaft (DFG) to MS (SCHN 1080/2-1). The authors owe thanks for technical support to Anja Klahr, Greifswald.

## References

- ADL, S.M., A. HABURA & Y. EGLIT 2014: Amplification primers of SSU rDNA for soil protists. – *Soil. Biol. Biochem.* **69**: 328–342.
- ADL, S.M., B.S. LEANDER, A.G. SIMPSON, J.M. ARCHIBALD, O.R. ANDERSON et al. 2007: Diversity, nomenclature and taxonomy of protists. – *Syst. Biol.* **56**: 684–689.
- AGUILAR, M., A.M. FIORE-DONNO, C. LADO & T. CAVALIER-SMITH 2013: Using environmental niche models to test the ‘everything is everywhere’ hypothesis for *Badhamia*. – *ISME J.* **8**: 737–745.
- BASS, D., T.A. RICHARDS, L. MATTHAI, V. MARSH & T. CAVALIER-SMITH 2007: DNA evidence for global dispersal and probable endemism of protozoa. – *BMC Evol. Biol.* **7**: 162.
- CHANTANGSI, C., D.H. LYNN, M.T. BRANDL, J.C. COLE, N. HETRICK et al. 2007: Barcoding ciliates: a comprehensive study of 75 isolates of the genus *Tetrahymena*. – *Int. J. Syst. Evol. Microbiol.* **57**: 2412–2425.

- CHAO, A., R.L. CHAZDON, R.K. COLWELL & T.J. SHEN 2006: Abundance-based similarity indices and their estimation when there are unseen species in samples. – *Biometrics* **62**: 361–371.
- CLARK, J. & E.F. HASKINS 2014: Sporophore morphology and development in the myxomycetes: a review. – *Mycosphere* **5**: 153–170.
- COLWELL, R.K. 2009: EstimateS: Statistical estimation of species richness and shared species from samples. Version 8.2. User's Guide and application. <http://purl.oclc.org/estimates>. Accessed 12 April 2012.
- COLWELL, R.K., A. CHAO, N.J. GOTELLI, S.-Y. LIN, C.X. MAO et al. 2012: Models and estimators linking individual-based and sample-based rarefaction, extrapolation and comparison of assemblages. – *J. Plant. Ecol.* **5**: 3–21.
- DE BARY, A. 1859: Die Mycetozoen. Ein Beitrag zur Kenntnis der niedersten Thiere. – *Zeitschr. Wiss. Zool.* **10**: 88–175.
- EDGAR, R.C. 2004: MUSCLE: multiple sequence alignment with high accuracy and high throughput. – *Nucl. Acids Res.* **32**: 1792–1797.
- ELIASSON, U. 1977: Recent advances in the taxonomy of Myxomycetes. – *Bot. Not.* **130**: 483–492.
- ELIASSON, U. 2015: Review and remarks on current generic delimitations in the myxomycetes, with special emphasis on *Licea*, *Listerella* and *Perichaena*. – *Nova Hedwigia*, online first (doi: 10.1127/nova\_hedwigia/2015/0283).
- ERASTOVA, D.A., M.V. OKUN, Y.K. NOVOZHILOV & M. SCHNITTLER 2013: Phylogenetic position of the enigmatic myxomycete genus *Kelleromyxa* revealed by SSU rDNA sequences. – *Mycol. Progress* **12**: 599–608.
- FENG, Y. & M. SCHNITTLER 2015: Sex or no sex? Independent marker genes and group I introns reveal the existence of three sexual but reproductively isolated biospecies in *Trichia varia* (Myxomycetes). – *Org. Divers. Evol.* **15**: 631–650.
- FERRIS, P.J., V.M. VOGT & C.L. TRUITT (1983): Inheritance of extrachromosomal rDNA in *Physarum polycephalum*. – *Mol. Cell. Biol.* **3**: 635–642.
- FIORE-DONNO, A.M., C.J. BERNEY, J. PAWLOWSKI & S.L. BALDAUF 2005: Higher-order phylogeny of plasmodial slime molds (Myxogastria) based on elongation factor 1-A and small subunit rRNA gene sequences. – *J. Euk. Microbiol.* **52**: 201–210.
- FIORE-DONNO, A.M., M. MEYER, S.L. BALDAUF & J. PAWLOWSKI 2008: Evolution of dark-spored Myxomycetes (slime-molds): Molecules versus morphology. – *Mol. Phylogenet. Evol.* **46**: 878–889.
- FIORE-DONNO, A.M., E.F. HASKINS, J. PAWLOWSKI & T. CAVALIER-SMITH 2009: *Semimorula liquescens* is a modified echinostelid myxomycete (Mycetozoa). – *Mycologia* **101**: 773–776.
- FIORE-DONNO, A.M., S.I. NIKOLAEV, M. NELSON, J. PAWLOWSKI, T. CAVALIER-SMITH et al. 2010: Deep phylogeny and evolution of slime moulds (Mycetozoa). – *Protist* **161**: 55–70.
- FIORE-DONNO, A.M., Y.K. NOVOZHILOV, M. MEYER & M. SCHNITTLER 2011: Genetic structure of two protist species (Myxogastria, Amoebozoa) suggests asexual reproduction in sexual amoebae. – *PLoS ONE* **6**: e22872.
- FIORE-DONNO, A.M., A. KAMONO, M. MEYER, M. SCHNITTLER, M. FUKUI et al. 2012: 18S rDNA phylogeny of *Lamproderma* and allied genera (Stemonitales, Myxomycetes, Amoebozoa). – *PLoS ONE* **7**: e35359.
- FIORE-DONNO, A.M., F. CLISSMANN, M. MEYER, M. SCHNITTLER & T. CAVALIER-SMITH 2013: Two-gene phylogeny of bright-spored Myxomycetes (slime moulds, superorder Lucisporidia). – *PLoS ONE* **8**: e62586.

- FROMMLET, J.C. & M.D. IGLESIAS-RODRÍGUEZ 2008: Microsatellite genotyping of single cells of the dinoflagellate species *Lingulodinium polyedrum* (Dinophyceae): A novel approach for marine microbial population genetic studies. – *J. Phycol.* **44**: 1116–1125.
- GENTEKAKI, E. & D.H. LYNN 2009: High-level genetic diversity but no population structure inferred from nuclear and mitochondrial markers of the peritrichous ciliate *Carchesium polypinum* in the Grand River basin (North America). – *Appl. Environ. Microbiol.* **75**: 3187–3195.
- GUINDON, S. & O. GASCUEL 2003: A simple, fast, and accurate algorithm to estimate large phylogenies by maximum likelihood. – *Syst. Biol.* **52**: 696–704.
- HAUGEN, P., O.G. WIKMARK, A. VADER, D.H. COUCHERON, E. SJØTTEM et al. 2005: The recent transfer of a homing endonuclease gene. – *Nucl. Acids Res.* **33**: 2734–2741.
- HEBERT, P.D., A. CYWINSKA, S.L. BALL & J.R. DEWAARD 2003: Biological identifications through DNA barcodes. – *Proc. Biol. Sci.* **270**: 313–321.
- HOPPE, T. & M. SCHNITTLER 2015: Characterization of myxomycetes in two different soils by TRFLP-analysis of partial 18S rRNA gene sequences. – *Mycosphere* **6**: 216–227.
- HORTON, T.L. & L.F. LANDWEBER 2000: Evolution of four types of RNA editing in myxomycetes. – *RNA* **6**: 1339–1346.
- HUGERTH, L.W., E.E. MULLER, Y.O. HU, L.A. LEBRUN, H. ROUME et al. 2014: Systematic design of 18S rRNA gene primers for determining eukaryotic diversity in microbial consortia. – *PLoS ONE* **9**: e95567.
- JOHANSEN, T., S. JOHANSEN & F.B. HAUGLI 1988: Nucleotide sequence of the *Physarum polycephalum* small subunit ribosomal RNA as inferred from the gene sequence: secondary structure and evolutionary implications. – *Curr. Genet.* **14**: 265–273.
- KAMONO, A., M. MEYER, T. CAVALIER-SMITH, M. FUKUI & A.M. FIORE-DONNO 2013: Exploring slime mould diversity in high-altitude forests and grasslands by environmental RNA analysis. – *FEMS Microbiol. Ecol.* **84**: 98–109.
- KATOH, K. & D.M. STANDLEY 2013: MAFFT multiple sequence alignment software version 7: improvements in performance and usability. – *Mol. Biol. Evol.* **30**: 772–780.
- LADO, C. 2015: An on line nomenclatural information system of Eumycetozoa. 2005–2015. <http://www.nomen.eumycetozoa.com>. Accessed 10 July 2015.
- LEONTYEV, D.V., M. SCHNITTLER, G. MORENO, S.L. STEPHENSON, D.W. MITCHELL et al. 2014a: The genus *Alwisia* (Myxomycetes) revalidated, with two species new to science. – *Mycologia* **106**: 936–948.
- LEONTYEV, D.V., S.L. STEPHENSON & M. SCHNITTLER 2014b: A new species of *Alwisia* (Myxomycetes) from New South Wales and Tasmania. – *Mycologia* **106**: 1212–1219.
- LEONTYEV, D.V., S.L. STEPHENSON & M. SCHNITTLER 2015. A critical revision of the *Tubifera ferruginosa* complex. – *Mycologia* **107**: 959–985.
- LI, W. & A. GODZIK 2006: Cd-hit: a fast program for clustering and comparing large sets of protein or nucleotide sequences. – *Bioinformatics* **22**: 1658–1659.
- LINNÉ, C. 1753: *Species Plantarum*. Uppsala.
- LISTER, A. 1894: *A monograph of the Mycetozoa*. London.
- LISTER, A. 1911: *A monograph of the Mycetozoa*, ed. 2, revised by G. Lister. London.
- LISTER, A. 1925: *A monograph of the Mycetozoa*, ed. 3, revised by G. Lister. London.
- LUNDBLAD, E.W., C. EINVIK, S. RØNNING, K. HAUGLI & S. JOHANSEN 2004: Twelve group I introns in the same pre-rRNA transcript of the myxomycete *Fuligo septica*: RNA processing and evolution. – *Mol. Biol. Evol.* **21**: 1283–1293.

- MAGURRAN, A.E. 2004: Measuring biological diversity. – Blackwell Publishing, Malden, Massachusetts.
- MARTIN, G.W. & C.J. ALEXOPOULOS 1969: The Myxomycetes. – Iowa Univ. Press, Iowa City.
- MILNE, I., D. LINDNER, M. BAYER, D. HUSMEIER, G. MCGUIRE et al. 2009: TOPALi v2: a rich graphical interface for evolutionary analyses of multiple alignments on HPC clusters and multi-core desktops. – *Bioinformatics* **25**: 126–127.
- NANDIPATI, S.C., K. HAUGLI, D.H. COUCHERON, E.F. HASKINS & S.D. JOHANSEN 2012: Polyphyletic origin of the genus *Physarum* (Physariales, Myxomycetes) revealed by nuclear rDNA mini-chromosome analysis and group I intron synapomorphy. – *BMC Evol. Biol.* **12**: 166.
- NANNENGA-BREMEKAMP, N.B. 1991: A guide to temperate Myxomycetes (Feest A. & E. Burgraff: De Nederlandse Myxomyceten, Engl. transl.). – Biopress Ltd., Bristol.
- NEUBERT, H., W. NOWOTNY & K. BAUMANN 1993: Die Myxomyceten Deutschlands und des angrenzenden Alpenraumes unter besonderer Berücksichtigung Österreichs. 1 Ceratiomyxales, Echinosteliales, Liceales, Trichiales. – Baumann Verl., Gomaringen.
- NEUBERT, H., W. NOWOTNY & K. BAUMANN 1995: Die Myxomyceten Deutschlands und des angrenzenden Alpenraumes unter besonderer Berücksichtigung Österreichs. 2 Physariales. – Baumann Verl., Gomaringen.
- NEUBERT, H., W. NOWOTNY & K. BAUMANN 2000: Die Myxomyceten Deutschlands und des angrenzenden Alpenraumes unter besonderer Berücksichtigung Österreichs. 3 Stemonitales. – Baumann Verl., Gomaringen.
- NOVOZHILOV, Y.K., M.V. OKUN, D.A. ERASTOVA, O.N. SHCHEPIN, I.V. ZEMLYANSKAYA et al. 2013a: Description, culture and phylogenetic position of a new xerotolerant species of *Physarum*. – *Mycologia* **105**: 1535–1546.
- NOVOZHILOV, Y.K., M. SCHNITTLER, D.A. ERASTOVA, M.V. OKUN, O.N. SCHEPIN et al. 2013b: Diversity of nivicolous myxomycetes of the Teberda State Biosphere Reserve (Northwestern Caucasus, Russia). – *Fungal Divers.* **59**: 109–130.
- NOVOZHILOV, Y.K., D.W. MITCHELL, M.V. OKUN & O.N. SHCHEPIN 2014: New species of *Diderma* from Vietnam. – *Mycosphere* **5**: 554–564.
- OGEDENGBE, J.D., R.H. HANNER & J.R. BARTA 2011: DNA barcoding identifies *Eimeria* species and contributes to the phylogenetics of coccidian parasites (Eimeriorina, Apicomplexa, Alveolata). – *Int. J. Parasitol.* **41**: 843–850.
- PAWLOWSKI, J., S. AUDIC, S.M. ADL, D. BASS, L. BELBAHRI et al. 2012: CBOL protist working group: barcoding eukaryotic richness beyond the Animal, Plant, and Fungal Kingdoms. – *PLoS Biol* **10**: e1001419.
- PERSOON, C.H. 1790–1793: Illustrations of the fungi. – Paris.
- POULAIN, M., M. MEYER & J. BOZONNET 2011: Les myxomycetes. – Féd. Mycol. Bot. Dauphiné-Savoie, Delémont.
- ROSS, I.K. 1973: The Stemonitomycetidae, a new subclass of Myxomycetes. – *Mycologia* **65**: 477–485.
- RONQUIST, F. & J.P. HUELSENBECK 2003: MrBayes 3: Bayesian phylogenetic inference under mixed models. – *Bioinformatics* **19**: 1572–1574.
- SCHNITTLER, M. & D.W. MITCHELL 2000: Species diversity in Myxomycetes based on the morphological species concept – a critical examination. – *Stapfia* **73**: 55–62.
- SCHOCH, C.L., K.A. SEIFERT, S. HUHNDORF, V. ROBERT, J.L. SPOUGE et al.; Fungal Barcoding Consortium 2012: Nuclear ribosomal internal transcribed spacer (ITS) region as a universal DNA barcode marker for Fungi. – *Proc. Natl. Acad. Sci. USA* **109**: 6241–6246.



- SHADWICK, L.L., F.W. SPIEGEL, J.D. SHADWICK, M.W. BROWN & J.D. SILBERMAN 2009: *Eumycetozoa = Amoebozoa?*: SSUrDNA phylogeny of protosteloid slime molds and its significance for the amoebozoan supergroup. – PLoS ONE **4**: e6754.
- SHCHEPIN, O., Y.K. NOVOZHILOV & M. SCHNITTLER 2014: Nivicolous myxomycetes in agar culture: some results and open problems. – Protistology **8**: 53–61.
- SPANGENBERG, A., K. BILLWITZ, I. HERZBERG & L. LANDGRAF 2003: Das Naturschutzgebiet Eldena. – Greifswalder Geographische Arbeiten **30**: 7–23.
- STEPHENSON, S.L., I. KALYANASUNDARAM & T.N. LAKHANPAL 1993: A comparative biogeographical study of myxomycetes in the mid-Appalachians of eastern North America and two regions of India. – J. Biogeogr. **20**: 645–657.
- STEPHENSON, S.L., M. SCHNITTLER & Y.K. NOVOZHILOV 2008: Myxomycete diversity and distribution from the fossil record to the present. – Biodivers. Conserv. **17**: 285–301.
- TAMURA, K., M. NEI & S. KUMAR 2004: Prospects for inferring very large phylogenies by using the neighbor-joining method. – Proc. Natl. Acad. Sci. USA **101**: 11030–11035.
- TAMURA, K., D. PETERSON, N. PETERSON, G. STECHER, M. NEI et al. 2011: MEGA5: molecular evolutionary genetics analysis using maximum likelihood, evolutionary distance, and maximum parsimony methods. – Mol. Biol. Evol. **28**: 2731–2739.
- TORRES-MACHORRO, A.L., R. HERNÁNDEZ, A.M. CEVALLOS & I. LÓPEZ-VILLASEÑOR 2010: Ribosomal RNA genes in eukaryotic microorganisms: witnesses of phylogeny? – FEMS Microbiol. Rev. **34**: 59–86.
- UNTERSEHER, M., M. SCHNITTLER, C. DORMANN & A. SICKERT 2008: Application of species richness estimators for the assessment of fungal diversity. – FEMS Microbiol. Lett. **282**: 205–213.
- WIKMARK, O.G., P. HAUGEN, E.W. LUNDBLAD, K. HAUGLI & S.D. JOHANSEN 2007: The molecular evolution and structural organization of group I introns at position 1389 in nuclear small subunit rDNA of myxomycetes. – J. Euk. Microbiol. **54**: 49–56.

Manuscript submitted September 7, 2016; accepted October 30, 2015.



## 4. Declaration



Hiermit erkläre ich, dass diese Arbeit bisher von mir weder an der Mathematisch-Naturwissenschaftlichen Fakultät der Ernst-Moritz-Arndt-Universität Greifswald noch einer anderen wissenschaftlichen Einrichtung zum Zwecke der Promotion eingereicht wurde.

Ferner erkläre ich, dass ich diese Arbeit selbständig verfasst und keine anderen als die darin angegebenen Hilfsmittel und Hilfen benutzt und keine Textabschnitte eines Dritten ohne Kennzeichnung übernommen habe.

Greifswald

Date

06.11.2015

Yun Feng

## Declaration about the contribution of each author and storage of primary data

This thesis work contains four publications and manuscripts:

Feng, Y., Schnittler, M. 2015: Sex or no sex? Independent marker genes and group I introns reveal the existence of three sexual but reproductively isolated biospecies in *Trichia varia* (Myxomycetes).

*Organisms Diversity and Evolution*, online first (doi: 10.1007/s13127-015-0230-x).

YF designed the study. The sequences of homing endonuclease genes in the introns of the nuclear small-subunit ribosomal RNA genes were as well discovered and evaluated by YF. All laboratory work and the evaluation of sequences and intron data, including phylogenetic analyses, were carried out by the first author (YF). Most of the specimens used for the study were obtained by loan; MS took part in organizing these specimen loans. The manuscript was written jointly by YF and MS.

Feng, Y., Klahr, A., Janik, P., Ronikier, A., Hoppe, T., Novozhilov, Y.K., Schnittler, M. 2015: What an intron may tell: several sexual biospecies coexist in *Meriderma* spp. (Myxomycetes). *Protist*, reviewed, resubmission needed.

MS designed the study. The first two authors (YF and AK) did the laboratory work, including the cloning of sequences. MS compiled the primary sequence alignment. This alignment was corrected by YF. All phylogenetic analyses and the subsequent data evaluation was carried out by YF. Three authors (PJ, AR, YKN) contributed determined specimens for the study. MS contributed the population genetic model. TH worked on the thin sections and fluorescence staining to count the number of nuclei per spore. The manuscript was written jointly by YF and MS.

Schnittler, M., Feng, Y., Heinrich, E., Janik, P., Ronikier, A., Klahr, A., Erastova, D.A., Novozhilov, Y.K., Meyer, M. 2015: Biological or morphological species? A revision of *Meriderma* spp. (Myxomycetes). (*manuscript*).

MS designed the study, invented a method for the analysis of SEM micrographs using the image analysis language ImageJ, and carried out multivariate analyses. YF carried out the SSU sequences of specimens, assisted by AK; further sequences were provided by DAE and YKN. All sequence alignments and phylogenetic analyses were contributed by YF. In the frame of a diploma thesis, EH examined the specimens and compiled a set of morphological characters used for multivariate analyses. JP, AR, and YKN provided SEM micrographs of spores prepared by critical point drying. MM provided the initial taxonomic concept for a revision of the genus *Meriderma* and designed the formal taxonomic descriptions. The manuscript was written by MS and corrected by all remaining authors.

Feng, Y., Schnittler, M. 2015: Molecular or morphological species? Myxomycete diversity in a deciduous forest in northeastern Germany. *Nova Hedwigia*, accepted.

YF designed the study and carried out all field work. The novel method for high throughput PCR of myxomycete specimens from spores was established for myxomycetes by YF, who compiled as well alignments and carried out the phylogenetic analyses. Specimens were morphologically determined by YF; these determinations were cross-checked by MS. Statistical analyses were done by MS and YF. The manuscript was written jointly by YF and MS.

The primary data for this thesis include collections of specimens and sequence data of several marker genes, namely the nuclear small-subunit ribosomal RNA gene (SSU, partial and complete sequences); the elongation factor 1 alpha gene (EF1A, partial sequences), and the cytochrome oxidase subunit 1 gene (COI, partial sequences). All specimens were accessed to the collection of MS which will be deposited at the Botanical State Collection Munich (M), the largest public collection for myxomycetes in Germany. Via the digitalization of locality data, this information will be uploaded to the portal of the Global Biodiversity Information Facility (GBIF). All sequence data were submitted to GenBank (NCBI); alignments used for phylogenetic analyses are provided with the publications as supplementary files or retrieved from the public database TreeBASE.

Seen by the thesis supervisor (M. Schnittler):

## Updated status of publications

Feng, Y., Schnittler, M. 2015: Sex or no sex? Independent marker genes and group I introns reveal the existence of three sexual but reproductively isolated biospecies in *Trichia varia* (Myxomycetes). *Organisms Diversity and Evolution* 15:631–650.

Feng, Y., Klahr, A., Janik, P., Ronikier, A., Hoppe, T., Novozhilov, Y.K., Schnittler, M. 2016: What an intron may tell: several sexual biospecies coexist in *Meriderma* spp. (Myxomycetes). *Protist*, online first (doi: 10.1016/j.protis.2016.03.003).

Feng, Y., Schnittler, M. 2016: Molecular or morphological species? Myxomycete diversity in a deciduous forest in northeastern Germany. *Nova Hedwigia*, online first (doi: 10.1127/nova\_hedwigia/2016/0326).

Greifswald

Date

09.05.2016

Yun Feng





## 5. Curriculum Vitae



## Curriculum Vitae

### Personal Information

Name: Feng, Yun

Address: Bahnhofstraße 2/3, D-17489, Greifswald, Germany

E-mail: yun.feng@uni-greifswald.de

Telephone: +49-3834-864125

Gender: Female; Date and place of birth: June 11, 1970, Beijing, P.R. China

### Education

2011 – Present, Ph.D. student at the Institute of Botany and Landscape Ecology, Ernst-Moritz-Arndt University of Greifswald, Germany. Research focused on the genetic diversity and reproductive systems of myxomycetes.

2000 – 2003, M.S. at the Department of Biology, Duke University, USA. Research focused on the phylogeny and historical biogeography of the genus *Platanus*.

1992 – 1995, M.S. at the Department of Plant Molecular and Developmental Biology, College of Life Sciences, Peking University, P.R. China. Research focused on the reproductive systems of the endangered species *Cimicifuga nanchuanensis*, and *in vitro* organogenesis of *Lilium davidii*.

1988 – 1992, B.S. in Botany, Department of Biology, Peking University, P.R. China. Degree thesis focused on the expression of the embryo-specific gene at the cellular and tissue level in the somatic embryogenesis of transgenic carrot. Be awarded the university scholarship of study (1989 – 1990) and the third-class university scholarship for outstanding students (1990 – 1991).

1982 – 1988, attending Beijing No. 80 Middle School, P.R. China. Be awarded the second-class prize of the first session of the Beijing language knowledge competition (1986).

### Professional Experience

2011 – Present, Institute of Botany and Landscape Ecology, Ernst-Moritz-Arndt University of Greifswald, Germany. Assistant Researcher in the project “Reproductive systems of myxomycetes” funded by the Deutsche Forschungsgemeinschaft (DFG project SCHN 1080/2-1).

2005 – 2011, Assistant Researcher, TEDA School of Biological Sciences and Biotechnology, Nankai University, P.R. China. Research focused on the genomics of plants and fungi.

2000 – 2003, Teaching Assistant in the course "General Microbiology", Duke University, USA.

1995 – 2000, Assistant Researcher, Department of Botany, Beijing Museum of Natural History, P.R. China. Research focused on the systematics of freshwater green algae. Main participant of the plant exhibition "Green Homeland".

Spring 1993, Teaching Assistant in the course "Plant Embryology", Peking University, P.R. China.

### Publications

Yun Feng, Anja Klahr, Paulina Janik, Anna Ronikier, Thomas Hoppe, Yuri K. Novozhilov, Martin Schnittler. 2016. What an intron may tell: several sexual biospecies coexist in *Meriderma* spp. (Myxomycetes). Protist, online first (doi: 10.1016/j.protis.2016.03.003).

Yun Feng, Martin Schnittler. 2016. Molecular or morphological species? Myxomycete diversity in a deciduous forest in northeastern Germany. Nova Hedwigia, online first (doi: 10.1127/nova\_hedwigia/2016/0326).

Yun Feng, Martin Schnittler. 2015. Sex or no sex? Independent marker genes and group I introns reveal the existence of three sexual but reproductively isolated biospecies in *Trichia varia* (Myxomycetes). Organisms Diversity and Evolution 15:631–650.

Hongchao Wang, Haiqin Chen, Guangfei Hao, Bo Yang, Yun Feng, Yu Wang, Lu Feng, Jianxin Zhao, Yuanda Song, Hao Zhang, Yong Q. Chen, Lei Wang, Wei Chen. 2013. Role of the phenylalanine-hydroxylating system in aromatic substance degradation and lipid metabolism in the oleaginous fungus *Mortierella alpina*. Applied and Environmental Microbiology 79:3225–3233.

Ahmad Yamin Rahman\*, Abhilash O. Usharraj\*, Biswapriya B. Misra\*, Gincy P. Thottathil\*, Kandakumar Jayasekaran\*, Yun Feng, Shaobin Hou, Su Yean Ong, Fui Ling Ng, Ling Sze Lee, Hock Siew Tan, Muhd Khairul Sakaff, Beng Soon Teh, Bee Feong Khoo, Siti Suriawati Badai, Nurohaida Ab Aziz, Anton Yuryev, Bjarne Knudsen, Alexandre Dionne-Laporte, Nokuthula P Mchunu, Qingyi Yu, Brennick J Langston, Tracey Allen Freitas, Aaron G. Young, Rui Chen, Lei Wang, Nazalan Najimudin, Jennifer A. Saito, Maqsudul Alam. 2013. Draft genome sequence of the rubber tree *Hevea brasiliensis*. BMC Genomics 14:75. (\*equal contributors)

Tiezheng Yuan, Yan Ren, Kun Meng, Yun Feng, Peilong Yang, Shaojing Wang, Pengjun Shi, Lei Wang, Daoxin Xie, Bin Yao. 2011. RNA-Seq of the xylose-fermenting yeast *Scheffersomyces stipitis* cultivated in glucose or xylose. Applied Microbiology and Biotechnology 92:1237–1249.

- Hongchao Wang, Bo Yang, Guangfei Hao, Yun Feng, Haiqin Chen, Lu Feng, Jianxin Zhao, Hao Zhang, Yong Q. Chen, Lei Wang, Wei Chen. 2011. Biochemical characterization of the tetrahydrobiopterin synthesis pathway in the oleaginous fungus *Mortierella alpina*. *Microbiology* 157:3059–3070.
- Jinkui Yang\*, Lei Wang\*, Xinglai Ji\*, Yun Feng, Xiaomin Li, Chenggang Zou, Jianping Xu, Yan Ren, Qili Mi, Junli Wu, Shuqun Liu, Yu Liu, Xiaowei Huang, Haiyan Wang, Xuemei Niu, Juan Li, Lianming Liang, Yanlu Luo, Kaifang Ji, Wei Zhou, Zefen Yu, Guohong Li, Yajun Liu, Lei Li, Min Qiao, Lu Feng, Ke-Qin Zhang. 2011. Genomic and proteomic analyses of the fungus *Arthrobotrys oligospora* provide insights into nematode-trap formation. *PLoS Pathogens* 7:e1002179. (\*equal contributors)
- Lei Wang\*, Wei Chen\*, Yun Feng, Yan Ren, Zhennan Gu, Haiqin Chen, Hongchao Wang, Michael J. Thomas, Baixi Zhang, Isabelle M. Berquin, Yang Li, Jiansheng Wu, Huanxin Zhang, Yuanda Song, Xiang Liu, James S. Norris, Suriguga Wang, Peng Du, Junguo Shen, Na Wang, Yanlin Yang, Wei Wang, Lu Feng, Colin Ratledge, Hao Zhang, Yong Q. Chen. 2011. Genome characterization of the oleaginous fungus *Mortierella alpina*. *PLoS One* 6:e28319. (\*equal contributors)
- Ray Ming\*, Shaobin Hou\*, Yun Feng\*, Qingyi Yu\*, Alexandre Dionne-Laporte, Jimmy H. Saw, Pavel Senin, Wei Wang, Benjamin V. Ly, Kanako L. T. Lewis, Steven L. Salzberg, Lu Feng, Meghan R. Jones, Rachel L. Skelton, Jan E. Murray, Cuixia Chen, Wubin Qian, Junguo Shen, Peng Du, Moriah Eustice, Eric Tong, Haibao Tang, Eric Lyons, Robert E. Paull, Todd P. Michael, Kerr Wall, Danny W. Rice, Henrik Albert, Ming-Li Wang, Yun J. Zhu, Michael Schatz, Niranjana Nagarajan, Ricelle A. Acob, Peizhu Guan, Andrea Blas, Ching Man Wai, Christine M. Ackerman, Yan Ren, Chao Liu, Jianmei Wang, Jianping Wang, Jong-Kuk Na, Eugene V. Shakirov, Brian Haas, Jyothi Thimmapuram, David Nelson, Xiyin Wang, John E. Bowers, Andrea R. Gschwend, Arthur L. Delcher, Ratnesh Singh, Jon Y. Suzuki, Savarni Tripathi, Kabi Neupane, Hairong Wei, Beth Irikura, Maya Paidi, Ning Jiang, Wenli Zhang, Gernot Presting, Aaron Windsor, Rafael Navajas-Pe'rez, Manuel J. Torres, F. Alex Feltus, Brad Porter, Yingjun Li, A. Max Burroughs, Ming-Cheng Luo, Lei Liu, David A. Christopher, Stephen M. Mount, Paul H. Moore, Tak Sugimura, Jiming Jiang, Mary A. Schuler, Vikki Friedman, Thomas Mitchell-Olds, Dorothy E. Shippen, Claude W. dePamphilis, Jeffrey D. Palmer, Michael Freeling, Andrew H. Paterson, Dennis Gonsalves, Lei Wang, Maqsudul Alam. 2008. The draft genome of the transgenic tropical fruit tree papaya (*Carica papaya* Linnaeus). *Nature* 452:991–996. (\*equal contributors)
- Cuixia Chen, Qingyi Yu, Shaobin Hou, Yingjun Li, Moriah Eustice, Rachel L. Skelton, Olivia Veatch, Rachel E. Herdes, Lauren Diebold, Jimmy Saw, Yun Feng, Wubin Qian, Lee Bynum, Lei Wang, Paul H. Moore, Robert E. Paull, Maqsudul Alam, Ray Ming. 2007. Construction of a sequence-tagged high density genetic map of papaya for comparative structural and evolutionary genomics in Brassicales. *Genetics* 177:2481–2491.
- Yun Feng, Sang-Hun Oh, Paul S. Manos. 2005. Phylogeny and historical biogeography of the genus *Platanus* as inferred from nuclear and chloroplast DNA. *Systematic Botany* 30:786–799.
- Wang Zhixue, Feng Yun. 1999. Studies on the Chlorococcales from Beijing and Hebei Province (III) - Studies on genus *Nephroclytium*. *Memoirs of Beijing Natural History Museum* 58:7–9.
- Feng Yun, Wang Zhixue. 1999. Studies on the Chlorococcales from Beijing and Hebei Province (IV) - Studies on genus *Monoraphidium*. *Memoirs of Beijing Natural History Museum* 58:11–16.
- Wang Zhixue, Feng Yun. 1999. Studies on the Chlorococcales from Beijing and Hebei Province (V) - Studies on genus *Scenedesmus*. *Memoirs of Beijing Natural History Museum* 58:17–47.
- Qi Wen-qing, Feng Yun, Chenzhu Xi-zhao, Li Zheng-li, You Rui-lin. 1997. Studies on the reproductive characteristics of *Cimicifuga nanchuanensis* (Ranunculaceae), an endemic endangered species to China. *Acta Botanica Sinica* 39:7–10.
- Wang Zhixue, Feng Yun. 1997. The studies on the Chlorococcales from Beijing and Hebei Province (II) - Some new plants of Chlorococcales in the area (Chlorophyta). *Memoirs of Beijing Natural History Museum* 56:39–44.
- Wang Zhixue, Feng Yun. 1997. The studies on the Chaetophorales in Beijing and Hebei area (IV) Two new species of the Chaetophorales (Chlorophyta). *Memoirs of Beijing Natural History Museum* 56:45–48.
- Wang Zhixue, Feng Yun, Su Wentuan. 1996. Studies on the Chaetophorales from Beijing and Hebei Province II. Report of the genus of *Draparnaldia*. *Memoirs of Beijing Natural History Museum* 55:39–42.
- Wang Zhixue, Feng Yun, Su Wentuan. 1996. Studies on the Chaetophorales from Beijing and Hebei Province III. Report of several new record species of Chaetophorales. *Memoirs of Beijing Natural History Museum* 55:43–46.
- Zhou Yibing, Feng Yun, You Rui-lin. 1995. Some isozyme changes related to organogenesis of bulblets from bulb scales of *Lilium davidii* *in vitro*. *Acta Scientiarum Naturalium Universitatis Pekinensis* 31:499–507.

Greifswald

Date

09.05.2016

Yun Feng

## 6. Acknowledgements



I wish to thank all the current and past members of the lab of General Botany and Plant Systematics for their kind support. I would like to thank especially Anja Klahr for helping me with all aspects of the lab work and for creating a nice working atmosphere in the lab. I owe as well thanks to all colleagues and collectors who contributed to specimens from their myxomycete collections.

Furthermore I would like to thank Prof. Steven L. Stephenson from the University of Arkansas, USA for agreeing to work as the second reviewer of this dissertation.

I would like to thank my supervisor, Prof. Martin Schnittler, for endless support, for introducing me to the world of myxomycetes, and for guidance on doing good research.

Finally, I am grateful to my parents, Yicun Wang and Huairong Feng, for their encouragement and continuous support.

This study was funded by the Deutsche Forschungsgemeinschaft DFG (grant number SCHN 1080/2-1).

